

Rhodium-catalysed hydroformylation of long-chain alkenes in aqueous multiphase systems: Kinetic studies and systematic process development

Vorgelegt von
Diplom-Ingenieur
Tobias Pogrzeba
geb. in Berlin

von der Fakultät II – Mathematik und Naturwissenschaften
der Technischen Universität Berlin
zur Erlangung des akademischen Grades

Doktor der Ingenieurwissenschaften
Dr.-Ing.

genehmigte Dissertation

Promotionsausschuss:

Vorsitzender: Prof. Dr. Thomas Friedrich, TU Berlin
Berichter: Prof. Dr. Reinhard Schomäcker, TU Berlin
Berichter: Prof. Dr. Dieter Vogt, TU Dortmund

Tag der wissenschaftlichen Aussprache: 02. Februar 2018

Berlin 2018

Danksagung

Ich möchte an dieser Stelle die Gelegenheit nutzen, mich bei allen Personen zu bedanken, die zum Gelingen dieser Arbeit beigetragen haben.

Mein besonderer Dank gilt zunächst Herrn Prof. Dr. Reinhard Schomäcker, der mir das Vertrauen geschenkt hat an seinem Lehrstuhl promovieren zu können und dessen guten Rates ich mir in all den Jahren stets gewiss sein konnte. Ich danke außerdem Herrn Prof. Dr. Dieter Vogt für die Übernahme des Zweitgutachtens meiner Dissertation und für die sehr gute und vertrauensvolle Zusammenarbeit innerhalb des SFBs.

Ich danke der Deutschen Forschungsgemeinschaft (DFG) für finanzielle Unterstützung im Rahmen des Sonderforschungsbereichs Transregio 63, Integrierte chemische Prozesse in flüssigen Mehrphasensystemen (*InPROMPT*).

Ein ganz großes Dankeschön gebührt allen aktuellen und ehemaligen Mitgliedern des Arbeitskreises von Prof. Dr. Reinhard Schomäcker, einer Gruppe von wunderbaren Menschen mit denen ich die vergangenen 8 Jahre meines Lebens sehr gerne verbracht habe. Ich danke euch für das kollegiale und freundliche Miteinander und für all die gemeinsam verbrachten Stunden, auch neben der Arbeitszeit. Herausheben möchte ich meinen Dank an dieser Stelle nur an eine besondere Person: Marcel Schmidt. Es war mir über die vergangenen 4 Jahre eine enorm große Freude mit dir zusammen zu arbeiten und dich auch in schwierigen Zeiten stets als meinen Kollegen und Freund an meiner Seite zu wissen. Danke für all die Diskussionen, Gespräche und witzige Plaudereien, welche wir beiden miteinander geführt haben!

Für die tolle Zusammenarbeit innerhalb des SFB möchte ich mich des Weiteren bei all meinen Kollegen in Berlin, Magdeburg, Darmstadt und Dortmund bedanken. Insbesondere gilt mein Dank Markus Illner, David Müller und Erik Esche für die außergewöhnlich gute und vertrauensvolle Kooperation, ohne die wir unsere gemeinsamen Projektziele niemals so erfolgreich realisiert hätten.

Herzlich bedanken möchte ich mich bei Nataša Milojevic, Carolina Urban, Ariane Weber und Julia Bauer für ihre tatkräftige Unterstützung. Durch eure unermüdliche und ausgezeichnete Mitarbeit habt ihr maßgeblich zum Gelingen meiner Dissertation beigetragen.

Zuletzt gilt mein Dank meiner Familie: Meiner Schwester, die stets für mich da ist, und meinen Eltern, die mich zeitlebens unterstützt, gefördert und beraten haben. Ohne euch wäre all dies niemals möglich gewesen. Ihr seid mir das Wichtigste im Leben, danke, dass es euch gibt!

Abstract

In the course of the development of new sustainable industrial chemical processes the exploitation of switchable solvent systems is increasingly investigated in various fields. The application of highly efficient catalysts and safer solvents is mandatory to make a step towards a greener chemistry, as well as to find innovative ways to reduce waste from chemical reactions. Consequently, the use of water as solvent for chemical processes is a very promising approach. The focus of this thesis is the kinetic study of rhodium-catalysed hydroformylation of long-chain alkenes in aqueous multiphase systems (microemulsion systems, surfactant-free multiphase emulsions, and Pickering emulsions) and the investigation of the applicability of these systems in a mixer-settler process. Based on the example of the hydroformylation of 1-dodecene in a microemulsion system, a step-by-step approach is presented on how to investigate these complex multiphase systems and to transfer the results of lab-scale experiments into a continuously operated process in miniplant scale. In addition, the hydroformylation of 1-dodecene is also investigated in surfactant-free multiphase emulsions and Pickering emulsions in a more fundamental approach. The goal for these two multiphase systems is to prove their applicability as reaction systems for organic transition metal-catalysed chemistry.

The hydroformylation of 1-dodecene was successfully performed in all three investigated microemulsion systems with very high selectivity towards the desired linear product (n:iso selectivity of 98:2). In microemulsion systems, the catalyst recycling after the reaction could be easily conducted by simple phase separation, maintaining the activity and very high selectivity. In a second step, the results from the lab experiments were successfully transferred into miniplant scale. A 200 h long campaign in continuous operation could be performed, showing similar product yield and selectivity as on the lab-scale. In addition, a stable steady state operation was achieved, showing an efficient phase separation and recycling of surfactant and catalyst.

Furthermore, the influence of phase behaviour and the selected non-ionic surfactant on the hydroformylation reaction in microemulsion systems has been investigated. The results revealed that the applied surfactant can have a strong impact on the performance of the catalytic reaction, in particular on the reaction rate. Based on a proposed mechanism and the gained experimental data an adapted kinetic model has been derived, including the unique influences of the regarded multiphase system on the reaction (in particular the surfactant concentration and ligand to metal ratio).

Zusammenfassung

Im Zuge der Entwicklung neuer, nachhaltiger chemischer Prozesse im industriellen Maßstab wird in verschiedensten Bereichen der Einsatz von schaltbaren Lösungsmittelsystemen zunehmend untersucht. Die Verwendung von hocheffizienten Katalysatoren und sicheren Lösungsmitteln, sowie innovative Lösungen um den entstehenden Abfall zu verringern, sind zwingend notwendig für einen Schritt in Richtung einer *grüneren* Chemie. Der Einsatz von Wasser als Lösungsmittel ist daher ein sehr vielversprechender Ansatz. Der Fokus der hier vorliegenden Arbeit ist die kinetische Untersuchung der Rhodium-katalysierten Hydroformylierung von langkettigen Alkenen in wässrigen Mehrphasensystemen (Mikroemulsionssysteme, tensidfreie mehrphasige Emulsionen, und Pickering Emulsionen) und deren Einsatzfähigkeit in einem Mixer-Settler Prozess. Anhand des Beispiels der Hydroformylierung von 1-Dodecen in Mikroemulsionssystemen wird schrittweise ein Ansatz präsentiert, wie diese komplexen Mehrphasensysteme untersucht und die Resultate der Laborexperimente auf eine kontinuierlich betriebene Miniplant übertragen werden können. Des Weiteren wurde die gleiche Reaktion in tensidfreien mehrphasigen Emulsionen und Pickering Emulsionen grundlegend untersucht, um deren Einsatzfähigkeit als Reaktionsmedien für die organische, übergangsmetallkatalysierte Chemie zu überprüfen.

Die Hydroformylierung von 1-Dodecen konnte in allen drei Systemen erfolgreich durchgeführt werden und zeigte eine sehr hohe Selektivität zum gewünschten linearen Produkt (n:iso Selektivität von 98:2). In Mikroemulsionssystemen konnte der Katalysator nach der Reaktion durch eine einfache Phasentrennung zurückgewonnen und ohne Verlust in seiner Aktivität und Selektivität mehrfach wiederverwendet werden. Die Übertragung der Ergebnisse vom Labor- in den Miniplantmaßstab verlief ebenfalls erfolgreich. Der Prozess in der Miniplant konnte in einer 200 h langen Kampagne kontinuierlich und stabil betrieben werden. Die Ergebnisse bestätigen die Vorhersagen der Laborresultate und belegen außerdem ein effizientes Recycling von Tensid und Katalysator durch Phasentrennung.

Des Weiteren wurde der Einfluss des Phasenverhaltens und des gewählten nicht-ionischen Tensids auf die Hydroformylierung in Mikroemulsionssystemen untersucht. Hierbei konnte ein mitunter starker Einfluss des Tensids auf den Ablauf der katalytischen Reaktion gefunden werden. Basierend auf einem vorgeschlagenen Reaktionsmechanismus und den gesammelten experimentellen Daten wurde anschließend ein angepasstes kinetisches Modell entwickelt, welches die besonderen Einflüsse dieser Mehrphasensysteme auf die Reaktion mit berücksichtigt (insbesondere die Einflüsse der Tensidkonzentration und des Ligand:Metall-Verhältnisses).

Erklärung zur Dissertation

Ich erkläre hiermit, dass ich bislang an keiner anderen Hochschule oder Fakultät meine Promotionsabsicht beantragt habe.

Die vorliegende Dissertation wurde bereits in Form von wissenschaftlichen Publikationen veröffentlicht. Es handelt sich hierbei um die folgenden Veröffentlichungen (chronologisch):

Paper 1: Rhodium-Catalyzed Hydroformylation of Long-Chain Olefins in Aqueous Multiphase Systems in a Continuously Operated Miniplant

Tobias Pogrzeba, David Müller, Tobias Hamerla, Erik Esche, Niklas Paul, Günter Wozny, and Reinhard Schomäcker

Industrial & Engineering Chemistry Research, 2015, 54, 11953-11960

Eigenanteil: Erstautor; In diesem Beitrag wurden die Ergebnisse aus semi-Batch Experimenten zur rhodiumkatalysierten Hydroformylierung von 1-Dodecen in Mikroemulsionssystemen im Labormaßstab auf eine kontinuierlich betriebene Miniplant übertragen. Die Labormessungen zum Einfluss verschiedener Parameter auf die Reaktion wurden von mir durchgeführt und bereits in der Doktorarbeit von Tobias Hamerla beschrieben. Die Übertragung der Messwerte auf die Miniplant erfolgte in Zusammenarbeit mit David Müller. Des Weiteren habe ich beim Betrieb der Miniplant mitgearbeitet.

Paper 2: Systematic Phase Separation Analysis of Surfactant-Containing Systems for Multiphase Settler Design

David Müller, Erik Esche, Tobias Pogrzeba, Markus Illner, Felix Leube, Reinhard Schomäcker, and Günter Wozny

Industrial & Engineering Chemistry Research, 2015, 54, 3205-3217

Eigenanteil: dritter Autor; Bei dieser Arbeit handelt es sich um die Anleitung zur Auslegung eines Mixer-Settler-Prozesses für tensidbasierte Mehrphasensysteme. Die Anleitung wurde anhand eines Fallbeispiels zur Hydroformylierung in Mikroemulsionssystemen erläutert. Ich habe die Untersuchungen des dynamischen Phasentrennverhaltens dieser Systeme angeleitet, auf deren Basis ein entsprechendes Phasentrennmodell erstellt und zur Auslegung eines Dekanters für den kontinuierlichen Prozess verwendet wurde.

Paper 3: Verteilungsgleichgewichte von Liganden in mizellaren Lösungsmittelsystemen

Marcel Schmidt, Tobias Pogrzeba, Dmitrij Stehl, René Sachse, Michael Schwarze, Regine von Klitzing, and Reinhard Schomäcker

Chemie Ingenieur Technik, 2016, 88, 119-127

Eigenanteil: zweiter Autor; In diesem Beitrag wurde das Verteilungsgleichgewicht von vier repräsentativen Liganden für die homogene Katalyse in unterschiedlichen wässrig-mizellaren Systemen analysiert, um tiefgreifendere Erkenntnisse bzgl. der Einflussfaktoren auf das Katalysatorrecycling in diesen Medien zu erlangen. Die Hydrophobizität und Grenzflächenaktivität der Liganden stellten sich als wichtige Größen für den Verteilungskoeffizienten heraus. Ich habe Marcel Schmidt bei der Durchführung und Auswertung der Experimente unterstützt.

Paper 4: Superior catalyst recycling in surfactant based multiphase systems – Quo vadis catalyst complex?

Tobias Pogrzeba, David Müller, Markus Illner, Marcel Schmidt, Yasemin Kasaka, Ariane Weber, Günter Wozny, Reinhard Schomäcker, and Michael Schwarze

Chemical Engineering and Processing, 2016, 99, 155-166

Eigenanteil: Erstautor; In dieser Arbeit wurde der Einfluss von verschiedenen Parametern/Faktoren auf die Verteilung von Katalysatorkomplexen in Mikroemulsionssystemen untersucht. Ich habe die Phasenuntersuchungen zu den verschiedenen Systemen und die Bestimmung der Katalysatorkonzentration in den Einzelphasen in Zusammenarbeit mit Marcel Schmidt durchgeführt. Die erhaltenen Informationen wurden im Anschluss dazu verwendet (gemeinsam mit David Müller und Markus Illner) ein Prozesskonzept für Reaktionen in mizellaren Medien zu erarbeiten.

Paper 5: Catalytic Reactions in Aqueous Surfactant-Free Multiphase Emulsions

Tobias Pogrzeba, Marcel Schmidt, Lena Hohl, Ariane Weber, Georg Buchner, Joschka Schulz, Michael Schwarze, Matthias Kraume, and Reinhard Schomäcker

Industrial & Engineering Chemistry Research, 2016, 55, 12765-12775

Eigenanteil: Erstautor; Der Einsatz von wässrigen, tensidfreien Mehrphasenemulsionen als Reaktionsmedien für die übergangsmetallkatalysierte homogene Katalyse wird in dieser Publikation

erstmalig am Beispiel von zwei verschiedenen Reaktionen berichtet. Die Emulsionen wurden mit Hilfe des Amphiphils Diethylenglycolbutylether formuliert und mittels Endoskopmessungen (durchgeführt von Lena Hohl) charakterisiert. Die Phasenuntersuchungen und Experimente zur Hydroformylierung von 1-Dodecen in diesen Reaktionsmedien wurden unter meiner Aufsicht von Ariane Weber im Zuge ihrer Bachelorarbeit durchgeführt.

Paper 6: Halloysites Stabilized Emulsions for Hydroformylation of Long Chain Olefins

Regine von Klitzing, Dimitrij Stehl, Tobias Pogrzeba, Reinhard Schomäcker, Renata Minullina, Abhishek Panchal, Svetlana Konnova, Rawil Fakhrullin, Joachim Koetz, Helmuth Möhwald, and Yuri Lvov

Advanced Materials Interfaces, 2016, 1600435

Eigenanteil: dritter Autor; Der Einsatz von Halloysite-stabilisierten Emulsionen für die rhodiumkatalysierten Hydroformylierung von 1-Dodecen wird in dieser Publikation erstmalig berichtet. Die Durchführung der Reaktion über einen Zeitraum von 24 h verlief erfolgreich. Ich habe die Reaktion in diesen Emulsionen experimentell untersucht und in Abstimmung mit Dimitrij Stehl (zuständig für Herstellung und Charakterisierung der Emulsionen) die Zusammensetzung der Emulsionen bezüglich der Reaktionsperformance optimiert.

Paper 7: Hydroformylation in Microemulsions: Proof of Concept in a Miniplant

Markus Illner, David Müller, Erik Esche, Tobias Pogrzeba, Marcel Schmidt, Reinhard Schomäcker, and Jens-Uwe Repke

Industrial & Engineering Chemistry Research, 2016, 55, 8616-8626

Eigenanteil: dritter Autor; In diesem Beitrag wurden ausführlich der Aufbau und erfolgreiche Betrieb einer Miniplant zur Hydroformylierung von 1-Dodecen in Mikroemulsionssystemen beschrieben. Ein Hauptaugenmerk lag dabei auf der kontinuierlichen Phasentrennung in einem horizontalen Dekanter. Ich habe mit experimentellen Daten bei der Entwicklung des Phasentrennmodells für den Dekanter mitgeholfen. Des Weiteren habe ich die Durchführung des Prozesses in der Miniplant mit Labormessungen zur Hydroformylierung und deren Analytik grundlegend unterstützt, sowie am eigentlichen Betrieb der Anlage mitgearbeitet. Hauptverantwortlich für die Miniplant waren Markus Illner und David Müller.

Paper 8: Microemulsion Systems as Switchable Reaction Media for the Catalytic Upgrading of Long-Chain Alkenes

Tobias Pogrzeba, Markus Illner, Marcel Schmidt, Jens-Uwe Repke, and Reinhard Schomäcker

Chemie Ingenieur Technik, 2017, 89, 459-463

Eigenanteil: Erstautor; Dieser Kurzbeitrag beschäftigt sich mit der Anwendung von Mikroemulsionssystemen als schaltbare Reaktionsmedien für chemische Prozesse. Am Beispiel der Hydroformylierung von 1-Dodecen wird der Einfluss von Temperatur und Ethoxylierungsgrad auf die katalytische Reaktion diskutiert. Ich habe diese Experimente durchgeführt. Im Anschluss wird die erfolgreiche Umsetzung der Hydroformylierung in einer kontinuierlich betriebenen Miniplant präsentiert. Beim Betrieb der Miniplant habe ich Markus Illner mit Rat und Tat unterstützt.

Paper 9: Understanding the Role of Nonionic Surfactants during Catalysis in Microemulsion Systems on the Example of Rhodium-Catalyzed Hydroformylation

Tobias Pogrzeba, Marcel Schmidt, Natasa Milojevic, Carolina Urban, Markus Illner, Jens-Uwe Repke, and Reinhard Schomäcker

Industrial & Engineering Chemistry Research, 2017, 56, 9934-9941

Eigenanteil: Erstautor; In diesem Beitrag wurde der Einfluss von nicht-ionischen Tensiden auf katalytische Reaktionen in Mikroemulsionssystemen am Beispiel der Hydroformylierung systematisch untersucht. Es konnte gezeigt werden, dass das Phasenverhalten von Mikroemulsionen keinen Einfluss auf den Ablauf von katalytischen Reaktionen hat. Die Auswahl des Tensids ist hingegen von großer Bedeutung und kann das Resultat der Reaktionen entscheidend beeinflussen. Die Experimente für diese Publikation wurden teils direkt von mir und teils unter meiner Betreuung (Bachelorarbeit von Natasa Milojevic und Carolina Urban) durchgeführt.

Paper 10: Kinetics of Hydroformylation of 1-Dodecene in Microemulsion Systems using Rhodium Sulfoxantphos Catalyst

Tobias Pogrzeba, Markus Illner, Marcel Schmidt, Natasa Milojevic, Jens-Uwe Repke, and Reinhard Schomäcker

Industrial & Engineering Chemistry Research, eingereicht im Dez 2017

Eigenanteil: Erstautor; in diesem Beitrag wurde die Hydroformylierung von 1-Dodecen in Mikroemulsionssystemen kinetisch untersucht, mit dem Ziel ein adaptiertes kinetisches Modell für die Reaktion in diesen Medien aufzustellen. Aus dem Zusammenspiel von Experimenten und Modellierung zeigte sich, dass vor allem die Katalysator- und die Tensidkonzentration entscheidende Parameter für den Ablauf der Reaktion sind. Die veröffentlichten Messdaten in dieser Publikation und deren Auswertung wurden von mir erbracht. Die Modellierung der Kinetik wurde von Markus Illner durchgeführt.

Jeweils ein Exemplar der hier aufgeführten Publikationen ist dieser Dissertation beigelegt.

Ort, Datum Tobias Pogrzeba

Table of Contents

1	Introduction	1
1.1	Motivation.....	1
1.2	Research scope and outline of this work	2
2	Theoretical background	6
2.1	Chemical engineering aspects.....	6
2.1.1	Surfactant-modified multiphase systems	7
2.1.2	Kinetics of rhodium-catalysed hydroformylation	9
2.2	Process engineering aspects	12
3	Methods and materials	15
3.1	Preparation of catalyst solution.....	15
3.2	Investigation of phase behaviour and catalyst distribution.....	15
3.3	Determination of the rhodium concentration	16
3.4	Hydroformylation experiments.....	16
3.5	Gas chromatography and data evaluation.....	17
4	Results and discussion.....	19
4.1	Design of process	19
4.1.1	Catalyst distribution in microemulsion systems	19
4.1.2	Process constraints and general concept.....	21
4.2	Phase separation analysis for multiphase settler design	23
4.2.1	Phase separation dynamics.....	24
4.2.2	Full mapping of phase separation	25
4.2.3	Design of multiphase settler	26
4.3	From lab to miniplant.....	27
4.3.1	Parameter studies	27
4.3.2	Miniplant operation	28
4.4	Influence of non-ionic surfactants on catalysis in microemulsion systems.....	30

4.4.1	Degree of ethoxylation	31
4.4.2	Effect of surfactant concentration	32
4.5	Reaction kinetics of hydroformylation	33
4.5.1	Catalyst concentration.....	34
4.5.2	Formulation of an adapted kinetic model	35
4.6	Catalytic reaction in surfactant-free multiphase emulsions	38
4.7	Pickering Emulsions	39
5	Conclusions and outlook	41
6	References	42

List of Abbreviations

Abbreviation	Description
C4E2	Diethylene glycol butyl ether
cmc	Critical micelle concentration
EO	Ethoxylation degree of the surfactant
GC	Gas chromatography
MES	Microemulsion system
o/w (emulsions)	Oil-in-water (emulsion)
RDS	Rate determining step
Rh-SX	Rhodium-SulfoXantphos catalyst
SFME	Surfactant-free multiphase emulsion
SX	SulfoXantphos, ligand
TOF	Turnover frequency
TPP	Triphenylphosphine, ligand
TPPTS	Tri-(natrium-meta-sulfonatophenyl)-phosphine, ligand
w/o (emulsion)	Water-in-oil (emulsion)

1 Introduction

1.1 Motivation

The goal of sustainable and green chemistry is to find innovative ways to reduce waste, conserve energy, and to generate chemical products with less hazardous syntheses. According to the 12 principles of green chemistry, developed by Anastas and Warner ¹, the use of renewable feedstocks and the application of highly efficient catalysts and safer solvents is mandatory to make a step towards a greener chemistry. Consequently, this leads the design of new and efficient chemical processes. Water is the solvent preferred by Nature for biochemical processes and it is environmentally benign. However, it is only a feasible solvent for organic chemicals that have polar groups, such as alcohols ². To widen the scope of substrates and enable the transfer of the already established organic transition metal-catalysed chemistry into the medium water, micellar catalysis can provide the crucial “solution” ³. Often it is sufficient to employ a suitable surfactant or a micelle producing agent to solubilize the reactants and to enable the reaction. So-called microemulsion systems are a special type of aqueous, surfactant-modified multiphase systems. These systems provide a temperature-induced switchability in their phase behaviour that offers many interesting options for chemical processes with industrial relevance in aqueous media.

The hydroformylation reaction is one of the most important homogeneously catalysed reactions practiced on the industrial scale. The production of aldehydes from short-chain alkenes (e.g. propylene or butylene) exceeds nowadays 12 million metric tons per year ^{4,5}. Aldehydes are valuable intermediates and used in the production of a wide range of products such as detergents, plasticizers, flavours or surfactants. In general, a product mixture is obtained from the hydroformylation reaction since the formyl group can be formed at both C atoms of the double bond (Figure 1).

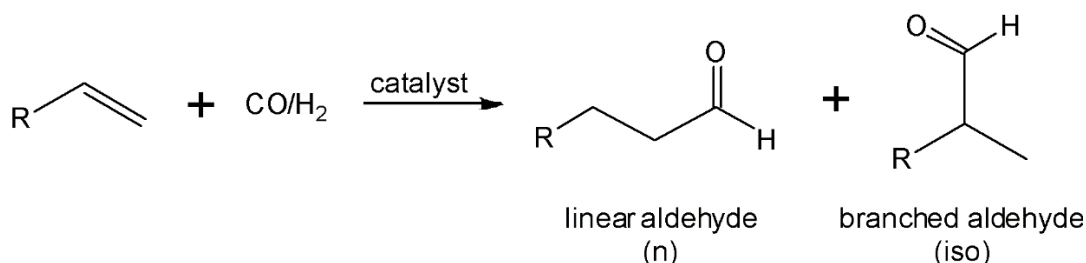


Figure 1 Schematic reaction path of hydroformylation.

Since the discovery of the hydroformylation reaction by Otto Roelen in 1938 ⁶, the chemical processes to produce aldehydes from alkenes underwent many development steps. The current state of the art in industry is the implementation of the reaction in an aqueous two-phase system with highly active rhodium catalysts consisting of water-soluble ligands, which was developed and established at Ruhrchemie in 1982 ⁷. The major drawback of this process is the limitation to short-chain alkenes ($C \leq 5$), due to the poor solubility of long-chain alkenes in the aqueous phase. Therefore, long-chain alkenes ($C > 5$) are today still converted by cobalt- or rhodium-catalysed processes in homogeneous phase, requiring complex and expensive product separation and catalyst recycling, especially in the case of rhodium. Thus, a novel and “greener” process concept based on surfactant-modified multiphase systems has been investigated over the last 8 years within the Collaborative Research Centre SFB/TRR 63 (InPROMPT).

1.2 Research scope and outline of this work

The focus of this thesis is the kinetic study of rhodium-catalysed hydroformylation of long-chain alkenes in aqueous multiphase systems (microemulsion systems, surfactant-free multiphase emulsions, and Pickering emulsions) and the investigation of the applicability of these systems in a mixer-settler process. Based on the example of the hydroformylation of 1-dodecene in a microemulsion system, a step-by-step approach is presented on how to investigate these complex multiphase systems and to transfer the results of lab-scale experiments into a continuously operated process in miniplant scale. In addition to this case study for microemulsion systems, the hydroformylation of 1-dodecene is also investigated in surfactant-free multiphase systems and Pickering emulsions in a more fundamental approach. The goal for these two multiphase systems is to prove their applicability as reaction systems for organic transition metal-catalysed chemistry.

With the objective to enable a continuous process for the rhodium-catalysed hydroformylation of long-chain alkenes in aqueous multiphase systems, this work is based on two main axes:

1. Chemical engineering aspects; e.g. investigation on the phase behaviour of the reaction systems, distribution of the components in the different phases, reaction kinetics, influence of the additives on the reaction
2. Process engineering aspects; e.g. phase separation behaviour under process conditions, design of a multiphase settler, operation of the continuous process.

This thesis is based on 10 full-text peer-reviewed articles from contributions in scientific journals, which deal with the different aspects of the process development for the hydroformylation of long-chain alkenes in aqueous multiphase systems. Figure 1.1 displays the structure of this thesis and illustrated the connection of the different aspects from the articles in a unified framework. The topics of each article are briefly summarized in the following (chronologic order):

Paper 1 deals with the transfer of results of lab-scale hydroformylation experiments in microemulsion systems into a continuously operated process in miniplant scale. At first, the reaction parameters have been optimized to give high turnover frequencies and high selectivity to the desired linear aldehyde. In a second step, the hydroformylation was operated continuously in a miniplant for a total of 130 h, including phase separation and catalyst recycling.

Paper 2 presents a guideline for the multiphase settler design for a mixer-settler process in surfactant-modified multiphase systems. In addition, the guideline is applied in a case study for microemulsion systems in a hydroformylation miniplant. The systematic analysis of the most relevant parameters for phase separation of these systems resulted in the design of a highly flexible, modular settler for the separation of up to three liquid phases.

Paper 3 deals with the distribution of homogeneous catalyst systems in surfactant-modified multiphase systems. For that purpose, the equilibrium distribution of four representative ligands in different surfactant-containing systems was investigated and the dependency of their distribution in the different phases of these systems was discussed.

Paper 4 is divided in two parts. At first, the influence of different parameters/factors on the distribution of catalyst complexes in microemulsion systems is analyzed. In the second part, the derived information is then used for the optimal design of a mixer-settler process for the hydroformylation of long-chain alkenes. Hereby, special attention is given to the separation step with the aim to reduce catalyst leaching into the product streams.

Paper 5 reports of the first applications of aqueous surfactant-free multiphase emulsions as reaction media for homogeneously catalysed reactions (hydroformylation and Suzuki coupling). The formulated multiphase systems were investigated with respect to reaction engineering and catalyst recycling to evaluate their application potential for new chemical processes based on switchable solvents.

Paper 6 presents the results of the first application of halloysites stabilized Pickering emulsions for hydroformylation of long-chain alkenes. The formulated emulsions were investigated and characterized by spectroscopic methods. Then the reaction was performed in one selected (o/w) Pickering emulsion system to give a proof of concept.

Paper 7 reports of the proof of concept for rhodium-catalysed hydroformylation in microemulsion systems carried out during a 200 h miniplant operation. The challenges of the miniplant operation (e.g. foaming, phase separation) are discussed and methods to overcome them are presented. In addition, the results of the miniplant operation are discussed in detail.

Paper 8 is a short communication concerning the application of microemulsion systems as switchable reaction media. The influence of temperature and the selected surfactant on the reaction kinetics in these systems is discussed. The results from lab-scaled experiments are also compared to the results of a long-term steady state continuous operation of the hydroformylation process in the miniplant.

Paper 9 deals with the influence of non-ionic surfactants during catalysis in microemulsion systems. On the example of rhodium-catalysed hydroformylation the impact of phase behaviour, surfactant structure and hydrophilicity of the applied surfactant has been investigated experimentally and discussed in detail.

Paper 10 presents the results of kinetic experiments on rhodium-catalysed hydroformylation in microemulsion systems. The influence of different parameters on the rate of the reaction has been investigated. The results were then used in order to formulate an adapted kinetic model for the reaction in these reaction media.

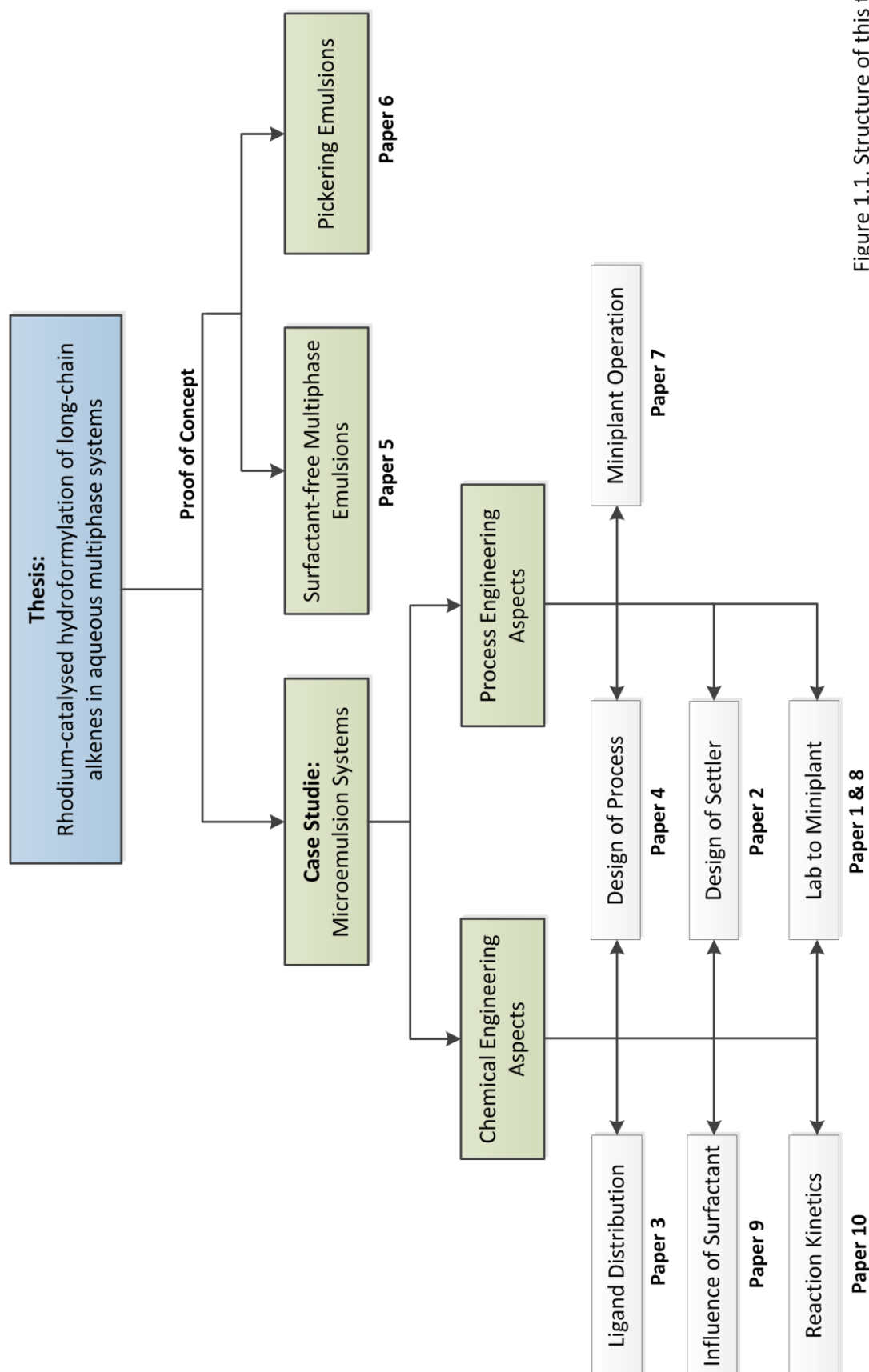


Figure 1.1. Structure of this thesis.

2 Theoretical background

This chapter summarizes the important aspects of this work from a theoretical point of view. Further issues are clarified and referenced in the discussion part in chapter 4, once it is necessary.

2.1 Chemical engineering aspects

Chemical reactions proceed with the highest rates when all the reactants are dissolved in the same phase and thus no mass transport limitation occurs. However, this ideal situation is often hindered by poor miscibility or different aggregate states of the reactants. For that reason, many examples for two- or three phase reaction systems (with reactants in gaseous, liquid and solid state) can be found in industrial applications. Since mass transfer is a key factor for this type of reactions, the size of the interfacial area between the reactants and the phases they are dissolved in becomes a very important parameter. An increase of the interfacial area usually leads to a better mass transfer between the phases and also gives the reaction more space to proceed, which all in all results in a higher reaction rate. In case of reactions performed by homogeneously dissolved catalysts, additionally the separation of product and catalyst after the reaction becomes a major task. For this purpose aqueous two-phase systems have been established in industry, providing efficient consecutive reaction and separation steps during the process. The most common examples for these processes are the Ruhrchemie-Rhône-Poulenc process for the hydroformylation of propylene and butylene ⁷, the shell higher olefin process (SHOP) for the production of higher olefins ⁸, or the Wacker process for the fabrication of acetaldehyde ⁹. Since the homogeneous catalyst is dissolved in an aqueous phase in all three processes, it can be easily separated from the organic phase that contains remaining reactants and the product after the reaction. However, the concentrations of the reactants in the catalyst containing phase have to be sufficiently high in order to achieve high reaction rates. In case of the three mentioned examples the solubility of the substrates (short-chain alkenes) is good enough to enable the reaction, but often enough this is not applicable for other conventional two-phase systems. To overcome the disadvantage of limited substrate solubility in the catalyst phase, several additives are available that allow to tune the properties of reaction media or make them switchable. Ideally, a reaction medium should be homogenous during the reaction and afterwards switchable to a two-phase system for the product isolation step. So-called switchable solvents, meaning liquids that can be reversibly switched from one state to another, thus have a great potential for process intensification. Well-known examples for switchable solvent systems in literature are supercritical media based on CO₂ ¹⁰, thermomorphic multicomponent systems ¹¹, switchable-polarity solvents ¹², or microemulsions systems (MES) ¹³. A case study on the application

of MES as switchable solvents for rhodium-catalysed hydroformylation of long-chain alkenes in a continuously operated chemical process was the main goal of this work.

2.1.1 Surfactant-modified multiphase systems

Aqueous solutions can be applied as reaction media for organic transition metal-catalysed chemistry by the use of surfactants as phase agents. Micellar solutions enhance the solubility and mass transfer of organic non-polar reactants in the polar aqueous phase and thus enable reactions under mild conditions^{14–18}. However, the recovery of the catalyst from micellar solutions after the reaction is not easily done and requires the application of filtration techniques, for example, ultrafiltration. With the so-called micellar enhanced ultrafiltration (MEUF) technique, an active catalyst that is embedded in the micelles can be recycled within the retentate and reused for the reaction, if a micelle rejecting membrane is applied^{19,20}.

A more versatile approach to combine reaction and catalyst recycling in surfactant-modified multiphase systems is the application of microemulsion systems (MES) as switchable solvents. Microemulsion systems are ternary mixtures consisting of an organic component, water and a surfactant. Usually, non-ionic surfactants of the type C_iE_j are chosen in this context to formulate the MES (see Figure 2). In C_iE_j , i is the number of hydrocarbon groups of the surfactant's hydrophobic part, and j is the number of ethoxylate groups of its hydrophilic part.

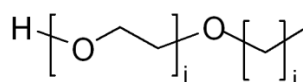


Figure 2. Typical structure of an aliphatic non-ionic surfactant of type C_iE_j .

According to Winsor, microemulsions are thermodynamically stable and can be of different phase behaviour dependent on the composition and temperature of the system. They can be either a one-phase system (Winsor IV) or part of a multiphase system (Winsor I, II, III) in which the microemulsion can be one of three different types: water-in-oil (w/o), oil-in-water (o/w), or bicontinuous^{21,22}. The different Winsor systems are schematically illustrated in the fish-type diagram in Figure 3. The important composition parameters to characterize the MES are the weight fractions of oil (α) and surfactant (γ) (Equation 1), which are calculated from the mass m of the corresponding component:

$$\alpha = \frac{m_{oil}}{m_{oil} + m_{H_2O}} \quad \gamma = \frac{m_{Surf}}{m_{oil} + m_{H_2O} + m_{Surf}} \quad (1)$$

Theoretical background

The left-hand diagram in Figure 3 shows the temperature dependant phase behaviour of microemulsion systems, where the phase boundaries resemble the shape of a fish. The sequence of the phases as a function of temperature, the so-called phase inversion, is a result of a gradual change in the surfactant's solubility. Typically, non-ionic surfactants are mainly soluble in water at low temperatures, whereas they become better soluble in an organic component at higher temperatures. This means that the characteristics of non-ionic surfactant can be switched between hydrophilic and hydrophobic by temperature changes. The sequence of phases in the fish-type diagram is described in detail in the following: Starting from surfactant concentrations in the mixture that exceed the critical micelle concentration (cmc), the two phases (organic and water phase) and the macroscopic interfaces are saturated with the surfactant. As a result, the surfactant molecules are forced to form microscopic oil/water interfaces – microemulsions. At low temperatures, these microemulsions consist of oil-bearing micelles in a continuous water phase ($\underline{2}$, o/w microemulsion). Due to the changing solubility of the surfactant, at higher temperatures water-bearing inverse micelles are formed in a continuous organic phase ($\bar{2}$, w/o microemulsions). Both microemulsions coexist with a pure organic or aqueous excess phase, forming the biphasic Winsor systems I and II. At intermediate temperatures exists a three-phase system (Winsor III) where a surfactant-rich microemulsion phase is formed in the middle of two excess phases, because the surfactant is almost equally soluble in both solvents at that point. Furthermore, a one-phase system (Winsor IV) can be obtained at high surfactant concentrations.

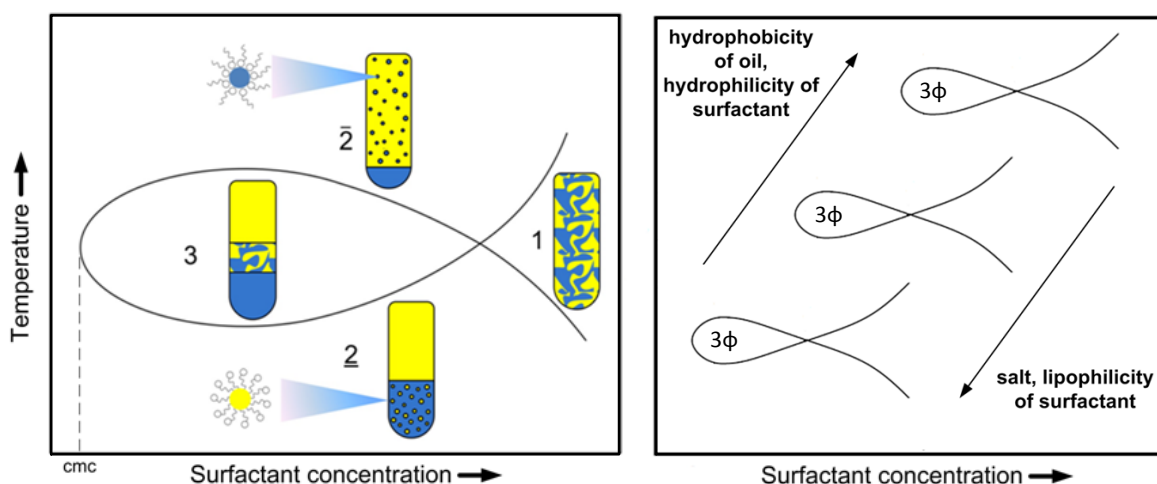


Figure 3. Left: Fish-type phase diagram of a microemulsion system for varying surfactant concentration (γ) at a constant oil/water ratio (α). Right: Qualitative effect of different additives on the phase behaviour of microemulsion systems with non-ionic surfactants.

The phase diagram is an important tool for process development, since the reaction and separation steps are based on it. In general, each Winsor system can be applied as a reaction system for a catalytic reaction. However, for the subsequent separation step the three-phase area is the most viable phase state since the MES needs here the shortest time to separate completely¹³. With that in mind, it has to be considered that the phase behaviour of MES strongly depends on the composition of the reaction mixture. The right-hand diagram in Figure 3 schematically illustrates the shift of the phase behaviour as a function of increasing oil hydrophobicity, salinity, and changing hydrophilicity of the non-ionic surfactant. For example, concentration changes of reactants and products during the course of a chemical reaction are constantly influencing the phase behaviour of the MES. This has a major impact on the application of microemulsion systems in a chemical process with a continuously conducted phase separation, since the changes in phase behaviour have to be constantly tracked and the temperature for phase separation has to be adjusted accordingly in order to maintain the three-phase area. The consequences of this issue on process development are further discussed in section 2.2.

2.1.2 Kinetics of rhodium-catalysed hydroformylation

Despite the fact that the hydroformylation reaction has already been performed for more than 60 years in industry, there exists still a great interest in the detailed investigation of the reaction mechanism. The basis for the generally accepted reaction mechanism was developed by Heck and Breslow during their research on cobalt-catalysed hydroformylation^{23–25} and was found to be valid for the hydroformylation with modified rhodium catalysts in its elementary steps by Wilkinson et al.^{26,27}

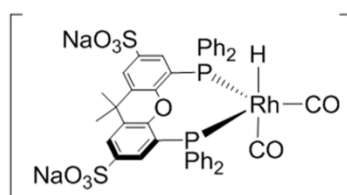


Figure 4. Structure of the hydrophilic Rhodium-Sulfoxantphos catalyst.

Based on this fundamental mechanism, Figure 5 shows the dissociative mechanism of the rhodium-catalysed hydroformylation in aqueous media using a bidentate diphosphine (sulfoxantphos) as ligand (see Figure 4). It is assumed, that in a first step the precursor $\text{Rh}(\text{CO})_2(\text{acac})$ reacts with sulfoxantphos in the presence of CO and H_2 to give principally species (**1a**)²⁸, which is in equilibrium to the non-selective unmodified Rh-tetracarbonyl complex (**1b**)²⁹ and the catalytically inactive Rh-

Theoretical background

dimer (**1c**)^{30,31} under reaction conditions. The catalytic cycle of hydroformylation starts with the dissociation of one CO from species (**1a**) to give the 16-valence electron rhodium hydride complex (**2**). The alkene can coordinate to species (**2**) forming the π -complex (**3**) followed by insertion into the Rh-H bond to form the alkyl species (**4**). In this step the orientation of the ligand at the rhodium centre dictates the regioselectivity of the reaction, since the insertion of the alkene determines whether a linear or a branched aldehyde will be formed. The cycle continues by addition of CO forming the coordinatively saturated alkylrhodium(I) complex (**5**) and proceeds with the migratory insertion of CO into the Rh-alkyl bond to form the acyl complex (**6a**). At this stage a high excess of CO can lead to the formally uncompetitive inhibition of reaction by formation of the catalytically inactive acyl species (**6b**) that is in equilibrium with (**6a**)³² and has been detected by NMR and *in situ* IR techniques^{33–35}. Finally, addition of H₂ to species (**7**) and reductive elimination of the aldehyde closes the cycle and reforms the species (**2**).

It is today widely accepted, that the rate determining step (RDS) of the hydroformylation reaction can be of two different types: (I) the coordination/insertion of the olefin double bond to species (**2**) leading to the formation of the alkyl species (**4**) and (II) the oxidative addition of hydrogen to the acyl complex (**6a**). Dependent on the ligand type and on the steric interaction between ligand and substrate the RDS can differ for the same catalyst and thus makes a general prediction very difficult^{36,37}.

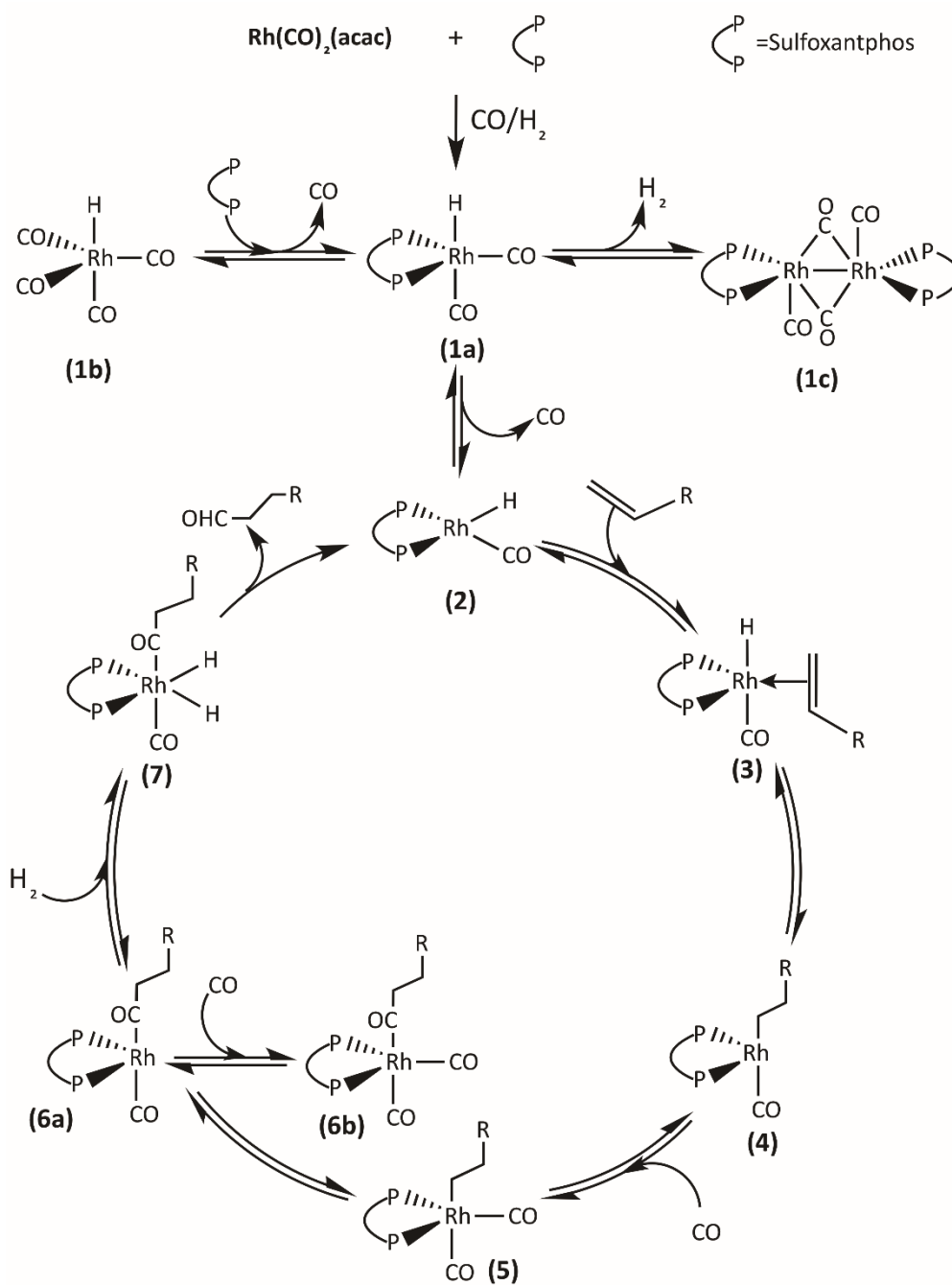


Figure 5. Mechanism of ligand modified hydroformylation with a bidentate diphosphine ligand (path to linear aldehyde) based on the mechanism by Wilkinson et al.²⁶.

2.2 Process engineering aspects

Process design for homogeneous catalysis in microemulsion systems enables the development of new chemical processes with high reaction rates and efficient catalyst recycling. The switchability of these multiphase systems offers many interesting options for combined mixer-settler applications in chemical processes with industrial relevance, like Suzuki and Heck coupling reactions^{38,39} as sub-steps in the total synthesis of complex organic molecules (e.g. total synthesis of Boscalid®⁴⁰). The basic concept for the application of MES as switchable solvents for chemical processes in aqueous media is illustrated in Figure 6: For a given chemical reaction, a stable microemulsion system (including all the reactants and the catalyst) has to be formulated in a first step to enable the reaction under optimal conditions. The catalyst recycling and product isolation can then be performed in a subsequent, temperature-induced phase separation step. Although the three-phase area is the most viable phase state for this step due to the short time for phase separation¹³, generally the biphasic Winsor systems I and II (see Figure 3) could be also applied for this task. Which state of the MES is finally used for the reaction or a combined reaction and separation process, strongly depends on the applied reactants and products and their solubility in the different phases. For instance, the three-phase area offers the interesting possibility to separate a hydrophobic product (upper phase) from the catalyst/surfactant (middle phase) and also from hydrophilic side-products, e.g. salts (bottom phase).

As mentioned earlier in section 2.1.1, the phase behaviour of microemulsion systems is a function of temperature and their composition. The challenging aspect of operating a process with these systems is the shifting of the ideal separation region to different temperatures due to concentration changes. This can be caused by consumption of the reactants, product formation, changing oil-to-water ratio, or changing surfactant concentration.

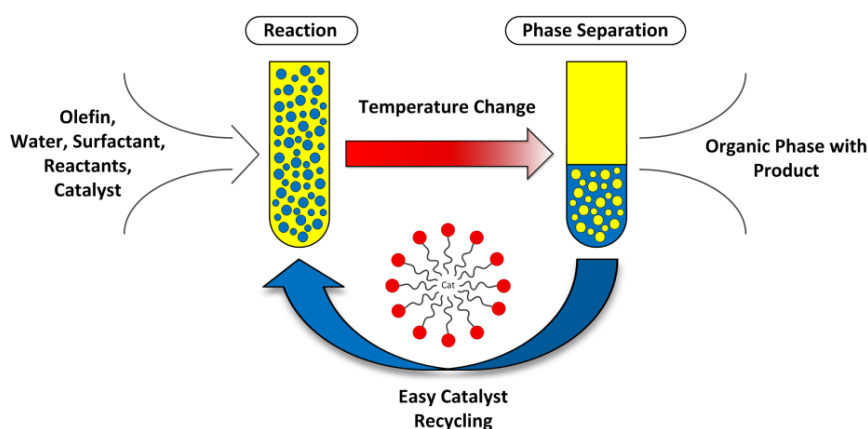


Figure 6. Basic concept for the application of microemulsion systems as switchable solvents for chemical processes in aqueous media.

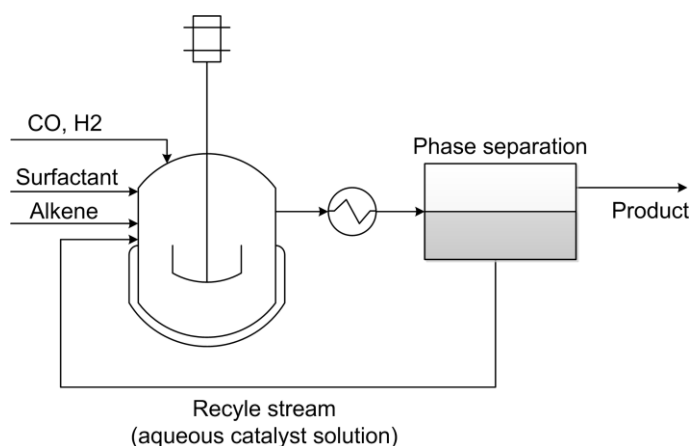


Figure 7. Process concept for the hydroformylation of long-chain alkenes in microemulsion systems; basic operation units and main gas/liquid streams.

Hence, an important requirement for the preparation of operating a continuous process with microemulsion systems is a detailed mapping of the phase behaviour, including all the components of the reaction system. The information received from this mapping is needed to determine a suitable operating area for the process: In order to operate the process continuously and to obtain a considerable product phase, the phase separation must be operated within a certain temperature window. Since this temperature window can be rather narrow for certain applications, especially if an operation in the three-phase area is intended, particular requirements are imposed to the temperature control and design of the separation unit. In addition, online concentration measurements of the mixture inside the separation unit are necessary for the operator of the process to adjust the optimal temperature for phase separation.

Figure 7 shows the general scheme of the process concept for the rhodium-catalysed hydroformylation of long-chain alkenes in microemulsion systems. The reaction is performed in a continuously operated reactor with a constant feed of reactants. The reaction mixture is subsequently led to a settler, in which the phase separation takes place, continuously. Here, the organic product-containing phase is removed and forwarded to downstream processes, whereas the surfactant and aqueous catalyst solution are recycled to the reactor. To achieve an economical viable process, it is of utmost importance that the catalyst loss into the organic phase stays at a minimum. Thus the backbone of this concept is the correct execution of the phase separation step during the entire operation time. On the basis of the here presented process concept for microemulsion systems, a fully automated miniplant was designed and build at Technische Universität Berlin ^{41,42}. The miniplant setup is schematically depicted in Figure 8. It consists of three main sections: a feed section holding containers for the applied substances, a main reaction section holding the reactor (1.5 L volume), and a recycle section holding a decanter (0.5 L volume). The decanter has three drains

to enable a reliable separation of the product-containing organic phase from the surfactant and catalyst-rich middle phase (depicted as “Mix”) and the lower aqueous phase. Each drain is connected to a separate pump, so that each of the phases can be recycled with different flow rates. To adjust the phase separation of the microemulsion system during the operation of the process, the temperature of the settler can be regulated independent from the reactor. This increases the flexibility of the process and allows for the adjustment of optimal reaction and separation conditions under any circumstances. A more detailed description of the miniplant and its single units is given in **PAPER 7**.

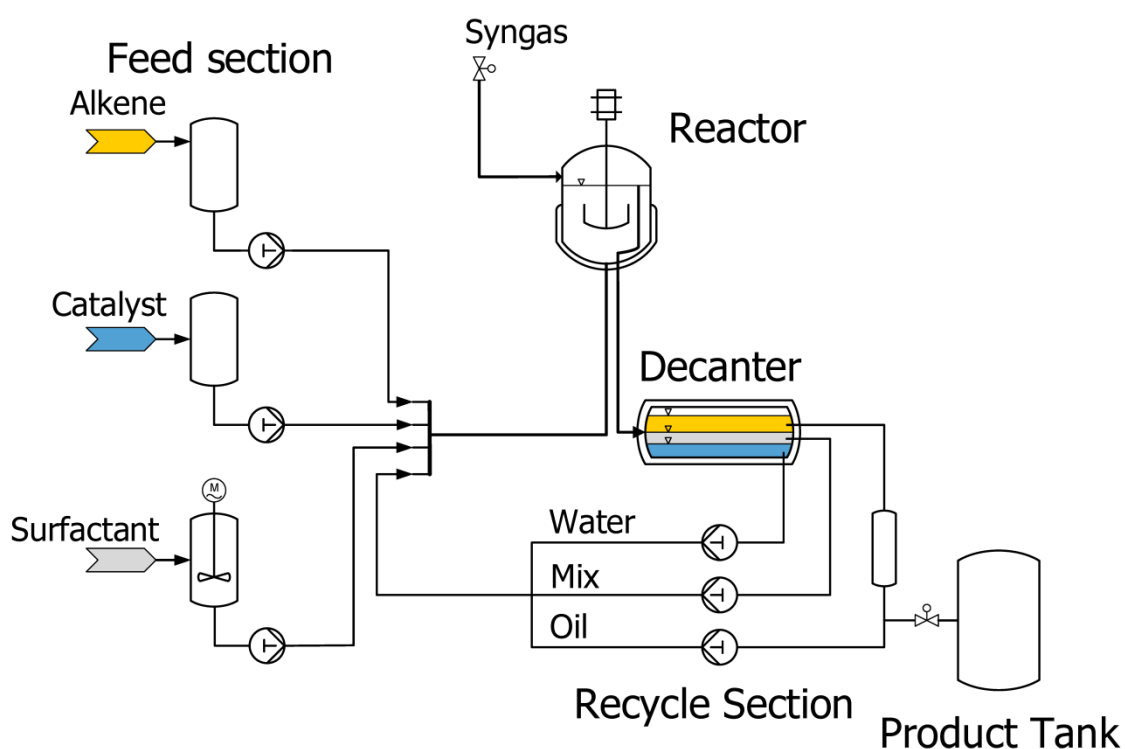


Figure 8. Schematic setup of the mini-plant system for the continuous hydroformylation of 1-dodecene in microemulsion systems; build at the Technische Universität Berlin.

3 Methods and materials

3.1 Preparation of catalyst solution

For the preparation of the catalyst solution, usually 12.9 mg (0.05 mmol, 1 equiv) of the precursor acetylacetonato)dicarbonylrhodium(I) $[\text{Rh}(\text{acac})(\text{CO})_2]$ and 156.7 mg (0.20 mmol, 4 equiv) of the ligand 2,7-Bissulfonate-4,5-bis(diphenylphosphino)-9,9-dimethylxanthene (SulfoXantphos, SX) were evacuated three times in a Schlenk tube and flushed with argon. The solvent (5 g degassed water, HPLC grade) was added through a septum. Then the catalyst solution was stirred over night at room temperature to ensure the formation of the catalyst complex.

3.2 Investigation of phase behaviour and catalyst distribution

Investigations on the phase behaviour of the microemulsion systems were performed by using small glass reactors (50 mL volume) with a heating jacket (see Figure 9). The lid of such a reactor offers connections for sampling, for vacuum establishment, and argon inertisation. The microemulsion systems were formulated from 1-dodecene/water/non-ionic surfactant. The applied non-ionic surfactant was usually from the Marlipal 24 series with varying degree of ethoxylation (EO), from Marlipal 24/50 (average EO = 5) to Marlipal 24/90 (average EO = 9). In addition, every mixture consisted of the catalyst complex and 1 wt-% sodium sulfate. The oil-to-water ratio (α) and the surfactant concentration (γ) were varied. For each sample the different amounts of oil, water, sodium sulfate, and the particular surfactant were weighted into the reactor and evacuated and flushed with argon for at least three times. Then the catalyst solution was injected with a syringe.

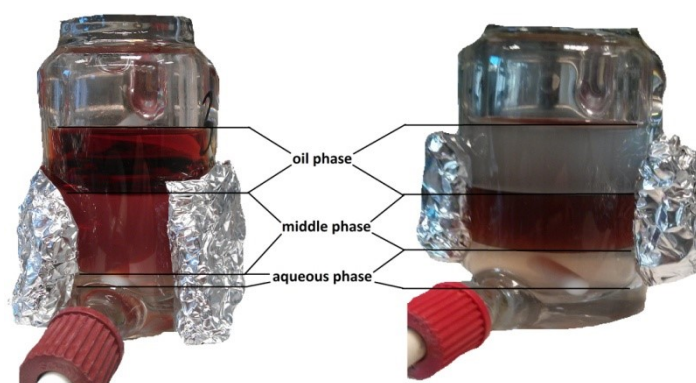


Figure 9. Examples for the phase behaviour investigation: Catalyst distribution obtained for the three-phase area of the MES with Marlipal 24/70 + Rh/Xantphos catalyst (left) and Marlophen NP7 + Rh/SulfoXantphos catalyst (right). (**PAPER 4**)

The phase behaviour was usually investigated from 50 °C to 90 °C in 2 °C steps. The microemulsions were stirred during the heating periods by a magnetic stirrer. After the desired temperature was reached, the stirrer was stopped and the phase separation was observed. If necessary, samples of the different phases were taken with a syringe to determine the catalyst (rhodium) concentration in each.

3.3 Determination of the rhodium concentration

The rhodium concentration in the different phases of the microemulsion systems was determined by inductively coupled plasma optical emission spectrometry (ICP-OES) using Varian ICP-OES 715 ES instrument. Usually, only the aqueous phase and the middle phase of the different three-phase systems were analyzed. Therefore, 2 mL of the water or 1 mL of the middle phase were added to an ICP tube and treated with freshly prepared aqua regia. Afterwards, the samples were diluted with degassed water and the rhodium concentration was measured at a wavelength of 369 nm. A calibration of the setup was performed with rhodium standard solutions (1, 5, 20, 50, and 150 mg/L).

3.4 Hydroformylation experiments

The hydroformylation reactions were performed in a 100 mL stainless steel high-pressure vessel from Premex Reactor AG, equipped with a gas dispersion stirrer and mounted in an oil thermostat from Huber (K12-NR). The reactor setup is illustrated in Figure 10. A mass flow controller (**3**) and a pressure transmitter (**4**) in the gas feed line allow for isobaric reaction conditions. In addition, connections for sampling (**6**) and inertisation of the reaction mixture (**7**) are implemented. The typical reaction conditions for the hydroformylation were 2-40 bar pressure of syngas, an internal reactor temperature of 65–120 °C, and a stirring speed of 1200 rpm, using a gas dispersion stirrer. The reaction mixture usually consisted of 120 mmol (20 g) 1-dodecene, water (HPLC grade, $\alpha = 0.5$), 1.0 wt-% sodium sulfate, non-ionic surfactant (Marlipal 24 series), and catalyst solution. The ratio of rhodium/ligand/alkene was 1/4/2500 in every experiment.

The reaction procedure was performed as described in the following. At first the reactor was filled with the desired amounts of alkene, water, sodium sulfate, and surfactant. Then the catalyst solution was transferred by a syringe to the reactor. The reactor was closed and evacuated and purged with nitrogen for at least three times. The stirrer was started at a rate of 500 rpm and the reactor was heated up to the desired temperature. After reaching the temperature the stirring was slowed down (200-300 rpm) and the reactor was pressurized with syngas. Then the reaction was started by

increasing the stirring speed again to 1200 rpm. For the evaluation of reaction progress, samples were withdrawn at several time intervals (after 0, 1, 2, 3, and 4 hours) via a sampling valve and analyzed by gas chromatography (GC). To ensure homogeneous liquid sampling, the stirring speed was not changed, while the samples were taken from the reactor. In addition, consumption of syngas during the experiments has been recorded via the mass flow controller.

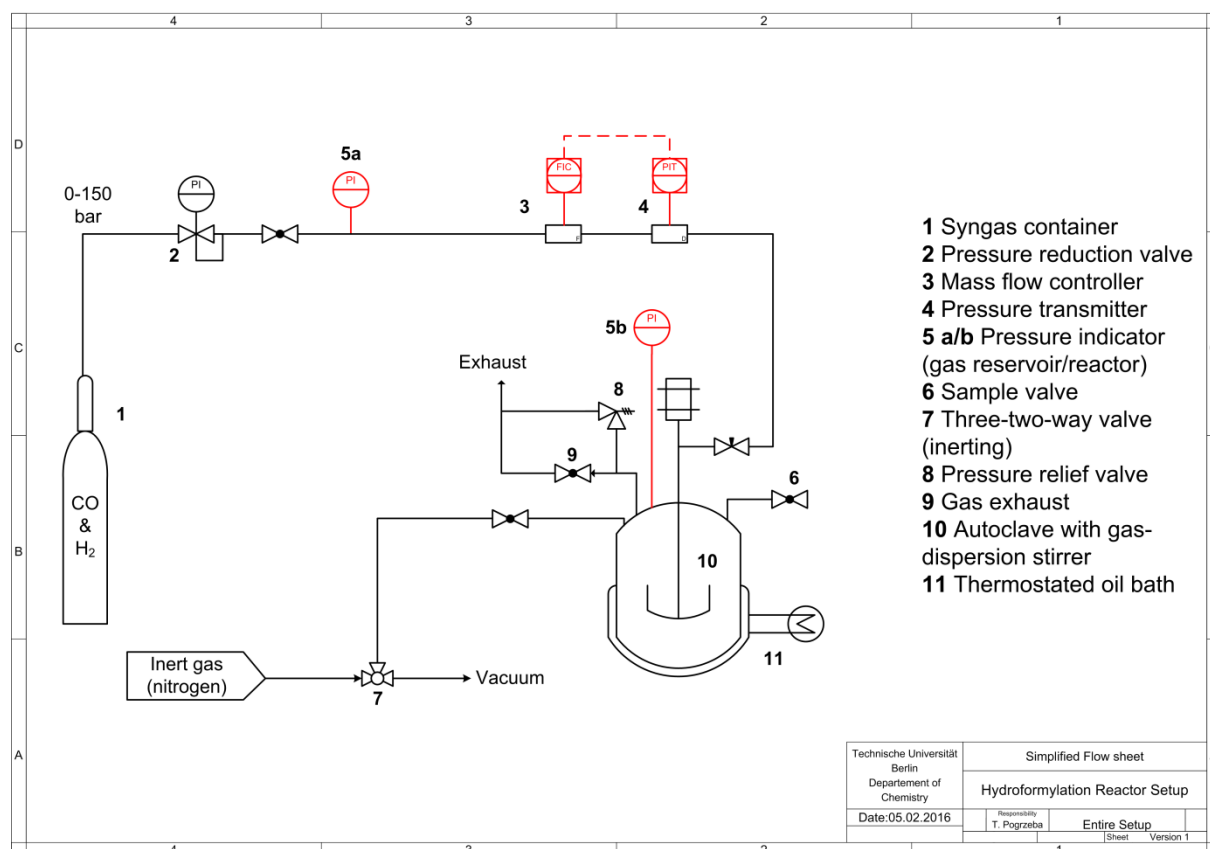


Figure 10. Setup of the hydroformylation reactor.

3.5 Gas chromatography and data evaluation

Reaction progress and selectivity of hydroformylation reactions were analyzed by gas chromatography on a Shimadzu model GC-2010, equipped with a RTX-5MS capillary column (30 m length, 0.25 mmID, 0.25 μ m film thickness), a flame ionization detection analyzer, and nitrogen as carrier gas. The temperature ramp of the applied GC method is shown in Table 1. A calibration of the setup was performed with the single substances in high-purity.

Table 1. Temperature ramp of the GC method.

Level	Heating rate [°C/min]	Starting temperature [°C]	Final temperature [°C]	Holding time [min]
0	-	100	-	7
1	10	100	145	2
2	5	145	207	-
3	50	207	330	30

The important parameters (conversion X , yield Y , selectivity S , and TOF) for the evaluation of experimental data were calculated as shown in Equation 2-5, where n is the amount of substance, 1-dodecene is the substrate and 1-tridecanal is the product.

$$X(t) = \frac{n_{t=0,Substrate} - n_{t,Substrate}}{n_{t=0,Substrate}} \quad (2)$$

$$Y(t) = \frac{n_{t,Product}}{n_{t=0,Substrate}} \quad (3)$$

$$S(n: iso) = \frac{n_{Product}}{n_{iso-Aldehydes}} \quad (4)$$

$$TOF_{Ald} = \frac{n_{t=0,Substrate} \cdot Y_{Ald}(t)}{n_{cat} \cdot t} \quad (5)$$

4 Results and discussion

Based on the example of the hydroformylation of 1-dodecene in a microemulsion system, a step-by-step approach is presented in the following on how to investigate these complex multiphase systems as reaction media and on how to transfer the results of lab-scale experiments into a continuously operated process in miniplant scale. Due to the preliminary studies of Rost⁴³ and Hamerla⁴⁴ on the hydroformylation of 1-dodecene in microemulsion systems, the experimental selection of the non-ionic surfactant for the reaction and the formulation of a basic kinetic model is not discussed in detail in this work. However, since these are important aspects for reaction engineering and process design, it will be part of the discussions on the influence of surfactants on reactions in microemulsion systems in section 4.4 and the formulation of a more detailed kinetic model in section 4.5.

4.1 Design of process

Microemulsions can be applied as smart switchable solvents for a homogeneously catalysed reaction. Regarding the economical feasibility of a chemical process in these media, the quantitative recycling of the applied catalyst is one critical aspect. Thus, in order to exploit the characteristics of microemulsion systems for chemical processes in aqueous media, information about the distribution of the catalyst complex in each of the single phases is of utmost importance. In a second step, the derived information can then be used for the design of a process that simultaneously meets the constraints for the reaction step and for the recycling step of the catalyst.

4.1.1 Catalyst distribution in microemulsion systems

The influence of different parameters/factors on the distribution of catalyst complexes in microemulsion systems has been analysed, e.g. type of ligand, temperature (phase behaviour), structure of surfactant, and chain length of surfactant (**PAPER 3+4**). For the quantitative recycling of the catalyst complex, it is essential to estimate or manipulate the interactions between the catalyst complex and the surfactant. Figure 11 illustrates the experimental results for the distribution of the rhodium catalyst in the 1-dodecene/water/non-ionic surfactant microemulsion system with different surfactants/amphiphiles and ligands. If one compares the results for short-chain amphiphiles like C₄E₁ and long-chained aliphatic surfactants, it becomes evident that the change in chain-length only influences the distribution of the Rhodium-SulfoXantphos (Rh-SX) catalyst in both the water-containing phases. This change in distribution is mainly due to the different polarity of the single phases of the corresponding (micro)emulsion systems. Since an amphiphile like C₄E₁ is rather non-polar, the amphiphile-rich middle phase is too non-polar to dissolve much of the hydrophilic catalyst

(only 33.7% of the overall catalyst amount). The drastic increase of the rhodium content in the middle phase with one additional ethoxylate group on the amphiphile (C_4E_2 , 82.5% catalyst in middle phase) confirms this assumption. For the long-chain surfactants nearly all of the rhodium catalyst is located in the middle phase. Apparently, the Rh-SX catalyst follows the surfactant into this phase due to its own surface active properties. It could be demonstrated by surface tension measurements that these properties belong to the water-soluble ligand SulfoXantphos (**PAPER 3**). Since the middle phase of a three-phase microemulsion system offers a very high interfacial area, the catalyst complex is mainly located in this phase as well and acts there as a small ionic surfactant at the interface. A change of the ethoxylation degree (EO) of the non-ionic surfactant thus does not lead to a further increase of catalyst concentration in the middle phase, since the EO does not significantly change the interfacial area in this phase at a constant surfactant concentration in the system. The rhodium amount in the organic phase was found to be in the order of 0.1 ppm for all investigated systems. A similar result was also found for the oil-in-water microemulsion (Winsor I system) using Marlipal 24/70, where over 99.99% of the catalyst was located in the aqueous microemulsion phase. On the contrary, in the water-in-oil microemulsion (Winsor II) the Rh-SX catalyst was equally distributed between both co-existing phases (**PAPER 4**).

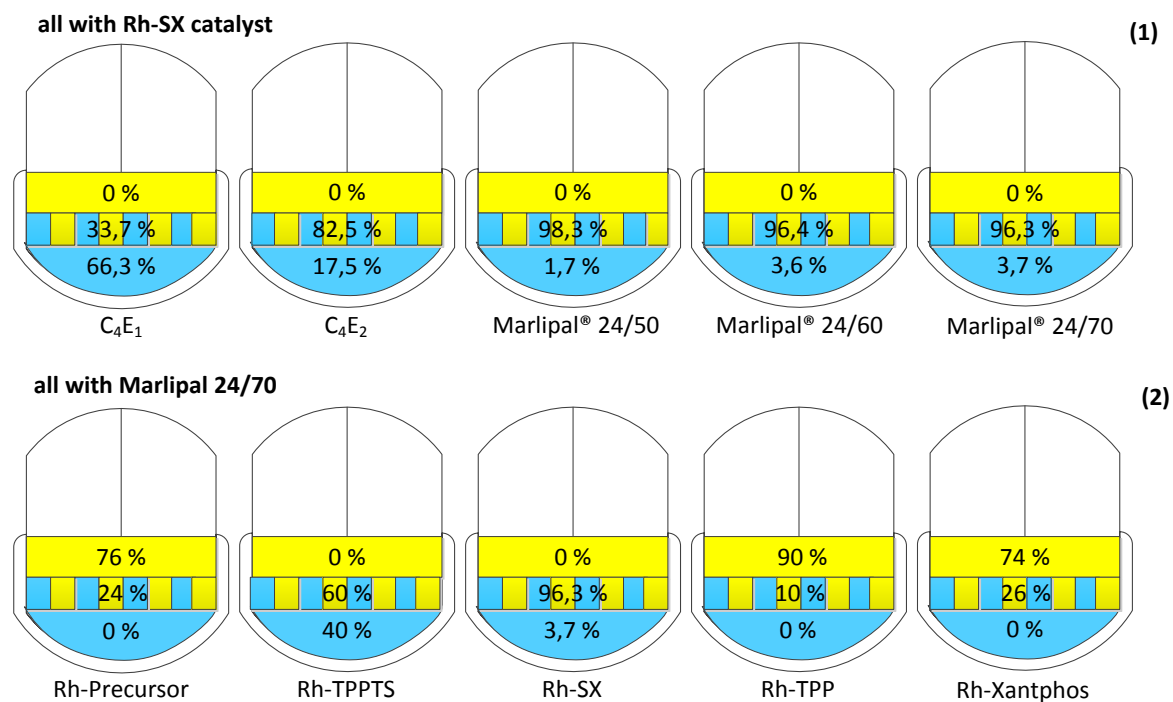


Figure 11. Distribution of the rhodium catalyst between the co-existing phases of the 1-dodecene/water/non-ionic surfactant microemulsion system: (1) With different surfactants/amphiphiles ($\alpha = 0.5$, $\gamma = 0.08$ ($\gamma = 0.2$ for C_4E_1 and C_4E_2) for Rh-SX, $n(\text{Rh}(\text{acac})(\text{CO})_2) = 0.05$ mmol, $n(\text{SX}) = 5$ equiv; (2) With different ligands ($\alpha = 0.5$, $\gamma = 0.08$ (Marlipal 24/70)), $n(\text{Rh}(\text{acac})(\text{CO})_2) = 0.05$ mmol, $n(\text{bidentate}) = 5$ equiv, $n(\text{monodentate}) = 10$ equiv). (**PAPER 4**)

The type of ligand has also a strong influence on the catalyst distribution in the microemulsion system (see Figure 11, (2)). It is obvious that the hydrophobicity of the ligand is crucial for the distribution. The water-soluble ligands TPPTS and SulfoXantphos lead to high concentrations of the catalyst complex in the middle phase and nearly no traces of catalyst in the organic phase. In comparison, the complexes bearing the hydrophobic ligands TPP and Xantphos (as well as the unmodified rhodium catalyst) are mainly located in the organic phase. Considering these results, changing the hydrophobicity of the applied ligand can be an important tool to adjust the catalyst distribution in the microemulsion system with respect to an optimal catalyst recycling, without changing the actual catalyst.

4.1.2 Process constraints and general concept

The task was to design a process with reliable catalyst recycling and minimized catalyst leaching into the product streams (zero leaching at best). With the information at hand regarding the catalyst distribution (Figure 11, Rh-SX), the polarity of the product n-tridecanal and possible side-products (always organic components), and the applied surfactant (Marlipal 24 series), the two following options were available for the phase separation step: Separation in a biphasic (Winsor I) system or in a three-phase (Winsor III) system. Besides catalyst leaching and long-term stability, another important issue in terms of optimal operation conditions and equipment sizing (costs) is that of the phase separation dynamics. Figure 12 exemplary shows the separation time of a microemulsion system as a function of temperature and phase behaviour. Obviously, the system needs the shortest time for separation in Winsor III state (between 1-2 min at best), which is a general characteristic of microemulsion systems. This information is of high importance for the design of process, because it

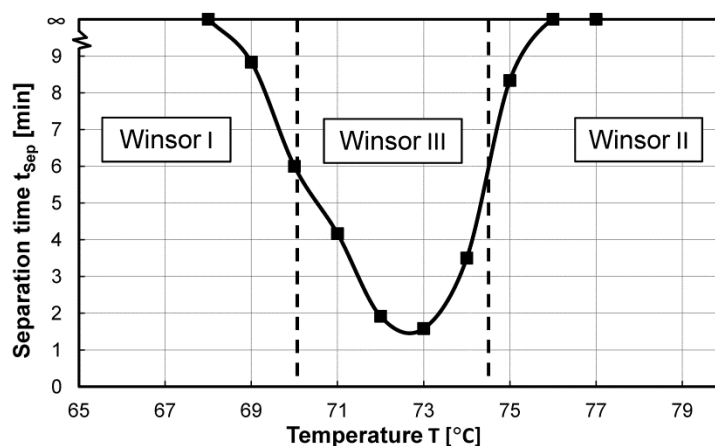


Figure 12. Temperature-dependent phase separation time of a microemulsion system consisting of 1-dodecene/water/Marlipal(24/70) ($\alpha = 0.5$, $\gamma = 0.08$, 1 wt-% Na_2SO_4 , $n(\text{Rh}(\text{acac})(\text{CO})_2) = 0.05$ mmol, $n(\text{SulfoXantphos}) = 5$ equiv). (**PAPER 4**)

means that the operation unit for the phase separation can be built smaller or the through-put can be increased. Thus the Winsor III state can usually be considered as the most beneficial state for the separation step from an economic point of view, if all the mentioned constraints regarding the distribution of catalyst, reactants and products are met as well.

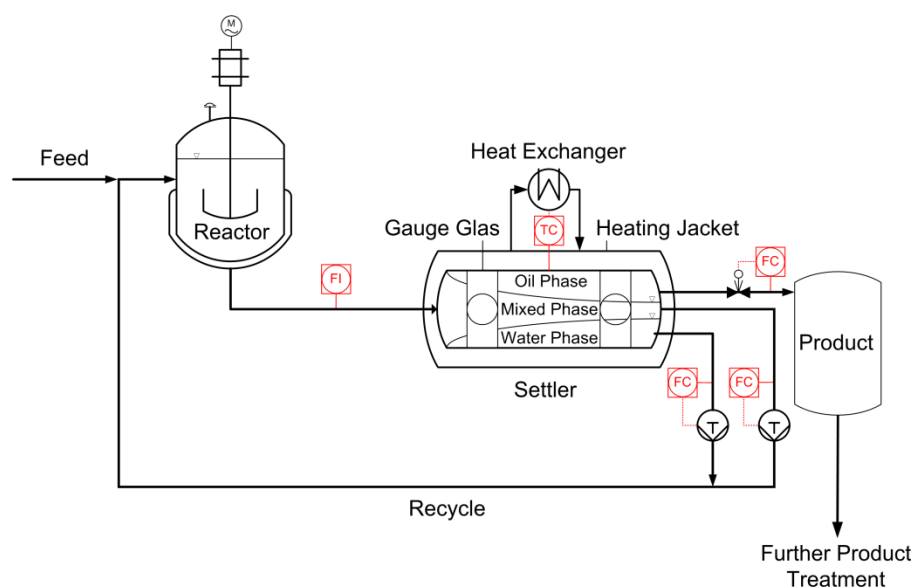


Figure 13. General mixer-settler setup for the separation of a microemulsion system with up to three liquid phases. (PAPER 4)

Based on the process constraints, a general process concept for the investigated hydroformylation reaction is depicted in Figure 13. The setup consists of two main operation units: a mixer (reactor) and a settler. The reactants 1-dodecene and syngas, the Rhodium-SulfoXantphos catalyst and the surfactant are constantly fed into the reactor where the hydroformylation is performed. Afterwards the reaction mixture is heated up or cooled down to the desired temperature for phase separation (Winsor III state) in the settler. Since the reaction product 1-tridecanal is mainly dissolved in the organic phase, the goals of the separation step are (1) to obtain a catalyst-free organic phase and (2) the recycling of the catalyst, water, and surfactant within the mixed phase and the water phase. If the phase separation is conducted optimally, it is possible to recycle all of the applied catalyst and surfactant in the process. In this case, only the substrate 1-dodecene has to be replenished in the same amount as organic phase is extracted from the settler during a continuous operation. As mentioned in section 2.2, the challenging aspect of operating a process with microemulsion systems is the shifting of the ideal separation region to different temperatures. Thus, in order to enable a continuously operated phase separation a detailed mapping of the phase behaviour and separation time has been performed, including all the components of the reaction system.

4.2 Phase separation analysis for multiphase settler design

The phase behaviour of the investigated microemulsion system consisting of 1-dodecene, water, and the technical grade surfactant Marlupal 24/70 has been recorded in several steps according to systematic guideline in **PAPER 2**. Figure 14 shows the fish-type diagram that was received from a prescreening in basic lab-scale experiments (described in section 3.2). It is of importance that the investigation of the phase behaviour is done with all the components of the reaction system, including the Rhodium-SulfoXantphos catalyst and sodium sulfate. The presence of these “additives” in the mixture leads to a considerable shift of the phase boundaries (~ 5 K) to lower temperatures in comparison to the simple microemulsion system of 1-dodecene, water and non-ionic surfactant. The use of sodium sulfate in the mixture is of high importance for a feasible phase separation and will be explained in the following section. For the investigated mixture, a surfactant concentration of 6-10 wt-% ($\gamma = 0.06 - 0.10$) and operating temperatures of 65-85 °C mark the three-phase area which allows for an optimal phase separation under process conditions. Furthermore, it was found that the α value should be in range of 0.4 to 0.6 because (1) a too low oil-to-water ratio leads to a small organic phase and thus increases the difficulty to remove it in the settler, (2) for $\alpha < 0.3$ foaming can be observed, and (3) for $\alpha > 0.6$ the switchability of the microemulsion system decreases since the three-phase area becomes smaller.

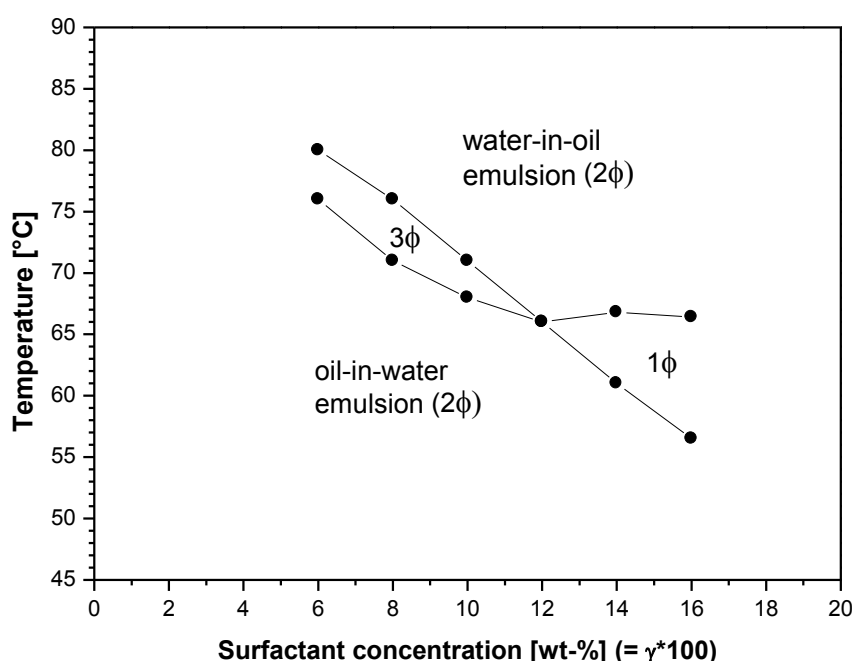


Figure 14. Phase diagram of 1-dodecene/water/Marlupal(24/70) ($\alpha = 0.5$, 1 wt-% Na_2SO_4 , $n(\text{Rh}(\text{acac})(\text{CO})_2) = 0.05$ mmol, $n(\text{SulfoXantphos}) = 4$ equiv). (**PAPER 9**)

4.2.1 Phase separation dynamics

In a temperature and pressure controlled glass reactor with a gas dispersion stirrer, the dynamics of phase separation of the reaction mixture have been investigated for different stirring speeds and pressures of argon and syngas (for experimental setup and results see **PAPER 2**) under process conditions. The change of the stirring speed from 700 to 1500 rounds per minute (rpm) showed no influence on phase separation dynamics. The pressure on the other hand did. The relative phase height of the organic phase after 20 min of separation differed by roughly 5% for argon pressures between 1 to 10 bar, with 1 bar resulting in the fastest separation and 10 bar in the slowest. However, the most decisive factor for the separation turned out to be the switch from argon to syngas (see Figure 15).

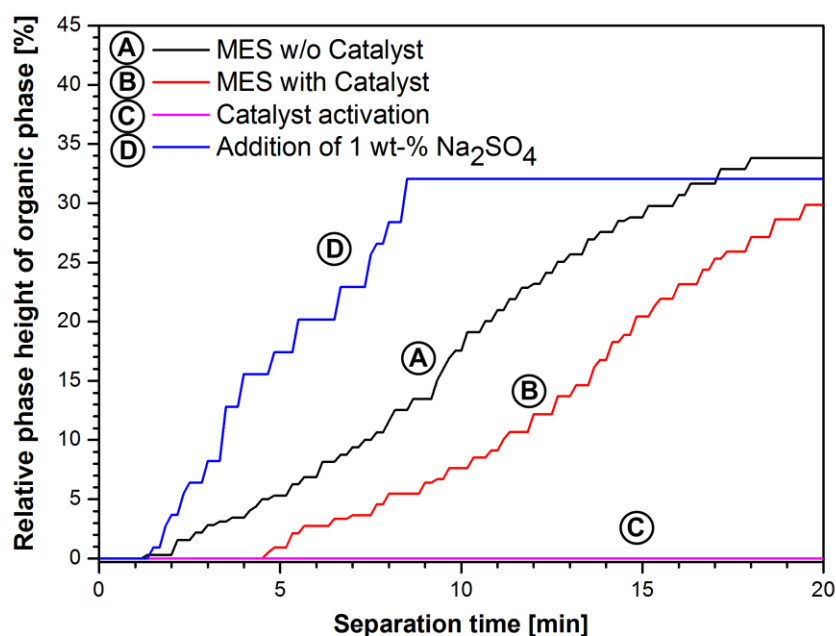


Figure 15. Relative height of organic (product) phase over separation time under process conditions. All experiments were performed at 85°C and 10 bar pressure of argon (for A+B) or 10 bar pressure of syngas (C+D). MES was formulated from 1-dodecene, water, and Marlupal 24/70 ($\alpha = 0.5$, $\gamma = 0.08$). Additionally, 0.05 mmol [Rh(acac)(CO)₂] and 0.2 mmol SulfoXantphos were added for B, C, and D. (**PAPER 9**)

It becomes apparent that the activation of the catalyst with syngas inhibits the separation of the microemulsion system drastically. The time for complete phase separation of the system increased from 18 min for the pure MES (Figure 15, A) to around 25 min after the addition of the catalyst (B) and in the end to over several hours after the addition of 10 bar syngas (C). Moreover, it has to be noted that a complete phase separation of the mixture under these conditions could not be

observed. The surface activity of the catalyst complex has been observed before during parameter studies in lab scale (see discussion in section 4.1.1 and **PAPER 1+3**). However, such a strong impact of the catalyst on the phase separation was not expected and has not been reported before in literature for other microemulsion systems. On the other hand, it explains the observations from the first continuous operation of the hydroformylation process (integrated reaction and separation) on miniplant scale, where almost no phase separation of the reaction mixture could be achieved (**PAPER 1**). To overcome this undesirable effect, the microemulsion system has been modified by the addition of 1.0 wt-% sodium sulfate. Since the catalyst complex acts as a small ionic surfactant, the adjustment of the ionic strength in the aqueous part of the reaction mixture mostly suppresses the emulsion-stabilizing ability of the catalyst by electrostatic screening. As a result, the addition of the electrolyte significantly improves the phase separation dynamics of the mixture to a separation time of about 8 min (see Figure 15, D). Subsequent to these findings, the effect of sodium sulfate on the reactivity and stability of the catalyst during hydroformylation has been investigated. As reported in **PAPER 9**, the stability of the catalyst remains unchanged with only a small decrease in reactivity compared to a reaction system without the additional electrolyte. This decrease can be explained with an increasing destabilization of the microemulsion system with higher amount of sodium sulfate, which leads to larger emulsion droplets and consequently to a smaller interface for reaction. Another explanation could be a decreased solubility of syngas in the microemulsion system with increasing concentration of sodium sulfate.

4.2.2 Full mapping of phase separation

Based on the results of the investigation on phase behaviour and separation dynamics of the applied microemulsion system, a full mapping of the phase behaviour was performed and presented in **PAPER 2**. Therefore, the lower and upper temperature boundaries of the three-phase area have been detected for mixtures with different concentrations of surfactant, organic educt, and product that lie in range of the expected process values. Figure 16 illustrates the results of the mapping: By using linear and quadratic functions the influence of the variables on the phase behaviour was modelled, generating a multidimensional region in which the operator is allowed to operate the process. It is apparent that due to the small temperature window of 4 K, the online tracking of the composition of the mixture entering the settler during the process is of high importance. Fast analysis methods like online Raman or Infrared spectrometry are the most feasible for this task, however they are not easy to implement into a process. Offline GC-measurements on the other hand are also feasible and much easier to handle, on condition that the process runs slow enough to allow for analysis times of 30 min or more (which is often required for microemulsion systems).

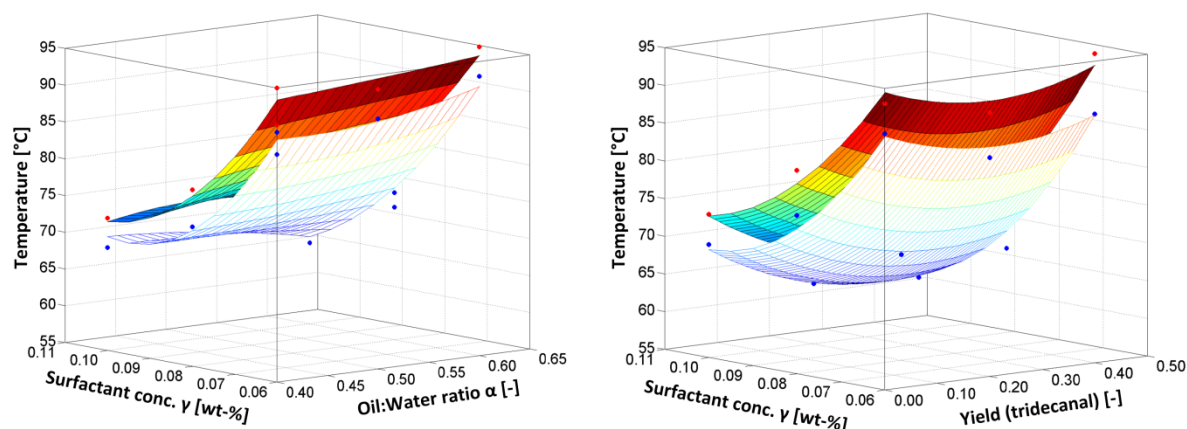


Figure 16. Phase boundaries of the 1-dodecene/water/Marlipal(24/70) microemulsion system (with 1 wt-% Na_2SO_4 , $n(\text{Rh}(\text{acac})(\text{CO})_2) = 0.05 \text{ mmol}$, $n(\text{SulfoXantphos}) = 4 \text{ equiv}$). Left: For varying fractions of α and γ at a constant degree of conversion ($X = 0.0\%$). Right: For varying X and γ at a constant oil-to-water ration ($\alpha = 0.5$). **(PAPER 2)**

4.2.3 Design of multiphase settler

With the information gained from the systematic analysis of the phase behaviour of the reaction system, a modular, multiphase settler was developed **(PAPER 2)**. The settler can be operated at up to 120 °C and up to 20 bar. The material is stainless steel of type EN steel no. k.h.s. DIN 1.4571, the sealings consist of PTFE and the gauge glasses are made of borosilicate. As already mentioned, particular requirements are imposed to the temperature control and design of the separation unit due to the narrow temperature window for the optimal phase separation in the Winsor III state. Therefore several Pt100 measurement devices are installed along the length of the settler and each segment of the settler is connected to a thermostat. Thus, the desired temperature can be controlled and observed in each segment separately. Figure 17 shows the final settler setup for the investigated hydroformylation process.

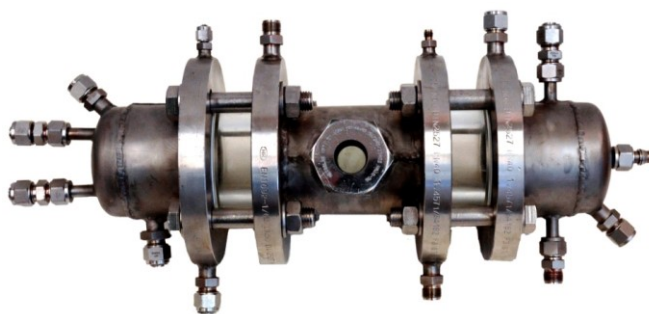


Figure 17. Picture of the modular, multiphase settler developed for the hydroformylation process: One module containing two mirror-inverted sight glasses (middle) and two modules with cylindrical glasses for the observation of the phase separation during the process. **(PAPER 2)**

4.3 From lab to miniplant

To enable the continuous process in the miniplant, a systematic optimization of the reaction parameters was performed in lab-scale semibatch experiments. Based on the preliminary studies of Rost⁴³ and Hamerla⁴⁴ on the rhodium-catalysed hydroformylation of 1-dodecene in microemulsion systems, and considering the results from the phase separation experiments discussed in section 4.2 in this work, the reaction system consisted of the following components: 120 mmol 1-dodecene, 20 g water ($\alpha = 0.5$), Marlipal 24/70 as surfactant, 1 wt-% sodium sulfate, 0.05 mmol Rh(acac)(CO)₂, and 0.2 mmol SulfoXantphos.

4.3.1 Parameter studies

The following parameters had to be assigned for the continuous process: temperature, syngas pressure, and surfactant concentration. In **PAPER 1** the experimental results for pressure and temperature variation are presented, which originate from the preliminary work of Hamerla⁴⁴. It was found that the reaction can already be performed at very low syngas pressures with a minimum pressure of 3 bar. An increase in pressure does not lead to a significant increase in reaction rate. After 4 hours reaction time at 3 bar syngas the observed yield of aldehyde was 16%, whereas for 30 bar syngas 19.3% product could be found. Based on the experimental results and considering safety and economy of the overall process in the miniplant, an operating pressure of 15 bar syngas was finally chosen. The variation of reaction temperature showed, that an increase in temperature generally leads to an increase in the reaction rate of the hydroformylation. The best reaction results could be observed for a temperature of 95 °C: an aldehyde yield of 31.3% and a high n:iso selectivity of 98:2 were obtained after 4 hours reaction time. The investigation on the effect of temperature was then further extended with respect to the catalyst activity (**PAPER 8**). It was found that the reaction rate increases exponentially, indicating a simple Arrhenius behaviour. As illustrated in Figure 18, the TOF of the catalyst could be raised from 50 h⁻¹ at 68 °C to 380 h⁻¹ at 110 °C with a constantly high n:iso selectivity of 99:1 and 98:2. An activation energy of 59 kJ/mol could be calculated for the reaction. However, an increase of the reaction temperature beyond 100 °C turned out to be not beneficial for the process due to decreased long-term stability of the catalyst and increasing rate of side-reaction, e.g. hydrogenation and isomerisation. As consequence, a reaction temperature of 95 °C was chosen for the process. At last, the surfactant concentration was set to 8 wt-% ($\gamma = 0.08$) and underwent no further optimization because it was more or less dictated by the process constraints for the phase separation in the settler. Since the concentration of surfactant cannot be changed between reactor outlet and settler inlet during the operation of the process, it can only be varied between 6 and 10 wt-% in general to ensure a feasible phase separation (see Figure 14). In

conclusion, a surfactant concentration of 8 wt-% was the best choice for the continuous process because it offers the most stable operation point regarding the robustness of the phase separation against possible fluctuations in concentration.

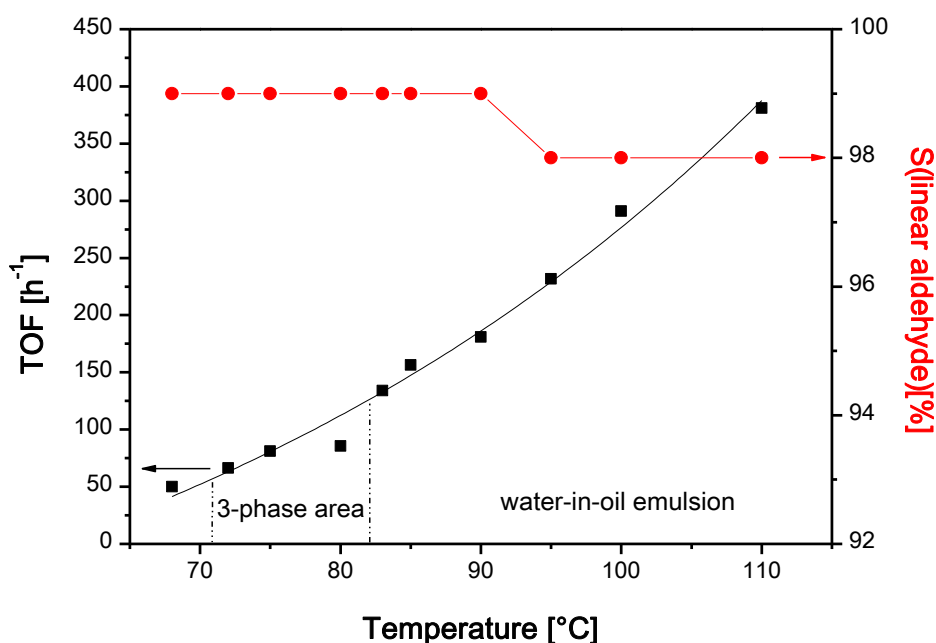


Figure 18. Effect of temperature on hydroformylation reaction. Test conditions: 0.05 mmol Rh(acac)(CO)₂, 0.2 mmol SulfoXantphos, 120 mmol 1-dodecene, water ($\alpha = 0.5$), $\gamma = 0.08$ (Marlipal 24/70), 1 wt-% Na₂SO₄, V_R = 50 mL, p = 15 bar, stirring speed = 1200 rpm, t_R = 4 h. Statistic deviation of results: ± 3 %. (**PAPER 8**)

4.3.2 Miniplant operation

The proof of concept for the continuously operated rhodium-catalysed hydroformylation of long-chain alkenes in microemulsion systems was performed within a technical miniplant system. Several long-term miniplant operations were performed in order to test the feasibility of the reaction system and the stability of the process. The results can be found in **PAPER 1**, **PAPER 7**, and **PAPER 8**, respectively. Figure 19 shows the trajectories for the conversion of 1-dodecene and yield of tridecanal from a miniplant campaign with over 100 hours in continuous operation. After feeding and starting up the plant, hydroformylation was successfully initiated (operation hour 12). The plant was operated in full recycle-mode from then on to quickly increase the yield of product. At operation hour 35, the continuous operation was started with the introduction of fresh substrate and extraction of the maintained organic phase from the settler. The product yield stabilized at a value of 39% (n:iso = 99:1) which could be sustained during steady-state operation for more than 50 hours. Most notably, the reaction results are in good agreement to the findings from lab-scale experiments.

The continuous phase separation was successfully accomplished, leading to a nearly pure organic phase (substrate and product content of 99.8%) and very low rhodium leaching into the product-containing phase (lower than 0.1 ppm). The remaining 0.2% content of the organic phase was mainly surfactant; since a technical grade surfactant was applied for the process, a large number of surfactants with different chain-length are always present in the mixture. The shorter chained surfactants (ethoxylation degrees of 4 and 5) are more lipophilic and thus can be dissolved in the organic phase at the applied separation temperature in the settler. Due to this “surfactant leaching” into the product phase, the introduction of fresh surfactant to the reactor becomes necessary during the process operation. In case of a purer product phase would be required for a certain application, a purification of the product phase, e.g. by organophilic nanofiltration, could be a feasible approach. All aspects considered, the miniplant operation proved the applicability of microemulsion systems as switchable reaction media in a chemical process. In **PAPER 7** the results of a more than 200 hour long miniplant campaign are presented. The aim of this campaign was to adjust a stable continuous operation, change the working point, and investigate the effect of disturbances on the process. The successful performance of the process under these different conditions proved again the feasibility of the process concept and also the stability of the overall process.

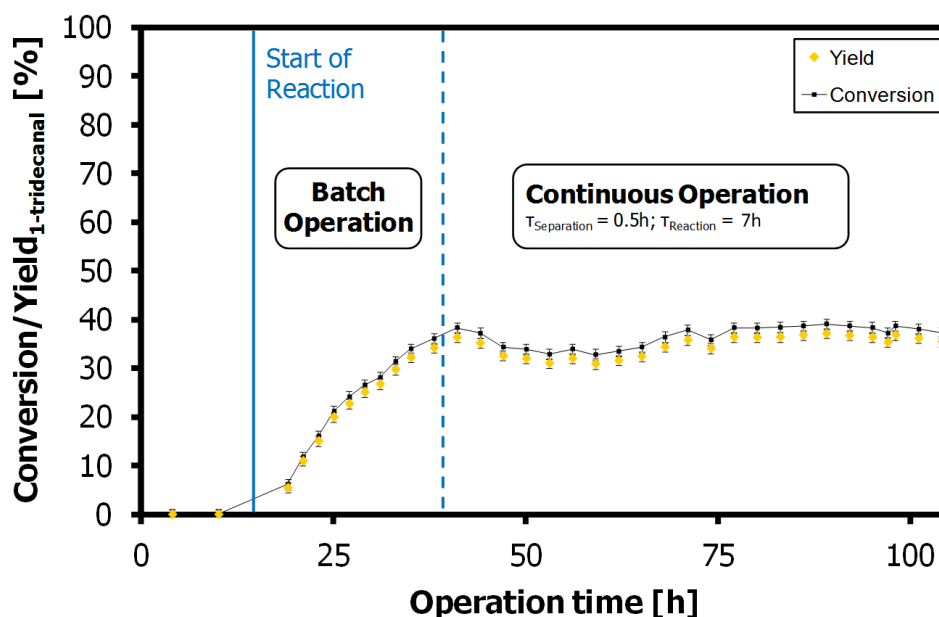


Figure 19. Miniplant operation results. Conversion of 1-dodecene and yield of tridecanal over the operation time. Reaction residence time indicates equivalent time of a batch experiment. Operation conditions: 0.04 mol% Rh(acac)(CO)₂, 0.2 mol% SulfoXantphos, $\alpha = 0.5$, $\gamma = 0.08$ (Marlipal 24/70), 1 wt-% Na₂SO₄, T = 95 °C, p = 15 bar(g). (**PAPER 8**)

4.4 Influence of non-ionic surfactants on catalysis in microemulsion systems

The switchability of microemulsion systems offers many interesting options for chemical processes in aqueous media with industrial relevance. However, these complex multiphase systems require a profound knowledge of the influence of a variety of system parameters regarding reaction and separation, as already partly discussed in the previous sections of this thesis. In particular, the applied surfactant can have a strong impact on the results of a catalytic reaction. A systematic investigation on the influence of non-ionic surfactants on catalytic reactions in microemulsions systems is presented in **PAPER 9** on the example of the rhodium-catalysed hydroformylation. An important finding to understand the role of surfactant during catalysis was that the phase behaviour of microemulsion systems has no major impact on the catalytic reaction. As illustrated in Figure 18, the reaction rate follows the increase of temperature with no abrupt alteration that would indicate a major change of mass transfer conditions for the reaction. Consequently, it is likely to assume that the hydroformylation of long-chain alkenes in microemulsion systems is a kinetically controlled two-phase reaction. Since the applied Rhodium-Sulfoxantphos catalyst is surface active and thus mainly located at the oil-water interface, the reaction should take place at the interface as well (see Figure 20). With that, the role of the surfactant for the catalytic reaction is of utmost importance. In its function as emulsifier it determines the stability of the microemulsions system and the local concentrations of the reactants at the oil-water interface. In addition, it also provides the interfacial area for the reaction. Since the surfactant and catalyst are in immediate vicinity to each other at the interface, electronic interactions between them are possible that might hinder the catalytic reaction. However, these interactions are not very predictable because they depend on the chemical structure of both the surfactant and the catalyst complex. Thus the selection of an appropriate surfactant type (e.g. aliphatic, aromatic, or ionic) for a certain reaction can only be based on experimental results.

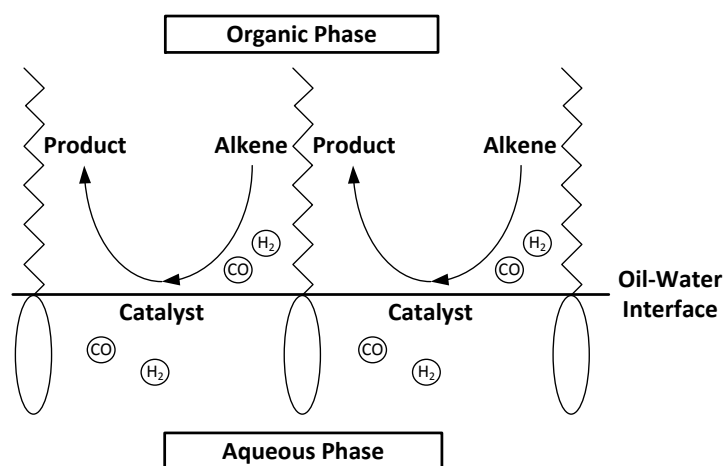


Figure 20. Schematic illustration of two-phase catalysis in microemulsion systems on the example of the hydroformylation reaction. (**PAPER 9**)

4.4.1 Degree of ethoxylation

While the selection of a surfactant type (anionic, cationic, non-ionic) for a chemical reaction is mainly based on the compatibility of the surfactant with the reaction system, the optimal ethoxylation degree (EO) of the surfactant is determined by the temperature of the process. In general, a higher EO number results in a higher temperature required for the surfactant to work efficiently as emulsifier. As a result, long chained surfactants work better at higher temperatures than short chained surfactants and vice versa. A good indicator for the working range of a specific surfactant is the position of the fish body of the resulting microemulsion system in the phase diagram. The effect of the EO on the rate of a reaction has been elaborately discussed in **PAPER 9** and is reflected in Table 2 on the example of the rhodium-catalysed hydroformylation of 1-dodecene.

Table 2. Experimental results for the hydroformylation of 1-dodecene with different surfactants at constant temperature ^a. (**PAPER 9**)

no.	surfactant	conversion 1-dodecene [%]	yield (linear aldehyde) [%]	n:iso selectivity
1	Marlipal 24/50	28	25	99:1
2	Marlipal 24/60	25	24	98:2
3	Marlipal 24/70	34	29	98:2
4	Marlipal 24/80	38	33	98:2
5	Marlipal 24/90	43	38	98:2
6	Marlophen NP5 ^b	4	4	99:1
7	Marlophen NP6 ^b	8	6	99:1
8	Marlophen NP7 ^b	10	9	98:2
9	Marlophen NP9 ^b	15	13	98:2

^aReaction conditions [1-5]: 0.04 mol-% Rh(acac)(CO)₂, 0.16 mol-% SulfoXantphos, 120 mmol 1-dodecene, water ($\alpha = 0.5$), $\gamma = 0.08$, 1 wt-% Na₂SO₄, V_R = 50 mL, T = 95 °C, p = 15 bar, stirring speed = 1200 rpm, t_R = 4 h. Statistic deviation of results: ± 3 %.

^bReaction conditions [6-9]: 0.05 mol-% Rh(acac)(CO)₂, 0.25 mol-% SulfoXantphos, 180 mmol 1-dodecene, water ($\alpha = 0.88$), $\gamma = 0.10$, V_R = 50 mL, T = 110 °C, p = 40 bar, stirring speed = 1000 rpm, t_R = 4 h. *Data extracted from ⁴⁵.

Based on the experimental data depicted in Table 2 it is evident that the surfactant with the highest EO, Marlipal 24/90, is clearly superior at the selected reaction temperature of 95 °C. In addition, a linear increase of the conversion of 1-dodecene with an increasing EO is indicated. However, this trend can be reversed if the reaction temperature is decreased: Already at 80 °C the reaction performs best with Marlipal 24/50 and worst with Marlipal 24/90, underlining the precise tunability of microemulsion systems for a certain application by the selection of the surfactant. As expected, this characteristic is reflected for the surfactants from the Marlophen NP series. The noticeable

inferior reaction performance for these surfactants is most probably due to their different chemical structure. The aromatic ring of the surfactant interacts with the catalyst complex and hinders the catalytic reaction considerably¹⁷. With that in mind, these results are also a good example of a poor surfactant selection for the investigated reaction, as discussed in the previous section.

4.4.2 Effect of surfactant concentration

Considering the biphasic character of microemulsion systems at low surfactant concentrations, an increase of the surfactant concentration generally means a larger interfacial area for a reaction and thus a higher potential reaction rate. Figure 21 shows the dependency of the reaction rate on the surfactant concentration for the rhodium-catalysed hydroformylation. At first, the reaction does not occur if no surfactant is added to the mixture. Beyond that, the reaction rate clearly increases with the surfactant concentration. The product yield after 4 hours reaction time increased from roughly 4% with 1 wt-% surfactant in the mixture to 53% with 30 wt-% surfactant. However, in case of the investigated reaction the increase in reaction rate cannot be solely addressed to the larger interfacial area. Since the catalyst complex is surface active, it should be mainly located at the oil-water interface even at low surfactant concentrations. Thus, this finding could be explained by a change in

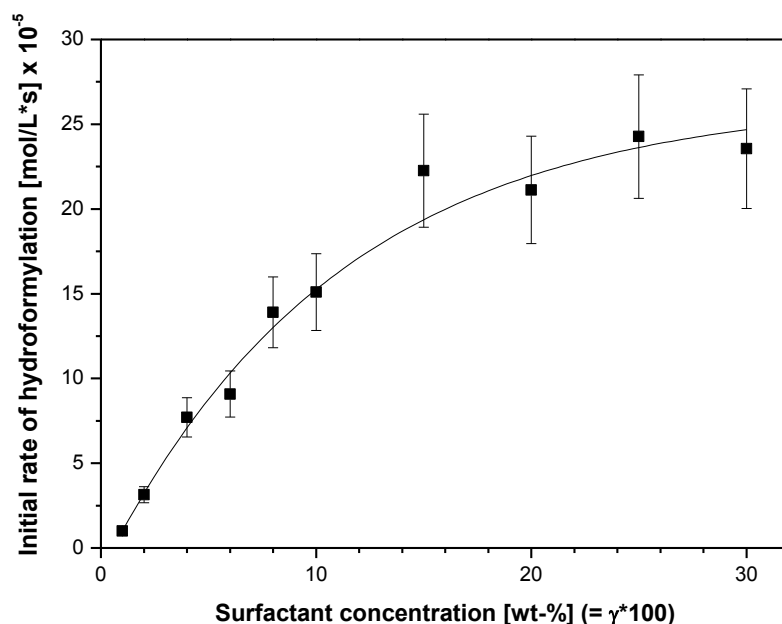


Figure 21. Effect of surfactant concentration on the reaction rate of hydroformylation. Test conditions: 0.05 mmol Rh(acac)(CO)₂, 0.2 mmol SulfoXantphos, 120 mmol 1-dodecene, water ($\alpha = 0.5$), Marlipal 24/70, 1 wt-% Na₂SO₄, V_R = 50 mL, T = 95 °C, p = 15 bar, stirring speed = 1200 rpm. Initial rates were calculated from syngas consumption. Statistic deviation of results: ± 15 %. **(PAPER 9)**

the local catalyst concentration at the oil-water interface. If the interfacial area of the reaction system (which corresponds to the volume of the emulsion phase) is increased, the catalyst becomes more diluted at the interface within the emulsion phase. In consequence, the local catalyst concentration in the emulsion phase should decrease. This affects the pre-equilibrium of the catalyst complex (see Figure 5) and thus the reactivity in hydroformylation. A decrease of the local catalyst concentration should lead to a higher amount of active monomeric species and thus to a higher reaction rate.

4.5 Reaction kinetics of hydroformylation

In order to achieve a precise kinetic model to describe the rhodium-catalysed hydroformylation in microemulsion systems in a continuous process, a detailed kinetic study of the reaction has been performed and presented in **PAPER 10**. One of the important questions in this work was to find and understand the important parameters for the hydroformylation reaction kinetics in microemulsion systems that are different from the kinetics in homogeneous media. However, an important requirement to clearly isolate the effect of the reaction parameters on kinetics in these complex multiphase systems had been to initially gain a profound knowledge about the role of surfactants during the catalytic reaction (see section 4.4 and **PAPER 9**). To study the kinetics of the reaction, the effects of 1-dodecene concentration, catalyst concentration, ligand:Rh ratio, and syngas pressure on the initial rate of hydroformylation have been investigated. The investigation was performed under the following standard conditions: 2.4 mol/L (120 mmol) 1-dodecene, 20 g water ($\alpha = 0.5$), 3.5 g Marlipal 24/70 ($\gamma = 0.08$), 1 wt-% Na_2SO_4 , 1.0×10^{-3} mol/L (0.05 mmol) catalyst and SulfoXantphos:Rh ratio = 4:1 (P:Rh ratio = 8:1), temperature of 95 °C, and syngas pressure of 15 bar.

For the concentration of 1-dodecene, the reaction rate was found to increase linearly indicating a first order dependence. Due to the surface activity of the applied Rhodium-SulfoXantphos catalyst, the hydroformylation takes mainly place at the oil-water interface in the microemulsion system. Since 1-dodecene is not a strongly coordinating olefin, higher concentrations at the interface are necessary to generate more of the olefin coordinated Rhodium complex (Figure 5, species 3) and thus will lead to an enhancement in reaction rate. The effect of syngas pressure has been investigated in range of 1 to 40 bar while the other reaction parameters were kept constant. A complex dependency of the reaction rate on the pressure was found, as illustrated in Figure 22. This reaction behaviour is very characteristic for hydroformylation reaction and mainly due to the increase of the partial pressure of CO. The reaction is generally driven by the concentrations of CO and H_2 in the reaction mixture, but also inhibited by side reactions leading to the formation of inactive dicarbonyl rhodium species with increasing CO partial pressure (Figure 5, species 6b). As a

consequence, the apparent reaction order of CO changes with the partial pressure: It starts at a positive value at low CO concentrations in solution, passes zero, and then has a negative value for higher CO concentrations. The effect of the H_2 partial pressure on the hydroformylation reaction is usually of positive order and can be of zero order at higher pressures.

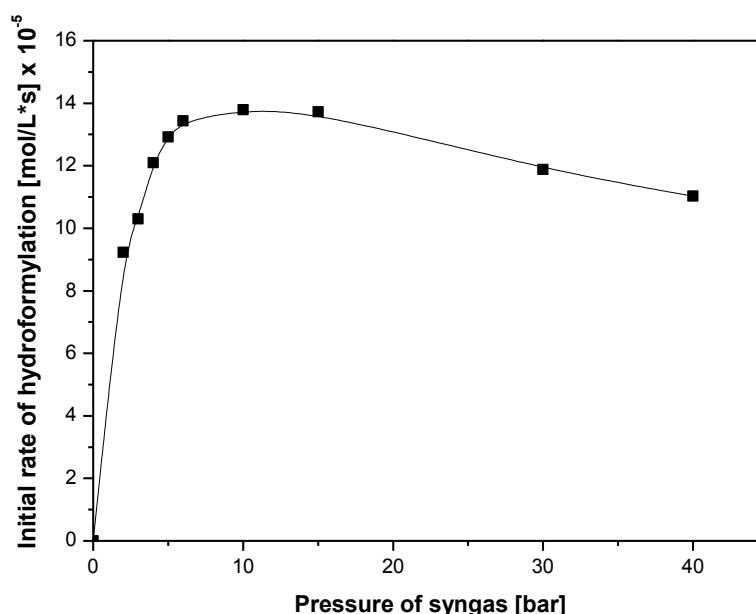


Figure 22. Effect of syngas pressure on the rate of hydroformylation. Test conditions: 0.05 mmol $\text{Rh}(\text{acac})(\text{CO})_2$, 0.2 mmol SulfoXantphos, 120 mmol 1-dodecene, water ($\alpha = 0.5$), Marlupal 24/70 ($\gamma = 0.08$), 1 wt-% Na_2SO_4 , $V_R = 50$ mL, $T = 95$ °C, stirring speed = 1200 rpm. Initial rates were calculated from syngas consumption. Statistic deviation of results: ± 15 %. **(PAPER 10)**

4.5.1 Catalyst concentration

The effect of catalyst concentration on the rate of hydroformylation has been investigated at two different temperatures and, in general, an increase of the rate with increasing catalyst concentration could be found (see Figure 23). However, at low catalyst concentrations the increase of the rate was found to be significantly higher than at high concentrations, which indicates that not all Rh atoms are working as catalyst at the same TOF dependent on the catalyst loading in the reaction mixture. Most probably this reaction behaviour is due to the two pre-equilibria of the active Rhodium-SulfoXantphos complex (Figure 5, species 1a) with the corresponding dimeric Rh species (1c) and the unmodified Rh species (1b). At low catalyst concentrations the formation of the unmodified species could be enhanced due to the relatively low concentration of ligand compared to the concentration of CO in solution. At high catalyst concentrations the formation of the dimeric species should be increased, leading to a partial deactivation of the applied catalyst complex. Interestingly, this finding

fits very well to the experimental results from Figure 21 where the effect of surfactant concentration on the reaction rate has been illustrated. It is evident, that in case of the investigated reaction both experiments (the change of catalyst concentration and of surfactant concentration) showed the same impact on the reactivity of the catalyst. In conclusions, this confirms the proposition from section 4.4 that the hydroformylation reaction in microemulsion systems takes mainly place at the oil-water interface. As a result, the local concentrations of the reactants and the catalyst are of high importance for the rate and selectivity of the reaction.

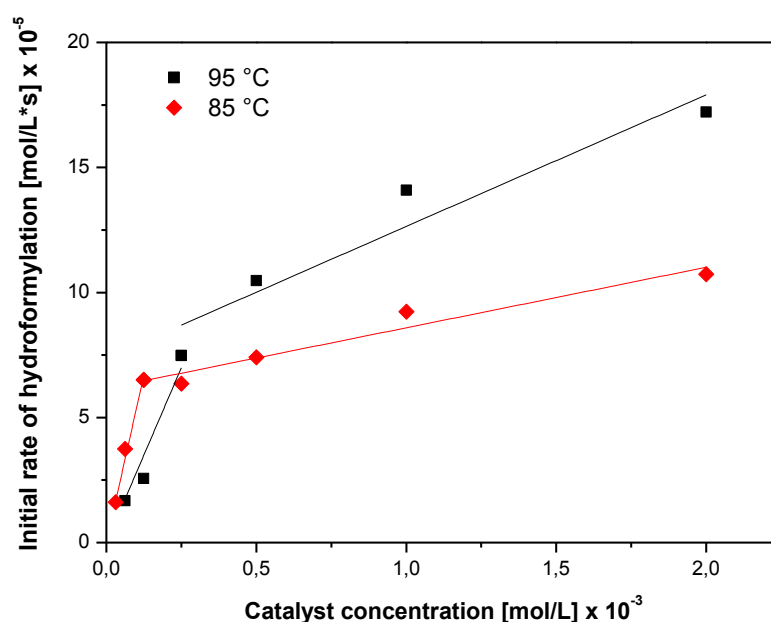


Figure 23. Effect of catalyst concentration on the rate of hydroformylation. Test conditions: SulfoXantphos:Rhodium ratio = 4:1 (P:Rh ratio = 8:1), 120 mmol 1-dodecene, water ($\alpha = 0.5$), Marlipal 24/70 ($\gamma = 0.08$), 1 wt-% Na_2SO_4 , $V_R = 50$ mL, $p = 15$ bar, stirring speed = 1200 rpm. Initial rates were calculated from syngas consumption. Statistic deviation of results: ± 15 %. (**PAPER 10**)

4.5.2 Formulation of an adapted kinetic model

To receive a model description for the rhodium-catalysed hydroformylation of 1-dodecene in microemulsion systems including the unique influences of the regarded multiphase system on the reaction, a parameter estimation using according dynamic experimental data has been performed (**PAPER 10**). The applied kinetic model (eq. 6) is based on the works of Kiedorf et al.⁴⁶ who originally derived the model from hydroformylation experiments in homogeneous thermomorphic solvent systems using a Rhodium-BiPhePhos catalyst. In order to adapt this basic model to the hydroformylation in microemulsion systems, a rate-based correction factor has been implemented which accounts for the effect of the surfactant concentration on the reaction rate (eq. 7). As it

appears from the kinetic experiments depicted in Figure 21, this factor is very crucial to express the special influence of the surfactant and the local catalyst concentration at the oil-water interface on the activity and selectivity of the catalyst. As a result, the modified kinetic model is able to describe the variation of temperature, pressure, and (in some degree) the surfactant concentration and ligand:metal ratio (see Table 3). Unfortunately, an even better description of the reaction kinetics including the effect of the catalyst pre-equilibria on the reaction was not possible using this approach, because the exact concentration of active catalyst during a hydroformylation experiment remains unknown and can only be estimated. Thus the parameter estimation is not able to predict more accurate the equilibrium constants for the pre-equilibria. However, regardless the slight impreciseness of the model it is still of high value for the better comprehension of the reaction progress during a process. In particular, with the herein investigated mixer-settler process in mind it allows for an implementation of the recycle streams into the kinetic model and therefore offers the possibility to easier find optimal operating conditions.

$$Rate_{Hyfo} = \frac{[Rh(CO)_2H]}{1 + K_{eq,cat,a} \cdot [CO] + K_{eq,cat,b} \cdot \frac{[CO]}{[H_2]}} \cdot \frac{k_{Hyfo}^{ref} \exp\left(\frac{-E_{A,Hyfo}}{R} \cdot \left(\frac{1}{T} - \frac{1}{T_{ref}}\right)\right) [CO][H_2][alkene]}{1 + K_{a,Hyfo} \cdot [alkene] + K_{b,Hyfo} \cdot [CO][alkene] + K_{a,Hyfo} \cdot [CO][H_2][alkene]} \quad (6)$$

$$Rate^*_{Hyfo} = \frac{K_{eq,Lig} \cdot [Surfactant] \cdot K_{eq,Surfactant}}{1 + [SX]^{n_{eq,Lig}}_{Hyfo}} \cdot Rate_{Hyfo} \quad (7)$$

$$k_{Hyfo}^{ref,**} = K_{eq,Lig} \cdot K_{eq,Surfactant} \cdot k_{Hyfo}^{ref} \quad (8)$$

Table 3. Comparison of the estimation results for the basic kinetic model (eq. 6) and the adapted model (eq. 7). The relative deviation between model and experimental data for each component in the regarded set of experiments is depicted. Additionally, the estimated parameters are listed for the adapted model. (PAPER 10)

Component	Model 1 (eq. 6) Variation of T, p	Model 2 (eq. 7) Variation of T, p, [SX], [Surfactant]	
1-dodecene	1.63%	4.52%	
iso-dodecene	0.48%	2.73%	
iso-aldehyde	< 0.01%	0.54%	
dodecane	0.18%	0.21%	
tridecanal	1.43%	1.42%	
<div> <div> Hydroformylation $k_{Hyfo,a}^{ref,**} = 7.895 \cdot 10^3 \frac{L^3}{g_{cat} \cdot min \cdot mol^2}$ $E_{A,Hyfo,a} = 120844 \frac{J}{mol}$ $n_{Hyfo,a}^{eq,Lig} = 0.002$ $k_{Hyfo,b}^{ref,**} = 4.885 \cdot 10^7 \frac{L^3}{g_{cat} \cdot min \cdot mol^2}$ $E_{A,Hyfo,b} = 59000 \frac{J}{mol}$ $n_{Hyfo,b}^{eq,Lig} = 0.854$ $k_{Hyfo,b}^{ref,**} = 6.650 \cdot 10^{-5} \frac{L^3}{g_{cat} \cdot min \cdot mol^2}$ $E_{A,Hyfo,b} = 59000 \frac{J}{mol}$ $n_{Hyfo,c}^{eq,Lig} = 0.999$ $K_{a,Hyfo} = 4.816 \cdot 10^{-3} \frac{L}{mol}$ $K_{b,Hyfo} = 1.826 \cdot 10^{-2} \frac{L}{mol}$ $K_{c,Hyfo} = 5.908 \cdot 10^4 \frac{L}{mol}$ </div> <div> Hydrogenation $k_{Hyd,a}^{ref,**} = 46.486 \frac{L^2}{g_{cat} \cdot min \cdot mol}$ $E_{A,Hyd,a} = 102260 \frac{J}{mol}$ $n_{Hyfo,b}^{eq,Lig} = 0.002$ $k_{Hyd,b}^{ref,**} = 3.568 \cdot 10^4 \frac{L^2}{g_{cat} \cdot min \cdot mol}$ $E_{A,Hyd,b} = 76105 \frac{J}{mol}$ $n_{Hyfo,b}^{eq,Lig} = 0.999$ $K_{a,Hyd} = 3.311 \frac{L}{mol}$ $K_{b,Hyd} = 0.368 \frac{L}{mol}$ $K_{c,Hyd} = 2.916 \cdot 10^4 \frac{L}{mol}$ </div> <div> Catalyst Equilibrium $K_{eq,cat,a} = 8505.973 \frac{L}{mol}$ $K_{eq,cat,b} = 1$ Isomerization $k_{Iso}^{ref,**} = 4.878 \cdot 10^4 \frac{L}{g_{cat} min}$ $E_{A,Iso} = 136891 \frac{J}{mol}$ $n_{Hyfo,b}^{eq,Lig} = 3.668$ $\Delta G_{R,Iso} = 1099.999 \frac{J}{mol}$ $K_{a,Iso} = 132.859 \frac{L}{mol}$ $K_{b,Iso} = 8.134 \cdot 10^{-3} \frac{L}{mol}$ </div> </div>			

4.6 Catalytic reaction in surfactant-free multiphase emulsions

So-called surfactant-free multiphase emulsions (further denoted as SFME) are switchable solvent systems that provide the possibility to create new chemical processes in aqueous media. Same as for microemulsion systems, processes with SFMEs are based on temperature-induced phase transition. However, they offer the advantage of an easily handled and removable additive instead of usually highly viscous and high-boiling long-chain surfactants. Since this is a rather new technology, first experimental attempts had the goal to gain more knowledge about the application of these multiphase systems as reaction media. Therefore, the systems were tested for two catalytic reactions, namely the rhodium-catalysed hydroformylation of 1-dodecene and the Suzuki coupling reaction of 1-chloro-2-nitrobenzen and 4-chlorobenzenboronic acid. The applied reaction systems consisted of organic component (reactant and solvent), aqueous catalyst solution, and diethylene glycol butyl ether (denoted as C4E2). All the experimental results are reported in **PAPER 5**, in the following only the results for the hydroformylation will be discussed exemplarily.

The phase behaviour of SFMEs is slightly different from the one of microemulsion systems, since only two different states can be observed: a biphasic oil-in-water emulsion at low amphiphile concentrations and/or temperatures, and a three-phase area at high temperatures featuring multiple emulsions, where the middle phase is dispersed inside the dispersed aqueous phase. Interestingly, the phase behaviour of the applied SFME has no effect on the reaction rate of the hydroformylation, which is similar to the findings for microemulsion systems (see section 4.4). A simple Arrhenius approach is sufficient to describe the temperature dependency of the reaction, yielding in a calculated activation energy of 53.9 kJ/mol for the hydroformylation compared to the 59 kJ/mol that were calculated for microemulsion systems. The effect of amphiphile concentration on the other hand was found to be more complex. In general, an increased amount of C4E2 in the mixture (and by that a larger emulsion phase) benefits the reaction. However, for concentrations above $\gamma = 0.2$ catalyst decomposition was observed after several hours of experiment. A possible explanation for this could be that the equilibrium of the Rhodium-SulfoXantphos complex gets misaligned if the amount of C4E2 reaches a certain level. The short-chain amphiphile replaces SulfoXantphos as ligand, resulting in a very instable complex which in consequence should lead to a facilitated oxidation of rhodium by dissolved oxygen or the formation of hardly soluble rhodium clusters. This behaviour could be diminished by an increase of the ligand:metal ratio from 4:1 to 10:1, but not completely avoided.

The applicability of SFMEs as switchable solvents for the rhodium-catalysed hydroformylation of long-chain alkenes was finally tested in a number of consecutive recycling experiments. The experimental results are depicted in Figure 24. The applied catalyst could be successfully recycled for

four times and the hydroformylation reaction performed in a total of five runs with high selectivity toward the desired linear aldehyde. Furthermore, the results also show a considerable decrease in activity of the catalyst over the number of experiments which could be due to catalyst decomposition. Evidence on the quantitative amount of remaining active catalyst after the each run would require the implementation of extensive in situ measurement techniques which have not been applied yet, but would be an interesting option for future experiments. However, all aspects considered the experimental results gave a proof of concept for the application of SFMEs as switchable reaction media in homogeneous catalysis.

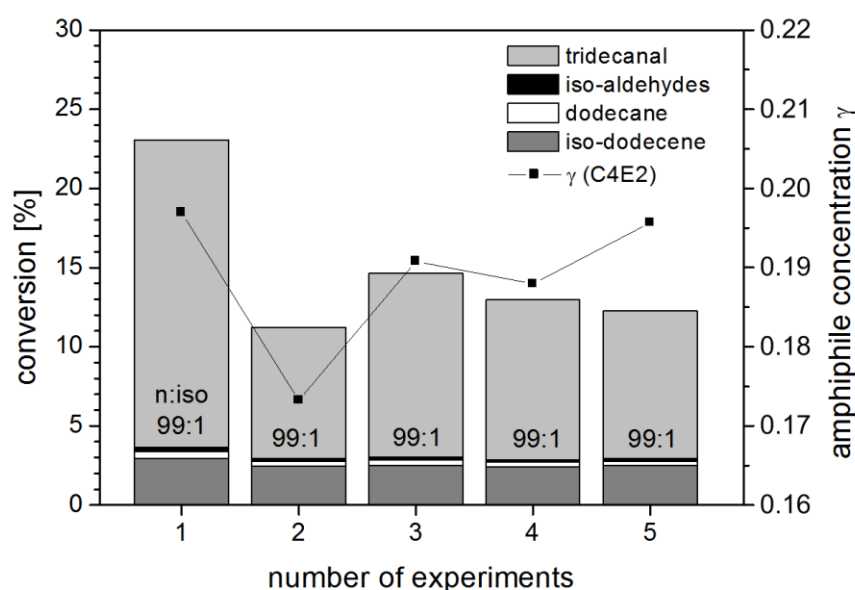


Figure 24. Recycling experiment for hydroformylation of 1-dodecene in SFME. Test conditions: 0.05 mmol $\text{Rh}(\text{acac})(\text{CO})_2$, 0.5 mmol SulfoXantphos, 80 mmol 1-dodecene, water ($\alpha = 0.4$), C4E2 ($\gamma = 0.2$), $V_R = 50$ mL, $T = 95$ °C, $p = 15$ bar, stirring speed = 1200 rpm, $t_R = 4$ h. Statistic deviation of results: ± 3 %. (**PAPER 5**)

4.7 Pickering Emulsions

Emulsions may be formulated not only by the addition of an amphiphile or surfactant, but also by nano- and microparticles that accumulate at the droplets' interface and stabilize them against coalescence in non-miscible liquids. These so-called Pickering emulsions⁴⁷ are able to stabilize oil-in-water emulsions and thus could be a useful tool for homogeneously catalysed reactions in aqueous media. They can be formulated by particles of silica, latex, or even natural clay nanotubes with different hydrophobicity which determines the stability of the resulting emulsion. In **PAPER 6**, the impact of halloysites stabilized Pickering emulsions on the rhodium-catalysed hydroformylation of 1-dodecene are reported for the first time. The experimental results of a long-term reaction are

illustrated in Figure 25. The hydroformylation was successfully performed, yielding in 36% tridecanal after 24 h reaction time with a very high n:iso selectivity of 99:1. Side-products from hydrogenation or isomerisation reaction were found in only small amounts (roughly 1% each). However, the reaction rate was found to be rather slow with a TOF of 15-20 h⁻¹, which is only 1/10 of the value of a comparable experiment in microemulsion systems. These results indicate that there still might be a great optimization potential for Pickering emulsions as reaction media. A large benefit of Pickering emulsions is the easy separation of the organic product and water-soluble catalyst after the reaction by the use of membrane filtration techniques. The emulsion can be concentrated to more than 90% without breakthrough of the organic phase, meaning the oil droplets remain stable during filtration. In conclusion, Pickering emulsions may unfold a very high process efficiency in future applications, however, more investigation on the effect of their composition on the reactivity and a number of successful recycling experiments are required first for the final proof of concept and further evaluation.

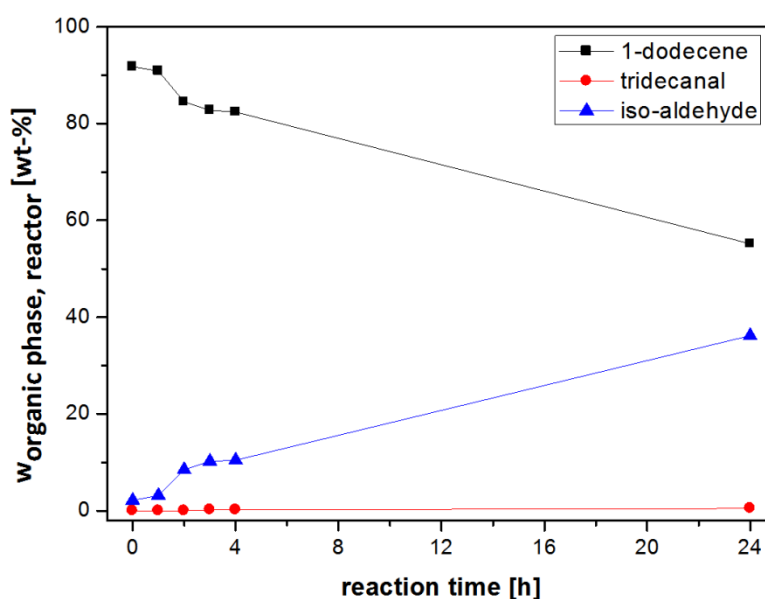


Figure 25. Hydroformylation of 1-dodecene in Pickering emulsions. Test conditions: 0.10 mmol Rh(acac)(CO)₂, 0.40 mmol SulfoXantphos, 48 mmol (8 g) 1-dodecene, 24 g water, 0.16 g (0.50 wt-%) of pristine halloysites (750 ± 200 nm), V_R = 35 mL, T = 95 °C, p = 15 bar, stirring speed = 1200 rpm, t_R = 24 h. Statistic deviation of results: ±3 %. (**PAPER 6**)

5 Conclusions and outlook

The application of aqueous multiphase systems as reaction media for homogenous catalysis offers many interesting options for the development of new “green” chemical processes. Regarding the already numerous examples for transition metal catalysis in surfactant based reaction media it seems to be only a question of time until the first industrial application in these systems becomes reality. In fact, Gallou and co-workers from Novartis Pharma AG reported very recently of a new straightforward and highly advantageous process for the production of an active pharmaceutical ingredient by the use of a nonionic surfactant as emulsifier ⁴⁸. However, regarding the implementation of transition metal catalysed reactions in microemulsion systems it is apparent that they require a profound knowledge of the influence of a variety of system parameters regarding reaction and separation. The impact of the applied surfactant on the outcome of a reaction can be rather strong and thus has to be taken into consideration during the development of a process. Thus the selection of an appropriate surfactant for a process is a very crucial task and should already be done at an early stage of the development. To answer the question, whether the application of a surfactant for the realization of a new process is useful or not, it might be a feasible approach to initially perform a small number of test reactions with different types of surfactants (e.g. non-ionic, anionic, cationic). The result of these primal experiments could then be very beneficial for the further development and enhancement of the chemical processes in surfactant-based media. All aspects considered in this thesis point out the good applicability of microemulsion systems as switchable reaction media in homogeneous catalysis and their high optimization potential for any given application by the selection of a proper surfactant.

6 References

- (1) Anastas, P. T.; Warner, J. C. *Green Chemistry: Theory and Practice*; Oxford University Press: Oxford, 1998.
- (2) Breslow, R. The Principles of and Reasons for Using Water as a Solvent for Green Chemistry. In *Green Solvent Vol. 5: Reactions in Water*; Anastas, P. T., Li, C.-J., Eds.; WILEY-VCH Verlag: Weinheim, 2010.
- (3) Lipshutz, B. H.; Gallou, F.; Handa, S. Evolution of Solvents in Organic Chemistry. *Sustain. Chem. Eng.* **2016**, *4*, 5838.
- (4) Wiese, K.-D.; Obst, D. *Catalytic Carbonylation Reactions*; Beller, M., Ed.; Springer: New York, 2006.
- (5) Bahrmann, H.; Bach, H.; Frey, G. D. Oxo Synthesis. In *Ullmann's Encyclopedia of Industrial Chemistry*; WILEY-VCH Verlag: Weinheim, 2000; pp 1–8.
- (6) Roelen, O. Verfahren Zur Herstellung von Sauerstoffhaltigen Verbindungen. DE 849548, 1949.
- (7) Cornils, B.; Hibbel, J.; Konkol, W.; Lieder, B.; Much, J.; Schmidt, V.; Wiebus, E. Verfahren Zur Herstellung von Aldehyden. DE 3234701, 1982.
- (8) Vogt, D. Nonaqueous Organic/Organic Separation (SHOP Process). In *Aqueous-Phase Organometallic Catalysis*; Cornils, B., Herrmann, W. A., Eds.; WILEY-VCH Verlag: Weinheim, 2004; pp 639–645.
- (9) Behr, A.; Onken, U. Organische Zwischenprodukte. In *Technische Chemie*; Baerns, M., Behr, A., Brehm, A., Gmehling, J., Hofmann, H., Onken, U., Renken, A., Eds.; WILEY-VCH Verlag: Weinheim, 2006; pp 573–574.
- (10) Leitner, W. Supercritical Carbon Dioxide as a Green Reaction Medium for Catalysis. *Acc. Chem. Res.* **2002**, *35*, 746.
- (11) Schäfer, E.; Brunsch, Y.; Sadowski, G.; Behr, A. Hydroformylation of 1-Dodecene in the Thermomorphic Solvent System Dimethylformamide/Decane. Phase Behavior – Reaction Performance – Catalyst Recycling. *Ind. Eng. Chem. Res.* **2012**, *51*, 10296.
- (12) Jessop, P. G.; Mercer, S. M.; Heldebrant, D. J. CO₂-Triggered Switchable Solvents, Surfactants, and Other Materials. *Energy Environ. Sci.* **2012**, *5*, 7240.
- (13) Schwarze, M.; Pogrzeba, T.; Volovych, I.; Schomäcker, R. Microemulsion Systems for Catalytic Reactions and Processes. *Catal. Sci. Technol.* **2015**, *5*, 24.
- (14) Dwars, T.; Paetzold, E.; Oehme, G. Reactions in Micellar Systems. *Angew. Chem. Int. Ed. Engl.* **2005**, *44*, 7174.
- (15) Lipshutz, B. H.; Taft, B. R. Heck Couplings at Room Temperature in Nanometer Aqueous Micelles. *Org. Lett.* **2008**, *10* (7), 1329.

- (16) Lipshutz, B. H.; Ghorai, S.; Abela, A. R.; Moser, R.; Nishikata, T.; Duplais, C.; Krasovskiy, A.; Gaston, R. D.; Gadwood, R. C. TPGS-750-M: A Second-Generation Amphiphile for Metal-Catalyzed Cross-Couplings in Water at Room Temperature. *J. Org. Chem.* **2011**, *76* (11), 4379.
- (17) Schwarze, M.; Milano-Brusco, J. S.; Strempe, V.; Hamerla, T.; Wille, S.; Fischer, C.; Baumann, W.; Arlt, W.; Schomäcker, R. Rhodium Catalyzed Hydrogenation Reactions in Aqueous Micellar Systems as Green Solvents. *RSC Adv.* **2011**, *1*, 474.
- (18) La Sorella, G.; Strukul, G.; Scarso, A. Recent Advances in Catalysis in Micellar Media. *Green Chem.* **2015**, *17*, 644.
- (19) Dwars, T.; Haberland, J.; Grassert, I.; Oehme, G.; Kragl, U. Asymmetric Hydrogenation in a Membrane Reactor: Recycling of the Chiral Catalyst by Using a Retainable Micellar System. *J. Mol. Catal. A Chem.* **2001**, *168* (1–2), 81.
- (20) Schwarze, M.; Schmidt, M.; Nguyen, L. A. T.; Drews, A.; Kraume, M.; Schomäcker, R. Micellar Enhanced Ultrafiltration of a Rhodium Catalyst. *J. Memb. Sci.* **2012**, *421–422*, 165.
- (21) Winsor, P. A. Hydrotrophy, Solubilisation and Related Emulsification Processes. Part I. *Trans. Faraday Soc.* **1948**, *44*, 376.
- (22) Kahlweit, M.; Strey, R.; Busse, G. Microemulsions: A Qualitative Thermodynamic Approach. *J. Phys. Chem.* **1990**, *94*, 3881.
- (23) Heck, R. F.; Breslow, D. S. The Reaction of Cobalt Hydrotetracarbonyl with Olefins. *J. Am. Chem. Soc.* **1961**, *83*, 4023.
- (24) Heck, R. F.; Breslow, D. S. Acylcobalt Carbonyls and Their Triphenylphosphine Complexes. *J. Am. Chem. Soc.* **1962**, *84*, 2499.
- (25) Heck, R. F. Addition Reactions of Transition Metal Compounds. *Acc. Chem. Res.* **1969**, *2*, 10.
- (26) Evans, D.; Osborn, J. A.; Wilkinson, G. Hydroformylation of Alkenes By Use of Rhodium Complex Catalysts. *J. Chem. Soc.* **1968**, 3133.
- (27) Brown, C. K.; Wilkinson, G. Homogeneous Hydroformylation of Alkenes with Hydridocarbonyltris-(triphenylphosphine)rhodium(I) as Catalyst. *J. Chem. Soc.* **1970**, 2753.
- (28) Silva, S. M.; Bronger, R. P. J.; Freixa, Z.; Dupont, J.; van Leeuwen, P. W. N. . High Pressure Infrared and Nuclear Magnetic Resonance Studies of the Rhodium-Sulfoxantphos Catalysed Hydroformylation of 1-Octene in Ionic Liquids. *New J. Chem.* **2003**, *27*, 1294.
- (29) Li, C.; Widjaja, E.; Chew, W.; Garland, M. Rhodium Tetracarbonyl Hydride: The Elusive Metal Carbonyl Hydride. *Angew. Chemie Int. Ed.* **2002**, *41*, 3785.
- (30) Sandee, A. J.; Slagt, V. F.; Reek, J. N. H.; Kamer, P. C. J.; van Leeuwen, P. W. N. M. A Stable and Recyclable Supported Aqueous Phase Catalyst for Highly Selective Hydroformylation of Higher Olefins. *Chem. Commun.* **1999**, 1633.

References

- (31) Bronger, R. P. J.; Berman, J. P.; Herwig, J.; Kamer, P. C. J.; van Leeuwen, P. W. N. . Phenoxaphosphino-Modified Xantphos-Type Ligands in the Rhodium-Catalysed Hydroformylation of Internal and Terminal Alkenes. *Adv. Synth. Catal.* **2004**, *346*, 789.
- (32) Helfferich, F. G. Kinetics of Multipstep Reactions. In *Comprehensive Chemical Kinetics Vol. 40*; Green, N. J. B., Ed.; Elsevier Science: Amsterdam, 2004.
- (33) Garland, M.; Pinot, P. Kinetics of the Formation and Hydrogenolysis of Acylrhodium Tetracarbonyl. *Organometallics* **1991**, *10*, 1693.
- (34) van der Slot, S. C.; Kamer, P. C. J.; van Leeuwen, P. W. N. M.; Iggo, J. A.; Heaton, B. T. Mechanistic Studies of the Hydroformylation of 1-Alkenes Using a Monodentate Phosphorus Diamide Ligand. *Organometallics* **2001**, *20*, 430.
- (35) Gellrich, U.; Seiche, W.; Keller, M.; Breit, B. Mechanistic Insights into a Supramolecular Self-Assembling Catalyst System: Evidence for Hydrogen Bonding during Rhodium-Catalyzed Hydroformylation. *Angew. Chemie Int. Ed.* **2012**, *51*, 11033.
- (36) Rooy, A. Van; Orij, E. N.; Kamer, P. C. J.; Leeuwen, P. W. N. M. Van. Hydroformylation with a Rhodium/Bulky Phosphite Modified Catalyst. Catalyst Comparison for Oct-1-Ene, Cyclohexene, and Styrene. *Organometallics* **1995**, *14*, 34.
- (37) Rooy, A. Van; Kamer, P. C. J.; Leeuwen, P. W. N. M. Van; Goubitz, K.; Fraanje, J.; Veldman, N.; Spek, A. L. Bulky Diphosphite-Modified Rhodium Catalysts: Hydroformylation and Characterization. *Organometallics* **1996**, *15*, 835.
- (38) Nowothnick, H.; Blum, J.; Schomäcker, R. Suzuki Coupling Reactions in Three-Phase Microemulsions. *Angew. Chem. Int. Ed. Engl.* **2011**, *50*, 1918.
- (39) Volovych, I.; Kasaka, Y.; Schwarze, M.; Nairoukh, Z.; Blum, J.; Fanun, M.; Avnir, D.; Schomäcker, R. Investigation of Sol–gel Supported Palladium Catalysts for Heck Coupling Reactions in O/w-Microemulsions. *J. Mol. Catal. A Chem.* **2014**, *393*, 210.
- (40) Volovych, I.; Neumann, M.; Schmidt, M.; Buchner, G.; Yang, J.-Y.; Wölk, J.; Sottmann, T.; Strey, R.; Schomäcker, R.; Schwarze, M. A Novel Process Concept for the Three Step Boscalid® Synthesis. *RSC Adv.* **2016**, *6*, 58279.
- (41) Müller, M.; Kasaka, Y.; Müller, D.; Schomäcker, R.; Wozny, G. Process Design for the Separation of Three Liquid Phases for a Continuous Hydroformylation Process in a Miniplant Scale. *Ind. Eng. Chem. Res.* **2013**, *52*, 7259.
- (42) Müller, D.; Minh, D. H.; Merchan, V. A.; Arellano-Garcia, H.; Kasaka, Y.; Müller, M.; Schomäcker, R.; Wozny, G. Towards a Novel Process Concept for the Hydroformylation of Higher Alkenes: Mini-Plant Operation Strategies via Model Development and Optimal Experimental Design. *Chem. Eng. Sci.* **2014**, *115*, 127.

- (43) Rost, A. Rhodium-Katalysierte Hydroformylierung von 1-Dodecen Mit Zweizähnigen Liganden in Mikroemulsionssystemen (Dissertation), Technische Universität Berlin, 2013.
- (44) Hamerla, T. Hydroformylierung Langkettiger Olefine Mit Zweizähnigen Rhodium-Komplexen in Mizellaren Lösungen Und Mikroemulsionen (Dissertation), Technische Universität Berlin, 2014.
- (45) Schwarze, M.; Pogrzeba, T.; Seifert, K.; Hamerla, T.; Schomäcker, R. Recent Developments in Hydrogenation and Hydroformylation in Surfactant Systems. *Catal. Today* **2015**, *247*, 55.
- (46) Kiedorf, G.; Hoang, D. M.; Müller, A.; Jörke, A.; Markert, J.; Arellano-Garcia, H.; Seidel-Morgenstern, A.; Hamel, C. Kinetics of 1-Dodecene Hydroformylation in a Thermomorphic Solvent System Using a Rhodium-Biphephos Catalyst. *Chem. Eng. Sci.* **2014**, *115*, 31.
- (47) S. Pickering. Pickering Emulsions. *J. Chem. Soc. Trans.* **1907**, *91*, 2001.
- (48) Gallou, F.; Isley, N. A.; Ganic, A.; Onken, U.; Parmentier, M. Surfactant Technology Applied toward an Active Pharmaceutical Ingredient: More than a Simple Green Chemistry Advance. *Green Chem.* **2016**, *18*, 14.

PAPER 1

Rhodium-Catalyzed Hydroformylation of Long-Chain Olefins in Aqueous Multiphase Systems in a Continuously Operated Miniplant

Tobias Pogrzeba, David Müller, Tobias Hamerla, Erik Esche, Niklas Paul, Günter Wozny, and Reinhard Schomäcker

Industrial & Engineering Chemistry Research, 2015, 54, 11953-11960

Online Article: <http://pubs.acs.org/doi/10.1021/acs.iecr.5b01596>

ActiveView PDF: <http://pubs.acs.org/doi/ipdf/10.1021/acs.iecr.5b01596>

Reproduced (or 'Reproduced in part') with permission from "Rhodium-Catalyzed Hydroformylation of Long-Chain Olefins in Aqueous Multiphase Systems in a Continuously Operated Miniplant; Tobias Pogrzeba, David Müller, Tobias Hamerla, Erik Esche, Niklas Paul, Günter Wozny, and Reinhard Schomäcker. Industrial & Engineering Chemistry Research, 2015, 54, 11953-11960." Copyright (2015) American Chemical Society.

Rhodium-Catalyzed Hydroformylation of Long-Chain Olefins in Aqueous Multiphase Systems in a Continuously Operated Miniplant

Tobias Pogrzeba,^{*,†} David Müller,[‡] Tobias Hamerla,[†] Erik Esche,[‡] Niklas Paul,[§] Günter Wozny,[‡] and Reinhard Schomäcker[†]

[†]Department of Chemistry, Technische Universität Berlin, Straße des 17. Juni 124, Sekr. TC-8, D-10623 Berlin, Germany

[‡]Chair of Process Dynamics and Operation, Technische Universität Berlin, Str. des 17. Juni 135, Sekr. KWT-9, D-10623 Berlin, Germany

[§]Chair of Chemical and Process Engineering, Technische Universität Berlin, Ackerstraße 76, D-13355 Berlin, Germany

ABSTRACT: We investigate aqueous multiphase systems for catalytic gas/liquid reactions, namely, the rhodium-catalyzed hydroformylation of the long-chain olefin 1-dodecene. The multiphase system was formulated from 1-dodecene, water, and a nonionic surfactant, which increases the solubility between the two nonmiscible liquid phases. On the basis of these systems, we present in this paper a transfer of lab experiments (semibatch) to a successful operation of a miniplant in continuous mode. Under optimized conditions, the reaction showed turnover frequencies of $\sim 200 \text{ h}^{-1}$ and high selectivity of 98:2 to the desired linear aldehyde. The miniplant was operated continuously for a total of 130 h. The control of the phase separation and catalyst recycling for product isolation for a long time period appeared to be challenging. Nevertheless, the separation was kept stable for over 24 h. The organic components in the product phase amounted to desired values between 95 and 99 wt %. The desired 99.99% of the catalyst remained in the aqueous catalyst phase.

1. INTRODUCTION

The hydroformylation reaction is one of the most important homogeneously catalyzed reactions practiced on the industrial scale, with the production of oxo-products exceeding 10 million metric tons per year. The reaction itself was originally discovered by Otto Roelen in 1938 at Ruhrchemie.^{1,2} In this reaction, unsaturated hydrocarbons react with a mixture of carbon monoxide and hydrogen (syngas) under high pressure and at high temperatures, catalyzed by transition-metal catalysts (predominantly cobalt-based catalysts), to linear and branched aldehydes (Figure 1).

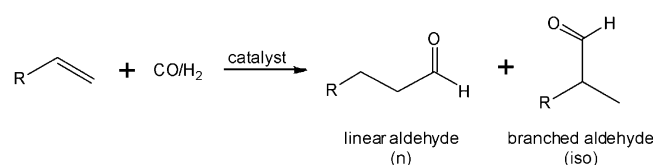


Figure 1. Hydroformylation reaction.

In general, the linear aldehydes are the favored products because they are important intermediates for the synthesis of alcohols, carbonic acids, and amines; furthermore, they have a better biodegradability. In recent years, a great effort has been made to improve the selectivity of the reaction toward the linear aldehydes by preparing transition-metal catalyst complexes with a variety of ligands. In 1968, the so-called “Wilkinson”-catalyst was described by Evans et al.³ It is a rhodium-based catalyst with monodentate phosphine ligands and gives selectivity of the linear aldehyde up to 75–80%. The use of rhodium as a noble-metal catalyst increases the activity of the hydroformylation reaction in comparison to the use of

cobalt-based catalysts, which are the standard catalyst for the hydroformylation of long-chain olefins in industrial applications so far. This has led to the development of new process concepts that on the one hand require a lower energy input⁴ and on the other hand are focused on catalyst recycling and prevention of catalyst leaching, because of the much higher price of rhodium compared to cobalt. The design of bidentate ligands, such as chelating diphosphines or diphosphites, led to a further improvement of the selectivity in hydroformylation reaction. In addition to the improvement of the selectivity, a new reaction concept was developed and established at Ruhrchemie in 1984,⁵ where the hydroformylation reaction was performed in a two-phase system with highly active rhodium catalysts consisting of water-soluble ligands. Although this concept offers the possibility of running the hydroformylation process with low catalyst deactivation and leaching, its major drawback is the limitation to short-chain olefins ($C \leq 5$), due to the poor solubility of long-chain olefins in the aqueous phase. On an industrial scale, long-chain olefins ($C > 5$) are still converted by cobalt- or rhodium-catalyzed processes in homogeneous phase with complex and expensive product separation and catalyst recycling, especially in the case of rhodium.

Therefore, a novel process concept based on surfactant-modified multiphase systems is currently investigated in the Collaborative Research Centre SFB/TRR 63 (InPROMPT), with the goal to investigate and utilize the advantages of biphasic catalysis using highly selective bidentate ligands for the hydroformylation of long-chain olefins ($C > 10$). The potential

Received: April 29, 2015

Revised: October 23, 2015

Accepted: November 2, 2015

Published: November 2, 2015

of the concept will be shown by a transfer of the reaction from the lab-scale to a miniplant. As previously shown by Hamerla et al.,⁶ the rhodium-catalyzed hydroformylation of 1-dodecene in a microemulsion system formed from 1-dodecene/water/Marlophen NP9 results in good activities (turnover frequency (TOF) > 300 h⁻¹) and very good selectivity ((*n*/iso) = 98:2, ratio of linear to branched aldehydes) by the use of the bidentate ligand SulfoXantPhos. On the basis of this promising results, a fully automated miniplant was designed and built at Technische Universität Berlin, which was described by Rost et al.⁷ and Müller et al.⁸ In this contribution we will present the results from the first successful run of a continuously operated miniplant with a microemulsion system. The aim of this miniplant run was to validate the lab-scale results for conversion and selectivity from semibatch experiments and to investigate unpredictable effects, such as effectiveness, stability, and loss of catalyst; accumulation of byproducts; the influence of the recycle stream on the reaction; and the controllability of the reaction in general. The miniplant was operated continuously for a total of 130 h. In preparation of the miniplant operation, additional semibatch lab-scale experiments have been performed to optimize the reaction system, which will be presented in this contribution as well.

2. BACKGROUND INFORMATION

2.1. State of the Art. Several examples of successful application of micellar reaction media can be found in the literature. Various media containing normal or inverse micelles are described. Fell and Papadogiannakis demonstrated the applicability of a water-soluble catalyst complex formed by Rh₄(CO)₁₂ and surface-active sulfobetaine-derived phosphine ligands for the hydroformylation of tetradec-1-ene.⁹ The hydroformylation of various olefins (C₆–C₁₆) in reverse micellar systems was presented by Van Vyve and Renken in 1991.¹⁰ In 2002, Haumann et al.¹¹ described the hydroformylation of 1-dodecene in microemulsions with the monodentate water-soluble ligand tris(3-sulfophenyl)-phosphine trisodiumsalt (TPPTS). All contributions showed that no conversion of long-chain olefins was detected without addition of surfactant, but fast reaction rates are obtained when surfactants are used to formulate a multiphase system. However, Schwarze et al.¹² recently have shown that the selection of an appropriate surfactant for a reaction is crucial and has to be done carefully. In using surfactant systems as part of an integrated reaction and separation process, the surfactant will have a huge impact on the phase behavior of the mixture and the distribution of catalyst and reactants between the aqueous and organic phase. Reaction kinetics as well as the dynamics of the separation process show a strong dependency on the surfactant concentration and the structure of the involved phases.¹³ Beside surfactant based media, several other promising approaches on hydroformylation of long-chain olefins in emulsions are being investigated currently, for example, the application of supramolecular emulsifiers by Potier and Vanbesi  n et al.^{14–16} or latices by Kunna et al.¹⁷

2.2. Surfactant-Based Multiphase Systems. Two-phase systems containing an aqueous and an oil phase can be modified by the addition of nonionic surfactants to form multiphase systems. These multiphase systems offer the possibility of increasing the interfacial area between the oil and aqueous phase by lowering the interfacial tension. It also enables an easy phase separation and catalyst recovery in a single step by temperature-induced phase transition after the

reaction. Addition of nonionic surfactants with balance solubility in both phases causes the formation of microemulsions. Important parameters to characterize a microemulsion are the weight fractions of oil (α) and surfactant (γ) (eqs 1 and 2, respectively), which are calculated with the mass m of the corresponding component:

$$\alpha = \frac{m_{\text{oil}}}{m_{\text{oil}} + m_{\text{H}_2\text{O}}} \quad (1)$$

$$\gamma = \frac{m_{\text{Surf}}}{m_{\text{oil}} + m_{\text{H}_2\text{O}} + m_{\text{Surf}}} \quad (2)$$

The so-called “Kahlweit’s fish”-diagram illustrates the phase behavior of microemulsion systems and can be drawn as a vertical section through the Gibb’s phase prism of a ternary mixture of water, oil, and nonionic surfactant at a constant α (see Figure 2) yielding in a pseudobinary phase diagram.¹⁸

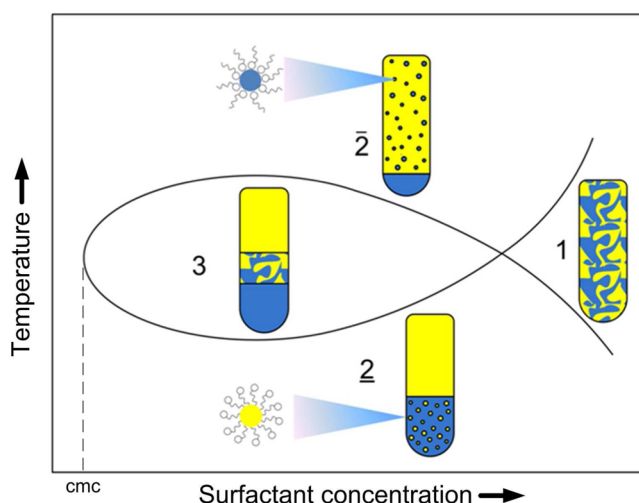


Figure 2. Schematic presentation of a Kahlweit’s fish diagram for a ternary mixture of oil, water, and nonionic surfactant at constant ratio of oil to water with normal (bottom) and inverse (top) micelles. Adapted with permission from ref 13. Copyright 2011 Wiley-VCH Verlag GmbH & Co. KGaA.

In Figure 2, four different phase states can be observed, which are dependent on the temperature and the surfactant concentration (γ). The latter has to be higher than the minimum concentration to form micelles, the critical micelle concentration (cmc). Micelles are nanoscale aggregates of surfactant monomers, which are able to act as microreactors by transferring a component (catalyst, educt) into the opponent phase. A detailed description of the complex phase behavior of microemulsion systems that is illustrated in the fish-diagram can be found in the literature.^{19,20}

In general, each of the four different phase states can be applied as a reaction medium for homogeneous catalysis. Compared to a binary system the reaction in a microemulsion system is carried out with considerably higher reaction rates, because the area for mass transfer is larger.²¹ The phase separation behavior of microemulsion systems allows for catalytic reactions with the possibility of catalyst recycling afterward, which is their major advantage in comparison to usual organic solvents.²² We found that in many cases the catalyst follows the surfactant into the corresponding microemulsion phase. Hence, catalyst recycling can be done by phase

separation after reaction when the state of the system is switched to (2) or (3) by changing temperature (see Figure 2); a process concept based on this consideration is shown in Figure 3.

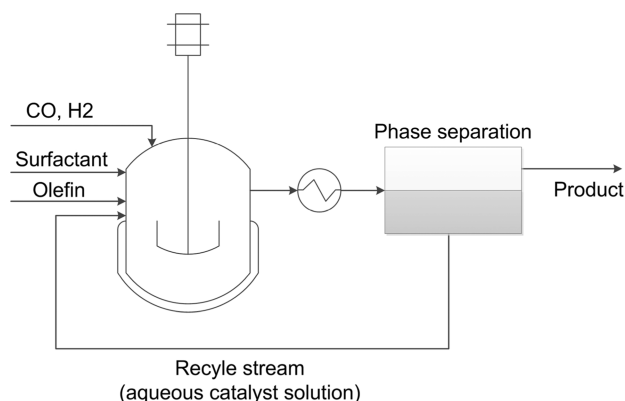


Figure 3. Process concept for the hydroformylation of long-chain olefins in microemulsion systems.

The composition of the reaction mixture and the kinetics of phase separation within the desired phase region are essential questions for the process development. Near the phase boundaries of the different microemulsion systems the phase separation often takes a long time because of low interfacial tension and high stability of the emulsified system; the composition of the phases in this region is quite similar, and separation of the components will often be incomplete. Thus, the kinetics of phase separation strongly depend on the temperature of the system and on the temperature distance to the phase boundaries.²³ For cost-efficient processes, time for the separation should be as low as possible. Because reaction and separation are strongly temperature- and composition-dependent, a thorough investigation of the phase behavior for each system is mandatory. Preliminary investigations on the hydroformylation of 1-dodecene indicated that the three-phase

region (3) is the most desirable state for an integrated process of reaction and catalyst separation.^{6,8} Additionally, it was observed that the separation time in the three-phase region was also considerably lower than in the also applicable lower two-phase region (2).²⁴ Therefore, the experimental conditions for the lab-scale experiments and for the miniplant were chosen to obtain the three-phase region.

3. MATERIAL AND METHODS

In this section, the applied substances and the experimental setup of the semibatch reactor as well as of the miniplant are described in detail.

3.1. Chemicals. The reactant 1-dodecene was purchased from VWR with a purity of 95 wt %. The precursor [Rh(acac)(CO)₂] was contributed by Umicore, Germany. The water-soluble ligand SulfoXantPhos (SX) was purchased from Molisa, where it was synthesized according to a procedure described by Goedheijt et al.²⁵ The technical-grade surfactants were provided by Sasol, Germany (former Hüls AG or Condea Chemicals, respectively).

3.2. Semi-Batch Reactor. The hydroformylation reactions in lab-scale are performed in a 100 mL stainless steel high-pressure vessel from Premex Reactor AG, equipped with a gas-dispersion stirrer and mounted in an oil thermostat from Huber (K12-NR). An overview of the complete reactor setup is given in Figure 4. Mass flow controller (4) and a pressure transmitter (5) in the syngas feed line enable isobaric reaction management (semibatch mode). For an alternative batch-mode (decreasing pressure), a 300 mL gas-reservoir (7) is connected to the reactor. A connection for the inertization of reaction mixture is implemented as well (9).

The typical reaction conditions for the hydroformylation were 15–40 bar pressure of syngas (1:1 mixture of CO and H₂, purity 1.6 for CO and 3.0 for H₂, purchased from Air liquide), an internal reactor temperature of 75–110 °C, and a stirring speed of 1200 rpm, using a gas dispersion stirrer. The reaction mixture usually consisted of 1-dodecene (0.120 mol, 20.0 g, 26 mL, purity 95%, $\alpha = 0.5$), water (1.11 mol, 20 mL, HPLC

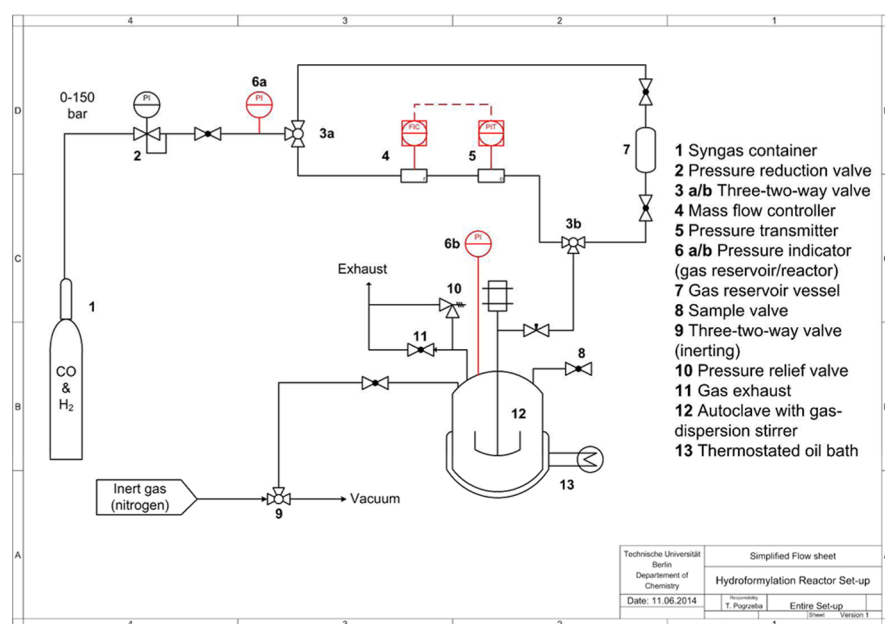


Figure 4. Lab-scale reactor setup.

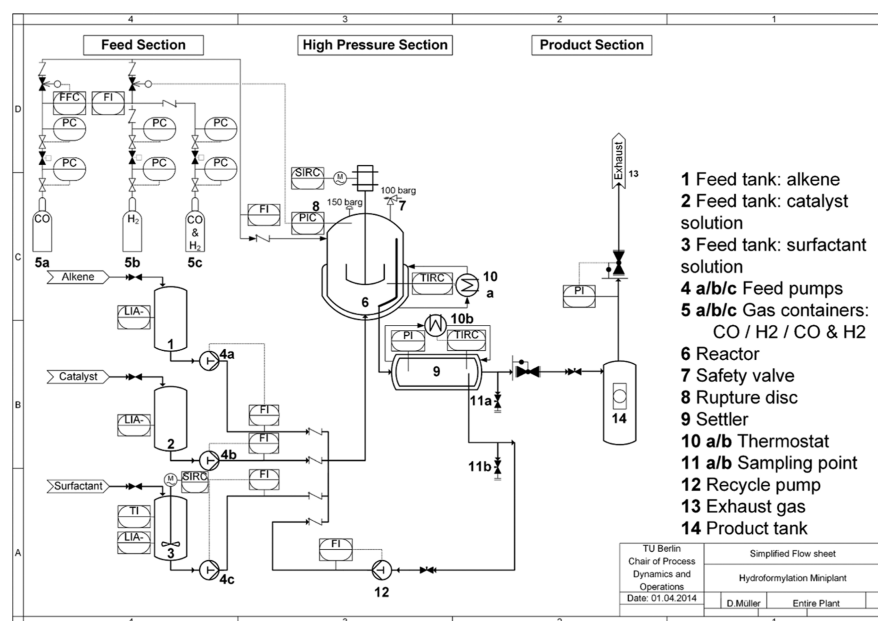


Figure 5. Simplified P&ID of the miniplant at Technische Universität Berlin.

grade), the nonionic surfactant Marlipal 24/70 (3.5 g, technical grade, $\gamma = 0.08$), rhodium precursor $[\text{Rh}(\text{acac})(\text{CO})_2]$ (0.05 mmol, 12.9 mg), and the ligand SulfoXantPhos (0.20 mmol, 158 mg). The metal-to-ligand ratio of the water-soluble catalyst complex was held constant at 1:4. The catalyst was prepared and the reaction procedure was carried out as described by Hamerla et al.,⁶ with the difference that the experiments were performed at isobaric conditions.

For the evaluation of reaction progress, samples were taken at several time intervals and analyzed by gas chromatography (GC) on a Hewlett-Packard model 5890, series II equipped with a RTX-SMS capillary column, a flame ionization detection analyzer, and nitrogen as the carrier gas. Inductively coupled plasma optical emission spectrometry (ICP-OES) was used to determine the amount of rhodium and phosphorus in the product phase.

3.3. Miniplant. To bridge the gap between lab-scale results and actual industrial application, a miniplant has been constructed with the aim of validating the results from semibatch experiments and investigating unpredictable effects, such as effectiveness, stability, and loss of catalyst; accumulation of byproducts; the influence of the recycle stream on the reaction; and the controllability of the reaction in general.

The design of the miniplant has been described by Müller et al.^{8,24} Nevertheless, it will be briefly revisited here. The miniplant consists of three sections: a feed section storing the educts and reactants, a mixer–settler section, and a product storage section. In Figure 5, a simplified P&ID of the miniplant at Technische Universität Berlin is depicted. The plant is fully automated with the SIEMENS process control system PCS7. The operators receive information from over 50 sensors, including an online-GC instrument for the gas composition in the reactor as well as a Raman-spectrometer in the product phase of the settler. In the plant, 15 controllable variables exist, such as pumps for liquid mass flows, control valves for product and gas streams, and thermostats for the temperature in the reactor and settler.

The feed section of the miniplant consists of the three feed tanks (units 1–3 in Figure 5), each with a volume of 10 L, and

of the feed pumps (units 4a, 4b, and 4c in Figure 5) for all liquids as well as gas bottles (units 5a, 5b, and 5c in Figure 5). The pump 4a, feeding 1-dodecene, feeds up to 1500 g/h to the reactor. The feed streams of the catalyst solution (4b) and nonionic surfactant (4c) can be regulated to a maximum value of 500 g/h each.

The mixer–settler section consists of a reactor and of a settler. The reactor has a capacity of 1000 mL, while a drain is fixed at 70% height. The reactor features a 6-bladed Rushton turbine-type gas dispersion stirrer with a maximum rotation speed of 2880 rpm. For the process, it is operated below 1100 rpm because of foaming reasons. The settler has a volume of 300 mL. The product phase is removed via a control valve while the catalyst phase is recycled back to the reactor. The maximum flow of the recycle pump (unit 12 in Figure 5) lies at 500 g/h.

Next to the standard online measurements regarding temperatures, pressures, flows, and levels, two offline GC instruments are employed for an hourly analysis of the composition in the product drain (unit 11a in Figure 5) and in the recycle drain (unit 11b) of the settler. Two GC instruments are used because the analysis time takes roughly 30–45 min. Thus, a sample can be taken hourly from the two sampling points. Additionally, as for the semibatch experiments, an ICP-OES instrument is employed for estimating the rhodium amount lost in the product phase after the phase separation.

4. RESULTS AND DISCUSSION

To enable the continuous process in the miniplant, further investigations of the reaction system had to be made in lab-scale semibatch experiments. Therefore, a systematic optimization of the reaction parameters was performed. In this section, we will present the results of the investigations of the influence of syngas pressure and temperature on the hydroformylation reaction.

4.1. Semibatch Experiments. The previous investigations in surfactant-based multiphase reaction media reveal a strong dependency between the reaction rate and the temperature of

the reaction mixture, because a change in temperature affects the phase behavior and mass-transfer processes in these media in addition to the catalytic reaction. As described earlier, the three-phase state of a given mixture of 1-dodecene, water, and a nonionic surfactant seems to be the optimal state for the hydroformylation reaction in such a multiphase system. According to these investigations, only a certain temperature range seems to be beneficial for the reaction. When the surfactant is changed, this range has to be determined again. In preliminary experiments a clear three-phase region of a mixture of 1-dodecene, water, and Marlupal 24/70 was observed in test tubes only in a quite small temperature window in the phase diagram. After addition of the Rhodium-SulfoXantPhos (Rh-SX) catalyst complex, the desired area is observed in a temperature range of 85–88 °C at a gamma value of 8–10%. This kind of phase behavior can be explained by the technical grade of the applied surfactant, which means a distribution of the degree of ethoxylation and the carbon chain length. Consequently, for further investigations a surfactant concentration of 8 wt % and a reaction temperature of 85 °C was chosen.

The important parameters (conversion, X ; yield, Y ; and selectivity, S) for the evaluation of experimental data in the following sections were calculated as shown in eqs 3–5, where n is the amount of substance, 1-dodecene is the substrate, and 1-tridecanal is the product.

$$X(t) = \frac{n_{t=0, \text{Substrate}} - n_{t, \text{Substrate}}}{n_{t=0, \text{Substrate}}} \quad (3)$$

$$Y(t) = \frac{n_{t, \text{Product}}}{n_{t=0, \text{Substrate}}} \quad (4)$$

$$S = \frac{n_{\text{Product}}}{n_{\text{iso-Aldehydes}}} \quad (5)$$

4.1.1. Estimation of Optimal Syngas Pressure. For safety and economic reasons we investigated the hydroformylation of 1-dodecene in surfactant-based multiphase systems at syngas pressure lower than the usually applied 40 bar. In Figure 6 it can be seen that the hydroformylation reaction can already be

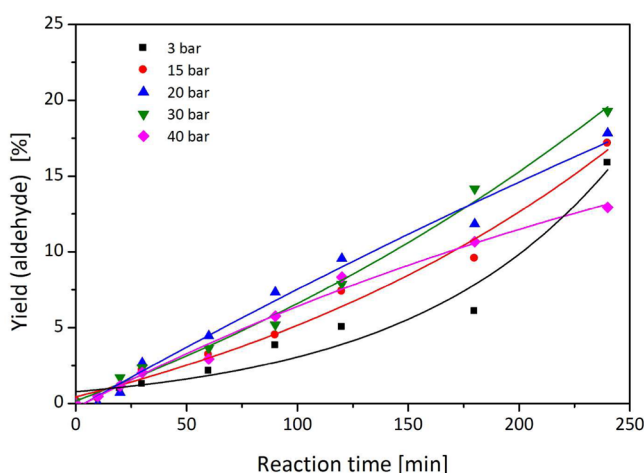


Figure 6. Influence of syngas pressure on the hydroformylation. Test conditions: 85 °C, 1200 rpm, 0.05 mmol Rh(acac) (CO)₂, 0.2 mmol SulfoXantPhos, 120 mmol 1-dodecene, $\alpha = 0.5$, $\gamma = 0.08$, $t_R = 240$ min, $V_R = 50$ mL. Statistic deviation: $\pm 3\%$.²⁸

done at very low pressure, e.g., 3 bar of syngas pressure. The observed yield of aldehyde after 4 h of reaction time at 3 bar syngas pressure was 16% and only about 3% smaller than for the hydroformylation at 30 bar syngas; it must be mentioned that the outstanding low value for the yield after 180 min at 3 bar is a result of insufficient sampling. Interestingly, the reaction rate for 40 bar syngas was the smallest of all performed experiments. This observation is in good agreement with the results of Deshpande et al.²⁶ who investigated the hydroformylation of 1-octene in ionic–organic biphasic media using Rh-SX catalyst and found a complex dependency of the reaction rate and partial pressure of CO. It first increased steeply and then decreased with further increase in CO pressure, exhibiting a maximum at 2–4 bar. This inhibition of the rate with an increase in partial pressure of CO seems to be typical for hydroformylation reactions. It can be explained by the formation of inactive dimeric catalyst species in the presence of CO. With an increase in CO pressure the concentration of the dimer increases as well, reducing the concentration of the active catalyst species and hence the reaction rate. For a better understanding of this issue we refer to the work of Markert et al.,²⁷ who analyzed the complex reaction network of the rhodium-catalyzed hydroformylation of 1-dodecene and suggested a catalytic cycle including the two main side reactions (isomerization and hydrogenation) as well as the deactivation of catalyst.

In Table 1 the results of the performed experiments at different pressures are given in detail. The influence of the

Table 1. Results of Experiments Shown in Figure 6 after 240 min of Reaction Time

syngas pressure [bar]	conversion [%]	yield _{Ald} [%]	selectivity (n:iso)	TOF _{Ald} [h ⁻¹]
3	19.1	15.9	97:3	94
15	19.2	17.2	97:3	102
20	20.4	17.8	99:1	106
30	21.7	19.3	98:2	114
40	15.7	12.9	97:3	77

syngas pressure on the n :iso selectivity is apparently very low; in all experiments the linear aldehyde is obtained with high selectivities in the range from 97:3 to 99:1. In contrast, the pressure dependency of the selectivity toward the hydroformylation reaction (ratio of produced aldehydes to overall products, see column three) is considerably stronger. The best results with selectivities around 90% are obtained for intermediate pressures between 15 and 30 bar. Furthermore, the catalyst activity is the highest in this range as well. Based on the experimental results and considering safety and economy of the overall process in the miniplant, an operating pressure of 15 bar syngas was finally chosen.

4.1.2. Variation of Temperature. As mentioned earlier, the temperature of the reaction mixture in microemulsion systems has a strong and complex influence on the reaction rate. A series of experiments was performed to investigate the influence of the temperature on the reaction at a syngas pressure of 15 bar and 4 h of reaction time. The experimental results are displayed in Figure 7. The best catalyst performance for the hydroformylation reaction was observed at 95 °C. After 4 h of reaction time, a yield of 31.3% aldehyde (n :iso = 98:2) and a TOF of 186 h⁻¹ are obtained (see Table 2). However, a relatively high amount of side products was detected in this

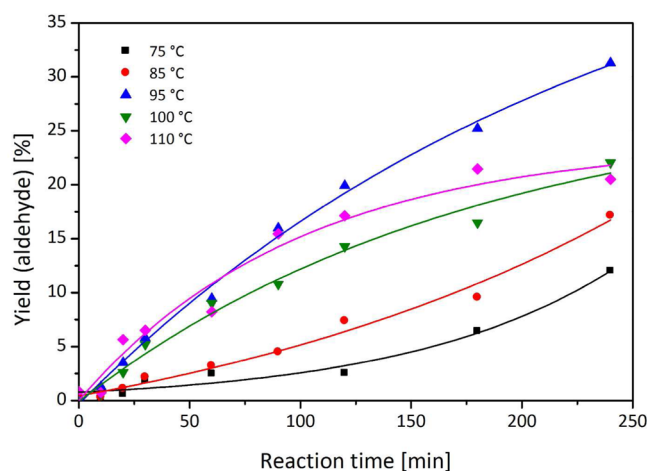


Figure 7. Influence of temperature on the yield of aldehyde. Test conditions: 15 bar, 1200 rpm, 0.05 mmol Rh(acac) (CO)₂, 0.2 mmol SulfoXantPhos, 120 mmol 1-dodecene, $\alpha = 0.5$, $\gamma = 0.08$, $t_R = 240$ min, $V_R = 50$ mL. Statistic deviation: $\pm 3\%$.²⁸

Table 2. Results of Experiments Shown in Figure 7 after 240 min of Reaction Time

reaction temperature [°C]	conversion [%]	yield _{ald} [%]	selectivity (n:iso)	TOF _{Ald} [h ⁻¹]
75	17.1	12.0	90:10	71
85	19.2	17.2	97:3	102
95	39.0	31.3	98:2	186
105	26.2	22.0	98:2	131
115	23.4	20.5	98:2	122

experiment. An increase of temperature from 95 to 115 °C resulted in a decrease in activity (TOF = 122 h⁻¹) but enhanced selectivity of the reaction. The catalyst performance at 75 °C was low, only a small yield of 12.0% aldehyde and low selectivities were obtained. An explanation for this result could be that the required catalyst species was not completely formed under these reaction conditions. Moreover, it was unexpected that the reaction rate at 85 °C was almost by half slower (TOF = 102 h⁻¹) than that at 95 °C. Regarding the results of preliminary batch experiments, this seems to be in contradiction, because the reaction should be the fastest in the three-phase region. For the applied microemulsion system the three-phase region was expected to be between 85 and 88 °C. The reason for the higher catalyst activity at 95 °C is a shift of the three-phase region to higher temperatures, induced by a change in composition of the reaction mixture (produced aldehyde and side products) and moreover the presence of the activated catalyst species. Recent investigations have revealed that the Rh-SX catalyst complex becomes surface active once it is activated by CO. As shown in Figure 8, the interfacial tension between 1-dodecene and water is considerably decreased when the activated catalyst complex is present in solution. We assume the appearing surface activity of the catalyst complex is due to a change in geometry between the nonactivated complex ([Rh(acac)(SX)], spherical, both ligands hydrophilic) and the activated complex ([Rh(CO)₂H(SX)], semispherical, only SX ligand hydrophilic). The impact of the activated catalyst on the phase behavior of the microemulsion system with Marlipal 24/70 seems to be very high. This observation is unexpected because this effect was not noticed for the microemulsion systems with surfactants from the Marlophen series, which were

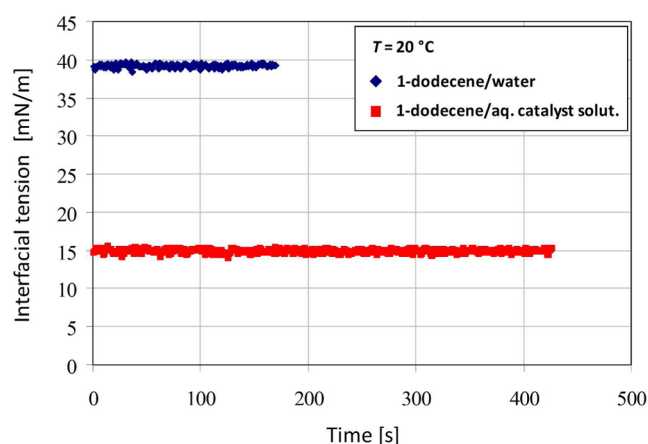


Figure 8. Dynamic interfacial tension of the binary system 1-dodecene/water measured by spinning drop method; with activated Rh-SX-catalyst (red line) and without Rh-SX-catalyst (blue line).

applied in the previous batch experiments by Rost et al.⁷ Nevertheless, this effect has to be studied in more detail in further investigations to give a detailed explanation.

As a result of the best catalyst performance, a reaction temperature of 95 °C was finally chosen for the continuous process.

4.2. Miniplant Operation. In a subsequent step the results obtained from the lab experiments were transferred to a continuous process in a miniplant. The miniplant was operated continuously; the reaction was performed at 15 bar syngas pressure and a temperature of 95 °C. The residence time of the reactants in the reactor was kept at about 1 h. This was achieved by adjusting a constant alkene feed of 100 g/h and a recycle stream of 500 g/h in total.

In the following, the results focus on three issues: a comparison with the semibatch experiments, phase separation and catalyst leaching, and additional observations regarding the process concept.

4.2.1. General Results and Experiment Comparison. The main results of the miniplant operation are shown in Figure 9. Herein, the results of the GC analysis of the product concentration in the top (Pos. 11a in Figure 5) and bottom phase (Pos. 11b in Figure 5) of the settler are depicted. A stable miniplant operation was difficult to achieve, and steady-state was reached only between 40 and 70 h of operation.

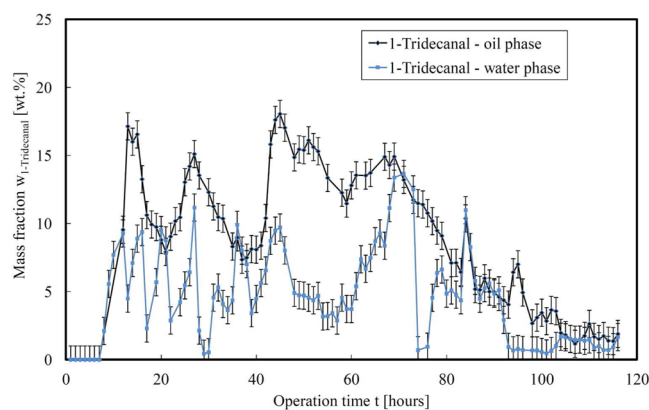


Figure 9. Miniplant operation results; tridecanal concentration in top and bottom sample position of the settler.

When the results to the batch experiments at similar conditions are compared, some differences become apparent. First, a predicted yield of 14% was successfully obtained and no catalyst deactivation during the entire operation time-span was observed. However, the selectivity of linear versus branched aldehyde was only around 93.3:6.6. This result is lower than that of the lab-scale semibatch experiments in section 4.1.2 (98:2). Additionally, during the operation large amounts (up to 20 wt %) of the side product *n*-dodecane were produced. This was not observed in the lab-scale experiments. As discussed in ref 29, reasons for this increased hydrogenation is a shift in the syngas composition of the reactor in combination with the higher reaction temperature.

4.2.2. Phase Separation and Catalyst Leaching. The second important step of the process is the phase separation in the mixer–settler. The goal therefore is to achieve high amounts (>95 wt %) of the organic components, such as *iso*/1-dodecene, aldehydes and *n*-dodecane, in the product phase. As described in section 4.1, the ideal separation region for the applied mixture with the surfactant Marlipal 24/70 is small (roughly 4 K). Thus, the control of the phase separation for a long time period is challenging, especially with a change in the composition of the system.

Nevertheless, a successful operation could be achieved. Figure 10 shows an excerpt from Figure 9 in which the

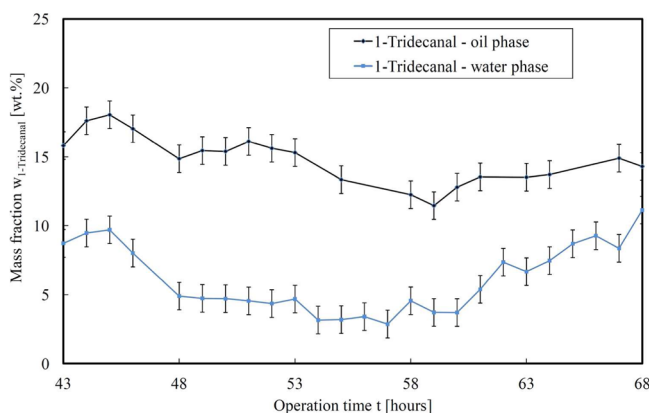


Figure 10. Miniplant operation results with stable phase separation.

separation was kept stable for more than 24 h. During this duration, the process was kept in steady-state. The organic components in the product phase amounted to the desired values between 95 and 99 wt %. Also the desired 99.99% of the catalyst remained in the catalyst phase. The rhodium loss was partially below the detectability limit of the ICP-MS (0.03 ppm for Rh), which is similar to lab-scale results and therefore considered to be a very successful result. For future investigations, increased effort will be made to keep the process stable.

Moreover, looking back at Figure 9, the difficulty of stabilizing the phase separation for a longer time period also is apparent. The main reason for this is the shift of the ideal separation behavior with temperature and changing concentrations of reactants and products. Because the analysis of the concentrations with the GCs took 30–45 min, a prediction of the current state of the plant was difficult.

Obviously, with a nonfunctioning phase separation, the catalyst leaching in the product phase is very high. The more catalyst is lost, the less is available for the reaction. This leads to

a lower yield, which can clearly be seen in Figure 9 after 70 h of operation.

4.2.3. Additional Observations. The stable continuous operation for over 24 h is seen as a success because a short-term proof of concept has been achieved, the reaction results were in the desired range, and the phase separation was kept stable. For future investigations, the stabilization of the phase separation is of utmost importance to perform a long-term proof of concept. Strategies such as applying online Raman-spectroscopy for compositive measurements combined with model-predictive control are taken into consideration.

The long-term operation of the miniplant revealed several effects that are highly important for the success of the process concept. Because the applied surfactant consists of a mixture of homologues, a fractioning occurs during the phase separation step. In test tube experiments, where no material is removed, such observations are not possible. In the miniplant, on the other hand, this effect becomes noticeable after a certain time period because of the shift of the optimal operating point. For future long-term operations, continuous surfactant feeding as well as strategies for additional surfactant separation from the product phase must be considered to counter this effect.

Another revealed effect was the occurrence of foam. In a previous setup of the miniplant, the catalyst phase was led to a recycle container. Here it was flashed and foam was created. The CO and H₂ still solved in the liquid degas because of the lower pressure. This has several drawbacks such as poor heat- and mass-transfer characteristics, and transport of mass with the available pumps is barely possible. First approaches to avoid the creation of foam were to remove the recycle container and thus directly feed the recycle phase into the reactor (thus resulting in the setup of Figure 5). Second, the stirrer speed was lowered to prevent foaming in the reactor due to the gassing stirrer. Third, the product phase is led directly into a larger flash with a possible injection of antifoam. Thus, pressure-release issues due to foam blocking were avoidable. These structural and process operating strategy changes have proven to be successful, and no foam was observed in the miniplant operation with the setup from Figure 5.

5. CONCLUSIONS AND OUTLOOK

In summary, we have shown that microemulsion systems are feasible reaction media for the rhodium-catalyzed hydroformylation of 1-dodecene. A nonionic surfactant is able to solubilize the hydrophobic substrate in an aqueous environment and thus supports the catalytic reaction and facilitates catalyst recycling in its active form. We investigated in lab-scale experiments the influence of pressure and temperature on the hydroformylation in a multiphase system formulated from 1-dodecene, water, and the nonionic surfactant Marlipal 24/70. We were able to show that a decrease of syngas pressure from 40 to 15 bar leads to an increase of catalyst activity. Furthermore, changing the reaction temperature in microemulsion systems influences not only the kinetics but also the phase behavior of the reaction system. Choosing the right process window is crucial for the activity and selectivity of the catalyst. The results of the lab-scale experiments established the basis for a continuous reaction process using surfactant systems. Finally, the proof of concept was successfully performed in the continuously operated miniplant. The results for the reaction were in the desired range, and the phase separation was kept stable for a time frame of 24 h. During this period, no rhodium loss into the product phase could be detected. However,

stabilizing the phase separation for a longer time period is still a challenging task. Therefore, new feeding strategies and methods of analysis for the surfactant as well as an optimization of the settler have to be considered.

AUTHOR INFORMATION

Corresponding Author

*E-mail: tobias.pogrzeba@tu-berlin.de.

Notes

The authors declare no competing financial interest.

ACKNOWLEDGMENTS

This work is part of the Collaborative Research Centre "Integrated Chemical Processes in Liquid Multiphase Systems" coordinated by the Technische Universität Berlin. Financial support by the Deutsche Forschungsgemeinschaft (DFG) is gratefully acknowledged (TRR 63). Furthermore, the authors gratefully acknowledge the support of the company Umicore for sponsoring the rhodium catalyst "Acetylacetonato-dicarbonylrhodium(I) (CAS: 14874-82-9)" and the company Sasol for the surfactant used in the described experiments. Additionally, the authors also acknowledge the support of SIEMENS for sponsoring the entire process control system SIMATIC PCS7 for the miniplant.

REFERENCES

- (1) Roelen, O. Verfahren zur Herstellung von sauerstoffhaltigen Verbindungen. 849548, 1949.
- (2) Roelen, O. Production of oxygenated carbon compounds. U.S. Patent 2,327,066, 1943.
- (3) Evans, D.; Osborn, J.; Wilkinson, G. *J. Chem. Soc. A* **1968**, 566 (1966), 3133–3142.
- (4) Weitkamp, J.; Gläser, R. In *Winnacker/Kuechler. Chemische Technik: Prozesse und Produkte*; Dittmeyer, R., Keim, W., Kreysa, G., Oberholz, A., Eds.; WILEY-VCH Verlag: Weinheim, 2004; pp 47–49.
- (5) Cornils, B.; Hibbel, J.; Konkol, W.; Lieder, B.; Much, J.; Schmidt, V.; Wiebus, E. Verfahren zur Herstellung von Aldehyden. DE3234701, 1982.
- (6) Hamerla, T.; Rost, A.; Kasaka, Y.; Schomäcker, R. *ChemCatChem* **2013**, 5, 1854–1862.
- (7) Rost, A.; Müller, M.; Hamerla, T.; Kasaka, Y.; Wozny, G.; Schomäcker, R. *Chem. Eng. Process.* **2013**, 67, 130–135.
- (8) Müller, M.; Kasaka, Y.; Müller, D.; Schomäcker, R.; Wozny, G. *Ind. Eng. Chem. Res.* **2013**, 52, 7259–7264.
- (9) Fell, B.; Papadogianakis, G. *J. Mol. Catal.* **1991**, 66 (2), 143–154.
- (10) Van Vyve, F.; Renken, A. *Catal. Today* **1999**, 48 (1–4), 237–243.
- (11) Haumann, M.; Jakuttis, M.; Franke, R.; Schönweiz, A.; Wasserscheid, P. *ChemCatChem* **2011**, 3 (11), 1822–1827.
- (12) Schwarze, M.; Pogrzeba, T.; Seifert, K.; Hamerla, T.; Schomäcker, R. *Catal. Today* **2015**, 247, 55–63.
- (13) Schomäcker, R.; Schwarze, M.; Nowothnick, H.; Rost, A.; Hamerla, T. *Chem. Ing. Tech.* **2011**, 83 (9), 1343–1355.
- (14) Potier, J.; Menuel, S.; Chambrier, M. H.; Burylo, L.; Blach, J. F.; Woisel, P.; Monflier, E.; Hapiot, F. *ACS Catal.* **2013**, 3 (7), 1618–1621.
- (15) Potier, J.; Menuel, S.; Monflier, E.; Hapiot, F. *ACS Catal.* **2014**, 4, 2342–2346.
- (16) Vanbésien, T.; Monflier, E.; Hapiot, F. *ACS Catal.* **2015**, 5 (7), 4288–4292.
- (17) Kunna, K.; Müller, C.; Loos, J.; Vogt, D. *Angew. Chem., Int. Ed.* **2006**, 45, 7289–7292.
- (18) Kahlweit, M.; Strey, R.; Busse, G. *J. Phys. Chem.* **1990**, 94 (1), 3881–3894.
- (19) Schwarze, M.; Pogrzeba, T.; Volovych, I.; Schomäcker, R. *Catal. Sci. Technol.* **2015**, 5, 24–33.
- (20) Sottmann, T.; Stubenrauch, C. In *Microemulsions: Background, New Concepts, Applications, Perspectives*; Stubenrauch, C., Ed.; John Wiley & Sons: Chichester, 2009.
- (21) Hamerla, T.; Schwarze, M.; Schomäcker, R. *Chem. Ing. Tech.* **2012**, 84 (11), 1861–1872.
- (22) Nowothnick, H.; Rost, A.; Hamerla, T.; Schomäcker, R.; Müller, C.; Vogt, D. *Catal. Sci. Technol.* **2013**, 3 (3), 600.
- (23) Schomäcker, R.; Holmberg, K. In *Microemulsions: Background, New Concepts, Applications, Perspectives*; Stubenrauch, C., Ed.; John Wiley & Sons: Chichester, 2009.
- (24) Müller, D.; Minh, D. H.; Merchan, V. A.; Arellano-Garcia, H.; Kasaka, Y.; Müller, M.; Schomäcker, R.; Wozny, G. *Chem. Eng. Sci.* **2014**, 115, 127–138.
- (25) Goedheijt, M. S.; Kamer, P. C. J.; van Leeuwen, P. W. N. M. *J. Mol. Catal. A: Chem.* **1998**, 134, 243.
- (26) Deshpande, R. M.; Kelkar, A. A.; Sharma, A.; Julcour-lebigue, C.; Delmas, H. *Chem. Eng. Sci.* **2011**, 66 (8), 1631–1639.
- (27) Markert, J.; Brunsch, Y.; Munkelt, T.; Kiedorf, G.; Behr, A.; Hamel, C.; Seidel-Morgenstern, A. *Appl. Catal., A* **2013**, 462–463, 287–295.
- (28) Hamerla, T. *Hydroformylierung langkettiger Olefine mit zweizähligen Rhodium-Komplexen in mizellaren Lösungen und Mikroemulsionen*. Ph.D. Dissertation, Technische Universität Berlin, 2014.
- (29) Müller, D.; Esche, E.; Pogrzeba, T.; Hamerla, T.; Barz, T.; Schomäcker, R.; Wozny, G. In *20th International Conference Process Engineering and Chemical Plant Design*, Berlin, 2014. ISBN: 978-3-00-047364-7.

PAPER 2

Systematic Phase Separation Analysis of Surfactant-Containing Systems for Multiphase Settler Design

David Müller, Erik Esche, Tobias Pogrzeba, Markus Illner, Felix Leube, Reinhard Schomäcker, and Günter Wozny

Industrial & Engineering Chemistry Research, 2015, 54, 3205-3217

Online Article: <http://pubs.acs.org/doi/10.1021/ie5049059>

ActiveView PDF: <http://pubs.acs.org/doi/ipdf/10.1021/ie5049059>

Reproduced (or 'Reproduced in part') with permission from "Systematic Phase Separation Analysis of Surfactant-Containing Systems for Multiphase Settler Design; David Müller, Erik Esche, Tobias Pogrzeba, Markus Illner, Felix Leube, Reinhard Schomäcker, and Günter Wozny. Industrial & Engineering Chemistry Research, 2015, 54, 3205-3217." Copyright (2015) American Chemical Society.

Systematic Phase Separation Analysis of Surfactant-Containing Systems for Multiphase Settler Design

David Müller,^{*,†} Erik Esche,[†] Tobias Pogrzeba,[‡] Markus Illner,[†] Felix Leube,[†] Reinhard Schomäcker,[‡] and Günter Wozny[†]

[†]Chair of Process Dynamics and Operations, Technische Universität Berlin, Straße des 17. Juni 135, Sekr. KWT-9, D-10623 Berlin, Germany

[‡]Department of Chemistry, Technische Universität Berlin, Straße des 17. Juni 124, Sekr. TC-8, D-10623 Berlin, Germany

ABSTRACT: The handling of multiphase systems applied in mixer–settler processes, in which phase separation characteristics are exploited, is to date still a challenge for the chemical industry. Approaches for analyzing the influencing parameters on these systems can be of use, especially regarding equipment design and technical applicability. In this contribution, a guideline is presented and applied in a case study for a surfactant-containing multiphase system implemented in a hydroformylation mini-plant. Herein, the most relevant investigated parameters such as temperature, concentrations of reactants, system pressure, and stirrer characteristics are analyzed. This is followed by an analysis of various internal fittings including their influence on the temperature profile within the settler. The results of the systematic analysis are used to design a highly flexible, modular, and efficient settler for the separation of up to three liquid phases.

1. INTRODUCTION AND MOTIVATION

The exploitation of multiphase separation characteristics is increasingly investigated in various fields in the chemical industry. Examples can be found both in academic contributions by Zagajewski et al.,¹ Rost et al.,² Brunsch et al.,³ and Haumann et al.⁴ as well as industry-oriented contributions by Kohlpainter et al.⁵ or Hirasaki et al.⁶ In most cases, an isolation of the product after a reaction or a separation of the applied catalyst from the reactants is desired. Descriptions of the phase separation characteristics of these systems is therefore of the utmost importance. Unfortunately, the correct thermodynamic modeling and simulation of these multiphase systems remains a challenge today.⁷ Larger amounts of knowledge originate from empirical studies or heuristics, which of course are cost intensive in terms of time and financial and chemical resources. This becomes especially critical when larger scale investigations are necessary in the form of mini-plant or pilot-plant operations.

One important area of multiphase systems is that of microemulsions. Therefore, in the following an approach to systematically analyze surfactant-containing multiphase systems regarding their applicability for technical application and pilot-plant operation in mixer–settler processes will be presented. In this contribution, it is assumed that the desired surfactant for the formulation of the microemulsion system is already selected. The primary goal is to reduce the necessary amount of experiments analyzing the influence of the surfactant on the phase separation to facilitate equipment design and operation point specifications. In the meantime, a secondary goal is to help bridge the gap between engineers and chemists regarding the focus of required experiments during the process development phase.

Based on the example of the hydroformylation of 1-dodecene in microemulsion systems, a guideline is given on how to investigate complex multiphase systems and take advantage of

them in continuous processes. This is followed by the design of a multiphase settler and its modification with respect to an accelerated phase separation. Lastly, the installation of the settler into a mini-plant at Technische Universität Berlin is presented.

2. ANALYSIS OF MICROEMULSION SYSTEMS

Preceding the discussion of a systematic guideline, a short review of the general phase separation characteristics of water–oil–surfactant systems will be given at this point. These separation characteristics are used as a basis for the subsequent guideline.

2.1. General Phase Separation Characteristics of Water–Oil–Surfactant Systems. By adding a surfactant to a mixture of oil and water, a microemulsion can be formed.⁸ On a macroscopic scale a microemulsion is regarded as homogeneous (a single phase system), despite being heterogeneous on a microscopic scale with coexisting, nanometer-thin hydrophobic and hydrophilic layers. The surface area of these domains is comparatively large and is occupied by a monolayer of surfactant molecules. However, the whole structure remains highly dynamic and is able to disintegrate and reshape within milliseconds.⁹ The microemulsion may act as a manipulable solvent, which not only increases the interfacial area during a reaction but also changes its phase separation behavior for different temperatures and surfactant concentrations. The latter allows for the possibility to adjust the reaction system between different process steps with varying requirements.¹⁰ Thus, mixer–settler-based process concepts,

Received: December 18, 2014

Revised: March 6, 2015

Accepted: March 11, 2015

Published: March 11, 2015

exploiting these characteristics, are developed in which water-soluble catalysts are applied to help react an oily educt.¹¹

In general, the phase separation characteristics of microemulsion systems can be described by Kahlweit's fish.^{12,13} The fish diagram is a slice of the Gibb's phase prism for oil–water–surfactant systems at an oil-to-water ratio of 1:1. The slice shows the different phase states at various temperatures and surfactant concentrations. Figure 1 shows a sketch of Kahlweit's

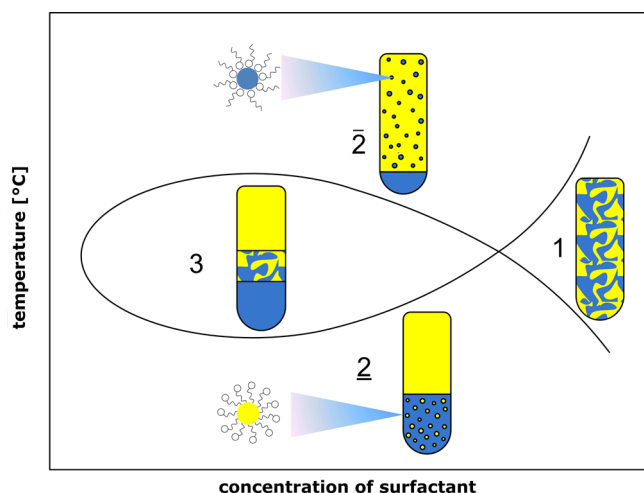


Figure 1. Qualitative image of Kahlweit's fish indicating different possible separation states of microemulsion systems.²

fish describing these possible separation states. Knowledge on these states is of importance for mixer–settler processes as their applicability varies.

According to Kahlweit's fish a two-phase region (2) is created at moderate surfactant concentrations and low temperatures. This implies a water- and surfactant-rich microemulsion at the bottom and an oil-rich phase on top. The surfactant is mainly dissolved in the water-rich phase due to its higher solubility there at lower temperatures. Hence, an oil-in-water (o/w) microemulsion is formed. This regime can be desired for the product separation step of a mixer–settler process as a pure product phase can be removed while recycling the surfactant and water (dissolved catalyst). If the temperature is increased, the three-phase region (3) is reached. Here, the lowest phase mainly consists of water. The surfactant bulk is suspended in the middle phase, which is yet again a microemulsion. Just as in (2), an oil-rich top phase is created, rendering this region also applicable for the separation step of a mixer–settler process.

The other two regions illustrated in Kahlweit's fish are the single-phase region on the right-hand side (entire mixture is a microemulsion) and the upper two-phase (2) region. In the latter, the surfactant lies dissolved in the top phase, which is a water-in-oil (w/o) microemulsion. Here, a separation would lead to great surfactant and water loss with the product phase, which could be detrimental for a process from an economic point of view.

With the information in mind regarding the general phase separation characteristics of oil–water–surfactant systems, the goals for research and analysis regarding process and equipment design become clear.

2.2. Systematic Phase Separation Analysis. As mentioned before, the aim is to provide a systematic approach to empirically analyze surfactant-containing systems with regards to their applicability for an actual mixer–settler process. Some ideas of this guideline concerning relevant investigation topics and equipment design issues can already be found in several contributions. Among these are papers by Kahlweit et al.¹⁴ and Sottmann et al.,¹³ in which the different aspects of nonionic technical-grade surfactants are analyzed. Important results concerning phase behavior and observability issues such as conductivity measurements in the different phase separation regions are discussed by the authors. Furthermore, in Müller et al.¹⁵ steps concerning operating point determination for mini-plants are discussed. Schlieper et al.,¹⁶ Mungma et al.,¹⁷ and Gerth and Heikamp¹⁸ show results concerning internal fittings (plates) and other coalescence acceleration in settlers, respectively. In this contribution, the different investigated issues, discussed ideas, and performed experiments are partially summarized and expanded to create a more general guideline. This guideline is divided into six steps (Figure 2).

Preceding the actual experimental analysis, the system goals for the mixer–settler system have to be defined. Hereby, the desired throughput, the maximal residence time in the settler as well as the separation quality have to be decided on. As a reminder, in this guideline it is assumed that the selection of the surfactant has already been performed. If this decision has been made, Step 2 can be carried out (Figure 3).

Hereby, a list as well as a range of interest for all influencing variables on the multiphase system in the mixer–settler process has to be set up. This step can be seen as a theoretical prescreening and definition of the investigation range. In general, the variables of interest are temperature, concentrations, pressure, and so forth; each of these variables of course has an influence on certain properties of the multiphase system in the mixer–settler process. In Figure 2, an example is given for pressure. Pressure has an influence on the reaction equilibrium and can change the overall viscosity, density, and

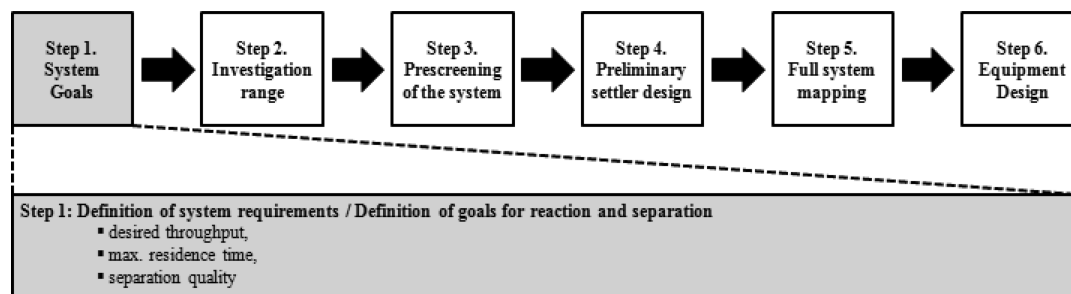


Figure 2. Step 1 of the guideline for the analysis of surfactant-containing systems.

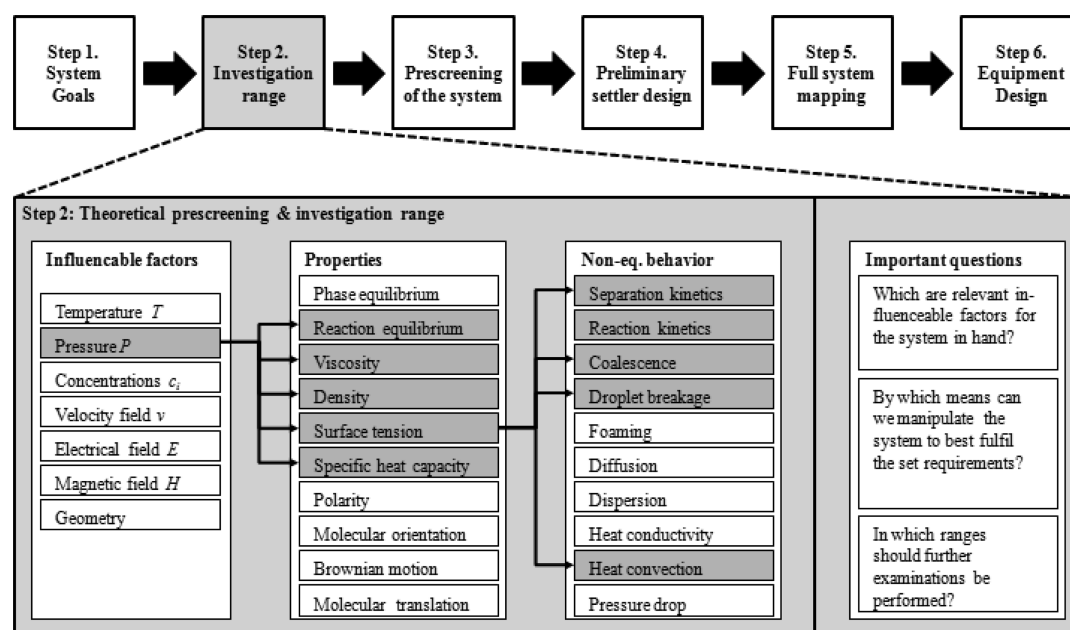


Figure 3. Step 2 of the guideline for the analysis of surfactant-containing systems.

surface tension of the system. Next, the contribution of this property on the nonequilibrium behavior of the system is characterized. A change in surface tension for example also means a change in the coalescence behavior and thus also on the separation kinetics.

The correct definition of the individual variable ranges of each of the influencing variables is crucial because it also defines the amount of required experiments. The influences can be selected and the ranges can be set depending on what is known of the thermodynamics of the system and the pure components applied. Vapor pressures, viscosities, and so forth should be checked here. In case thermodynamic data is available for the three-phase behavior of a similar system, this could be employed as an estimate. Additionally, information regarding plant specifications should be introduced. For the case that a plant already exists and solely a component switch is to be carried out, maximum pressures, throughputs, and maximum temperatures are already fixed.

After the ranges have been defined, the actual prescreening of the system is carried out. The goal is to obtain an overview of the separation characteristics of the system and thus keep the amount of required experiments low. Of interest are the following points: how long does the separation take, how large are each of the phases, where do desirable separations take place (concentrations and temperatures), and in which phase are the educts, the products, and the catalyst?

These questions can currently only be answered experimentally. First, from the authors' experience, so-called "shake and wait" experiments are of use, which can be carried out in a speedy manner. Multiple test tubes with varying compositions of the water–oil–surfactant system are prepared, immersed in thermostatic baths, and heated to temperatures within the range set above. Once the desired temperature is reached, the test tubes are removed from the bath, shaken heavily but shortly, and then returned to the bath to maintain the temperature. Afterward, the phase separation for each composition is observed for a fixed time frame. This process is repeated for several temperatures within the defined range. This way, the size of each of the phases as well as the separation

time depending on temperature and concentrations at a pseudo-equilibrium can be determined. A rough feasible operating region is thus obtained. This part of the investigation is part of "Investigation Deck 1" in Figure 4. Obviously, circumstances may exist under which systems will not separate quickly enough or as fast as desired. The experiments should therefore be limited to a certain time. This period will correspond to the maximum required residence time in an ideal settler.

The phase separation impediment may occur due to various reasons. In Figure 4 in "Observation Deck 1", several of these reasons are listed: high viscosity for certain concentrations, enhanced foaming, or surface active components. Obviously, if the system's viscosity is too high or if a large degree of foaming is noticed, a technical application becomes questionable. If such an impediment is observed, further steps are required. These may require additional investigations ("Investigation Deck 2") of the rheology of the system, degassing investigations or phase separation enhancement strategies such as applying magnetic or electric fields or even adding polarizing substances. The latter could be analyzed with spinning drop experiments. In the last mentioned cases, the "shake and wait" experiments have to be repeated under the new conditions, which unfortunately means more experiments. Again, from the author's experience, this step is inevitable but can be kept at a minimum by analyzing corner points of interest. The conclusions from this prescreening of the system are a preliminary minimal settling time τ_{\min} , the separation time τ as a rough function of temperature and concentrations as well as lower and upper temperature and concentration bounds.

In Step 4, a preliminary settler design is drafted based on the results of the preliminary screening (Figure 5). Depending on the factor with the strongest influence, a temperature controlled or concentration controlled settler should be chosen. In the former case, a common settler with a tight thermostatic control is required. In the latter case, an extraction-based system is necessary, in which a certain component needs to be added or accumulated in the settler. Additionally, it may be required to be able to measure the concentration of the mixture entering

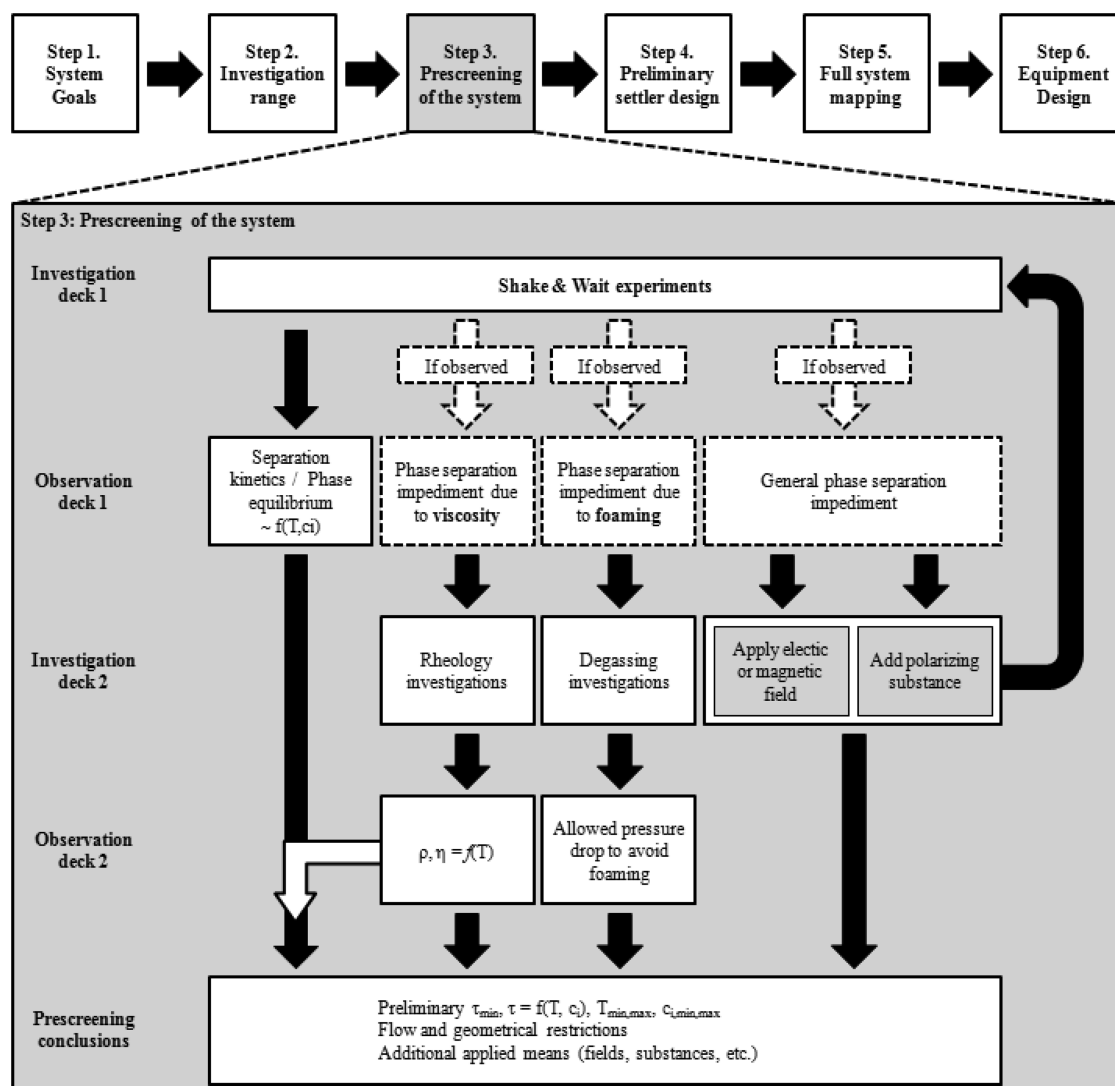


Figure 4. Step 3 of the guideline for the analysis of surfactant-containing systems.

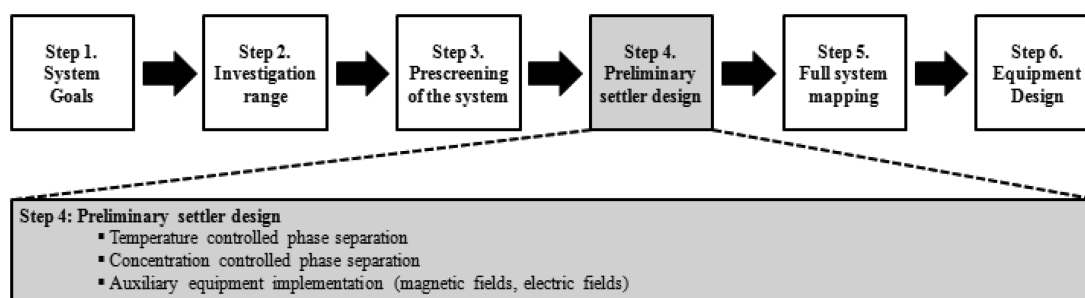


Figure 5. Step 4 of the guideline for the analysis of surfactant-containing systems.

the settler within a short time frame. For both settler types, the minimally required residence time can be estimated based on the “shake and wait” results. Furthermore, it may be necessary to consider auxiliary equipment such as magnetic or electric fields.

After determining a viable separation area regarding temperature and concentration, a more detailed mapping is required (Figure 6). For a process in which the oily components are to be removed (such as the process presented in the following chapter) this means two things: the phase

separation has to be adequately fast and the established product phase must be large and pure enough for removal from the process. The idea is to perform a detailed analysis of the phase separation dynamics in the sense of determining how quickly the desired phase is established. Then, step by step, different factors are analyzed. Among these are factors such as the stirrer type and speed. An important step in mixer–settler processes is the formation of the mixture which accompanies the reaction step. Conventionally, continuously stirred tank reactors are applied for the mixing. A higher stirrer speed in the reactor

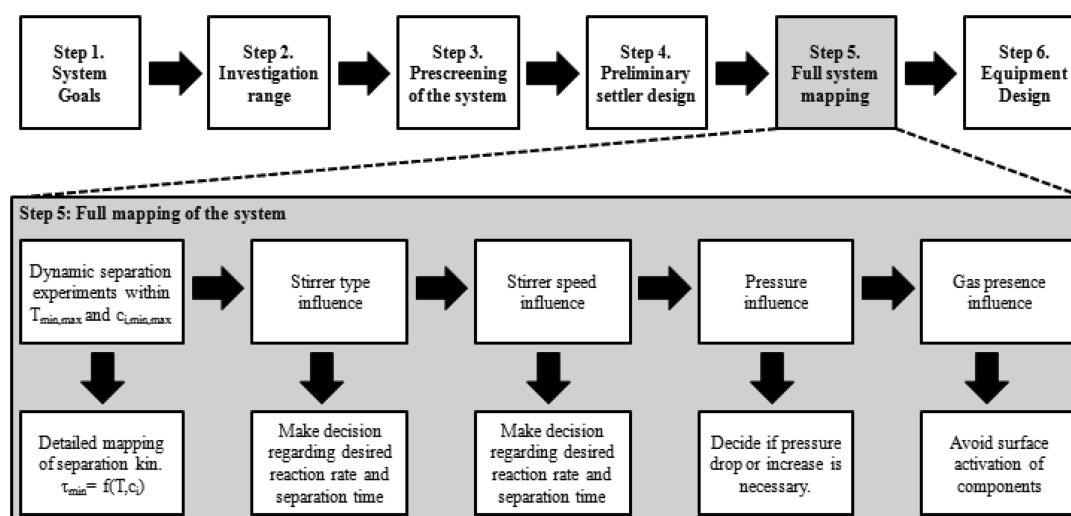


Figure 6. Step 5: Full mapping of the system.

implies a decrease of the droplet size of the emulsion and hence an increase in the overall reaction rate (a plateau or maxima may be reached as well).¹⁹ However, too high stirrer speeds may cause a too effective breakage of the droplets leading to the establishment of a stable microemulsion. In these cases, the separation time increases drastically. An optimum has to be found, at which the reaction can effectively be carried out and the required separation time does not cause an overly large hold-up of the settler. Next, total system pressure is important. Often enough, low to medium pressure has a negligible influence on the thermodynamic equilibrium of the phase separation. Nevertheless, influences on the separation dynamics due to the physically solved gas in the system are possible, which is an issue relevant for process design. It has to be remarked that additional influences can appear depending on the system. The stirrer type may have a tremendous influence the formation of the emulsion. Furthermore, partial pressures of various gases can change the behavior of the system entirely by catalyst surface activation or else. Hence, if relevant for the investigated system, these aspects should be included in the analysis.

With this information, the settler can then be designed in more detail in the final step, Step 6. Three main aspects should be considered: general operability, observability, and controllability of the phase separation. The operability should consider issues such as desired minimum and maximum liquid flow rate, minimum phase height, or required pressure resistance of the apparatus. Regarding observability, different strategies can be employed. Besides common pressure and temperature sensors, these could be gauge glasses to visually observe the quality of the phase separation, conductivity measurements at certain positions in the settler, or fast, continuous concentration measurements, for example, by Raman spectrometry. If gauge glasses or something similar are implemented, these can be enhanced by camera observation techniques with a connection to the process control system of the plant. Finally, regarding the controllability of the settler, methods for heating and cooling via thermostats or purposefully placed feeds to manipulate concentrations are thinkable. This of course has to be in accordance with the observation techniques applied. Additionally, if the separation dynamics are strongly influenced by any of the factors mentioned in Step 5, internal fittings should be considered in the settler. Different types exist, such as plates,

knitted fabrics, or baffles. These can drastically enhance the phase separation in the settler, reducing its necessary size.¹⁷

The application of this guideline is now shown in the following on a case study for the hydroformylation of long-chain alkenes in microemulsion systems.

3. CASE STUDY: HYDROFORMYLATION IN MICROEMULSION SYSTEMS

The previously presented guideline is applied on the example of a microemulsion system in which the rhodium-catalyzed hydroformylation of 1-dodecene is performed. First, the exact concept of the mixer–settler process as well as the applied substances are discussed. This is followed by an execution of the six steps to finally present a fully designed settler.

3.1. Investigated Process Concept and Applied Substances. The process concept discussed herein is concerned with the reaction known as hydroformylation. Hydroformylation is the coincident addition of carbon monoxide and hydrogen to an unsaturated hydrocarbon, thus forming either a linear or a branched aldehyde (Figure 7).²⁰

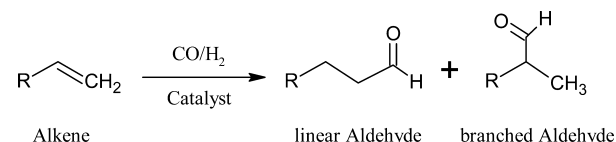


Figure 7. Concept of the reaction of alkenes with a transition metal catalyst.

These can be converted to alcohols, which are vital intermediate products in the chemical industry to produce detergents, softening agents, flavors, and other chemicals in further processing steps.

The production of aldehydes from short chain alkenes like propylene and butylene is nowadays one of the largest applications of homogeneous catalysis in chemical industry with a production of over 10 to 12 million metric tons per year.^{21,22} The challenging task of quantitative recovery of the expensive rhodium catalyst was solved in the Ruhrchemie–Rhone-Poulenc process by immobilization of the hydrophilic catalyst complex in the aqueous phase.⁵ The applicability of the process though is limited to short chain olefins (<C5) because

the solubility of higher olefins in water is poor. The process concept under investigation aims to solve this issue by applying a nonionic surfactant to promote the miscibility between the nonpolar alkene and an aqueous catalyst solution, thus increasing the interfacial area between both phases. This approach is called hydroformylation in microemulsions and is currently examined by various groups.^{23,24} Figure 8 shows the general scheme of the process concept investigated here.

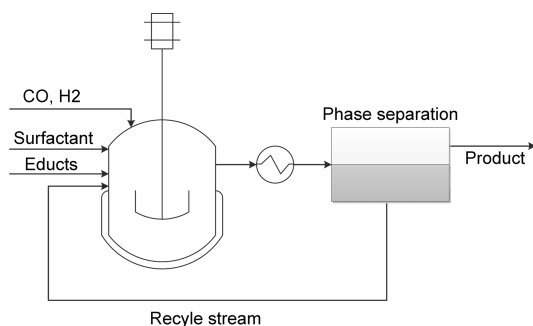


Figure 8. Process concept for the hydroformylation in microemulsions.

On a macroscopic scale, a homogeneously catalyzed reaction is performed in a two-phase system in the reactor. The reactants are subsequently led to a settler, in which the phase separation takes place. Here, the oily product phase is removed, whereas surfactant and aqueous catalyst solutions are recycled. As discussed in contributions by Müller et al.,^{15,26} the catalyst loss into the oil phase must stay at a minimum, to achieve an economically viable process. The backbone of the concept is the correct exploitation of the miscibility gap of the multiphase system. To date, it is basically impossible to operate a process such as this successfully without knowing the exact phase separation characteristics of the microemulsion system in hand.

The main chemicals applied in this study are as follows: As an educt, the linear C₁₂ alkene 1-dodecene (CAS: 14874-82-9) obtained from VWR International LLC is used. The product is the linear aldehyde 1-tridecanal (CAS: 14874-82-9), also obtained from VWR with a quality of 96%. The catalyst precursor Rh(acac)(CO)₂ (CAS: 14874-82-9) is sponsored by Umicore AG & Co. KG and the ligand SulfoXantPhos²⁶ is obtained from Molisa GmbH Magdeburg. The combination of Rh(acac)(CO)₂ with SulfoXantPhos has proven to be highly selective for the hydroformylation in aqueous reaction media leading to an *n*-aldehyde vs byproduct formation of 98:2. The surfactant applied is Marlipal 24/70 (CAS: 68439-50-9), which is sponsored by Sasol GmbH. Using these substances, the following analyses are carried out.

3.2. Steps 1 and 2: Goal Specification and Definition of the Investigation Range. As shown in Figure 2, the first step is the specification of process goals. As a mini-plant already exists, several of the process goals have already been determined.²⁵ An ideal separation time in the settler of the process lies around 0 to 90 min. Hereby, a product stream of roughly 100 to 200 g/h should be realized for the plant at TU Berlin. Next, a definition of the investigation range is carried out. The variables of interest for the system are the concentrations of educt (1-dodecene), product (1-tridecanal), surfactant, and water. Table 1 shows the according ranges, which have been specified based on results from previous investigations from Hamerla et al.^{20,25} and Rost et al.²

Table 1. Concentration Ranges

component	minimum [wt %]	maximum [wt %]
water	10	90
1-dodecene	10	90
surfactant	0	12
1-tridecanal yield	0	40

3.3. Step 3: Prescreening. As explained before, the phase behavior of a microemulsion system is a function of its composition and temperature. The challenging aspect of operating a process with these systems is the shifting of the ideal separation region to different temperatures due to concentration changes, that is, the reaction starts and product is produced, surfactant concentration changes due to purging with the product, or changing the oil-to-water ratio.

Hence, a mapping of the phase behavior is required in preparation of running a continuous process. Given that little thermodynamic data for the system on hand exists, the mapping depends solely on empirical research. For this purpose, using fully fledged factorial design of experiments, different compositions of the reaction mixture were prepared. It is known that the catalyst introduced into the system is surface active. This surface active substance hinders the coalescence of droplets during the presence of syngas. To counter this effect, 1 wt % Na₂SO₄ is added to all mixtures. The relevant variables hereby are the oil-to-water mass ratio (α), the surfactant mass fraction (γ), and the reaction conversion (X). The equations to calculate these values are shown in eq 1, 2, and 3, respectively

$$\alpha = \frac{m_{\text{olefin}}}{m_{\text{olefin}} + m_{\text{water}}} \quad (1)$$

$$\gamma = \frac{m_{\text{surfactant}}}{m_{\text{olefin}} + m_{\text{water}} + m_{\text{surfactant}}} \quad (2)$$

$$X = \frac{m_{\text{olefin}, t=0} - m_{\text{olefin}}}{m_{\text{olefin}, t=0}} \quad (3)$$

At this point, the “shake and wait” experiments are carried out for a wide range of temperatures and concentrations. Certain concentration regions can immediately be canceled due to various reasons:

- The temperature required for the separation is too high at very low surfactant concentrations (for our investigated surfactant).
- Low surfactant concentrations lead to a shifted temperaturewise operation region for the activated catalyst.
- A too low oil-to-water ratio leads to a small oil phase. In the actual settler apparatus, a removal of the oily components becomes difficult.
- At oil-to-water ratios below 30%, strong foaming of the system is observed.
- Too high surfactant concentrations quickly yield the undesired one phase region.

This leads to the conclusion that an oil-to-water ratio should lie between 40 and 60% and a surfactant concentration definitely above 6 but below 10 wt % should be analyzed in greater detail. Furthermore, Figure 9 shows a detailed result in which the temperature behavior around the region of interest for a fixed composition is displayed. Here, the two displayed surfaces show the phase boundary between water and mixture as well as between mixed and product phase. The upper surface is of interest for the process. The region where this “valley” is

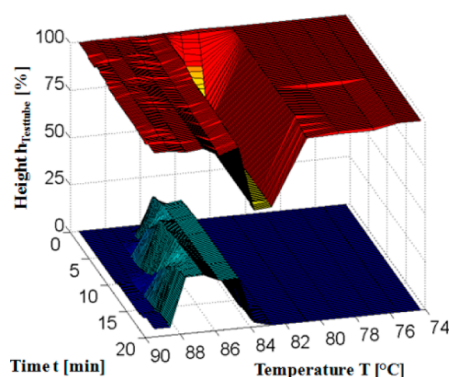


Figure 9. Experimental results for a mixture consisting of $\alpha = 50\%$, $\gamma = 9\%$, and $X = 0\%$.²⁷

created is ideal for operation as the largest product phase is created there.

3.4. Step 4: Preliminary Settler Design. Moving on, a critical conclusion is drawn from the detailed experimental result shown Figure 9: the system has a high temperature sensitivity. To operate the process continuously and to obtain a considerable product phase, the process must be operated within the “valley” of the top surface, which in this case implies a temperature window of 4K for the process. Thus, a temperature-controlled design is selected for the settler.

3.5. Step 5: Full Mapping. Based on the previous results, the region of interest shown Table 1 is narrowed to a domain in which the separation and reaction are ideal (Table 2). Next to a

Table 2. Modified Concentration Ranges

component	minimum [wt %]	maximum [wt %]
water	40	60
1-dodecene	40	60
surfactant	6	10
1-tridecanal yield	0	40

closer specification of concentrations, an analysis of pressure and stirring influence is also required (Table 3). Hereby, the

Table 3. Ranges for Other Influencing Factors

influence factor	minimum	maximum	unit
temperature	60	110	°C
pressure	1	100	bar (abs)
stirrer speed	700	1500	rpm

focus lies on the separation dynamics of the system. The faster a separation occurs, the larger the throughput and, thus, the higher the economic viability of the process concept can be.

An oil phase height of at least 20% is required after 20 min of separation in the settler. Knowledge on the shift of this 4 K window is needed for a stable operation. Therefore, a mapping of the lower and upper separation temperature is performed. This is schematically shown in Figure 10. The graph shows a qualitative cross section of the upper phase boundary shown in Figure 9 at 20 min of separation time.

Using linear and quadratic functions the influence of the variables is modeled. The general structure of this final function is shown in Figure 11. Thus, if the functions for lower and upper temperature bound are combined, a multidimensional

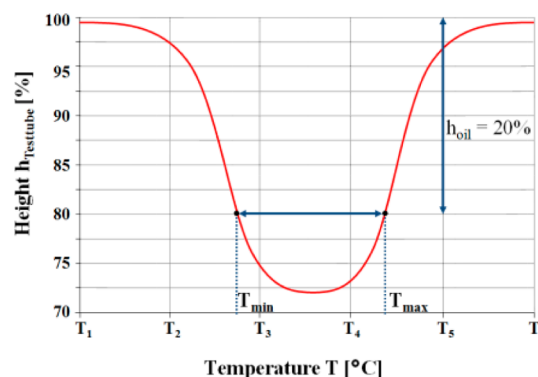


Figure 10. Schematic diagram of desired lower and upper temperature bounds.

region is created, in which the operator is allowed to operate the process.

With the information at hand regarding the suitable operating area, further analyses concerning the other influencing parameters on the phase separation are required. Among these are stirring in the reactor and system pressure. In order to analyze the influence of both on the system, an experimental setup shown in Figure 12 is used. A temperature and pressure controlled glass reactor with a gassing stirrer with four blades is used. A mixture with oil-to-water ratio α of 50%, a surfactant concentration γ of 8%, a product concentration X of 0%, and a catalyst concentration of 298 ppm with a metal to ligand ratio of 1:4 is filled into the reactor.

The mixture is heated to the previously determined operation temperature of 85 °C and continuously stirred at constant rotation speeds for 15 min. Afterward the stirrer is stopped and the phase separation is recorded for 20 min with a camera. This recording is then transferred to a PC and the phase heights are evaluated every 10 s via a MATLAB script. The procedure is repeated for stirring speeds of 700 to 1500 rounds per minute (rpm) in 200 rpm steps for 1, 5, and 10 bar absolute pressure of argon. Each experiment is performed twice to ensure reproducibility. For all experiments, results with minimal deviations were obtained. The results are summarized in Figure 13. Here, the development of the oil phase during phase separation in the reactor over time is exemplarily shown for different stirring speeds (left) and for different pressures at 1100 rpm (right).

It becomes apparent that the stirring speed in the analyzed range with the applied four-bladed gassing stirrer has no influence on the dynamics of the phase separation. The pressure on the other hand clearly has an influence on the dynamics. The relative phase height after 20 min of separation of 1 to 10 bar differs by roughly five percentage points. Higher pressures could not be investigated due to the maximum allowed pressure of the glass reactor. Given that the mini-plant shall be operated at 15 bar, the influence of the pressure on the dynamics of the phase separation is negligible. Nevertheless, coalescence enhancement is desired to increase the potential throughput of the system.

3.6. Internal Fittings and Temperature Profile Analysis. Following to the lab experiments the gathered information on phase separation characteristics was applied to design a settler for the continuous process in the mini-plant (see next section). In order to improve the performance of the settler in terms of phase separation time, various internal fittings were tested in cooperation with Rhodius GmbH.

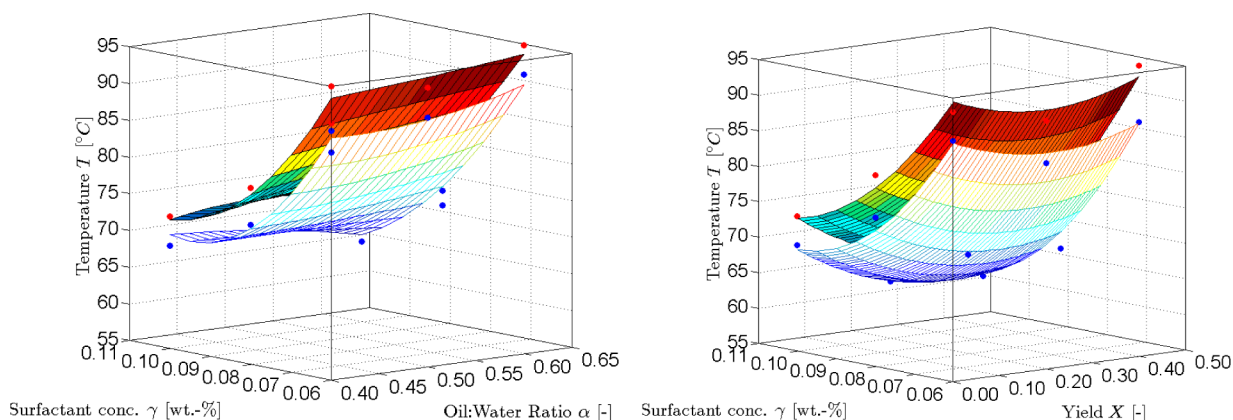


Figure 11. Temperature bound T_{\min} and T_{\max} as well as experimental data for varying fractions of α and γ at a constant degree of conversion X of 0% (left) and varying X and γ concentrations at a constant oil-to-water ratio α of 50% (right).

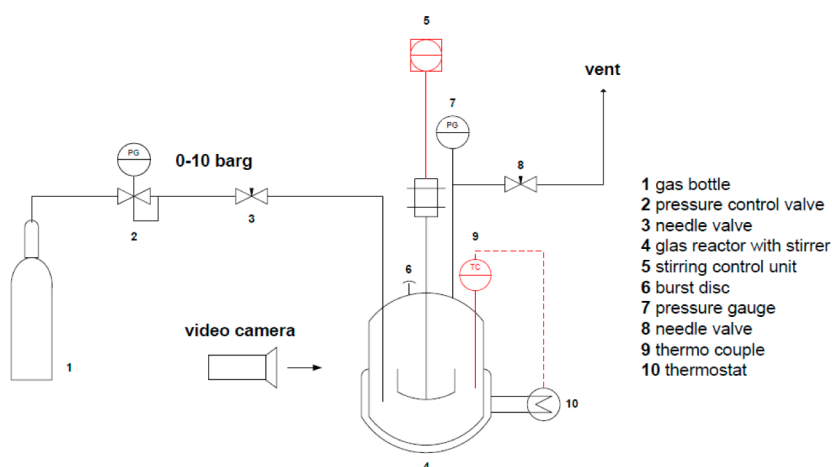


Figure 12. Experimental setup to analyze the stirrer speed and pressure influence on the phase separation.

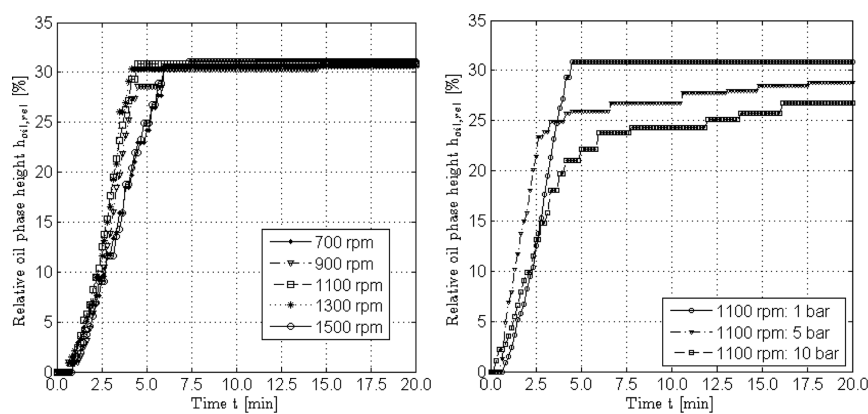


Figure 13. Relative height of the product phase at stirrer speeds from 700 to 1500 rpm for 1 bar absolute (left) and for argon pressures ranging from 1 to 10 bar absolute for 1100 rpm (right).

The experimental setup for this purpose is shown in Figure 14. The same mixture as used in the experiment before is inserted into a heated glass reactor with a volume of 1 L. The mixture is then fed into a settler (volume = 0.15 L) with a heating jacket. The settler is heated to the optimal separation temperature of 85 °C. The phase separation is then carried out, whereby different types of internal fittings and different geometries are tested.

The mixture is injected from the reactor into the settler via a pump. Depending on its frequency, the influence of various

settler residence times can be analyzed. This is quantified by measuring the height of the established oil phase in the settler at a certain residence time. Afterward, the mixture is led back to the reactor. Because the reactor volume is at least five times the size of the settler, it is assumed that no composition changes occur with the recycle of the settler streams.

Different knitted fabrics, sponsored by Rhodius, are tested in this experimental setup. The full scope of tested fabrics and internal fittings is shown in Figure 15. Exemplarily, a photo of the most relevant cases is shown in Figure 16. Starting from the

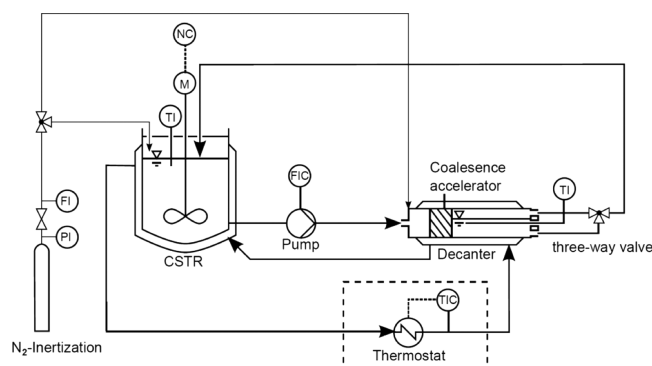


Figure 14. Experimental setup to test coalescence accelerators and internal fittings.

left, the figure shows a stainless steel accelerator (case 1). The general structure is that of a steel wool cylinder. Next to it is a combination of stainless steel and PTFE (case 2). The third is a modified stainless steel accelerator with a PTFE block in the middle (case 3). The fourth and fifth cases are modifications to analyze the influence of different geometries. Due to the successful experiments, focus is laid on cases 1 and 3.

The results of three tests are shown in Figure 17 (left). In the first test, the phase separation in an empty settler is measured. In the second, the stainless steel knitted fabric is affixed in the settler (case 1). Compared to the first test, a significant increase in the relative oil phase height is reached. In the third, the modified stainless steel fabric is analyzed (case 3). Because the centerpiece of the knitted fabric is replaced by a solid PTFE cylinder, the multiphase system is forced to pass directly along the wall of the settler. Here, the maximum oil phase height is almost immediately reached.

An explanation for these results can be found in the following deliberations: First, the stainless steel knitted fabric acts as a net. Droplets of oil or water are caught in this net or on the

steel fibers of this net. Additionally, the stainless steel net reduces the space available for the liquid flow. The liquid mass flow is increased locally and the pressure drop in the apparatus is increased as well. Thus, the probability for the coalescence of droplets is also increased. A further explanation and probably the most relevant cause for these results can be seen in Figure 15 (right). The temperature along the radius of the settler was measured for the three cases above. In the first case, a large temperature drop from top to bottom can be seen. The settler wall temperature was exemplarily set to 95 °C. At 75% settler radius, a temperature of roughly 92 °C is measured. Moving closer to the middle of the settler, the temperature drops below 80 °C. This means that the optimal separation temperature, as discussed in the previous section, is not obtained in a large part of the settler. In case of the settler without inner fixtures the separation will take more time or will not occur at all. For the other two tests, the temperature drop is not as large. The fabrics enforce a homogeneous temperature profile. The third test shows the most homogeneous temperature profile, thus enabling the best separation. This is due to the fact that the liquid has to directly pass the wall, because the middle of the settler is blocked with the PTFE cylinder. The exact positions of the temperature measurements are shown in Figure 18.

4. EQUIPMENT DESIGN

With the information gained from the systematic analysis of the system, a modular, multiphase settler is developed. The general requirements for the design of the settler can be divided into three categories: general operational criteria, automation and observability, and modularization. These requirements as well as their implementation are discussed in the following sections.

4.1. Modular Multiphase Settler. Regarding the operational criteria, the settler will be operated at up to 120 °C and at up to 20 bar. To guarantee temperature, pressure, and chemical stability, stainless steel of type EN steel no. k.h.s. DIN 1.4571 is

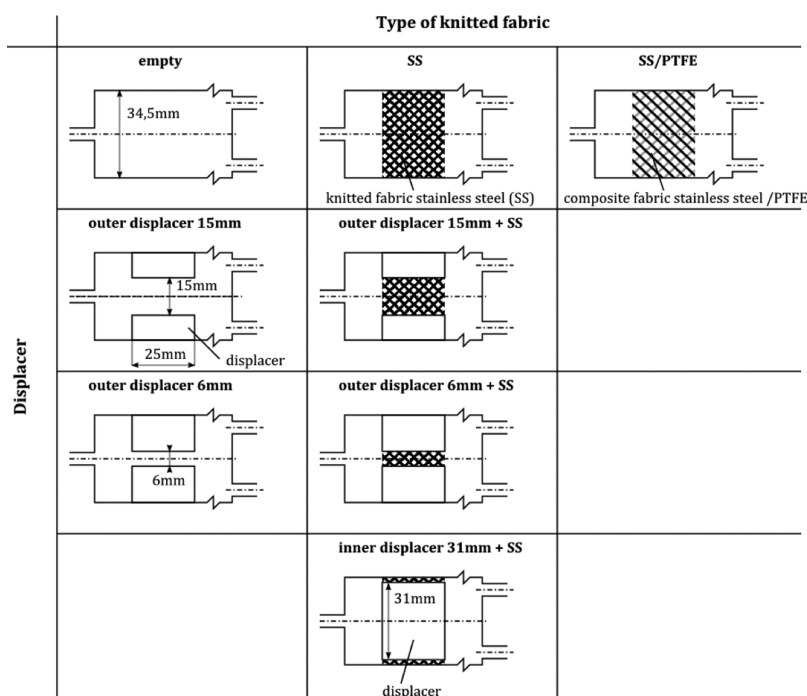


Figure 15. Settlers with different internal fittings.



Figure 16. Stainless steel (SS) fabric, SS/PTFE fabric, SS fabric with PTFE displacer inside, SS fabric with outer displacer (6 mm), SS fabric with outer displacer (15 mm).

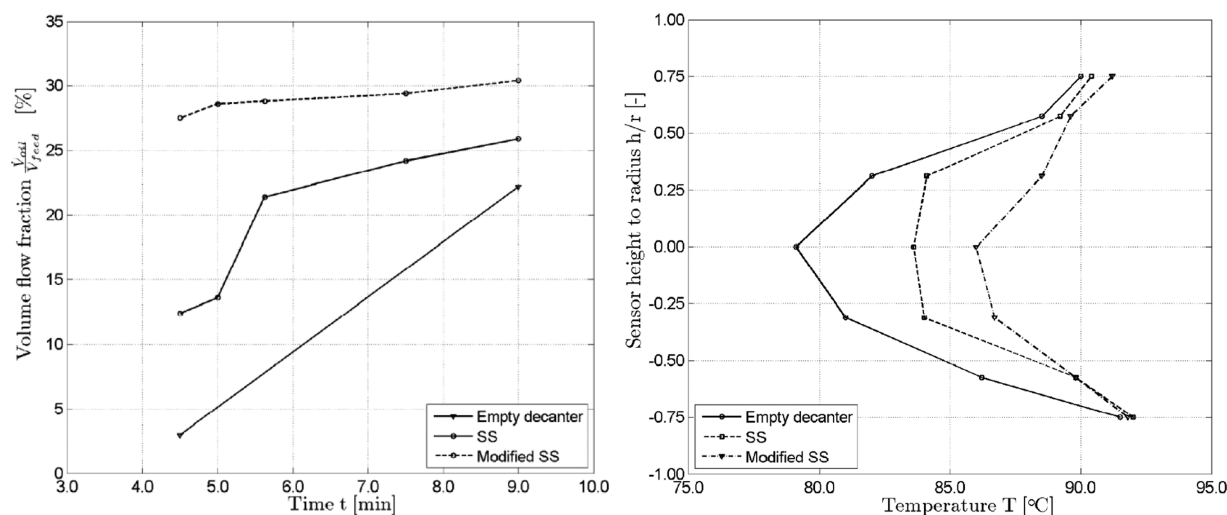


Figure 17. Comparison of the relative oil phase height over separation time (left) and temperature profile (right) in the settler for three tests: empty settler, stainless steel fabric (SS), modified stainless steel fabric (modified SS).

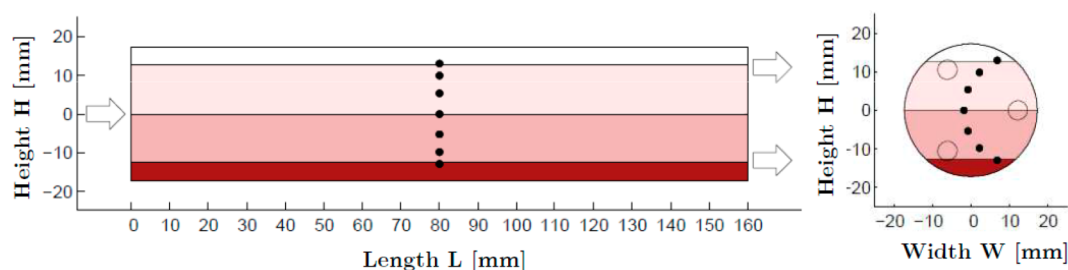


Figure 18. Temperature sensor positions in the settler. The different shades in the settler indicate the possible phases during the phase separation at the correct temperature.

used. The sealings consist of PTFE. The gauge glasses in the settler are made of borosilicate glass.

The requirements for the automation of the settler are mainly focused on the actual observability of the system. First, because the temperature has an enormous influence on the phase separation, knowledge on the temperature profile is required. Therefore, several Pt100 measurement devices are installed along the length of the settler. Each developed settler segment is connected to a thermostat. Thus, the desired temperature can be controlled and observed in each segment separately. Second, the observation of the phase separation is achieved through sight glasses.

Furthermore, to enhance the observability, a conductivity probe is installed in the top of the settler. This allows for immediate observation from the process control system once even a tiny oil phase forms at the top of the settler. Because a pressure of maximally 20 bar is allowed in the apparatus, a pressure sensor is added (plant operation at 15 bar).

Depending on the desired application, different settler modules are developed. Apart from two end pieces for feeding and removing the substances from the settler, three modules are developed. First, a module is desired in which different internal fittings and coalescence accelerators can be tested. This module mainly consists of flanges, a temperature sensor, and a double shell as a heating jacket. Differently designed internal fittings can be inserted herein. Second, a module is required for the conductivity measurement. Similarly to the first module, it features an additional temperature sensor and the double shell. The conductivity probe is inserted in the topside of the module. The third module contains two mirror-inverted sight glasses to observe the phase separation. Between each of these modules, cylindrical glass segments are used to enhance the observability. These three modules are shown in Figure 19. The inside of the settler is shown in Figure 20 as a 3D model; on the left, the inserted internal fitting is sketched, whereas on the right, the

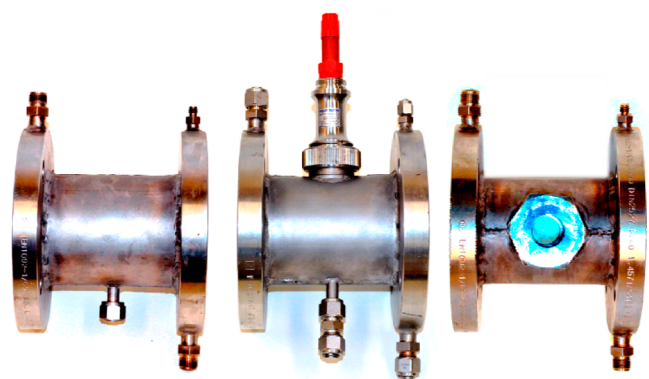


Figure 19. Settler modules: (left) empty settler module for the implementation of internal fittings, (middle) module with conductivity sensor, (right) module with sight glass.

flow of the heating fluid in the heating jacket is rendered. The settler with its end pieces is finally displayed in Figure 21.

4.2. Mini-Plant Implementation. The mini-plant at Technische Universität Berlin has already been described in greater detail in previous publications by Müller et al.^{15,27} and shall only be revisited shortly here. The implementation of the settler into the mini-plant is shown in Figure 22 in a simplified P&ID. The plant itself consists of three sections: a feed section, a high pressure section, and a product storage section.

From the feed section (units 1–5 in Figure 22), the alkene, the catalyst solution, the surfactant and the syngas are fed into the second section of the plant, the high pressure section. This part consists of the reactor, the settler and the recycle pumps (units 6–12 in Figure 22). After the reaction occurs in the reactor, the mixture is led to the settler (unit 9). The settler itself has three possible outlet streams, which can be recycled, depending on the height of each of the phases. Thus, if no separation occurs, pump 12c can be activated and the entire mixture is refilled into the reactor. If the middle phase is too large, the duty of pump 12b can be increased. This middle outlet stream has a height adjustable drain. In general, pump 12a will always be active to recycle the catalyst. The third section is the product storage section. If the phase separation is successful then the oil phase is led into unit 14, where it is stored and can be used for further investigations. Regarding automation, observation, and control, the plant is fully automated with SIEMENS' PCS 7. It incorporates over 50 sensors and actuators, including an online GC for measuring the reactor gas-phase composition and an online-Raman

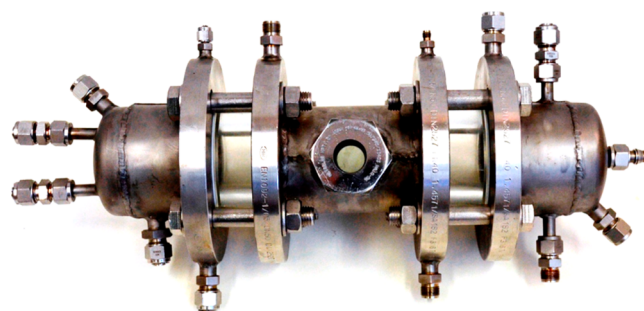


Figure 21. Settler construction with one module containing the two mirror-inverted sight glasses and the two cylindrical glasses.

spectrometer for measuring the alkene and aldehyde in the liquid entering the settler.

The combination of concentration measurements and temperature control has already proven to be successful in investigations carried out at Technische Universität Berlin. An example of the successful application can be seen in Figure 23. Here, a diagram is shown in which the temperature in the settler and gauge glass images at different points in time are compared. In the beginning, the settler temperature is roughly 82 °C. For the current concentration (measured with a GC), this is the wrong separation temperature according to the mapping shown in Figure 11 (only one phase can be monitored). The model created from this mapping recommends a temperature increase of roughly 1 K, which directly leads to the desired effect. After 30 min a phase separation can be observed in the gauge glass of the settler. After 1 h, a stable phase separation has been established and the process was operated in a desired fashion (two phase system).

The settler presented in section 3 has not been tested as a whole yet. In the future, with the relatively fast online measurement of the Raman spectrometer (below 3 min), a step toward online-optimization of the phase separation is taken. Therefore, the mapping of the optimal separation area in Figure 11 is to be used. Furthermore, the influence of the internal fittings will be exploited to establish the phase separation in the correct area as quickly as possible and thus guarantee a constant oil stream into the product tank.

5. CONCLUSIONS AND OUTLOOK

Concluding, the aim of this contribution was to present a guideline for analyzing surfactant-containing multiphase systems. The authors are aware that not all phase-separation relevant analysis topics are tackled with the guideline presented

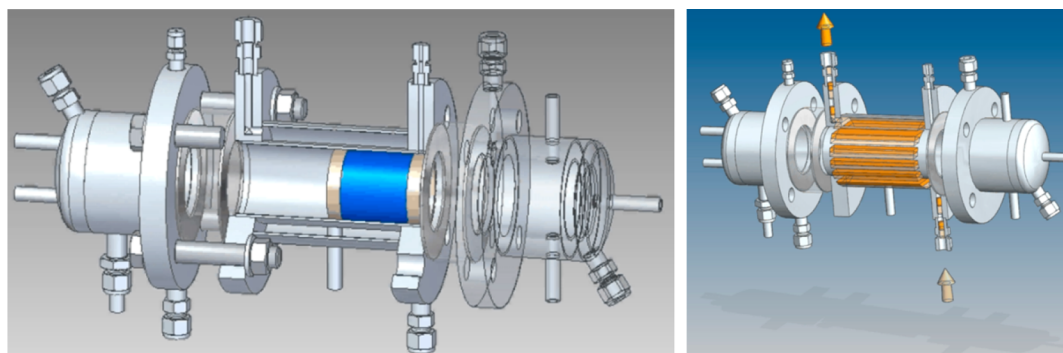


Figure 20. 3D settler: (left) with internal fitting, (right) heating fluid in the jacket of the settler.

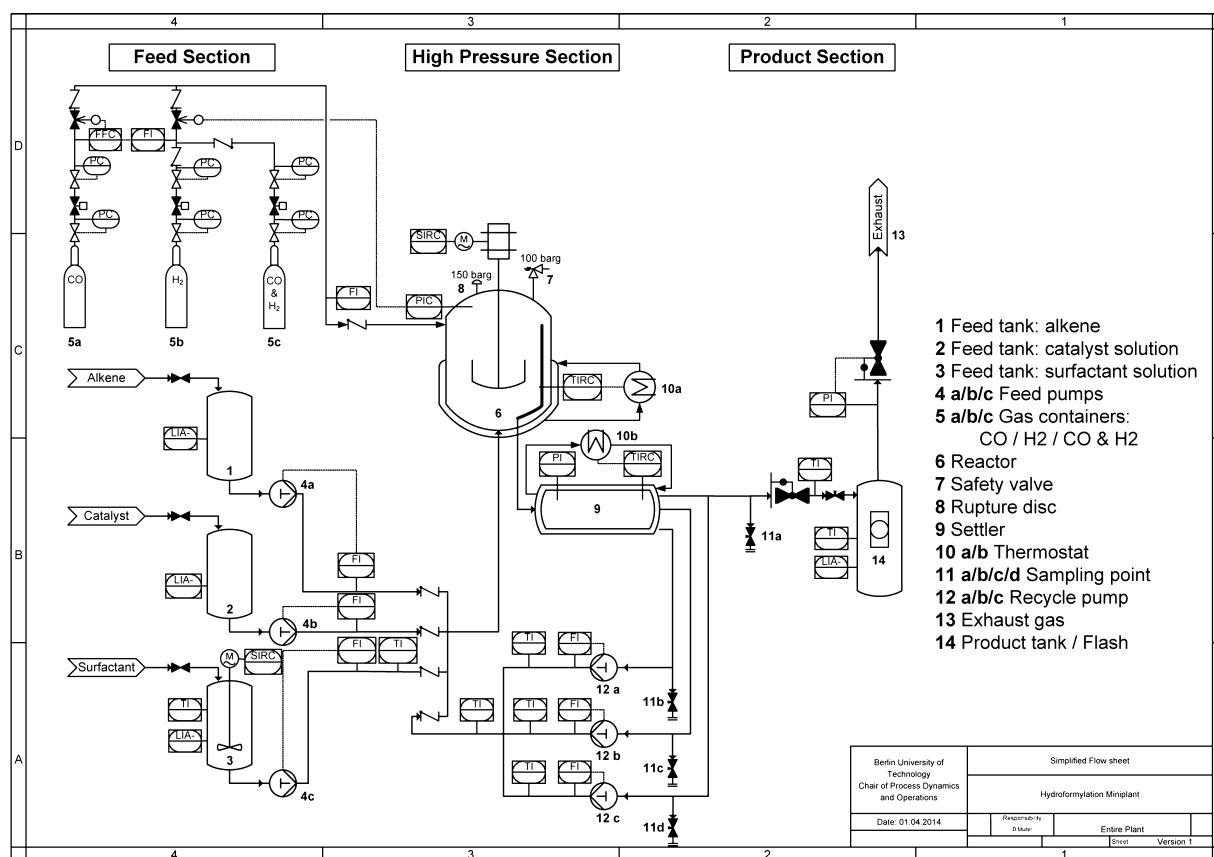


Figure 22. Simplified piping and instrumentation diagram of the hydroformylation mini-plant.

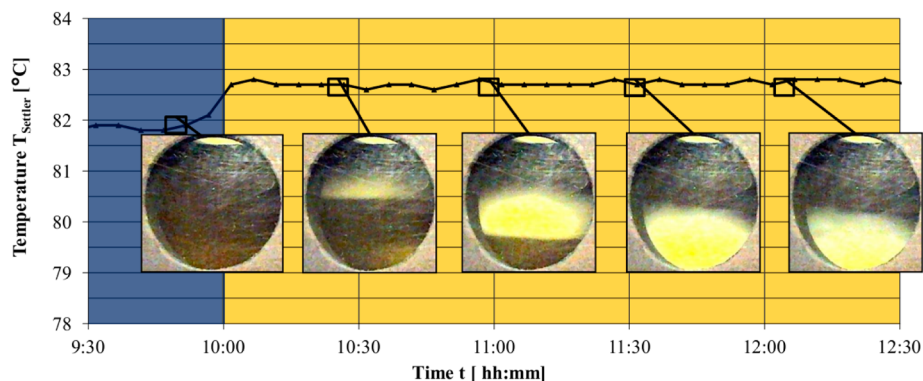


Figure 23. Gauge glass phase separation observation.

herein. Issues such as sludge accumulation and contamination or electrolyte influences were neglected. Nevertheless, we believe that with this guideline, the amount of relevant experiments is reduced and a more focused approach toward equipment design can be taken.

The guideline was successfully applied on an example of a multiphase system for a hydroformylation mini-plant, in which experiments of optimal separation temperature analysis, pressure influence analysis, and stirrer influence analysis were carried out. On the basis of the obtained results, a flexible, modular settler for the separation of the multiphase system was designed and constructed. The analysis was systematized to enable transferability to other multiphase systems for equipment design purposes.

AUTHOR INFORMATION

Corresponding Author

*E-mail: david.mueller@tu-berlin.de.

Funding

German Research Foundation (Deutsche Forschungsgemeinschaft "DFG").

Notes

The authors declare no competing financial interest.

ACKNOWLEDGMENTS

This work is part of the Collaborative Research Center "Integrated Chemical Processes in Liquid Multiphase Systems" coordinated by the Technische Universität Berlin. Financial support by the German Research Foundation (Deutsche Forschungsgemeinschaft, DFG) is gratefully acknowledged

(TRR 63). Furthermore, the authors gratefully acknowledge the support of Umicore N.V. for sponsoring the rhodium catalyst "Acetylacetonatodicarbonylrhodium(I) (CAS: 14874-82-9)", Sasol Ltd. for the surfactant used in the described experiments, the support of SIEMENS AG for sponsoring the entire process control system SIMATIC PCS7 for the automation of the mini-plant, and Rhodius GmbH for sponsoring the knitted fabrics.

REFERENCES

- (1) Zagajewski, M.; Dreimann, J.; Behr, A. Verfahrensentwicklung Vom Labor Zur Miniplant: Hydroformylierung von 1-Dodecen in Thermomorphen Lösungsmittelsystemen. *Chemie Ing. Tech.* **2014**, *86*, 449.
- (2) Rost, A.; Müller, M.; Hamerla, T.; Kasaka, Y.; Wozny, G.; Schomäcker, R. Development of a Continuous Process for the Hydroformylation of Long-Chain Olefins in Aqueous Multiphase Systems. *Chem. Eng. Process.: Process Intensif.* **2013**, *67*, 130.
- (3) Brunsch, Y.; Behr, A. Temperature-Controlled Catalyst Recycling in Homogeneous Transition-Metal Catalysis: Minimization of Catalyst Leaching. *Angew. Chem., Int. Ed. Engl.* **2013**, *52*, 1586.
- (4) Haumann, M.; Koch, H.; Hugo, P.; Schomäcker, R. Hydroformylation of 1-Dodecene Using Rh-TPPTS in a Microemulsion. *Appl. Catal., A* **2002**, *225*, 239.
- (5) Kohlpaintner, C. W.; Fischer, R. W.; Cornils, B. Aqueous Biphasic Catalysis: Ruhrchemie/Rhône-Poulenc Oxo Process. *Appl. Catal., A* **2001**, *221*, 219.
- (6) Hirasaki, G.; Miller, C. A.; Puerto, M. Recent Advances in Surfactant EOR. *SPE J.* **2011**, *16*, 889.
- (7) Sottmann, T.; Strey, R. Evidence of Corresponding States in Ternary Microemulsions of Water – Alkane – C₁₂E₈. *J. Phys. Chem.* **1996**, *39*, A39.
- (8) Kahlweit, M. Microemulsions. *Science* **1988**, *240*, 617.
- (9) Holmberg, K. Organic Reactions in Microemulsions. *Eur. J. Org. Chem.* **2007**, 731.
- (10) Schomäcker, R.; Schwarze, M.; Nowothnick, H.; Rost, A.; Hamerla, T. Mizellare Lösungen Und Mikroemulsionen Als Reaktionsmedien Für Katalytische Reaktionen. *Chemie Ing. Tech.* **2011**, *83*, 1.
- (11) Schomäcker, R.; Holmberg, K. Reactions in Organised Surfactant Systems. In *Microemulsions - Background, New Concepts, Applications, Perspectives*; Subenrauch, C., Ed.; John Wiley and Sons Ltd: Hoboken, NJ, 2009; pp 148 – 177.
- (12) Kahlweit, M.; Leßner, E.; Strey, R. Über Das Phasenverhalten Ternärer Systeme Des Typs H₂O - Öl - Nichtionisches Tensid. *Colloid Polym. Sci.* **1983**, *261*, 954.
- (13) Sottmann, T.; Lade, M.; Stolz, M.; Schomäcker, R. Phase Behavior of Non-Ionic Microemulsions Prepared from Technical-Grade Surfactants. *Tenside, Surfactants, Deterg.* **2002**, *39*, 20.
- (14) Kahlweit, M.; Strey, R.; Haase, D.; Firman, P. Properties of the Three-Phase Bodies in H₂O-Oil-Nonionic Amphiphile Mixtures. *Langmuir* **1988**, *4*, 785.
- (15) Müller, M.; Kasaka, Y.; Müller, D.; Schomäcker, R.; Wozny, G. Process Design for the Separation of Three Liquid Phases for a Continuous Hydroformylation Process in a Miniplant Scale. *Ind. Eng. Chem. Res.* **2013**, *52*, 7259.
- (16) Schlieper, L.; Chatterjee, M.; Henschke, M.; Pfennig, A. Liquid-Liquid Phase Separation in Gravity Settler with Inclined Plates. *AIChE J.* **2004**, *50*, 802.
- (17) Mungma, N.; Chuttrakul, P.; Pfennig, A. Jurnal Teknologi Liquid-Liquid Phase Separation in Batch Settling with Inclined Plate. *J. Teknol.* **2014**, *4*, 55.
- (18) Gerth, K.; Heikamp, W. Einrichtung Zum Trennen von Heterogenen Dispersionen. DE19717768C2.
- (19) Hamerla, T.; Paul, N.; Kraume, M.; Schomäcker, R. Aufklärung Der Stofftransportwege in Mizellaren Mehrphasenreaktionen Am Beispiel Der Hydroformylierung. *Chemie Ing. Tech.* **2013**, n/a.
- (20) Otto Roelen. Production of Oxygenated Carbon Compounds. 2327066, 1943.
- (21) Wiese, K.; Obst, D. Hydroformylation. In *Catalytic Carbon-ylation Reactions*; Beller, M., Ed.; Springer: New York, 2006; pp 1–33.
- (22) Bahrmann, H.; Bach, H.; Frey, G. D. Oxo Synthesis. *Ullmann's Encyclopedia of Industrial Chemistry*; Springer: New York, 2009; pp1–8.
- (23) Miyagawa, C. C.; Kupka, J.; Schumpe, A. Rhodium-Catalyzed Hydroformylation of 1-Octene in Micro-Emulsions and Micellar Media. *J. Mol. Catal. A Chem.* **2005**, *234*, 9.
- (24) Hamerla, T.; Rost, A.; Kasaka, Y.; Schomäcker, R. Hydroformylation of 1-Dodecene with Water-Soluble Rhodium Catalysts with Bidentate Ligands in Multiphase Systems. *ChemCatChem* **2013**, n/a–n/a.
- (25) Müller, M.; Kasaka, Y.; Müller, D.; Wozny, G.; Schomäcker, R. A Continuous Hydroformylation Process in a Miniplant Scale: Equipment Design for the Separation of Three Liquid Phases. In *11th International Symposium on Process Systems Engineering—PSE2012*; Elsevier B.V.: Amsterdam, 2012; p 710–714.
- (26) Schreuder Goedheijt, M.; Kamer, P. C.; van Leeuwen, P. W. N. A Water-Soluble Diphosphine Ligand with a Large "Natural" Bite Angle for Two-Phase Hydroformylation of Alkenes. *J. Mol. Catal. A: Chem.* **1998**, *134*, 243.
- (27) Müller, D.; Minh, D. H.; Merchan, V. A.; Arellano-Garcia, H.; Kasaka, Y.; Müller, M.; Schomäcker, R.; Wozny, G. Towards a Novel Process Concept for the Hydroformylation of Higher Alkenes: Mini-Plant Operation Strategies via Model Development and Optimal Experimental Design. *Chem. Eng. Sci.* **2013**, 1.

PAPER 3

Verteilungsgleichgewichte von Liganden in mizellaren Lösungsmittelsystemen

Marcel Schmidt, Tobias Pogrzeba, Dmitrij Stehl, René Sachse, Michael Schwarze, Regine von Klitzing, and Reinhard Schomäcker

Chemie Ingenieur Technik, 2016, 88, 119-127

Online Article: <http://onlinelibrary.wiley.com/doi/10.1002/cite.201500125/full>

ActiveView PDF: <http://onlinelibrary.wiley.com/doi/10.1002/cite.201500125/epdf>

Reprinted (adapted) with permission from “Verteilungsgleichgewichte von Liganden in mizellaren Lösungsmittelsystemen; Marcel Schmidt, Tobias Pogrzeba, Dmitrij Stehl, René Sachse, Michael Schwarze, Regine von Klitzing, and Reinhard Schomäcker. Chemie Ingenieur Technik, 2016, 88, 119-127.” Copyright (2016) John Wiley and Sons.

Verteilungsgleichgewichte von Liganden in mizellaren Lösungsmittelsystemen

Marcel Schmidt^{1,*}, Tobias Pogrezba¹, Dmitrij Stehl¹, René Sachse¹, Michael Schwarze², Regine von Klitzing¹ und Reinhard Schomäcker¹

DOI: 10.1002/cite.201500125

Herrn Prof. Dr.-Ing. Matthias Kraume zum 60. Geburtstag gewidmet

Im Rahmen des Sonderforschungsbereichs SFB/TRR 63 „InPROMPT“ (Integrierte chemische Prozesse in flüssigen Mehrphasensystemen) wird der Einsatz mizellarer Lösungsmittelsysteme als schaltbare mehrphasige Reaktionsmedien für die homogene Katalyse untersucht. In diesem Beitrag wird das Verteilungsgleichgewicht von vier repräsentativen Liganden in unterschiedlichen wässrig-mizellaren Systemen analysiert und die Abhängigkeit ihrer Verteilung – und damit auch der eines homogen gelösten Katalysators – in den einzelnen Phasen dieser Mehrphasensysteme diskutiert. Die Kenntnis der Verteilungskoeffizienten ist von entscheidender Bedeutung für eine effiziente und quantitative Katalysatorrückführung in wässrig-mizellaren Systemen.

Schlagwörter: Liganden, Mizellen, Tenside, Verteilungskoeffizient

Eingegangen: 14. August 2015; *akzeptiert:* 29. September 2015

Equilibrium Distribution of Ligands in Micellar Solutions

The applicability of micellar solvent systems as tuneable multiphase reaction media for homogeneous catalysis is being examined within the framework of the collaborative research centre SFB/TRR 63 “InPROMPT” (Integrated Chemical Processes in Liquid Multiphase Systems). In this contribution the equilibrium distribution of four representative ligands in different aqueous-micellar systems was investigated and the dependency of their distribution – and thereby the distribution of a homogeneously dissolved catalyst – in the different phases of these multiphase systems is discussed. The knowledge of the distribution coefficients is of utmost importance for an efficient and quantitative catalyst recycling in aqueous-micellar systems.

Keywords: Equilibrium distribution, Ligands, Micelles, Surfactants

1 Einleitung

Für die Wirtschaftlichkeit eines chemischen Prozesses in der homogenen Katalyse ist vor allem die quantitative Rückführung der teuren Edelmetall-Katalysatoren von entscheidender Bedeutung. Den Idealfall für homogene Reaktionsmedien stellen deshalb sogenannte schaltbare Reaktionssysteme dar, deren Phasenverhalten sich zwischen den

verschiedenen Prozessschritten verändern lässt. So sollte ein Reaktionsmedium während der Reaktion homogen sein, um Stofftransporthemmungen zu vermeiden, und für die Katalysatorabtrennung in ein Zweiphasensystem umschaltbar sein, in dem Produkt und Katalysator in unterschiedlichen Phasen vorliegen. Zur vollständigen Abtrennung des Katalysators vom Produkt empfiehlt sich der Einsatz von Zweiphasensystemen mit sehr breiten Mischungslücken, da darin die Verteilungskoeffizienten der Katalysatoren häufig große Werte zugunsten einer der beteiligten Phase annehmen. So bieten z. B. wässrig-organische Systeme oft optimale Verhältnisse für die Katalysatorabtrennung, da die Liganden für die Katalysatoren durch funktionelle Gruppen sehr gut in ihrer Löslichkeit (polar/unpolar) eingestellt werden können (s. Abb. 1). Durch einfache Modifikationen am Liganden (z. B. das Anbringen von Sulfonat-Gruppen zur

¹Marcel Schmidt (marcel.schmidt@tu-berlin.de), Tobias Pogrezba, Dmitrij Stehl, René Sachse, Prof. Regine von Klitzing, Prof. Reinhard Schomäcker, Technische Universität Berlin, Institut für Chemie, Straße des 17. Juni 124, 10623 Berlin, Deutschland; ²Prof. Michael Schwarze, Technische Universität Berlin, Fachgebiet Anlagen- und Sicherheitstechnik, Straße des 17. Juni 135, 10623 Berlin, Deutschland.

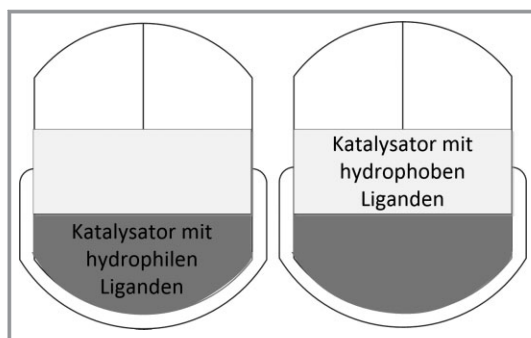


Abbildung 1. Schematische Darstellung zur Verteilung von Katalysatoren mit verschiedenen Liganden in einem flüssig-flüssig-Mehrphasensystem.

Erhöhung der Wasserlöslichkeit) kann somit dafür gesorgt werden, dass der Katalysator quantitativ in nur einer Phase vorliegt.

Das Hauptproblem der Anwendung von Wasser in der organischen Synthese ist die Unlöslichkeit vieler Reagenzien in diesem Medium. Neben zahlreichen Möglichkeiten wie dem Zusatz von hydrophilen Lösevermittlern, dem Einsatz von Phasentransfer-Katalysatoren oder pH-Regulierung der Reaktionslösung, bietet der Einsatz von Tensiden eine weitere Option zur Behebung des Löslichkeitsproblems. Hierbei übertragen Mizellen unpolare Reaktanden in die wässrige Phase oder polare Komponenten in die organische Phase. Diese Variante zur Modifikation von Zweiphasensystemen bietet eine hohe Flexibilität in ihrer Anwendung, da eine breite Palette an Tensiden auf dem Markt verfügbar ist. Außerdem eröffnet der Einsatz von Tensiden durch die Bildung von Mikroemulsionen den Zugang zu schaltbaren Reaktionsmedien, deren Phasenverhalten stark von der Zusammensetzung und Temperatur abhängig ist.

In den folgenden Kapiteln wird der Einfluss von unterschiedlichen Liganden und Tensiden auf die Katalysatorrückführung in mizellaren Systemen diskutiert. Für ausgewählte repräsentative Liganden wurden die Verteilungskoeffizienten in diesen Systemen experimentell und rechnerisch ermittelt. Auf Basis dieser Ergebnisse wird die Aussagekraft der Verteilungskoeffizienten zur Vorhersage der Qualität der Katalysatorrückführung in wässrigen Mehrphasensystemen überprüft.

2 Grundlagen und Methoden

Für die Bestimmung des polaren Charakters eines Substrates kann der Oktanol/Wasser-Verteilungskoeffizient P_{OW} , der nach Gl. (1) definiert ist, herangezogen werden.

$$P_{OW} = \frac{c_O^i}{c_W^i} \quad (1)$$

In Gl. (1) steht c_O^i für die Konzentration des Substrats in der Oktanolphase und c_W^i für die Konzentration in der Wasserphase. Für die Bestimmung des Wertes wird in der

Regel die Shake-Flask-Methode (OECD-Richtlinie 107) eingesetzt, bei der Oktanol und Wasser intensiv gemischt werden, wobei die zu verteilende Substanz in einer der Phasen vorgelöst wird. Nach erfolgter Phasentrennung wird die Konzentration der Substanz in den einzelnen Phasen bestimmt. Der Vorteil der Methode besteht darin, dass die Phasentrennung zumeist sehr schnell verläuft und die Versuche einfach zu realisieren sind. Für die Bestimmung von Verteilungskoeffizienten im Allgemeinen existieren aber auch andere experimentelle Methoden, z. B. über die Bestimmung von Löslichkeiten oder die Flüssigkeitschromatographie. Eine Übersicht ist in [1] gegeben. Anstelle der Konzentrationen kann der Verteilungskoeffizient auch über die Molenbrüche als K_{OW} (Gl. (2)) definiert werden.

$$K_{OW} = \frac{v_O}{v_W} \frac{c_O^i}{c_W^i} = 6,63 P_{OW} \quad (2)$$

In Gl. (2) steht v_O für das molare Volumen der Oktanolphase und v_W für das molare Volumen der Wasserphase. Da nach der Phasentrennung die Oktanolphase ca. 28 % Wasser enthält, während die Wasserphase nahezu rein vorliegt, muss dies bei der Berechnung berücksichtigt werden, weshalb sich ein Vorfaktor von 6,63 ergibt. Neben der experimentellen Bestimmung der Verteilungskoeffizienten kann auch eine Vorhersage durch Simulationsrechnung erfolgen. Hierfür bietet sich das freiverfügbare Programm ALOGPS2.1 an, das mithilfe künstlicher neuronaler Netze arbeitet. Dabei werden Modelle für die Lipophilie von chemischen Substanzen und die Löslichkeit in einer wässrigen Lösung kombiniert, um dies auf unbekannte Stoffe zu übertragen. So können Verteilungskoeffizienten anhand der chemischen Struktur kalkuliert werden – für weitere Informationen s. [2]. Dieses Programm eignet sich gut zur Vorhersage der Verteilungskoeffizienten von nicht-ionischen Verbindungen, wie z. B. Itaconsäureester [3]. Weiterhin bietet das Programm den Vorteil, dass auch Verteilungskoeffizienten bestimmt werden können, wo die experimentelle Erfassung sehr aufwendig ist, z. B. bei Substanzen deren Konzentration in einer Phase so gering ist, dass sie analytisch kaum erfassbar ist. Da die Verteilungskoeffizienten in der Regel über mehrere Zehnerpotenzen variieren können, wird zumeist der $\log P_{OW}$ bzw. $\log K_{OW}$ angegeben.

Auch in Tensidsystemen erfolgt die Verteilung eines Substrats zwischen Domänen unterschiedlicher Hydrophobizität. Im Vergleich zu den Oktanol/Wasser-Verteilungskoeffizienten ist jedoch die experimentelle Bestimmung der Verteilung in Tensidsystemen aufwendiger, da z. B. für wässrig-mizellare Lösungen oder Mikroemulsionen makroskopisch einphasige Systeme vorliegen. Weiterhin können in diesen Systemen, bedingt durch die Anwesenheit des Tensids, zusätzliche Effekte die Verteilung stark beeinflussen. Für wässrig-mizellare Lösungen findet man in der Literatur unterschiedliche Methoden zur Bestimmung des Verteilungskoeffizienten, die im Folgenden erläutert werden. Eine Methode, die sich gut für Feststoffe eignet, ist die Methode der erhöhten Löslichkeit (ESM; enhanced solubility

method). Dabei steigt die Löslichkeit eines Stoffes mit der Tensidkonzentration aufgrund einer größeren Anzahl an Mizellen, die für die Solubilisierung zur Verfügung stehen. Wie in [4] beschrieben, lässt sich der Verteilungskoeffizient aus Gl. (3) berechnen.

$$K_{MW} = \frac{(S_M - S_W)V_W}{S_W(C - \text{cmc})} \quad (3)$$

In Gl. (3) ist S_M die Löslichkeit des Substrates in der wässrig-mizellaren Lösung, S_W die Löslichkeit in Wasser, C die Tensidkonzentration, cmc die kritische Mizellbildungskonzentration und V_W das molare Volumen von Wasser ($55,55 \text{ mol L}^{-1}$). Die Methode ist einfach durchzuführen, da der Bodensatz des nicht gelösten Substrates abfiltriert und nur die gesättigte Lösung analysiert wird. Für nicht-ionische Tenside wird oft die Trübungspunktextraktion (CPE; cloud point extraction) angewendet. Dabei wird eine, mit dem Substrat gesättigte, wässrig-mizellare Lösung oberhalb der Trübungstemperatur in eine wasserreiche und tensidreiche Phase aufgespalten. Durch Bilanzierung der einzelnen Phasen kann der Verteilungskoeffizient aus Gl. (4) erhalten werden.

$$K_{MW} = \frac{x_M^i}{x_W^i} \quad (4)$$

In Gl. (4) ist x_M^i der Molenbruch des Substrates in der tensidreichen Phase und x_W^i der Molenbruch in der wasserreichen Phase. Da die CPE nur für nicht-ionische Tenside geeignet ist, können Verteilungen für ionische Tenside damit nicht bestimmt werden. Eine Methode, die für alle Tenside gleichermaßen geeignet ist, ist die Ultrafiltration wässrig-mizellarer Lösungen (MEUF; micellar enhanced ultrafiltration). Dabei wird eine mit dem Substrat gesättigte, wässrig-mizellare Lösung durch eine Membran mit einem Porendurchmesser unterhalb der Mizellgröße filtriert, wobei die Mizellen von der Membran zurückgehalten werden. Nur der Anteil an Substrat, der in der kontinuierlichen Wasserphase gelöst vorliegt, sowie das Tensid in monomerer Form passieren ungehindert die Membran. Durch Bilanzierung des Tensidsystems vor und nach der Filtration lässt sich der Verteilungskoeffizient, wie von Schwarze et al. in [3] gezeigt, bestimmen. Da die experimentellen Methoden sehr aufwendig sind, wurden Methoden zur Vorhersage der Verteilungskoeffizienten für Tensidsysteme untersucht. Eine Methode, die gute Vorhersagen liefert, ist COSMO-RS (conductor-like screening model for real solvents). Diese Methode konnte bereits anhand von Verteilungskoeffizienten aus CPE [5] oder MEUF [3] validiert werden.

3 Experimentelles

3.1 Chemikalien

Die Lösungsmittel 1-Dodecen (94 %) und Wasser (HPLC grade) wurden von VWR bezogen. 1-Oktanol (99 %) wurde von Roth erhalten. Die technischen Tenside Marlipal 24/40,

24/50 und 24/70 sind eine Spende der Firma Sasol. Die Tenside Triton X-114 und Triton X-100, sowie die Liganden Triphenylphosphin (TPP, 99 %), 4,5-Bis(diphenylphosphino)-9,9-dimethylxanthene (XantPhos, 97 %) und Tri-(natrium-meta-sulfonatophenyl)-phosphan (TPPTS, 95 %) wurden von Sigma-Aldrich erhalten. Das sulfonierte Analogum zum XantPhos Ligand, SulfoXantPhos, wurde von der Molisa GmbH hergestellt. Der Rhodium-Vorläufer $\text{Rh}(\text{acac})(\text{CO})_2$ ist eine Spende von Umicore. Alle Chemikalien wurden ohne Aufreinigung verwendet.

3.2 Methoden

Bestimmung des Oktanol/Wasser Verteilungskoeffizienten

Zur Bestimmung des Oktanol/Wasser-Verteilungskoeffizienten wurden jeweils 5 mL von mit Wasser gesättigtem Oktanol und mit Oktanol gesättigtem Wasser gemischt. Anschließend wurden 100 mg SulfoXantPhos bzw. TPPTS hinzugegeben und über Nacht auf einer Rüttelplatte vermischt. Die Konzentration der Liganden in den einzelnen Phasen wurde nach der Phasentrennung mit einer HPLC-Anlage der Serie 1200 von Agilent untersucht. Als Säule wurde eine Multospher 120 RP18-5 μL verwendet. Die Proben wurden bei einer Flussrate von 1 mL min^{-1} mit einem Lösemittelgemisch aus Wasser/Acetonitril von 30:70 vermessen.

Erhöhte Löslichkeitsmethode

Zur Bestimmung des Mizelle/Wasser-Verteilungskoeffizienten mittels der Methode der erhöhten Löslichkeit (ESM) wurden verschiedene tensidhaltige Lösungen hergestellt und der zu untersuchende Ligand bis zur Bodensatzbildung hinzugegeben. Die mizellare Lösung wurde über Nacht auf einer Rüttelplatte gemischt, anschließend filtriert und das Filtrat auf die Konzentration des Liganden analysiert.

Trübungspunkt-Extraktion

Für die Trübungspunkt-Extraktion (CPE) wurden 5 Gew.-% des Tensids mit den zu untersuchenden Liganden in einer wässrigen Lösung gemischt. Die Temperatur wurde schrittweise erhöht, bis der Trübungspunkt erreicht wurde. Nach erfolgter Phasentrennung wurden die einzelnen Phasen mittels HPLC hinsichtlich der Ligandenkonzentration untersucht. Für den Liganden XantPhos wurde die Konzentration mittels induktiv gekoppeltem Plasma mit optischer Emissionsspektroskopie (ICP-OES) bestimmt. Für die analytische Messung wurde das ICP-OES Varian 714 ES verwendet und zur Kalibrierung wurden Phosphorlösungen mit 1, 10, 100 und 1000 mg L^{-1} hergestellt. Die Auswertung erfolgte bei einer Wellenlänge von 213 nm.

Bestimmung der Oberflächenspannung der Liganden

Die Messungen zur Oberflächenspannung der Ligandenlösungen wurden mit einem DCAT 11 der Firma

DATAPHYSICS durchgeführt. Der Messkörper war ein Du Noüy-Ring bestehend aus einer Platin-Iridium-Legierung mit einer Ringhöhe von 25 mm, einen Ringdurchmesser von 18,7 mm und einer Drahtdicke von 0,37 mm. Es wurden verschieden konzentrierte Lösungen der Liganden TPPTS und SulfoXantPhos hergestellt und vermessen. Nach jeder Messung wurde der Messring mit einer Butangasflamme gereinigt.

Bestimmung der Verteilung des Katalysators in der Mikroemulsion

Die Konzentration von Rhodium in den unterschiedlichen Phasen eines mehrphasigen Mikroemulsionssystems wurde mittels ICP-OES bestimmt. Es wurde jeweils die wässrige Phase und die Mittelphase des Mikroemulsionssystems untersucht. Dazu wurden 2 mL der wässrigen bzw. 1 mL der Mittelphase mit Königswasser versetzt und mit destilliertem Wasser verdünnt. Die Rhodiumkonzentration wurde bei einer Wellenlänge von 369 nm gemessen. Die Kalibrierung erfolgte mit Rhodiumstandard-Lösungen der Konzentration 1, 5, 20, 50 und 150 mg L⁻¹.

4 Ergebnisse und Diskussion

Für die effektive Abschätzung der Verteilung von homogenen Katalysatorkomplexen in tensidmodifizierten Flüssig/flüssig-Mehrphasensystemen spielt die Polarität des Komplexes eine entscheidende Rolle. Diese kann maßgebend durch die Löslichkeitseigenschaften des verwendeten Liganden gesteuert werden. Das Wissen über die Verteilung des Liganden ist somit essentiell für die quantitative Abtrennung des homogenen Katalysatorkomplexes.

Das Verteilungsgleichgewicht eines homogenen Katalysatorkomplexes soll für mizellare Lösungsmittelsysteme qualitativ vorhergesagt werden, wobei ein besonderes Augenmerk auf die Art der Liganden und die Struktur des Tensids gelegt wird. Dazu wird schrittweise die Komplexität des Flüssig/flüssig-Mehrphasensystems erhöht um eine aussagekräftige Beurteilung zu gewährleisten.

4.1 Verteilungskoeffizienten für verschiedene Liganden zwischen 1-Oktanol und Wasser

Für die Auswahl eines Katalysatorkomplexes für Flüssig/flüssig-Mehrphasensysteme spielt der Verteilungskoeffizient des Liganden zwischen den nicht mischbaren Phasen eine entscheidende Rolle. Auf der einen Seite muss die lokale Konzentration aller Reaktionsteilnehmer so hoch sein, dass eine wirtschaftlich sinnvolle Reaktionsgeschwindigkeit resultiert. Auf der anderen Seite muss sichergestellt werden, dass ein Recycling des ligand-modifizierten, meist teuren Katalysatorkomplexes und eine Trennung des Reaktionsproduktes durch eine Phasentrennung ermöglicht wird.

Die Verteilungskoeffizienten von nicht-ionischen Liganden sind für Flüssig/flüssig-Mehrphasensysteme wie Oktanol/Wasser bekannt bzw. können mit verschiedenen Methoden berechnet werden, jedoch findet man kaum Informationen für ionische Liganden, die sulfoniert und somit wasserlöslich sind. Deshalb wurden die Oktanol/Wasser-Verteilungskoeffizienten K_{OW} für TPPTS und SulfoXantPhos – die sulfonierten Analoga zu TPP und XantPhos – bestimmt (Tab. 1). Für die Berechnung der Verteilungskoeffizienten wurde das Programm ALOGPS2.1 verwendet, das für nicht-ionische und nicht-geladene Moleküle gute Vorhersagen liefert.

Tabelle 1. Experimentelle und berechnete Oktanol-Wasser-Verteilungskoeffizienten K_{OW} für verschiedene Liganden (berechnet mit ALOGPS2.1).

Ligand	$\log(K_{OW})$ exp.	$\log(K_{OW})$ ber.
TPP	6,02 [6]	$6,2 \pm 0,5$
TPPTS	-3,07	-
XantPhos	-	$11,1 \pm 1,4$
SulfoXantPhos	-1,21	-

Die berechneten Oktanol/Wasser-Verteilungskoeffizienten zeigen, dass das bidentate XantPhos im Vergleich zu TPP viel hydrophober ist, was auf die größere Anzahl an Phenylringen zurückzuführen ist (Abb. 2). Der berechnete Wert für TPP stimmt dabei mit dem experimentell ermittelten Literaturwert überein. Eine Berechnung für die wasserlöslichen Analoga konnte aufgrund ihres ionischen Charakters nicht durchgeführt werden. Die experimentellen Daten zeigen jedoch deutlich, dass die Sulfonierung eine Umkehrung der Löslichkeit hervorruft und TPPTS bzw. SulfoXantPhos sich vorwiegend in der Wasserphase lösen. Dabei zeigt TPPTS im Vergleich zu SulfoXantPhos einen kleineren Oktanol/Wasser-Verteilungskoeffizienten, da drei

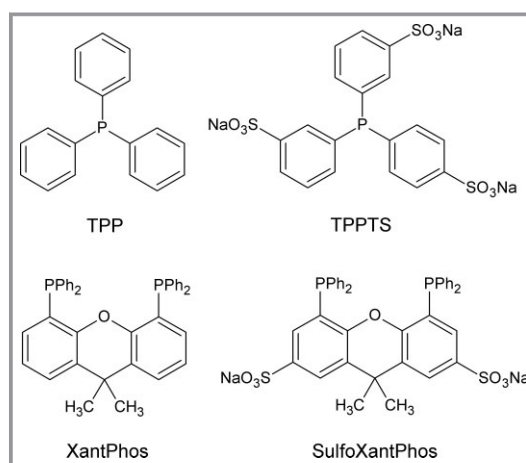


Abbildung 2. Strukturformeln der Liganden TPP, TPPTS, XantPhos und SulfoXantPhos.

statt zwei Sulfonat-Gruppen für eine größere Hydrophilie im Molekül sorgen. Außerdem besitzt SulfoXantPhos eine größere Anzahl an Phenylgruppen.

4.2 Verteilungskoeffizienten für verschiedene Liganden in einem mizellaren Lösungsmittelsystem

Ein basiertes Wissen über den Mizelle/Wasser-Verteilungskoeffizienten K_{MW} ist entscheidend, um den Trennungsprozess für homogene Katalysatorkomplexe in mizellaren Lösungsmittelsystemen zu verstehen und das Recycling zu optimieren. Für neutrale, nicht oberflächenaktive Komponenten besteht ein linearer Zusammenhang zwischen den Oktanol/Wasser- und Mizelle/Wasser-Verteilungskoeffizienten [7], der durch die Collander-Gleichung [8] beschrieben werden kann (Gl. (5)). Collander beobachtete in verschiedenen zweiphasigen Systemen einen linearen Zusammenhang zwischen den logarithmierten Verteilungskoeffizienten einer Komponente, wobei K_1 und K_2 die Verteilungskoeffizienten in den Systemen 1 und 2 widerspiegelt und a und b empirische Konstanten sind.

$$\log(K_1) = a \log(K_2) + b \quad (5)$$

Jedoch ist dieser Zusammenhang für ionische Spezies nicht nachweisbar, so dass dort zusätzliche Effekte bei der Verteilung in einem mizellaren Lösungsmittelsystem eine wesentliche Rolle spielen und untersucht werden müssen. Im Folgenden wird der Verteilungskoeffizient für einige Modell-Liganden, die häufig in Metallkomplexen eingesetzt werden, diskutiert, wobei ein Augenmerk auf die Tensidauswahl sowie auf die Struktur des Liganden gelegt wird.

4.2.1 Tensideinfluss

Zunächst wurde der Einfluss des Tensids auf die Verteilung des hydrophoben Liganden TPP und des hydrophilen Liganden SulfoXantPhos untersucht (Abb. 3). Dazu wurden die nichtionischen Tenside NP9, Triton X-100, Triton X-114, Marlipal 24/40, 24/50 und 24/70, und das anionische Tensid Natriumdodecylsulfat (SDS) verwendet. Typische Eigenschaften der Tenside sind in Tab. 2 aufgelistet und die Tensidstrukturen sind in Abb. 4 gezeigt.

Der Mizelle/Wasser-Verteilungskoeffizient K_{MW} von TPP liegt in der Größenordnung von K_{OW} für TPP. Demnach wird TPP vorwiegend innerhalb des hydrophoben Kerns der gebildeten Mizellen eingelagert. Des Weiteren war die Struktur des Tensids hinsichtlich des Mizelle/Wasser-Verteilungskoeffizienten von Interesse, weshalb zwei Tenside mit

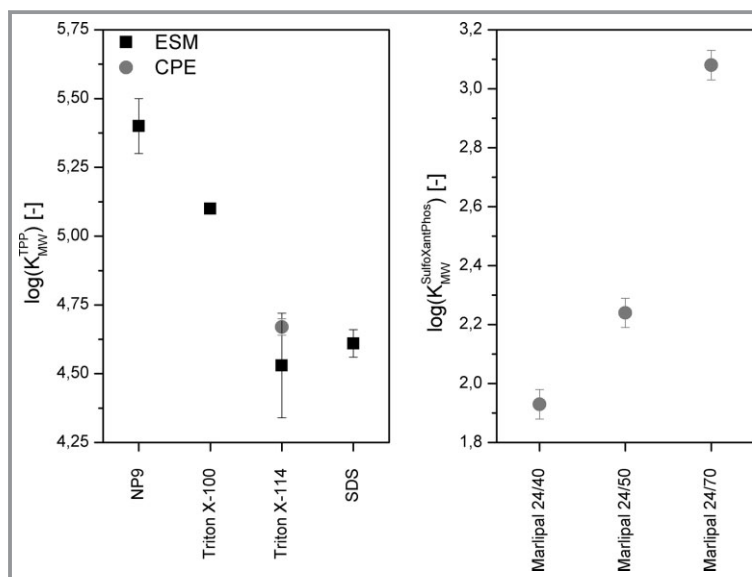


Abbildung 3. Verteilungskoeffizienten von TPP (links) und SulfoXantPhos (rechts) in mizellaren, wässrigen Lösungen mit der Methode nach der erhöhten Löslichkeit (ESM) und der Trübungspunkt Extraktion (CPE).

Tabelle 2. Molare Masse, Trübungspunkt, cmc und HLB-Wert der verwendeten Tenside.

Tensid	Molare Masse [g mol ⁻¹]	Trübungspunkt [°C]	cmc [mol L ⁻¹]	HLB-Wert
Triton X-100	≈ 625	65	2 · 10 ⁻⁴	13,5
Triton X-114	≈ 537	23	2 · 10 ⁻⁴	12,4
Marlophen NP9	≈ 600	52 – 56 ^{a)}	6,7 · 10 ⁻⁵	–
SDS	288,38	–	8,2 · 10 ⁻³	40 ^{d)}
Marlipal 24/40	≈ 376	66 – 68 ^{b)}	–	–
Marlipal 24/50	≈ 420	72 – 74 ^{b)}	–	–
Marlipal 24/70	≈ 508	53 – 56 ^{c)}	–	–

a) 1 % in deionisiertem Wasser, b) 10 % in 25 % BDG-Lösungen, c) 2 % in deionisiertem Wasser, d) nach der Methode von Davies.

identischen Ethoxylierungsgrad, aber unterschiedlichem hydrophoben Rest verglichen wurden: Triton X-100 besitzt einen verzweigten hydrophoben Rest und Marlophen NP9 weist eine lineare Alkylkette mit vergleichbarer Kohlenstoffanzahl auf. Es wurden bedingt durch die unterschiedlichen Alkylketten leicht unterschiedliche Verteilungskoeffizienten bestimmt. Durch die verzweigte Alkylkette ist der Kern der gebildeten Triton X-100-Mizelle hydrophiler im Vergleich zu Marlophen NP9. Dadurch ist der Verteilungskoeffizient geringer, da das stark hydrophobe TPP somit den Kern der Mizelle von Marlophen NP9 präferiert.

Weiterhin wurde der Einfluss des Ethoxylierungsgrad untersucht, wobei die Tenside Triton X-100 (9–10 Ethoxyeinheiten) und Triton X-114 (7–8 Ethoxyeinheiten)

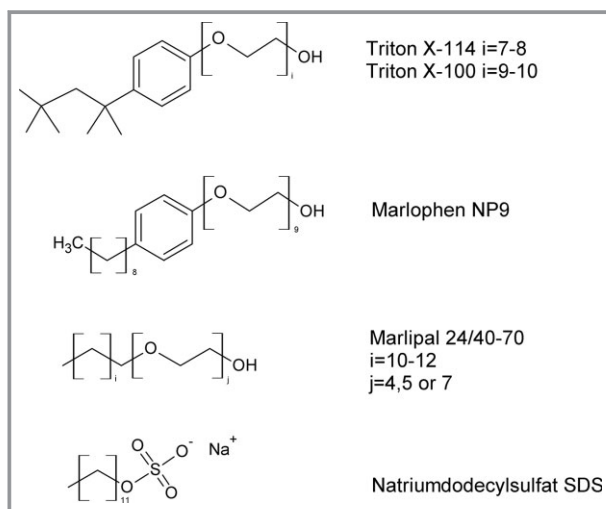


Abbildung 4. Strukturformeln der Tenside Triton X-100, Triton X-114, Marlophen NP9, Marlipal 24/40, 24/50 und 24/70 und SDS.

mit identischer hydrophober Alkylkette, jedoch unterschiedlicher Anzahl an Ethoxyeinheiten verglichen wurden. Die Schicht der hydrophilen Kopfgruppen von Triton X-100 ist im Vergleich zu Triton X-114 aufgrund der höheren Anzahl an Ethoxyeinheiten hydrophiler. Als Folge wird der Ligand TPP zusätzlich aus der kontinuierlichen wässrigen Phase verdrängt und es resultiert bei Triton X-100 ein höherer Verteilungskoeffizient im Vergleich zu Triton X-114. Für Triton X-100 und den Liganden TPP wurde mittels COSMO-RS ein Mizelle/Wasser-Verteilungskoeffizient von 7,1 bestimmt, der sich zwei Größenordnungen von den experimentellen unterscheidet [9]. Der Verteilungskoeffizient für SulfoXantPhos P_{MW} bestimmt durch eine Trübungspunkt-Extraktion, zeigt eine identische Tendenz. Je hydrophiler das Tensid ist, desto höher ist der Verteilungskoeffizient. Demzufolge reichert sich SulfoXantPhos, abhängig von der Hydrophilie des Tensids, bevorzugt in der tensidreichen Phase an, wobei jedoch zusätzliche Effekte eine entscheidende Rolle spielen, die im nächsten Abschnitt diskutiert werden. Überraschend ist dabei der positive Wert des Mizelle/Wasser-Verteilungskoeffizienten, da der Oktanol/Wasser-Verteilungskoeffizient $\log K_{OW}$ für SulfoXantPhos stark negativ war. Für Triton X-114 ist exemplarisch gezeigt, dass die gewählte Methode für die Bestimmung des Verteilungskoeffizienten keine Rolle für das Ergebnis spielt, da sich die $\log K_{MW}$ -Werte innerhalb der Messgenauigkeit decken. Zusätzlich wurde der Einfluss eines ionischen Tensids (SDS) auf den Verteilungskoeffizienten von TPP untersucht. Im Vergleich zu den anderen Tensiden erhält man hier einen ähnlichen Verteilungskoeffizienten wie für TX-114. Da TPP keine Ladung trägt, kann nur eine Wechselwirkung mit dem hydrophoben Mizellkern des SDS erfolgen und nicht zusätzlich mit den ionischen Kopfgruppen. Jedoch kann es zu attraktiven Wechselwirkungen kommen, wenn das Substrat ebenfalls Ladungen trägt.

Aus der Wasseraufbereitung mittels mizellgestützter Ultrafiltration (MEUF) ist bekannt, dass sich Metallionen an die negativen Kopfgruppen von anionischen Tensiden anbinden, wodurch aufgrund der vorliegenden Komplexbildung der Verteilungskoeffizient zugunsten der Mizelle verschoben wird. Dadurch können die Metallionen leicht abgetrennt werden [10,11]. Dasselbe Prinzip gilt auch für gelöste Anionen und kationische Tenside. So wurde in früheren Arbeiten zur Hydroformulierung von Olefinen in Gegenwart des kationischen Tensids Cetyltrimethylammoniumbromid (CTAB) unter Verwendung des hydrophilen Liganden TPPTS oft höhere Aktivitäten beobachtet, die sich neben einer höheren Eduktkonzentration im Mizellkern auch durch einen höheren Verteilungskoeffizienten von TPPTS erklären lassen; auch wenn dieser nie bestimmt wurde [12].

4.2.2 Ligandeneinfluss

Während in Abschn. 4.2.1 gezeigt wurde, dass sich durch die Auswahl des Tensids Einfluss auf die Verteilung des Liganden nehmen lässt, wird nun der Einfluss des Liganden selbst diskutiert. Für die beiden nicht-ionischen Tenside TX-100 und TX-114 sind die Verteilungskoeffizienten der untersuchten Liganden in Abb. 5 gezeigt.

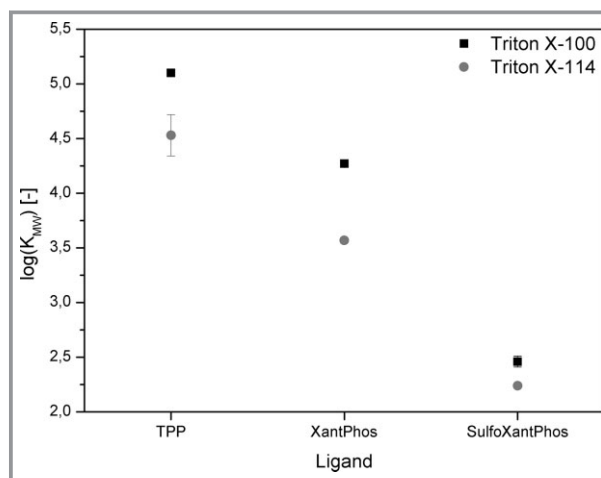


Abbildung 5. Verteilungskoeffizienten von TPP, XantPhos und SulfoXantPhos in mizellaren, wässrigen Lösungen mit Triton X-100 und Triton X-114, bestimmt mittels ESM.

Wie schon zuvor diskutiert, ist bei allen Liganden ein kleinerer Verteilungskoeffizient bei Triton X-114 zu beobachten. Überraschend ist, dass der Verteilungskoeffizient von XantPhos im Vergleich zu TPP kleiner ist, obwohl K_{OW} für XantPhos deutlich über den von TPP liegt. Weiterhin ist interessant, dass für das wasserlösliche SulfoXantPhos ein experimenteller Verteilungskoeffizient $\log K_{MW}$ von ca. 2,4 ermittelt wurde. Dies bedeutet, dass SulfoXantPhos vorwiegend in oder an der Mizelle eingelagert ist, was in Kontrast zu den Ergebnissen für K_{OW} steht. Erwartungsgemäß hätte

auch für den Mizelle/Wasser-Verteilungskoeffizienten aufgrund der Polarität von SulfoXantPhos ein negativer Wert resultieren müssen. Jedoch scheinen hier zusätzliche Effekte eine entscheidende Rolle zu spielen. Da das Molekül SulfoXantPhos ähnlich wie ein Tensid über einen hydrophoben und hydrophilen Teil verfügt, ist anzunehmen, dass SulfoXantPhos eine oberflächenaktive Substanz ist, die somit als Tensid fungieren kann. Demnach lagert sich SulfoXantPhos, bedingt durch dessen Oberflächenaktivität, an der Mizelle an und es ergibt sich ein vergleichsweise hoher Mizelle/Wasser-Verteilungskoeffizient. Dies wird auch durch die Messung der Oberflächenspannung von wässrigen Lösungen der Liganden bestätigt. Die sulfonierten Liganden SulfoXantPhos und TPPTS zeigen beide oberhalb einer Konzentration von $1 \cdot 10^{-4} \text{ mol L}^{-1}$ einen Abfall der Oberflächenspannung (Abb. 6). Dies erklärt den großen Mizelle/Wasser-Verteilungskoeffizienten von SulfoXantPhos.

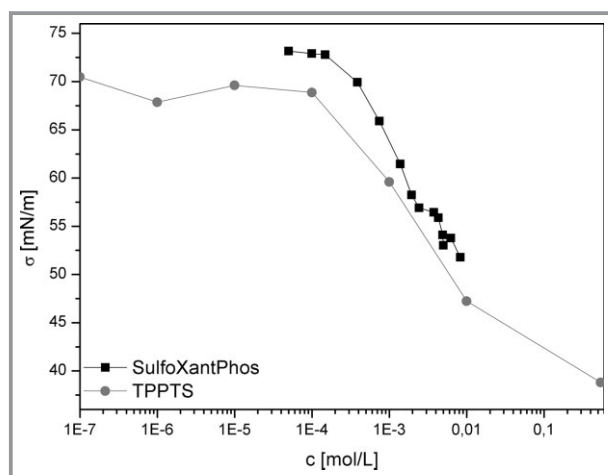


Abbildung 6. Oberflächenspannung σ von wässrigen TPPTS- und SulfoXantPhos-Lösungen in Abhängigkeit der Konzentration.

4.3 Verteilung des Katalysatorkomplexes in einem Mikroemulsionssystem

Die Wechselwirkungen zwischen verschiedenen Liganden und den Komponenten eines mizellaren Lösungsmittelsystems sind nun weitestgehend bekannt. Jedoch erhöht sich die Komplexität des Lösungsmittelsystems, wenn ein hydrophobes Lösungsmittel hinzukommt und eine Mikroemulsion gebildet wird. In Abb. 7 sind schematisch die Verteilungsgleichgewichte eines homogenen Katalysatorkomplexes zwischen den einzelnen Phasen eines Mikroemulsionssystems im Dreiphasengebiet aufgezeigt. Es wird angenommen, dass die Verteilung des Katalysatorkomplexes vorwiegend durch die Eigenschaften der Liganden bestimmt wird.

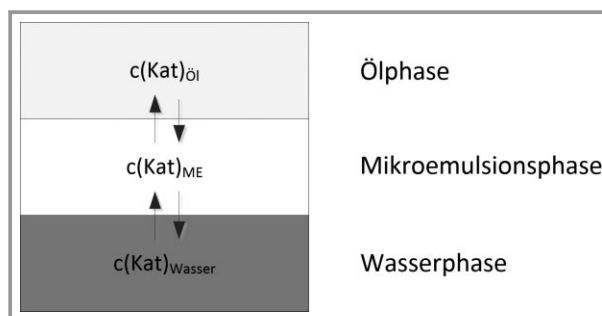


Abbildung 7. Schematische Darstellung des Verteilungsgleichgewichtes eines Katalysators in einer Mikroemulsion.

Durch die zusätzliche Ölkomponente spielt nicht nur die Verteilung des Katalysators zwischen der wässrigen und tensidreichen Phase, sondern auch die Verteilung zwischen der tensidreichen und öligen Phase eine Rolle. Für eine quantitative Abtrennung der teuren homogenen Katalysatoren ist es somit essentiell, die Verteilungsgleichgewichte zu kennen bzw. vorhersagen zu können. In Abb. 8 ist die Verteilung des Rhodium-Katalysators für die Liganden XantPhos und SulfoXantPhos in einem Mikroemulsionssystem dargestellt. Als Tensid wurde Marlipal 24/70 verwendet.

Es ist deutlich zu erkennen, dass die Hydrophilie und Grenzflächenaktivität des Liganden entscheidend für die Verteilung des Katalysatorkomplexes ist. Für den hydrophoben Liganden XantPhos ist der Katalysatorkomplex zu 74 % in der Ölphase enthalten, was auch optisch durch die intensive Rotfärbung der Ölphase ersichtlich ist. Der restliche Anteil befindet sich in der tensidreichen Mittelphase, die selbst ca. 1/4 der organischen Phase enthält. Interessant ist, dass für den wasserlöslichen Katalysatorkomplex mit SulfoXantPhos eine klare wässrige Phase vorhanden ist und sich der Großteil (96,3 %) des Katalysatorkomplexes in der tensidreichen Mittelphase anreichert. Dies ist, belegt durch die Mizelle/Wasser-Verteilungskoeffizienten K_{MW} von SulfoXantPhos, auf die attraktiven Wechselwirkungen und die Grenzflächenaktivität des Liganden mit dem Tensid zurückzuführen, wodurch der gesamte Katalysatorkomplex in die

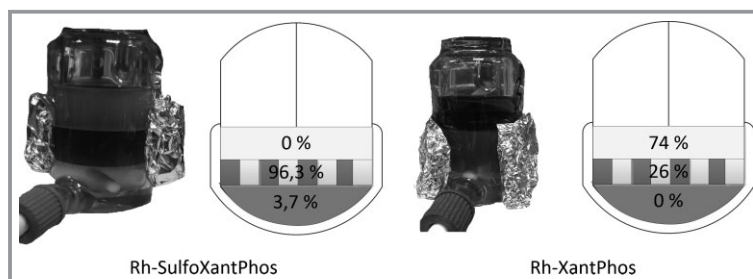


Abbildung 8. Verteilung des Rhodium-Katalysators bei Verwendung von SulfoXantPhos (links) und XantPhos (rechts) mit dem Tensid Marlipal 24/70 und 1-Dodecan als Lösungsmittel ($m_{\text{Wasser}} = m_{1\text{-Dodecan}} = 20 \text{ g}$, $m_{\text{Marlipal 24/70}} = 3,47 \text{ g}$, 1 Gew.-% Natriumsulfat, $\eta_{\text{Rh(acac)(CO)}_2} = 0,05 \text{ mmol}$, $\eta_{\text{Ligand}} = 5 \text{ eq.}$).

tensidreiche Mittelphase eingelagert wird. Somit können die Mizelle/Wasser-Verteilungskoeffizienten genutzt werden, um erste Hinweise über die Verteilung von Katalysatorkomplexen in einem Mikroemulsionssystem zu erhalten.

Die Ergebnisse für die Anreicherung des Rh/SulfoXanthophos-Komplexes in der tensidreichen Phase lassen sich auch auf einen kontinuierlichen Versuch in einer Miniplant übertragen, in der 1-Dodecen zu Tridecanal in einem Mikroemulsionssystem bestehend aus 1-Dodecen, Wasser und Marlupal 24/70 hydroformuliert wurde. Die Phasentrennung des Reaktionsgemisches wurde bei der kontinuierlichen Prozessführung von ca. 200 h in einem Dekanter realisiert. Dabei separierte das Reaktionsgemisch in eine Produktphase, die abgeführt wurde, und eine katalysatorreiche Phase, die zurück in den Reaktor geführt wurde. Über 99,99 % des Katalysators blieben in der Katalysatorphase im aktiven Zustand erhalten [13]. Die gute Trennung und hohe Rückführrate bestätigen die Vorhersagen zur Katalysatorverteilung auf der Grundlage der Verteilung des Liganden.

5 Zusammenfassung

Für Flüssig/flüssig-Zweiphasenreaktionen bieten sich tensidmodifizierte Reaktionsmedien an, da diese nicht nur zu wirtschaftlich sinnvollen Reaktionsgeschwindigkeiten führen, sondern es auch ermöglichen, homogene Katalysatoren vom Produkt abzutrennen und nochmals zu verwenden. Ein entscheidender Faktor für die quantitative Abtrennung des Katalysators ist die Wahl eines geeigneten Liganden und die Art des verwendeten Tensids. Es konnte gezeigt werden, dass die Struktur und Art des Tensids nur einen geringen Einfluss auf den Verteilungskoeffizienten von nichtionischen Liganden in einem mizellaren Reaktionssystem hat. Ausschlaggebenden Einfluss auf den Verteilungskoeffizienten in mizellaren Systemen hat nicht nur wie erwartet die Hydrophobizität der Liganden, sondern auch deren Grenzflächenaktivität. Für grenzflächenaktive sulfonierte Phosphinliganden konnte gezeigt werden, dass sich diese an die Tensidphase anlagern, wodurch ein unerwartet hoher Mizelle/Wasser-Verteilungskoeffizient resultiert.

Diese Arbeiten sind Teil des von der TU Berlin koordinierten Sonderforschungsbereichs/Transregio 63 „Integrierte chemische Prozesse in flüssigen Mehrphasensystemen“. Die Autoren bedanken sich bei der DFG für die finanzielle Unterstützung des Projektes (TRR63).

Formelzeichen

c_O^i	[mol L ⁻¹]	Konzentration des Substrats <i>i</i> in der Oktanolphase
c_W^i	[mol L ⁻¹]	Konzentration des Substrats <i>i</i> in der Wasserphase
cmc	[mol L ⁻¹]	kritische Mizellbildungskonzentration
K_{OW}	[-]	Verteilungskoeffizient Oktanol-Wasser, berechnet aus den Molenbrüchen
K_{MW}	[-]	Verteilungskoeffizient Mizelle-Wasser
<i>m</i>	[kg]	Masse
<i>n</i>	[mol]	Stoffmenge
P_{OW}	[-]	Verteilungskoeffizient Oktanol-Wasser, berechnet aus den Konzentrationen
S_M	[mol L ⁻¹]	Löslichkeit des Substrats in der mizellaren Lösung
S_W	[mol L ⁻¹]	Löslichkeit des Substrats in Wasser
V_W	[m ³ mol ⁻¹]	molares Volumen von Wasser
x_M^i	[-]	Molenbruch des Substrats <i>i</i> in der mizellaren Phase
x_W^i	[-]	Molenbruch des Substrats <i>i</i> in der Wasserphase
ν_O	[m ³ mol ⁻¹]	molares Volumen der Oktanolphase
ν_W	[m ³ mol ⁻¹]	molares Volumen der Wasserphase
σ	[mN m ⁻¹]	Oberflächenspannung

Abkürzungen

BDG	2-(2-Butoxyethoxy)ethanol
COSMO-RS	conductor-like screening model for real solvents
CPE	Trübungspunkt-Extraktion
CTAB	Cetyltrimethylammoniumbromid
ESM	erhöhte Löslichkeitsmethode
HLB	hydrophilic-lipophilic balance
ICP-OES	Optische Emissionsspektrometrie mit induktiv gekoppeltem Plasma
ME	Mikroemulsion
MEUF	micellar enhanced ultrafiltration
OECD	Organisation for Economic Cooperation and Development
SDS	Natriumdodecylsulfat
TPP	Triphenylphosphin
TPPTS	Tri-(natrium-meta-sulfonatophenyl)-phosphan
XantPhos	4,5-Bis(diphenylphosphino)-9,9-dimethylxanthene

Literatur

- [1] J. Sangster, *J. Phys. Chem. Ref. Data* **1989**, 18 (3), 1111 – 1229. DOI: 10.1063/1.555833
- [2] J. Dallos, A. Liszi, *J. Chem. Thermodyn.* **1995**, 27 (4), 447 – 448.
- [3] M. Schwarze, I. Volovych, S. Wille, L. Mokrushina, W. Arlt, R. Schomäcker, *Ind. Eng. Chem. Res.* **2011**, 51 (4), 1846 – 1852. DOI: 10.1021/ie2006565
- [4] K. Hanna, R. Denoyel, I. Beurroies, J. P. Dubès, *Colloids Surf., A* **2005**, 254 (1 – 3), 231 – 239. DOI: 10.1016/j.colsurfa.2004.12.016
- [5] T. Mehling, T. Ingram, I. Smirnova, *Langmuir* **2011**, 28, 118 – 124. DOI: 10.1021/la2028274
- [6] *Flame Retardants* (Eds: P. M. Visakh, Y. Arao), Springer International Publishing, Cham **2015**.
- [7] N. Chen, Y. Zhang, S. Terabe, T. Nakagawa, *J. Chromatogr. A* **1994**, 678, 327 – 332. DOI: 10.1016/0021-9673(94)80480-X
- [8] R. Collander, *Acta Physiol. Scand.* **1947**, 13 (4), 363 – 381.
- [9] S. Wille, L. Mokrushina, M. Schwarze, I. Smirnova, R. Schomäcker, W. Arlt, *Chem. Eng. Technol.* **2011**, 34 (11), 1899 – 1908. DOI: 10.1002/ceat.201100359
- [10] M. Schwarze et al., *J. Membr. Sci.* **2015**, 478, 140 – 147. DOI: 10.1016/j.memsci.2015.01.010
- [11] M. Schwarze, L. Chiappisi, S. Prévost, M. Gradzielski, *J. Colloid Interface Sci.* **2014**, 421, 184 – 190. DOI: 10.1016/j.jcis.2014.01.037
- [12] P. Baricelli et al., *Appl. Catal., A* **2015**, 490, 163 – 169. DOI: 10.1016/j.apcata.2014.11.028
- [13] D. Müller, E. Esche, T. Pogrzeba, T. Hamerla, T. Barz, R. Schomäcker, G. Wozny, in *20th Int. Conf. of Process Engineering and Chemical Plant Design* (Eds: M. Kraume, G. Wehinger), Copy Print, Berlin **2014**.

PAPER 4

Superior catalyst recycling in surfactant based multiphase systems – Quo vadis catalyst complex?

Tobias Pogrzeba, David Müller, Markus Illner, Marcel Schmidt, Yasemin Kasaka, Ariane Weber, Günter Wozny, Reinhard Schomäcker, and Michael Schwarze

Chemical Engineering and Processing, 2016, 99, 155-166

Online Article: <http://www.sciencedirect.com/science/article/pii/S0255270115300957>

ActiveView PDF: -/-

Reprinted (adapted) with permission from “Superior catalyst recycling in surfactant based multiphase systems – Quo vadis catalyst complex?; Tobias Pogrzeba, David Müller, Markus Illner, Marcel Schmidt, Yasemin Kasaka, Ariane Weber, Günter Wozny, Reinhard Schomäcker, and Michael Schwarze. Chemical Engineering and Processing, 2016, 99, 155-166.” Copyright (2015) Elsevier B.V.



Superior catalyst recycling in surfactant based multiphase systems – Quo vadis catalyst complex?



T. Pogrzeba^{a,*}, D. Müller^b, M. Illner^b, M. Schmidt^a, Y. Kasaka^a, A. Weber^a, G. Wozny^b, R. Schomäcker^a, M. Schwarze^c

^a Technische Universität Berlin, Department of Chemistry, TC-8, Str. des 17. Juni 124, 10623 Berlin, Germany

^b Technische Universität Berlin, Chair of Process Dynamics and Operation, KWT 9, Str. des 17. Juni 135, 10623 Berlin, Germany

^c Technische Universität Berlin, Chair of Plant and Process Safety, TK-01, Straße des 17. Juni 135, 10623, Berlin, Germany

ARTICLE INFO

Article history:

Received 9 March 2015

Received in revised form 7 July 2015

Accepted 3 September 2015

Available online 9 September 2015

Keywords:

Microemulsion systems

Surfactants

Catalyst Recycling

Process Design

Separation

ABSTRACT

Microemulsion systems are smart solvent systems which can be applied in homogeneous catalysis. We investigate these multiphase systems to exploit their characteristics for catalytic gas/liquid reactions and processes in aqueous media. One critical aspect from an economic perspective is the quantitative recycling of the catalyst complex dissolved in the multiphase system. Therefore, it is important to know the distribution of the catalyst complex in each of the single phases. In this contribution we analyse the different parameters/factors that may have an influence on the distribution of catalyst complexes in microemulsion systems, e.g. temperature, type of ligand, structure of surfactant, and chain length of surfactant. Afterwards, the derived information is used for the design of a real, industry-oriented application: hydroformylation of long chained alkenes. Hereby, special attention is given to the separation step of a process, which is performed after a homogeneously catalyzed reaction step in a microemulsion system. Process and economic constraints are briefly outlined and compared with operation data, aiming for the reuse of the catalyst in the reaction step and reduced leaching into product streams, even in the case of operational disturbances and shifts in the catalyst distribution.

© 2015 Elsevier B.V. All rights reserved.

1. Introduction

Expensive noble metal catalysts are often applied in homogeneous catalysis. The aims hereby are high activity and selectivity at moderate reaction conditions. However, to establish a large-scale process, the quantitative recovery of these catalysts is crucial and should be possible without loss in activity/selectivity. Hence, reaction media that combine the advantages of homogeneous catalysis (high turnover frequencies and high selectivity) and two-phase-catalysis (easy separation of catalyst and product) are of great interest. Beside the classical aqueous-organic two-phase systems, i.e. for the hydroformylation of 1-propene to n-butanal in the Ruhrchemie/Rhône-Poulenc Process [1], many new systems have been developed during the last decades. Well known examples are ionic liquids [2,3], supercritical media based on CO₂ [4,5], thermomorphic solvent mixtures [6], supported ionic liquid-phase (SILP) [7], or sol-gel immobilized catalyst systems [8]. An alternative approach is the application of microemulsion systems as tuneable solvents for the

recycling of water-soluble catalysts. Microemulsion systems are ternary mixtures consisting of a non-polar compound (oil), a polar compound (water), and a surfactant (often non-ionic surfactants are chosen in this context). They provide a high interfacial area between the polar and non-polar domains during the reaction. Additionally, their phase separation behaviour can be manipulated through temperature changes. However, for the application of microemulsion systems their phase behaviour, which not only depends on temperature but also on their composition and the interaction between the surfactant and the catalyst/reactants, has to be studied in detail [9]. Among the available green solvents, microemulsion systems, easily tuneable by the selection of an appropriate surfactant, show superior characteristics for catalytic reactions and processes in aqueous media. Furthermore, they fulfil all requirements needed for successful and efficient catalyst recycling. Examples for the application of microemulsions as reaction system are the hydrogenation of dimethyl itaconate with Rh/TPPTS [10], the Suzuki coupling of 2-bromobenzonitrile and 4-methylbenzeneboronic acid with Pd/TPPTS [11] and the hydroformylation of 1-dodecene with Rh/SX [12]. For further examples see also [9].

In this contribution we will evaluate and discuss the distribution of homogeneous catalyst complexes in microemulsion

* Corresponding author.

E-mail address: tobias.pogrzeba@tu-berlin.de (T. Pogrzeba).

systems by the variation of different parameters, e.g. temperature, ligand, structure of surfactant, and chain length of surfactant. We will also discuss several aspects which are important for the application of microemulsion systems for a closed recycle catalytic process with respect to the choice of the surfactant. In addition, we will present a case study to design a process for homogeneous catalysis in a microemulsion system with efficient catalyst recycling based on the results of the first part of this contribution.

2. Aqueous surfactant media

Water can act as a solvent for water-soluble catalysts and enables the biphasic extraction of non-polar products as well as the recycling of catalysts. However, in case of hydrophobic reactants it has the disadvantage of poor reactant solubility. The addition of a surfactant increases the solubility of non-polar reactants in the aqueous phase. Generally, there are two different approaches to create aqueous surfactant media for homogeneously catalysed reactions.

The first approach is to create an aqueous–micellar solution by the addition of a surfactant to water, which exceeds the critical micelle concentration (cmc). Micelles are nano-scale aggregates of surfactant monomers, which are able to solubilize organic components in their cores. Since the size of micelles is usually very small, the concentration of substrate in an aqueous–micellar solution is often lower than in conventional organic solvents. The cmc and the size of micelles depend on the type of surfactant. In general, non-ionic surfactants form larger micelles and have a low cmc in comparison to ionic surfactants.

The second approach is the use of microemulsion systems, which are formed at surfactant concentrations much higher than the cmc. By the addition of a non-ionic surfactant of the type C_iE_j to a biphasic mixture of water and oil, usually four different states can be observed that were classified by Winsor (Winsor systems I–IV). In C_iE_j , i is the number of hydrocarbon groups of the surfactant's hydrophobic part, and j is the number of ethoxylate groups of its hydrophilic part. Important parameters to characterize the mixture are the weight fractions α and γ . In Eq. (1) m_{oil} is the mass of oil, m_{water} is the mass of water and m_{surf} is the mass of non-ionic surfactant.

$$\alpha = \frac{m_{oil}}{m_{oil} + m_{water}} \quad \gamma = \frac{m_{surf}}{m_{oil} + m_{water} + m_{surf}} \quad (1)$$

In Fig. 1 the phase behaviour of a ternary mixture of oil, water and non-ionic surfactant is schematically shown for a constant value of α .

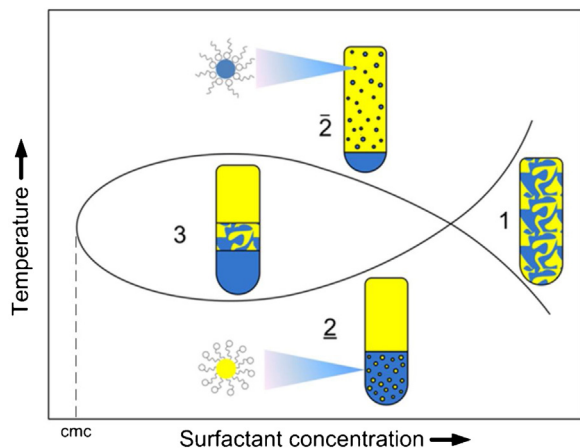


Fig. 1. Phase diagram (commonly called fish-diagram) for a ternary mixture of oil, water, and non-ionic surfactant at a constant ratio of oil and water with normal (bottom) and inverse (top) micelles. The figure has been modified from [13].

At low temperatures the surfactant is mainly solubilized in water, whereas its solubility in oil increases at higher temperatures. Thus, the illustrated sequence of phases as a function of temperature is the result of the gradual change in the surfactant's solubility from hydrophilic to hydrophobic. The phase sequence generally starts at low temperatures with an oil-in-water (o/w) microemulsion (2, Winsor I). This microemulsion consists of oil-bearing micelles in a continuous water phase which is in equilibrium with an organic excess phase. At intermediate temperatures a three-phase region (3, Winsor III) exists, where the surfactant is almost equally soluble in both liquids and forms a surfactant rich microemulsion phase in the middle of two excess phases. For even higher temperatures a water-in-oil (w/o) microemulsion (2-bar, Winsor II) is formed. Here, water-bearing inverse micelles exist in a continuous oil phase, which is in equilibrium with a water excess phase. If the concentration of surfactant in the ternary mixture is high enough for the complete solubilization of oil and water, a one-phase microemulsion (1, Winsor IV) of the entire volume will be formed, which can be an o/w-, bicontinuous- or w/o-microemulsion depending on the oil content in the mixture.

In general, each of the four Winsor states can be applied as a reaction medium for homogeneous catalysis. Since the phase behaviour of a microemulsion system can be changed as a function of temperature and surfactant concentration, it is possible to adjust the reaction system between different process steps with varying requirements [13]. The choice of the applied surfactant has to be made carefully so that the requirements for a homogeneously catalysed reaction with subsequent product separation and catalyst recycling, can be fulfilled. Besides its influence on the phase behaviour, the surfactant will have a strong impact on the distribution of reactants and catalysts between the aqueous and the organic phase. For the quantitative recycling of a homogeneously dissolved catalyst complex from multiphase systems as well as the evaluation of the reaction kinetics it is important to know the distribution of the catalyst complex between the single phases. In general, based on the experience with conventional organic–aqueous two-phase systems, water-soluble catalyst complexes are preferentially dissolved in the aqueous phase (see e.g. the Rh/TPPTS complex in the RCH/RP process) and hydrophobic counterparts are dissolved in the oil phase. For microemulsion systems, the interactions between the surfactant and the catalyst complex can influence the solubility of the latter considerably. In many cases the catalyst follows the surfactant into the corresponding microemulsion phase, which results in different separation tasks for the catalyst recycling during a process step depending on the phase behaviour of the microemulsion system. Therefore, it is necessary to indicate the parameters which are responsible for the catalyst distribution in such surfactant based multiphase systems to select the best surfactant as well as ideal operating conditions that result in a quantitative catalyst recycling and an optimal separation process.

3. Catalyst distribution in multiphase systems

To analyse the effects of the different parameters on the catalyst distribution multiple experiments were carried out. The obtained information from these experiments was then used for an actual industry-oriented application. In the following, details on these experiments as well as the results are presented.

3.1. Experimental

3.1.1. Chemicals

The solvents 1-dodecene (94%), water (HPLC grade), and tetrahydrofuran (THF, 99.5%) were purchased from VWR. The

surfactants Marlipal 24/50, Marlipal 24/60 and Marlipal 24/70 were a donation from Sasol. The surfactant Triton X-114, the amphiphiles C₄E₁ (99%) and C₄E₂ (99.2%), the hydrophobic ligands triphenylphosphine (TPP, 99%) and Xantphos (97%) and the rhodium standard solution (1011 mg/L) for ICP-OES analysis were received from Sigma–Aldrich. The water-soluble ligands 3,3',3''-phosphanetriyltris(benzenesulfonic acid) trisodium salt (sodium triphenylphosphine trisulfonate, TPPTS, 95%) and sulfonated 4,5-bis(diphenylphosphino)-9,9-dimethylxanthene (SulfoXantphos, SX) were purchased from ABCR and Molisa GmbH, respectively. The rhodium precursor Rh(acac)(CO)₂ was a donation from Umicore. To adjust the ionic strength we used sodium sulfate (Na₂SO₄, 99%) purchased from Merck. All the chemicals were used without further purification.

3.1.2. Preparation of the catalyst complex

For the preparation of the catalyst complex, 12.9 mg (0.05 mmol, 1 eq.) Rh(acac)(CO)₂ and the investigated ligand (10 eq. for the monodentate ligands and 5 eq. for the bidentate ligands) were evacuated three times in a Schlenk tube and flushed with argon. The solvent (2 g degassed water for the hydrophilic ligands and 3 g THF for the hydrophobic ligands) was added through a septum. Then the catalyst solution was stirred over night at room temperature to ensure the formation of the catalyst complex.

3.1.3. Investigation of the phase behaviour

Standard experiments were carried out by using a microemulsion system consisting of water as the hydrophilic compound, 1-dodecene as the hydrophobic oil ($\alpha = 50\%$), the investigated non-ionic surfactant ($\gamma = 8\%$) and a sodium sulfate amount of 1 wt%. To ensure the three phase region for the other amphiphiles, C₄E₁ and C₄E₂, the concentration had to be increased to $\gamma = 20\%$. The compounds were weighted into a glass reactor with a heating jacket. The lid of the reactor offers connections for sampling, for vacuum establishment, and argon inertisation. The samples were evacuated and flushed with argon three times. Then the catalyst solution was injected with a syringe. We studied the phase behaviour from 25 °C to 91 °C in 1 °C steps. For this purpose, we adjusted the temperature with a thermostat while stirring the microemulsion. After the desired temperature was reached, the

stirrer was stopped and the phase separation was observed. Samples of the different phases were taken to determine the rhodium concentration in each.

3.1.4. Determination of the rhodium concentration

The concentration of rhodium in the different phases was determined by inductively coupled plasma optical emission spectrometry (ICP-OES) using a Varian ICP-OES 715 ES instrument. In each case, we analysed the aqueous phase and the middle phase of the three phase system. Therefore, 2 mL of the water or 1 mL of the middle phase were added to an ICP tube and treated with freshly prepared aqua regia. Afterwards, the samples were diluted with degassed water and the rhodium concentration was measured at a wavelength of 369 nm. A calibration of the setup was performed with rhodium standard solutions having concentrations of 1, 5, 20, 50, and 150 mg/L.

3.2. Phase behaviour of the investigated microemulsion systems

To ensure an efficient recycling of the catalyst complex after the reaction, it is of utmost importance to know the phase behaviour of the reaction mixture. This phase behaviour strongly depends on the selected amphiphile. Several publications generalize observed effects [14,15], but to date and to the best of our knowledge the influence of the used catalyst complex has not been studied in detail. Therefore, we firstly tested different amphiphiles to obtain the influence of the chain length, structure, and the hydrophobic character of the amphiphiles towards the position of the three phase region on the temperature scale (see Fig. 2). Based on this information, the next step was to investigate the influence of ligands and thus the catalyst complex in particular in the subsequent sections. For the sake of completeness it has to be mentioned, that some of the applied chemicals are technical grade and may contain impurities which can have an impact on the phase behaviour of the investigated microemulsion systems and therefore have to be considered.

3.2.1. Hydrophobicity influence

It is well known that the three phase region for short chained amphiphiles, such as C₄E₁ and C₄E₂, has a broad temperature range. As expected, for the hydrophilic amphiphiles the position of the

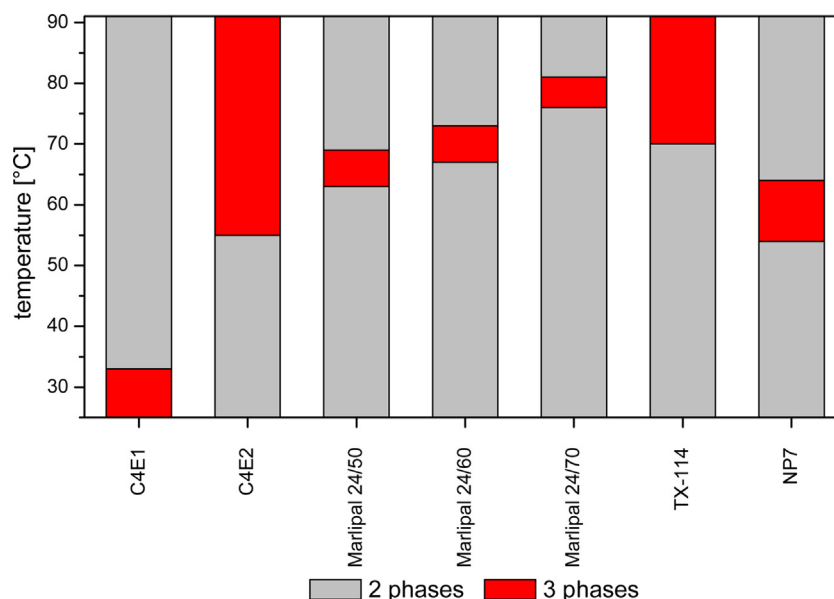


Fig. 2. Phase behaviour for different surfactants ($\alpha = 50\%$, $\gamma = 8\%$ ($\gamma = 20\%$ for C₄E₁ and C₄E₂), 1 wt.% sodium sulfate, $n_{\text{Rh(acac)CO}_2} = 0.05$ mmol, $n_{\text{SX}} = 5$ eq.).

three phase region is shifted to higher temperatures. The same effect of the three phase region being shifted to higher temperatures with increasing hydrophobicity exists for technical grade surfactants of the Marlipal series, which are long chain aliphatic surfactants (see Fig. 3). It is characteristic for these surfactants that they form micelles as a microstructure. By increasing the degree of ethoxylation from 5 in Marlipal 24/50 to 7 in Marlipal 24/70 the hydrophilic character increases and the three phase region is shifted to higher temperatures. In comparison to the short chained amphiphiles the temperature range of the three phase region is often limited to 5–10 K. It must be kept in mind that short chained amphiphiles only act as solubilisers and do not form micellar structures.

3.2.2. Chain length influence

The difference in the size of the temperature range of the three phase region of short compared to long chain amphiphiles is due to their different solubilisation properties in oil and water. Short chained amphiphiles, which act as an additional solvent, can dissolve more oil and water in their own phase compared to the technical grade surfactant Marlipal. This leads to a broad range of the three phase region.

3.2.3. Surfactant structure

Of special interest is the influence of the structure of the surfactant towards the position of the three phase region. Therefore, we compared different surfactants with the same degree of ethoxylation which are illustrated in Fig. 3: Triton X-114 with a linear hydrophobic carbon chain, Triton X-114 holding a branched carbon chain with a phenyl unit as linker, and NP7, which also has a phenyl unit as linker, but a linear carbon chain. Due to the different properties of the hydrophobic part of the surfactants, we obtain variable positions of the three phase region. Triton X-114 and NP7 have the same number of carbon atoms, but Triton X-114 is branched. Hence Triton X-114 is more hydrophilic than NP7 and so the three phase region is established at higher temperatures.

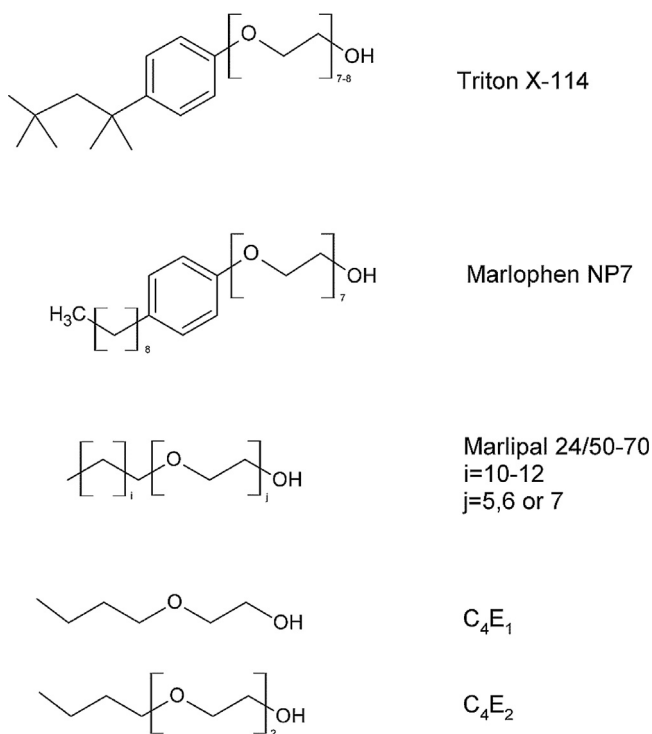


Fig. 3. Structures of the different investigated surfactants.

3.2.4. Ligand influence

Another important influence factor on the position of the three phase region is the type of applied ligand. The experimental results are shown in Fig. 4. The reference is a mixture with rhodium precursor without any ligand. We tested the monodentate ligands TPP and TPPTS and the bidentate ligands Xantphos and SulfoXantphos (see Fig. 5). At first glance, the water-soluble ligands TPPTS and SulfoXantphos shift the three phase region to higher temperatures. This is a result of the catalyst preparation though. The hydrophobic catalyst complexes were prepared using little amounts of THF, which is more hydrophilic in comparison to 1-dodecene. It is well known that the hydrophobicity of the oil influences the position of the three phase region [15]. The less hydrophobic the oil, the lower the position of the three phase region is. The difference of the position of the three phase region for TPPTS and SulfoXantphos is due to the ligand concentration. We used 10 eq. of the monodentate TPPTS and 5 eq. of the bidentate SulfoXantphos. As a result the water solubility of the surfactant decreases according to the salting out phenomenon of the sulfate anions [16], thus shifting the position of the three phase region to lower temperatures [14].

Based on these results, we moved on to investigate the parameters influencing the distribution of the whole catalyst complex.

3.3. Distribution of the catalyst complex

Not only is the temperature range for the different phases crucial for the separation process, but also the distribution of the catalyst complex between the different phases. For a feasible and economic process it is necessary to achieve a quantitative separation of the expensive catalyst complex. Therefore, it is essential to estimate or manipulate the interactions between the catalyst complex and the amphiphile. For this reason we investigated different amphiphiles and different ligands, which have an influence on the distribution characteristics of the catalyst complex. Qualitatively speaking, the distribution can be estimated visually by the colour of the different phases (see Fig. 6), but for quantification we measured the amount of rhodium by ICP-OES. In Fig. 7 the influence of different amphiphiles on the distribution of the water-soluble Rh/SX complex is shown. The rhodium content in the oil phase is negligible because of the water-soluble SulfoXantphos ligand as shown in [17,18]. So for the investigation of the catalyst complex distribution only the rhodium amount in the aqueous phase and the middle phase was considered. However, it should be mentioned that minor rhodium leaching into the oil phase was found in the order of 0.1 ppm [18] so that post-treatment of the organic phase would be necessary for complete rhodium recovery.

For the short chain amphiphiles C₄E₁ and C₄E₂ a high amount of the rhodium complex is present in the aqueous phase. The distribution of the rhodium complex depends on the partition coefficient between the phases. For the short chain amphiphiles, the major reason for the catalyst distribution is the different polarity of the phases, which increases from the oil phase over the amphiphile rich middle phase to the water phase. For the amphiphile C₄E₁, the middle phase is too non-polar to dissolve the catalyst complex to a sufficient extent and only 34% of the rhodium is located in the middle phase. For the amphiphile C₄E₂, the middle phase is more hydrophilic and allows for about 82% of the catalyst complex to be located there. As a consequence, the amount of rhodium in the aqueous phase is higher in the C₄E₁ system in comparison to the C₄E₂ system. In contrast, the rhodium amount in the aqueous phase of the Marlipal systems is only between 1.7% and 3.7% of the overall amount of rhodium in the system. Apparently, the catalyst complex follows the surfactant

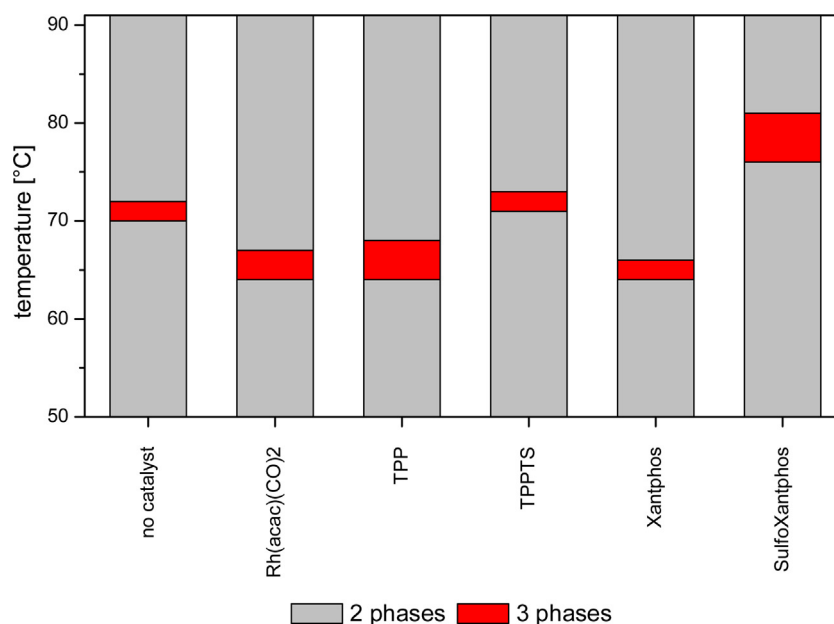


Fig. 4. Phase behaviour of Marlipal 24/70 in the presence of different ligands ($\alpha = 50\%$, $y = 8\%$, 1 wt% sodium sulfate, $n_{\text{Rh(acac)(CO)}_2} = 0.05$ mmol, $n_{\text{Ligand}} = 5$ or 10 eq.).

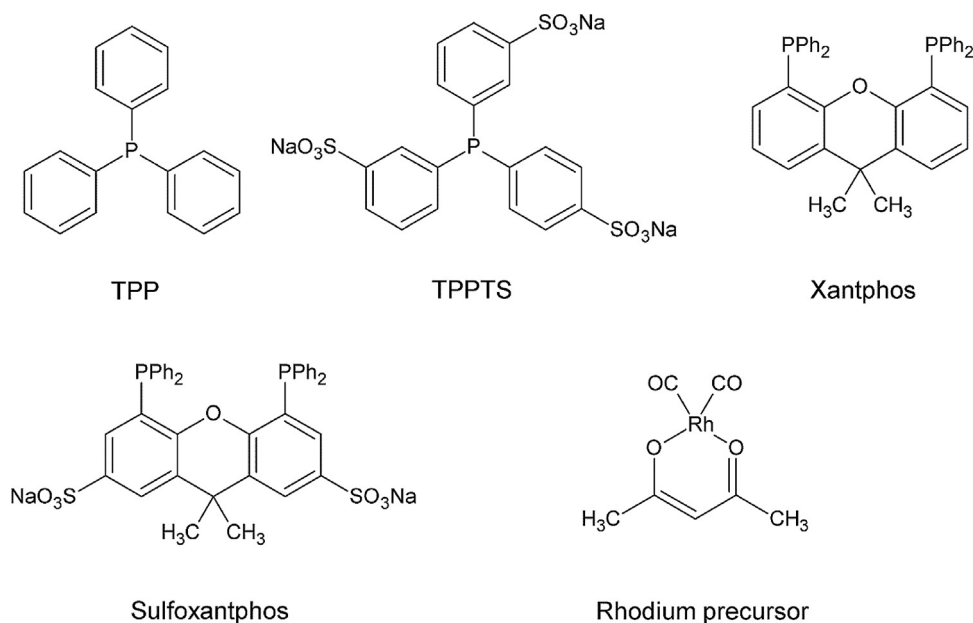


Fig. 5. Structures of the investigated ligands.

into the surfactant rich middle phase of the microemulsion systems. We assume that the water-soluble catalyst complex is also surface active and attaches itself to the oil–water interface of the bicontinuous phase of the microemulsion system.

Besides the amphiphile the kind of ligand has a strong influence on the distribution of the catalyst complex. In Fig. 8 the distribution of rhodium in the presence of different ligands is shown. It is clear that the hydrophobicity of the ligand is crucial for the distribution of the rhodium. For the water-soluble ligands TPPTS and SulfoXantphos the rhodium complex is located in the middle phase to a larger extend. The high amount of Rh/TPPTS in the aqueous phase (40%) is due to the high number of sulfonate groups per complex. In comparison to the water-insoluble ligands TPP and Xantphos, as well as for the unmodified rhodium precursor, the rhodium species is mainly located in the oil phase.

Here, only 10% of the Rh/TPP complex and 26% of the Rh/Xantphos complex are located in the middle phase. The comparison of mono- and bidentate ligands with respect to the distribution of the rhodium complex is difficult, because a different number of complex species can be formed. The number of coordinated ligands is important for the hydrophilic or hydrophobic character of the catalyst complex.

Furthermore, we investigated the distribution of the Rh/SulfoXantphos catalyst in a Winsor I and II system with the surfactant Marlipal 24/70, since this catalyst complex is of high interest for the discussion in Section 4. We found that in a Winsor I system over 99.99% of the catalyst is located in the microemulsion phase, whereas in a Winsor II system the catalyst is equally distributed between both phases.

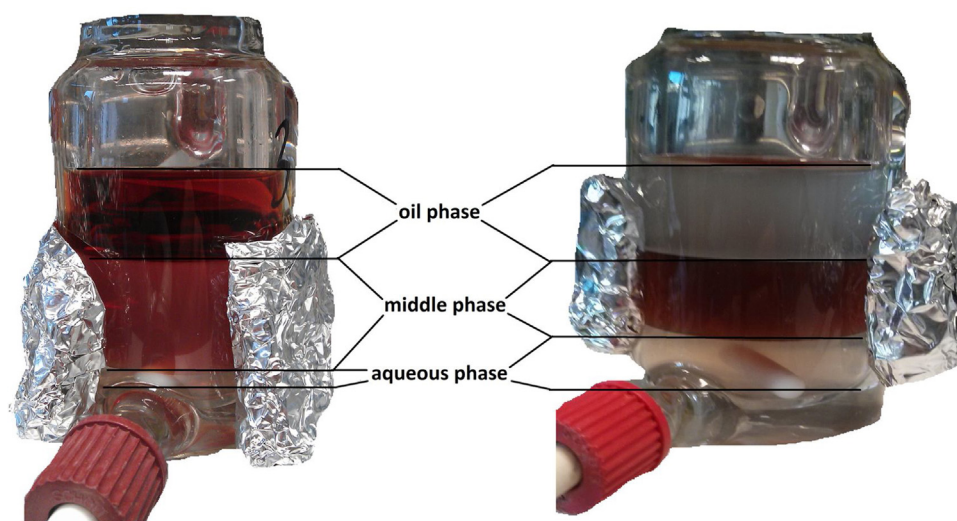


Fig. 6. Examples of catalyst distribution obtained for the three phase microemulsion system: Marlipal 24/70 and Rh/Xantphos (left) and Marlophen NP7 and Rh/SX (right).

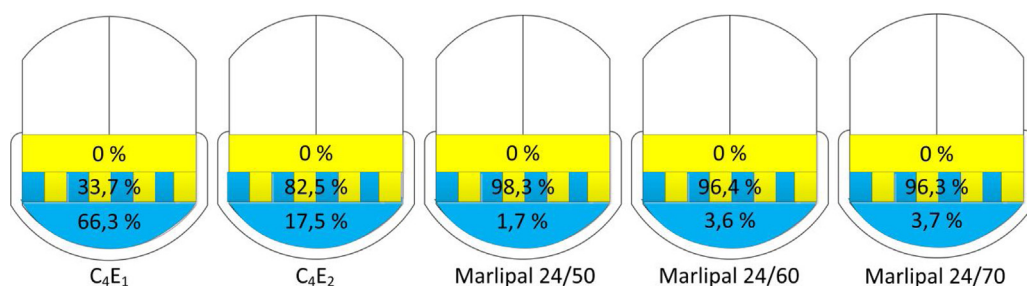


Fig. 7. Rh-content in the aqueous phase by the use of different amphiphiles ($\alpha = 50\%$, $y = 8\%$ ($\gamma = 20\%$ for C_4E_1 and C_4E_2), 1 wt% sodium sulfate, $n_{Rh(acac)CO_2} = 0.05$ mmol, $n_{SX} = 5$ eq.).

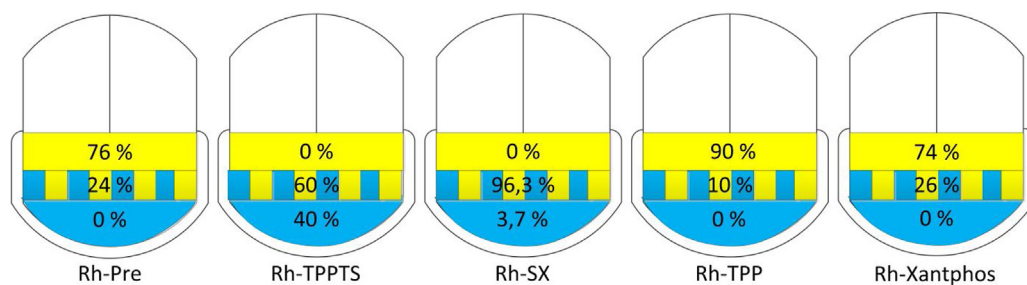


Fig. 8. Distribution of the Rh catalyst for different ligands ($\alpha = 50\%$, $y = 8\%$ (Marlipal 24/70), 1 wt% sodium sulfate, $n_{Rh(acac)CO_2} = 0.05$ mmol, $n_{bidentate} = 5$ eq., $n_{monodentate} = 10$ eq.).

However, concluding from these results it is clear that only water-soluble ligands should be used in connection with three-phase microemulsion systems, if an efficient recycling of the catalyst combined with a hydrophobic product isolation are desired.

3.4. Temperature influence

The prior results show that the distribution of the rhodium complex in a microemulsion system strongly depends on the hydrophobicity of the ligand and on the kind of the amphiphile. It

Table 1
Rhodium content in the aqueous phase at different temperatures with the amphiphile C_4E_2 ($\alpha = 50\%$, $y = 20\%$, 1 wt% sodium sulfate, $n_{Rh(acac)CO_2} = 0.05$ mmol ($m_{Rh} = 5145$ mg), $n_{SX} = 5$ eq.).

Temperature ($^{\circ}C$)	Volume aqueous layer (mL)	Volume middle layer (mL)	Volume oil layer (mL)	Rh-concentration aqueous layer (ppm)	Rh-content aqueous layer (mg)
60	16.0	10.4	24.6	34.5	0.55
70	17.0	9.0	25.0	52.7	0.90
80	17.0	8.0	26.0	60.3	1.03

is well known that the temperature shows a tremendous influence on the partition coefficient of salts like the catalyst complex. Hence, we investigated the rhodium content in the aqueous phase at different temperatures (see Table 1). Since most of the systems are extremely temperature sensitive, we decided to choose the microemulsion system formulated with of the amphiphile $C_{4}E_2$. As illustrated in Fig. 2 it has a broad three phase region, which allows us to study the effect of temperature without changing other experimental conditions.

The results listed in Tab. 1 state that the temperature has a strong influence on the distribution of the catalyst complex. The results are comparable, because the volume of the three layers stays almost constant. There is only a small reduction of the middle phase due to the fact that the solubility of the amphiphile in the oil phase increases with increasing temperature. Hence, the volume of the oil phase increases and that of the middle phase decreases. However, we can clearly show that the rhodium content in the aqueous layer is a function of the temperature. The higher the temperature, the higher is the rhodium content in the aqueous layer. The amount of rhodium was almost doubled by increasing the temperature from 333 K to 353 K. The results verify the typical properties for the solubility of a salt. Most salts (the water-soluble catalyst complex is an organic salt) show an increasing solubility in water with temperature. Thus, the separation temperature is also an important factor besides the kind of amphiphile and ligand to obtain a quantitative recycling of the catalyst complex.

3.5. Transfer of the lab results to a continuous process

The experimental results for the distribution of homogeneous catalyst complexes in microemulsion systems in the first part of this contribution demonstrate several possibilities to tune a reaction system with respect to an optimal catalyst recycling and separation process. The interactions between the surfactant and the catalyst complex influence the solubility of the latter and thus enable the control of catalyst distribution in the different phases by the choice of surfactant. For a fixed microemulsion system the application of different ligands has a strong influence on the distribution of the catalyst complex as well. However, a change of the applied ligand is rather unusual for an established reaction process and may result in a modification of the reaction kinetics. Therefore, the adjustment of the catalyst distribution by the choice of surfactant and the determination of the optimal

temperature range for the phase separation of the applied microemulsion system should be the preferred option for optimization of catalyst recycling.

In order to establish a closed recycle catalytic process, the Winsor III system is of great interest due to its two excess phases allowing for separation of hydrophobic products and hydrophilic side-products in the same separation step. Since the phase separation requires a certain amount of time depending on the state and temperature of the system, the reaction and catalyst recycling should be performed in different process steps to enable a continuous process.

Process design for homogeneous catalysis and catalyst recovery in microemulsion systems enables new paths in chemical engineering. Exemplarily, the homogeneously catalysed conversion of long chained olefins becomes feasible, as the surfactant compensates the miscibility gap between the olefin and a catalyst solved in an aqueous phase. As part of the Collaborative Research Center/Transregio 63, "Integrated Chemical Processes in Liquid Multiphase Systems" (InPROMPT) such a novel process concept is being investigated. One aim is to design, construct, and operate a mini-plant for the continuous hydroformylation in such a multicomponent system. Primary target is the combined homogeneous catalysis and catalyst recovery using this multiphase surfactant system. In the following, the task, the constraints, and the applied system is presented as well as an actual application in the mentioned mini-plant.

3.6. Task formulation

The task is to design a process in which the catalyst is recycled reliably in order to be reused in the reaction step and leaching via product streams is minimized or even eliminated. After the determination of a suitable tuned micellar solvent system, arising process constraints in terms of remaining catalyst leaching, catalyst stability, and separation dynamics have to be outlined, leading to the development of separation unit design for the given task. To keep things focussed, we consider that the product is always an oily component, thus forming the upper excess phase, and that the catalyst complex is hydrophilic. However, parts of the metal complex structure could be hydrophobic and thus inducing side effects, which have to be considered for the separation step. The thermomorphic behaviour of the microemulsion system and the catalyst behaviour described in Section 3 are summarized in

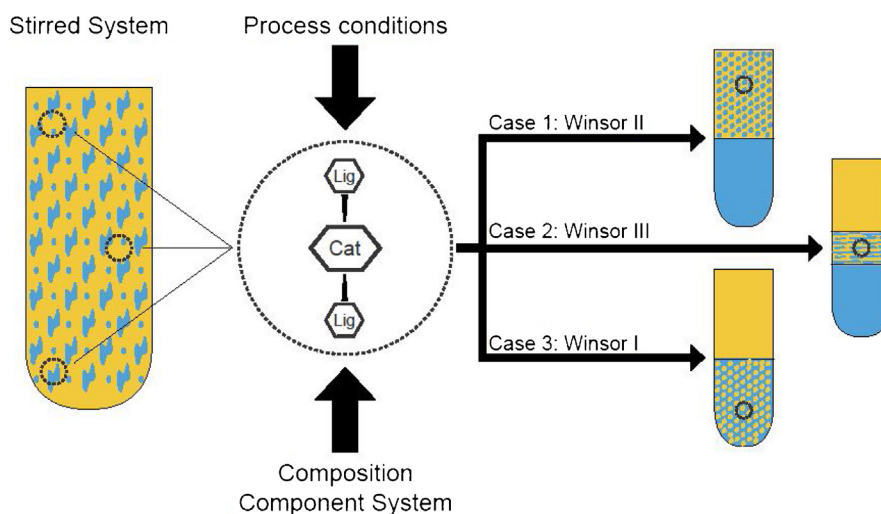


Fig. 9. Catalyst distribution and formed excess phases in the different phase separation systems for a microemulsion system tuned towards oily product separation and hydrophilic catalysts. Blue: aqueous excess phase, yellow: oily excess phase. The cycle indicates the location of the hydrophilic catalyst complex. (For interpretation of the references to colour in this figure legend, the reader is referred to the web version of this article.)

Fig. 9, showing the main catalyst position in the described Winsor systems, as well as formed excess phases.

We assume that the corresponding phase shows the major catalyst concentration. However, small amounts of catalyst could still remain in the directly neighbouring phases. The starting point for the separation process is right after a reaction step, in which a homogeneous emulsion is created.

3.6.1. Phase separation dynamics

An important issue which has to be considered in terms of operation conditions and equipment sizing (costs) is that of the phase separation dynamics. In the example shown in Fig. 10 the dependence of the separation time t_{sep} on the temperature can be seen. Fortunately, the Winsor III state shows a fast phase separation as opposed to the other states. This means, a short residence time in the separation step is possible. From an economic point of view this means a smaller settler, the operation unit in which the phase separation will take place, can be built or the through-put can be increased. Outside of the Winsor III temperature interval the separation time increases drastically. For the applied system, a separation in the Winsor I or Winsor II temperature interval was not observed, even after several hours. Other experimental results as well as a discussion on this issue regarding process applicability can be found in [19].

3.6.2. Process constraints

In addition to the determination of catalyst distribution and the overall phase separation dynamics, process constraints depending on the applied substances and microemulsion system need to be specified.

To maintain a viable lifetime of the active catalyst species in a continuous process, operation temperatures should be low, as the ligand-metal-complex is likely to decompose or initiate various side reactions at too high temperatures. This implies limitations for applicable thermal separation processes or prevents for example the use of distillation steps, as the catalyst complex would be completely deactivated and mainly transformed into metal particles in the reboiler. The system pressure should be kept constant or shifted smoothly for the overall process. Failing that, irreversible clustering of the metal-complexes may be observed, as shown in investigations of [20]. Moreover, aspects of chemical stability, such as degradation through the presence of oxygen, as well as electro chemical stability of the catalyst complex have to be

considered. Regarding the formation and thermomorphic behaviour of microemulsions, a variety of side effects could influence the separation dynamics [9]. It is obvious that for the surfactant concentration certain upper and lower bounds are required to maintain a microemulsion system. Impurities (salts) cause shifts in the observed temperature domains of the emulsion systems, as shown by Pfennig et al. [21]. Additionally, process pressure, stirrer speed in the reactor, and in general the occurring chemical reactions influence the phase separation dynamics and feasible temperature domains for the separation [19].

The previous findings are summarized in Fig. 11, which outlines feasible operation conditions and critical aspects of the phase separation states. At this point we define a critical rhodium loss, the rhodium mass fraction within the oil phase, which exits the plant as a product stream. Considering only rhodium precursor prices as catalyst costs, a value of 0.1 ppm equals monthly costs of around 200,000 for the catalyst (Rhodium price of 287/g [22], industrial scale product stream 10 t/h). This underlines the necessity for a low rhodium loss. According to the catalyst distribution in the Winsor system, the Winsor II state is highly economical infeasible, as high rhodium leaching would occur. Additionally, the separation dynamics are expected to be very slow, impairing the productivity of the plant. This fact also excludes the Winsor I system for operating points of a separator unit, because massively large units with high residence times would be necessary, although the rhodium loss poses to be optimally low. Therefore, only the Winsor III system seems economically feasible, concerning both criteria and is in scope for separator unit design and operating conditions.

3.7. Application example

The general process concept is depicted in Fig. 12 and consists of 2 main unit operations: mixing and settling. In the mixer part, the olefin, the surfactant, and an aqueous catalyst solution are mixed. By introducing syngas into the system, the hydroformylation reaction is initiated, thus forming aldehydes and byproducts [23]. Afterwards the reaction media is heated or cooled down to a desired temperature and separated accordingly. The idea is to exploit the thermomorphic behaviour and catalyst distribution according to Figs. 1 and 9. The goal is to obtain a catalyst-free oil phase, in which the product can be found, and a mixed phase, containing the vast majority of the dissolved catalyst. The mixed

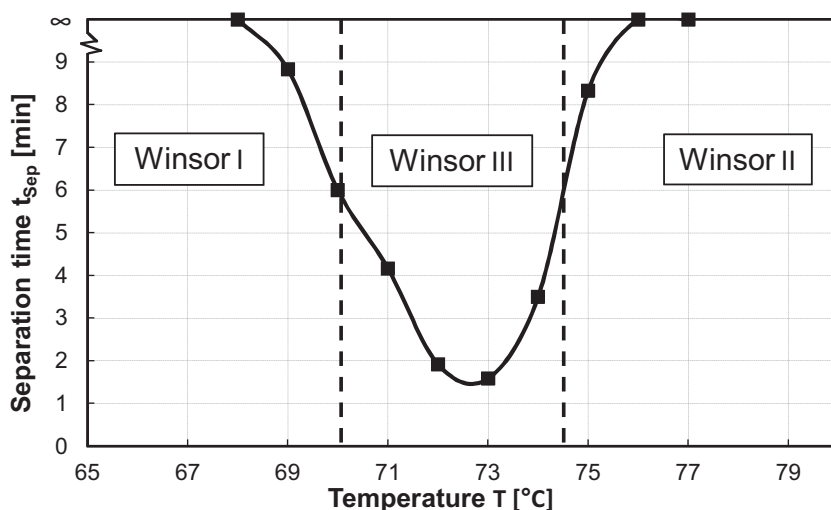


Fig. 10. Temperature dependency of the phase separation time and occurring phase states of a microemulsion system consisting of 1-dodecene/water/Marlipal 24/70 ($\alpha = 50\%$, $y = 8\%$, 1 wt% sodium sulphate, $n_{\text{Rh(acac)}\text{CO}_2} = 0.05 \text{ mmol}$, $n_{\text{SX}} = 5 \text{ eq.}$).

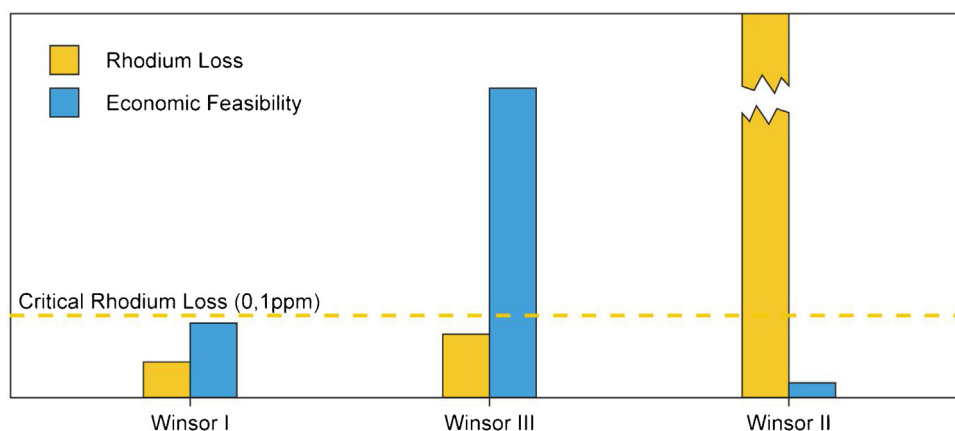


Fig. 11. Qualitative evaluation of the rhodium loss via the product phase and the economic feasibility of a settler operation in the corresponding Winsor systems. Phase separation dynamics are considered for the feasibility evaluation.

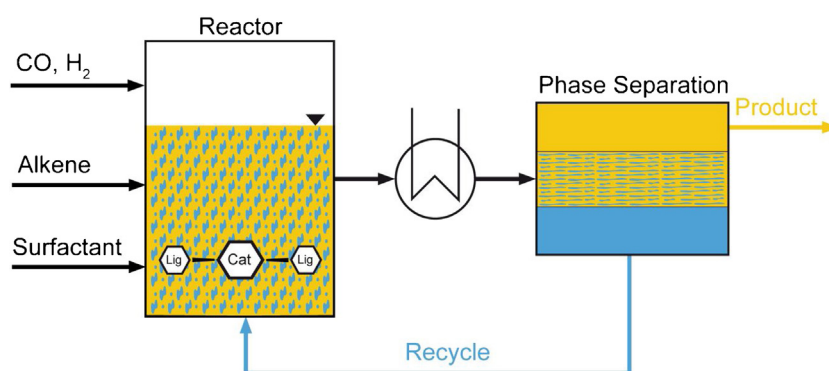


Fig. 12. Process concept for the hydroformylation of long-chained aldehydes in microemulsion systems [24].

phase is then recycled, thus enabling the reuse of catalyst and surfactant mixture.

For the investigated reaction system the hydrophilic catalyst complex, consisting of the rhodium precursor $\text{Rh}(\text{acac})(\text{CO})_2$ and the ligand SulfoXantphos, is applied. Hamerla et al. [12] have

shown that with this complex good reaction rates as well as a high selectivity regarding the linear aldehyde are achievable. Moreover, the application of a suitable surfactant is outlined, whereby according to experimental data the use of Marlupal 24/70 is

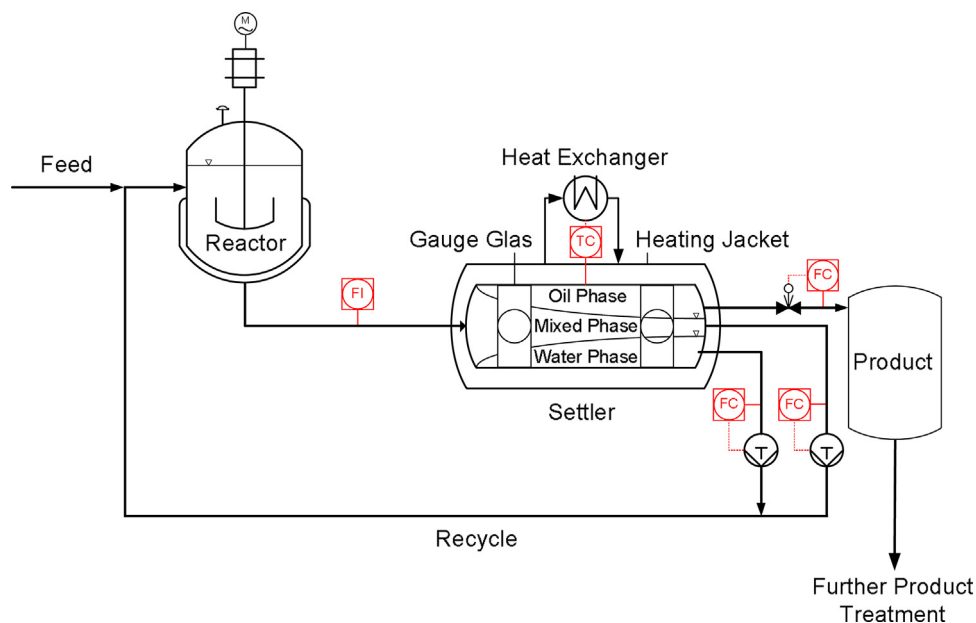


Fig. 13. General mixer-settler setup for the separation of up to three liquid phases.

preferential due to its applicability for the reaction and separation purposes [25].

3.8. Separation unit design and experimental data

Focussing on the separation step, the results from the first part of this contribution, together with outlined process constraints and challenges are applied for a separation unit design. Operational and economic aspects are then discussed on basis of experimental data of the respective unit.

3.8.1. Settler development

The pre-setting of a thermomorphic multiphase system, containing an oily component, water, and a surfactant for the regarded application offers the exploitation of suitable phase states. Due to the density differences of the components, a separation of the emulsion takes place in a composition dependent temperature domain, forming the three defined phases.

Fast phase separation dynamics for the Winsor III state and a suitable catalyst distribution (see Figs. 10 and 11) with almost no catalyst located in the oily product could be used in a simple settler setup. With the knowledge of the component concentration range in the reactor outlet and corresponding useful separation temperatures, we propose a temperature controlled settler setup, depicted in Fig. 13, for which the desired phase behaviour could be easily achieved. In this case a cylindrical tank with heating jacket, feed inlet, and 3 outlets for the corresponding phases is applicable. Adjusting the residence time via flow controllers and pumps and controlling the separation temperature, a phase split could be realized, gaining a pure oily product stream at the upper settler outlet. Lacking the input of mechanical and large quantities of thermal energy, along with needed internal, this set up offers low investment and operational costs.

In [19] a workflow is presented on how to systematically analyse surfactant containing multiphase systems regarding their applicability for mixer-settler processes. With respect to operational criteria, controllability and modularization a settler construction is presented, which was realised and integrated in the regarded mini-plant.

3.8.2. Settler operation

Given a settler design, as well as a specific microemulsion system, the economic and operational feasibility has to be validated. Therefore, experimental results of a mini-plant run will

be discussed in this section. Additional information about the hydroformylation mini-plant operation is given by Müller et al. [26].

The operating point for the reaction step of the hydroformylation in microemulsions was set to a pressure of 15 bar (g), temperature of 95 °C and a composition of $\alpha = 50\%$, $y = 8\%$, $w_{Rh}(\text{acac})\text{CO}_2 = 298 \text{ g/g}$, $w_{SX} = 4500 \text{ g/g}$, using Marlipal 24/70 as a technical grade surfactant. The plant was operated mostly in steady state condition (residence time settler approx. 40 min), using a settler with no internals.

For the observation of the phase separation state, samples at the outlet of the upper oily phase and the lower water phase were taken and analysed using offline gas chromatography. Taking a closer look at Fig. 14, it is possible to identify time periods where the separation was adequately. This is shown by the sum of the mass fraction of oily components, which reaches values close to 100% for the oily phase and simultaneously low values in the water phase. However, due to concentration shifts, caused by the ongoing reaction, the phase separation was partly lost.

It has to be mentioned that for the case of equal mass fractions in oil and water phase basically no separation took place and large amounts of surfactant and catalyst solution are introduced into the oil outlet stream. The overall high oil concentrations in both phases at these points indicate temporary shifts in the oil content of the settler, caused by inappropriate recycle ratios. By adjusting relevant process parameters, as temperature, recycle-ratio and surfactant concentration, the re-establishment of the separation was achieved, showing feasible settler operation for different operational states of the mini-plant.

In addition, Fig. 15 depicts the mass fraction of rhodium in the oil outlet stream of the settler. As this is the product stream, high rhodium contents cause a high economic loss.

Assuming a critical rhodium fraction of 0.1 ppm related to the oil phase, feasible operation periods are shown. For established phase separation, identified by a significant difference in the oil content of the regarded phases (Fig. 14), rhodium contents below 0.05 ppm were achieved (Operation time 35–60 h). With lost phase separation within the next 5 h of operation, the rhodium fraction increases immediately. Referring to the sampling point for operation time 63 h this behaviour is indicated and even higher rhodium contents are expected in the period of totally lost phase separation. Given the plant data, it could be seen that concentration shifts led to a drift towards the Winsor I state, where separation time increase massively. Interestingly no significant

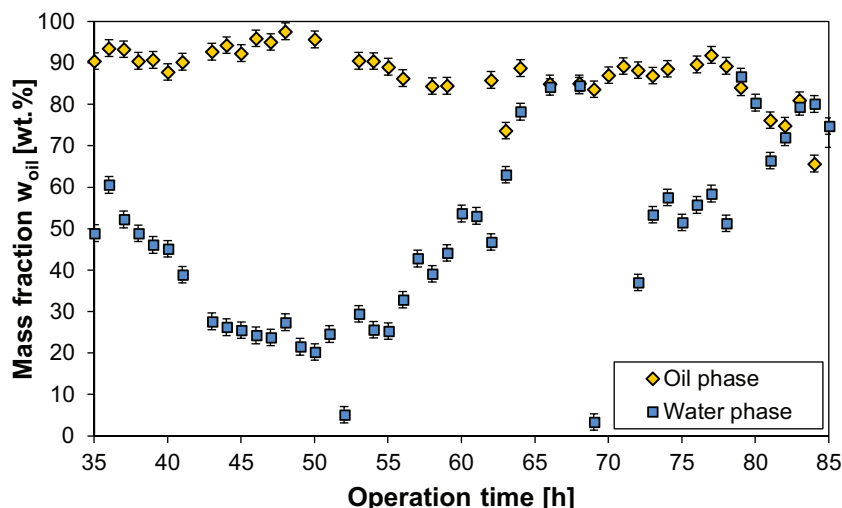


Fig. 14. Mini-plant operation data: mass fraction of total oily components in the upper oily phase and lower water phase.

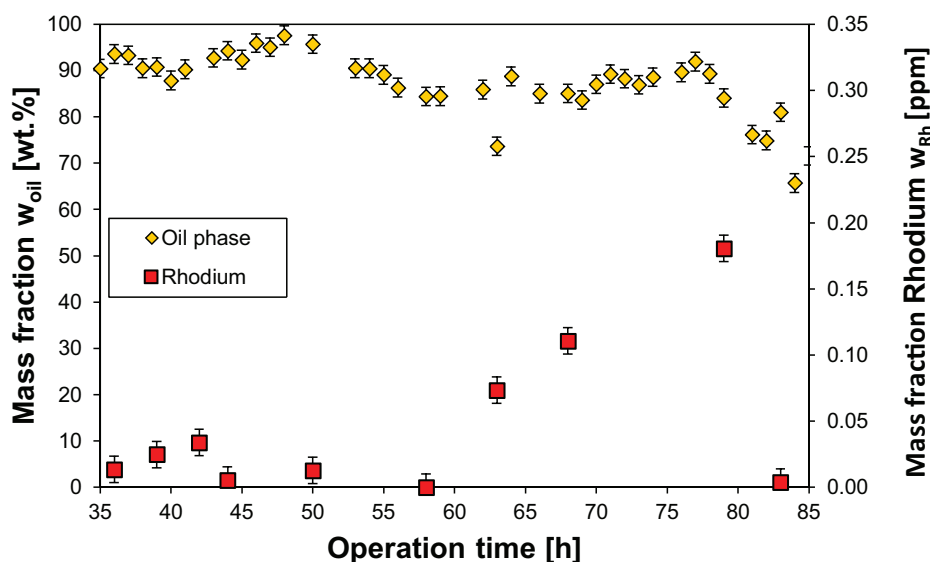


Fig. 15. Mini-plant operation data: mass fraction of total oily components (educt, products) in the upper oily phase and mass fraction of rhodium in the oily phase (product stream). Rhodium was measured using ICP-OES with a Varian ICP-OES 715 ES instrument, oil component data was gathered from gas chromatography.

decrease of rhodium concentration was achieved with re-established phase separation (70–80 h). In this case the settler temperature was set to high and the system moved towards the Winsor II state, whereas phase separation slowed down again and was subsequently lost.

Concluding, it is obvious that the expected behaviour for the catalyst distribution and phase separation dynamics is successfully confirmed in a mini-plant operation. However, challenges still exist to control the phase separation throughout all operational states and under process disturbances. For these cases different options for an advanced process concept seem possible and are in the scope of future investigations. Among these are liquid–liquid extraction for catalyst and surfactant separation from an oily phase or micellar enhanced ultrafiltration techniques, as described in [27,28].

4. Conclusions

The aim of this contribution was to analyse the effects that can have an influence on the distribution of homogeneous catalyst complexes between the different phase layers of microemulsion systems to ensure an efficient catalyst recycling for processes applying these multiphase systems. A profound knowledge of the thermodynamics of microemulsion systems and their phase behaviour as a function of temperature and composition is necessary to get a quantitative separation of the expensive catalyst complex. Especially the three-phase region is of great interest for a mixer-settler process due to its two excess phases allowing for separation of hydrophobic products and hydrophilic side-products in the same separation step. We have shown that the distribution of catalyst in a microemulsion system can be manipulated by the choice of the surfactant, the applied ligand, and the temperature. The surfactant seems to attract the catalyst complex, which follows the surfactant into the corresponding microemulsion phase. However, the higher the hydrophilicity of the ligand, the higher is the amount of catalyst that remains in the aqueous phase. In contrast, catalyst complexes involving hydrophobic ligands stay almost in the oil phase and should not be used in the presence of hydrophobic reactants as the separation is more challenging and requires further process steps. In addition, an increase of temperature improves the solubility of the catalyst complex in the aqueous phase as well. In summary, these results establish the

base for integrated processes using microemulsion systems. We presented a case study for the design of a continuous mixer-settler process, realized in a mini-plant for the Rh/SX catalysed hydroformylation of 1-dodecene to tridecanal in a microemulsion system. Analysing operation data, a temperature controlled settler is shown to be a feasible concept for a separation step, gaining an oily product phase and recycle a valuable catalyst rich phase. Due to disturbances, temporary high rhodium losses have to be tackled. Here, different process options like liquid–liquid extraction and membrane processes exist, which are of future research interest. However, summarizing the existing options for manipulating the phase behaviour of the microemulsion system for the application example, maintaining the three phase condition is desirable due to beneficial separation dynamics and moderate rhodium losses. Regarding microemulsion systems in general, this contribution gives information for a reasoned tailoring of the component system for an optimal catalyst distribution within the system, where a catalyst rich aqueous phase and fast separation dynamics is the desired situation for an easy and quantitative catalyst recycling.

Acknowledgements

This work is part of the Collaborative Research Centre “Integrated Chemical Processes in Liquid Multiphase Systems” coordinated by the Technische Universität Berlin. Financial support by the Deutsche Forschungsgemeinschaft (DFG) is gratefully acknowledged (TRR 63).

References

- [1] B. Cornils, J. Hibbel, W. Konkol, B. Lieder, J. Much, V. Schmidt, E. Wiebus, Verfahren Zur Herstellung von Aldehyden DE234701 (1982).
- [2] P.B. Webb, M.F. Sellin, T.E. Kunene, S. Williamson, A.M.Z. Slawin, D.J. Cole-Hamilton, *J. Am. Chem. Soc.* 125 (2003) 15577.
- [3] L. Leclercq, I. Suisse, F. Agbossou-Niedercorn, *Chem. Commun.* (2008) 311.
- [4] W. Leitner, *Acc. Chem. Res.* 35 (2002) 746.
- [5] P.G. Jessop, Y. Hsiao, T. Ikariya, R. Noyori, *J. Am. Chem. Soc.* 118 (1996) 344.
- [6] E. Schäfer, Y. Brunsch, G. Sadowski, A. Behr, *Ind. Eng. Chem. Res.* 51 (2012) 10296.
- [7] A. Riisager, P. Wasserscheid, R. Van Hal, R. Fehrmann, *J. Catal.* 219 (2003) 452.
- [8] I. Volovych, M. Schwarze, T. Hamerla, J. Blum, R. Schomäcker, *J. Mol. Catal. A Chem.* 366 (2013) 359.
- [9] M. Schwarze, T. Pogrzeba, I. Volovych, R. Schomäcker, *Catal. Sci. Technol.* 5 (2015) 24.

- [10] J.S. Milano-Brusco, M. Schwarze, M. Djennad, H. Nowothnick, R. Schomäcker, *Ind. Eng. Chem. Res.* 47 (2008) 7586.
- [11] H. Nowothnick, J. Blum, R. Schomäcker, *Angew. Chem. Int. Ed. Engl.* 50 (2011) 1918.
- [12] T. Hamerla, A. Rost, Y. Kasaka, R. Schomäcker, *ChemCatChem* 5 (2013) 1854.
- [13] R. Schomäcker, M. Schwarze, H. Nowothnick, A. Rost, T. Hamerla, *Chem. Ing. Tech.* 83 (2011) 1.
- [14] M.-J. Schwuger, K. Stickdorn, R. Schomäcker, *Chem. Rev.* 95 (1995) 849.
- [15] M. Kahlweit, E. Lessner, R. Strey, *J. Phys. Chem.* 87 (1983) 5032.
- [16] A. Kabalnov, U. Olsson, H. Wennerström, *J. Phys. Chem.* 99 (1995) 6220.
- [17] L. Wang, H. Chen, Y.E. He, Y. Li, M. Li, X. Li, *Appl. Catal. A Gen.* 242 (2003) 85.
- [18] H. Nowothnick, A. Rost, T. Hamerla, R. Schomäcker, C. Müller, D. Vogt, *Catal. Sci. Technol.* 3 (2013) 600.
- [19] D. Müller, E. Esche, T. Pogrzeba, M. Illner, F. Leube, R. Schomäcker, G. Wozny, *Ind. Eng. Chem. Res.* 54 (2015) 3205.
- [20] R.H. Crabtree, *Chem. Rev.* 115 (2015) 127.
- [21] A. Pfennig, A. Schwerin, *Ind. Eng. Chem. Res.* 37 (1998) 3180.
- [22] www.sigmaaldrich.com/catalog/product/aldrich/288101?lang=de®ion=D, 2015, (access 02.06.2015).
- [23] J. Markert, Y. Brunsch, T. Munkelt, G. Kiedorf, A. Behr, C. Hamel, A. Seidel-Morgenstern, *Appl. Catal. A Gen.* 462–463 (2013) 287.
- [24] D. Müller, E. Esche, M. Müller, G. Wozny, *Present. AIChE 2012, Pittsburgh*, 2012.
- [25] T. Hamerla, *Hydroformylierung Langkettiger Olefine Mit Zweizähnigen Rhodium-Komplexen, Mizellaren Lösungen Und Mikroemulsionen* (Dissertation), Technische Universität Berlin, 2014, 2015.
- [26] D. Müller, E. Esche, T. Pogrzeba, T. Hamerla, T. Barz, R. Schomäcker, G. Wozny, *20th Int. Conf. Process Eng. Chem. Plant Des.*, ISBN: 978-3-00-047364-7, Berlin, 2014.
- [27] M. Schwarze, M. Schmidt, L.A.T. Nguyen, A. Drews, M. Kraume, R. Schomäcker, *J. Membr. Sci.* 421–422 (2012) 165.
- [28] M. Schwarze, A. Rost, T. Weigel, R. Schomäcker, *Chem. Eng. Process. Process Intensif.* 48 (2009) 356.

PAPER 5

Catalytic Reactions in Aqueous Surfactant-Free Multiphase Emulsions

Tobias Pogrzeba, Marcel Schmidt, Lena Hohl, Ariane Weber, Georg Buchner, Joschka Schulz, Michael Schwarze, Matthias Kraume, and Reinhard Schomäcker

Industrial & Engineering Chemistry Research, 2016, 55, 12765-12775

Online Article: <http://pubs.acs.org/doi/10.1021/acs.iecr.6b03384>

ActiveView PDF: <http://pubs.acs.org/doi/ipdf/10.1021/acs.iecr.6b03384>

Reproduced (or 'Reproduced in part') with permission from "Catalytic Reactions in Aqueous Surfactant-Free Multiphase Emulsions; Tobias Pogrzeba, Marcel Schmidt, Lena Hohl, Ariane Weber, Georg Buchner, Joschka Schulz, Michael Schwarze, Matthias Kraume, and Reinhard Schomäcker. Industrial & Engineering Chemistry Research, 2016, 55, 12765-12775." Copyright (2016) American Chemical Society.

Catalytic Reactions in Aqueous Surfactant-Free Multiphase Emulsions

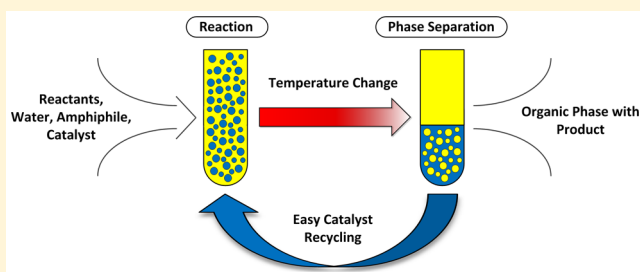
Tobias Pogrzeba,^{*,†} Marcel Schmidt,[†] Lena Hohl,[‡] Ariane Weber,[†] Georg Buchner,[†] Joschka Schulz,[‡] Michael Schwarze,[§] Matthias Kraume,[‡] and Reinhard Schomäcker[†]

[†]Department of Chemistry, Technische Universität Berlin, Straße des 17. Juni 124, Sekr. TC-8, D-10623 Berlin, Germany

[‡]Chemical and Process Engineering, Technische Universität Berlin, Ackerstraße 76, D-13355 Berlin, Germany

[§]Plant and Process Safety, Technische Universität Berlin, Straße des 17. Juni 135, TK-01, D-10623 Berlin, Germany

ABSTRACT: The first applications of aqueous surfactant-free multiphase emulsions as reaction media for rhodium-catalyzed hydroformylation of 1-dodecene and Suzuki coupling reaction of 1-chloro-2-nitrobenzene and 4-chlorobenzeneboronic acid are herein reported. The reaction systems were formulated from oil (reactant and solvent), aqueous catalyst solution, and diethylene glycol butyl ether [C₄H₉(C₂H₄O)₂OH]. We investigated these multiphase systems with respect to reaction engineering and catalyst recycling to evaluate their application potential for new chemical processes based on switchable solvents. For the hydroformylation, conversion of 23.4% after 4 h reaction time could be achieved at mild reactions conditions of 95 °C and 15 bar syngas pressure. The applied Rhodium-SulfoXantPhos catalyst could be successfully recycled for four times, maintaining its very high linear-to-branched selectivity of 99:1. For the Suzuki coupling reaction yields up to 90% were achieved within a single run. The Pd/SPhos catalyst could be recycled three times, but activity decreased at almost stable selectivity due to higher ligand leaching during the separation steps.



1. INTRODUCTION

In the course of the development of new sustainable industrial chemical processes the exploitation of switchable solvent systems is increasingly investigated in various fields. Several different approaches of switchable solvent systems have already been reported in the literature, like supercritical media based on CO₂,¹ switchable-polarity solvents,² thermomorphic multi-component solvents (TMS),³ or microemulsion systems (MES).⁴ Switchable solvents are liquids that can be reversibly switched from one state (or form) to another by the use of a simple trigger, for instance a change in temperature like for TMS and MES. The idea behind the application of these solvents in a chemical process is that they would meet the needs of one process step and could then be switchable to serve in the following step. For water-soluble catalysts, aqueous solutions can be applied as switchable solvent systems by the use of surfactants to formulate microemulsion systems. According to Winsor, microemulsions are thermodynamically stable and can be either a one-phase system (Winsor IV) or part of a multiphase system (Winsor I, II, or III) in which the microemulsion can be of three different types: water-in-oil (w/o), oil-in-water (o/w), or bicontinuous; the phase behavior is described in detail in the literature.^{4–7} It is believed that the surfactant is in any case necessary to stabilize the system by formation of an interfacial film between the aqueous and oil phases. However, in terms of sustainable processing it would be desirable to achieve aqueous two-phase systems that have a switchability similar to microemulsion systems but would not

need to be modified with a surfactant. Smith et al.⁸ reported in 1977 an oil-continuous (w/o) (micro)emulsion composed of hexane, 2-propanol, and water which could be considered as the first surfactant-free multiphase emulsion (denoted as SFME), since no traditional surfactant was involved in the system. Subsequently, the SFMEs have attracted much attention especially in physical chemistry,^{9–16} but besides their interesting physical properties SFMEs provide the possibility to create new chemical processes based on the concept of temperature-induced phase transition similar to TMS or MES systems. In addition, they offer the advantage of an easily handled and removable additive instead of nonenvironmentally friendly solvents or usually highly viscous and high-boiling long-chained surfactants.

In order to understand aqueous surfactant-free multiphase systems better for their application as switchable solvents in homogeneous catalysis, we decided to test these new multiphase systems using two model reactions, namely the hydroformylation of a long-chain olefin (1-dodecene) and the Suzuki coupling reaction of 1-chloro-2-nitrobenzene and 4-chlorobenzeneboronic acid in these systems. The applied reaction systems consist of oil (reactant and solvent), aqueous catalyst solution, and diethylene glycol butyl ether

Received: September 2, 2016

Revised: November 2, 2016

Accepted: November 28, 2016

Published: November 28, 2016

[C₄H₉(C₂H₄O)₂OH, denoted as C4E2]. Since the main goal of this work was to understand this new type of aqueous multiphase systems, we focused our experimental work on parametric studies and recycling experiments. In addition, we investigated the phase behavior of the resulting SFMEs and analyzed their structure by endoscopic measurement. The obtained results allow a characterization of the solvent properties of SFME and an evaluation of their application potential for new chemical processes.

2. MATERIALS AND METHODS

2.1. Materials. Chemicals for Hydroformylation Reactions. The reactant 1-dodecene was purchased from VWR with a purity of 95%. The precursor (acetylacetonato)-dicarbonylrhodium(I) (Rh(acac) (CO)₂) was contributed by Umicore, Germany. The water-soluble ligand 2,7-bissulfonate-4,5-bis(diphenylphosphino)-9,9-dimethylxanthene (SulfoXantPhos, SX) was purchased from Molisa, where it was synthesized according to a procedure described by Goedheijt et al.¹⁷ The syngas (1:1 mixture of CO and H₂, purity 2.1 for CO and 2.1 for H₂) was purchased from Air Liquide.

Chemicals for Suzuki Coupling Reactions. The reactants 1-chloro-2-nitrobenzene (purity 99.0%) and 4-chlorobenzeneboronic acid (purity 98.0%) were received from ABCR and Sigma-Aldrich, respectively. The precursor palladium(II) acetate (Pd(OAc)₂, purity 99.0%) was received from ABCR. The water-soluble ligand 2'-dicyclohexylphosphino-2,6-dimethoxy-sodium salt (SPhos, purity 97.0%) was received from Sigma-Aldrich. The base potassium carbonate (K₂CO₃, purity 98.0%) was received from Carl-Roth.

Miscellaneous Chemicals. The short-chain amphiphile diethylene glycol butyl ether (purity >99.0%) was purchased from Sigma-Aldrich. The solvent *n*-heptane (purity >99.0%) was received from Carl Roth. The solvents acetonitrile (HPLC, 99.9% purity) and water (HPLC, > 99.9% purity) were received from VWR. The ICP standards Rh (1011 ppm in 4.9 wt % HCl) and Pd (1011 ppm in 5.1 wt % HCl) were received from Sigma-Aldrich.

2.2. Investigation on Phase Behavior. Investigations on the phase behavior of the multiphase systems were performed by using tubes in a heatable water bath. Samples with different amounts of oil, water, and the particular amphiphile were prepared and heated up to the desired temperature. After reaching the temperature the test tubes were shaken to ensure homogeneity of mixture and put back into the water bath, and then phase separation was awaited. A phase diagram was constructed from the observed phase behavior as a function of amphiphile and temperature.

The important composition parameters to characterize the SFMEs are the weight fractions of oil (α) and amphiphile (γ) (eq 1), which are calculated with the mass m of the corresponding component:

$$\alpha = \frac{m_{\text{oil}}}{m_{\text{oil}} + m_{\text{H}_2\text{O}}} \quad \gamma = \frac{m_{\text{Amph}}}{m_{\text{oil}} + m_{\text{H}_2\text{O}} + m_{\text{Amph}}} \quad (1)$$

2.3. Endoscope Measurements. The experimental setup used for the endoscope measurements (Figure 1) consisted of a double-walled glass tank (DN 150, H/D = 1) equipped with four rectangular baffles and a Rushton turbine (stirrer diameter $d_{\text{st}} = 50$ mm, height of stirrer blade $h_{\text{st}} = 12.5$ mm). The Rushton turbine was installed at a constant bottom clearance ($h = 75$ mm). The temperature was maintained via an external

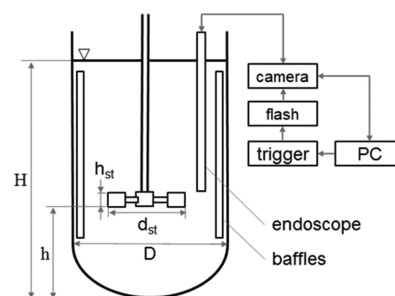


Figure 1. Experimental setup and endoscope measurement technique.

thermostat. The images were acquired using an endoscope, camera (GX 2750, Allied Visions Technology), trigger, and stroboscope at stirrer blade height. The drop sizes were determined using an automated image acquisition and drop detection software (SOPAT GmbH). Only spherical drops were taken into consideration. The minimum detectable drop size was 8–10 μm . Deviations of Sauter mean diameter were $\pm 10\%$.

2.4. Hydroformylation and Suzuki Coupling Experiments. **2.4.1. Catalyst Preparation.** For the preparation of the hydroformylation catalyst complex, 12.9 mg (0.05 mmol) of the rhodium precursor [Rh(acac) (CO)₂] and the ligand SulfoXantPhos (0.05–0.5 mmol) were dissolved in 4 mL of distilled water (degassed and flushed with nitrogen for at least 30 min) by using the Schlenk technique and stirred under argon atmosphere for a minimum of 12 h.

The homogeneous Pd/SPhos catalyst complex applied in Suzuki coupling reactions was prepared *ex situ* by stirring 7.5 mg (0.03 mmol) of the Pd(OAc)₂ catalyst precursor and 51.4 mg (0.10 mmol) of the water-soluble ligand SPhos in 3–5 mL of distilled water (degassed and flushed with nitrogen for at least 30 min) for 20 h under argon as inert gas.

2.4.2. Reaction Procedure. The hydroformylation reactions in lab-scale are performed in a 100 mL stainless steel high-pressure vessel from Premex Reactor AG, equipped with a gas dispersion stirrer and mounted in an oil thermostat from Huber (K12-NR). Reactor setup is illustrated in Figure 2. Mass flow controller (3) and a pressure transmitter (4) in the syngas feed line enable isobaric reaction management (semibatch mode). A connection for the inertization of reaction mixture is implemented as well (7).

The typical reaction conditions for the hydroformylation were 1–30 bar pressure of syngas, an internal reactor temperature of 75–100 $^{\circ}\text{C}$, and a stirring speed of 1200 rpm, using a gas dispersion stirrer. The reaction mixture usually consisted of 1-dodecene, water (HPLC grade), C4E2, rhodium precursor [Rh(acac) (CO)₂], and the ligand SulfoXantPhos.

The reaction was performed as described in the following. At first the reactor was filled with the desired amounts of olefin, water, and C4E2. Then the catalyst solution was transferred with a syringe to the reactor. The reactor was closed and evacuated and purged with nitrogen for at least three times. The stirrer was started at a rate of 500 rpm, and the reactor was heated up to the desired temperature. After reaching the temperature the stirring was slowed down (200–300 rpm), and the reactor was pressurized with syngas. Then the reaction was started by increasing the stirring speed again to 1200 rpm.

For the evaluation of reaction progress, samples were withdrawn at several time intervals via a sampling valve (Figure 2, (6)) and analyzed by gas chromatography (GC). To ensure

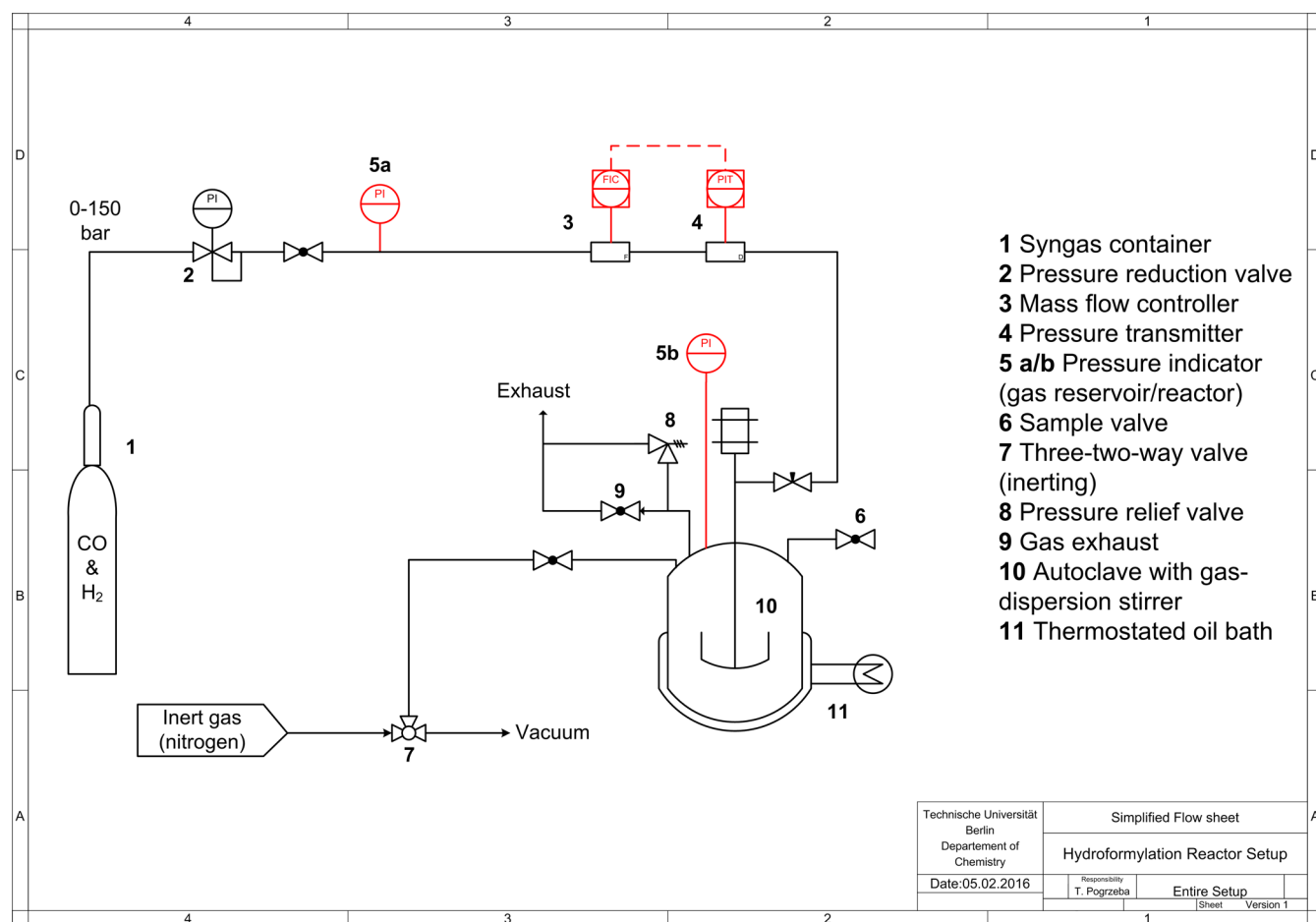


Figure 2. Reactor setup for hydroformylation experiments.

homogeneous liquid sampling, the stirring speed was not changed, while the samples were taken from the reactor. In addition, consumption of syngas during the experiments has been recorded via the mass flow controller.

The important parameters (conversion X , yield Y , selectivity S , and TOF) for the evaluation of experimental data were calculated as shown in eqs 2–5, where n is the amount of substance, 1-dodecene is the substrate, and 1-tridecanal is the product.

$$X(t) = \frac{n_{t=0, \text{Substrate}} - n_{t, \text{Substrate}}}{n_{t=0, \text{Substrate}}} \quad (2)$$

$$Y(t) = \frac{n_{t, \text{Product}}}{n_{t=0, \text{Substrate}}} \quad (3)$$

$$S(n:\text{iso}) = \frac{n_{\text{Product}}}{n_{\text{iso Aldehydes}}} \quad (4)$$

$$\text{TOF}_{\text{Ald}} = \frac{n_{t=0, \text{Substrate}} \cdot Y_{\text{Ald}}(t)}{n_{\text{cat}} \cdot t} \quad (5)$$

The Suzuki coupling reactions were performed in a double-walled glass reactor equipped with a condenser under nitrogen atmosphere. First, the reactor was evacuated and flushed with nitrogen. Second, the reactants were added under nitrogen flow (3 mmol of 4-chlorobenzenboronic acid, 3 mmol of 1-chloro-2-nitrobenzene, and 4 mmol of K_2CO_3) followed by water, C4E2, and heptane. The total mass was about 100 g. After

stirring at the desired reaction temperature, the reaction was started by the addition of the previously prepared Pd/SPhos catalyst. The reaction progress was followed by withdrawing samples which were analyzed by HPLC.

2.4.3. Analysis. GC Measurements. Reaction progress and selectivity of hydroformylation reactions were analyzed by gas chromatography on a Shimadzu model GC-2010, equipped with a Supelcowax 10 capillary column, a flame ionization detection analyzer, and nitrogen as carrier gas.

HPLC Measurements. The conversion and selectivity in all coupling reactions were determined by high performance liquid chromatography (HPLC) using an Agilent instrument 1200 series with 250×4 mm chromatographic column Multospher 120 RP18-5 μ from Ziemer Chromatographie Langerwehe/Germany. A mixture of acetonitrile/water (70 vol %/30 vol %) was used as eluent with a flow rate of 1 mL/min, $T = 25^\circ\text{C}$, $\lambda = 225$ nm, injection volume = 10 μL , $p = 110$ bar, and $t = 15$ min. All samples were dissolved in acetonitrile ($F = 100$).

ICP-OES Measurements. The residue solutions from different coupling reactions were analyzed for palladium and phosphorus content using a Varian 715-ES Optical Emission Spectrometer (ICP-OES) to determine catalyst leaching. Calibration of the instrument was performed with commercial palladium and phosphorus standards from Sigma-Aldrich.

3. RESULTS AND DISCUSSION

3.1. Hydroformylation Reaction. As a benchmark for the rhodium-catalyzed hydroformylation in aqueous multiphase

systems (Figure 3) we selected the 1-dodecene/water/Marlipal (24/70) microemulsion system, which was recently presented

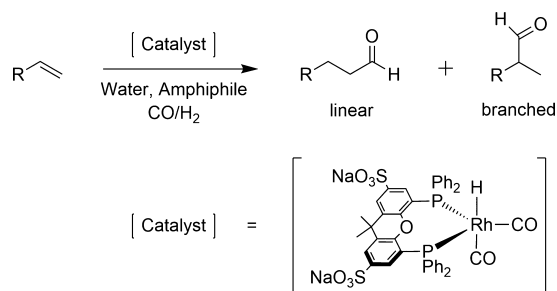


Figure 3. Hydroformylation reaction with the applied rhodium catalyst.

by our working group.¹⁸ The following parameters were found to be optimal for the reaction: $\alpha = 0.5$, $\gamma = 0.08$, 95 °C reaction temperature, 15 bar syngas pressure, 1200 rpm stirring speed, and 1:4 metal-to-ligand ratio. Hence we started the investigation of hydroformylation in the SFME system with these settings and subsequently optimized the parameters in several kinetic experiments. The results of these experiments are presented in the following chapters.

Investigation on Phase Behavior. At the beginning of our investigation the phase behavior of the applied 1-dodecene/water/C4E2 multiphase system was studied. For this purpose, several mixtures with different values for α (0.4, 0.5, 0.6) and γ (0.05 to 0.3) have been prepared. The phase behavior of the resulting emulsions was investigated from 25 to 95 °C in 2 °C steps (experimental procedure is described in section 2.2). Since the phase behavior was found to be similar for every investigated α value, in Figure 4 only the results for α

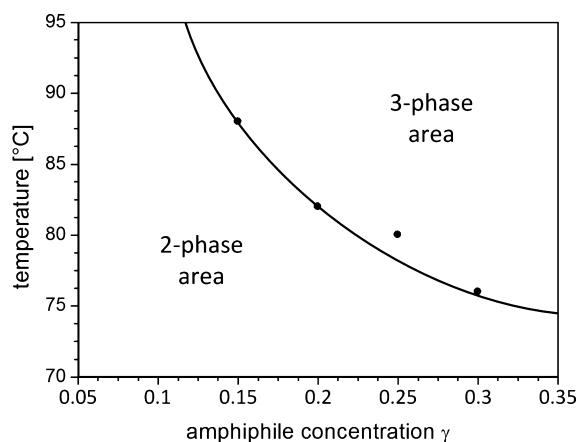


Figure 4. Phase diagram of the 1-dodecene/water/C4E2 multiphase system ($\alpha = 0.5$): 2-phase area = oil phase + aqueous phase, 3-phase area = oil phase, C4E2-rich middle phase, and aqueous phase.

$\alpha = 0.5$ are presented. A broad 3-phase area was found for the SFME beginning at 77 °C for $\gamma = 0.3$, at lower temperatures a 2-phase system was observed. The separation time of the system was less than 1 min in each case. With lower amphiphile concentration the phase transition temperature increased, for $\gamma = 0.15$ it was found at 88 °C. For $\gamma = 0.05$ and $\gamma = 0.1$ no 3-phase area could be observed. We assume that the required temperature for phase transition in these two systems is higher

than 95 °C, which was the maximal temperature we could adjust in the water bath.

Furthermore, the experiment for $\alpha = 0.5$ was repeated with rhodium-SX catalyst in the mixture to investigate the influence of the catalyst on phase behavior and the catalyst distribution in the multiphase system. As a result, no change of phase behavior could be detected with catalyst in the solution. However, the catalyst distribution between the phases changed with the phase behavior of the system. In the 2-phase area (depicted gray in Figure 4) all the catalyst was located in the aqueous phase. When the 3-phase area was adjusted by temperature, large amounts of the catalyst (82.5%) followed the amphiphile into the middle phase which was proved by ICP-OES measurements. The rest of the catalyst (17.5%) remained in the aqueous phase.

Furthermore, we observed decomposition of the catalyst for $\gamma > 0.2$ after several hours of experiment. The catalyst containing phase(s) changed color from yellow to brown and black rhodium particles adsorbed at the water–oil interface. Interestingly, this observation could not be verified for lower amphiphile concentrations. We heated and shook all emulsions for several days without observing any sign of catalyst decomposition. An explanation for this could be that if the amount of C4E2 reaches a certain level, the equilibrium of rhodium-SX complex formation gets misaligned and the short-chained amphiphile replaces SX as ligand. The resulting complex should be very instable, which in consequence would lead to a facilitated oxidation of rhodium by dissolved oxygen or the formation of hardly soluble rhodium clusters. Thus, we decided to apply a maximum of $\gamma = 0.2$ in the hydroformylation experiments.

Investigation on Phase Volumina. The influence of the oil/water ratio and amphiphile concentration on the phase volume fractions of the applied 1-dodecene/water/C4E2 system was studied (see Figure 5). For this purpose, different mixtures for α (0.3–0.5) and γ (0.175–0.225) were prepared, and the phase volume fractions were determined at two different temperatures. An increase of amphiphile concentration resulted in a larger middle phase volume fraction. Correspondingly, a decrease of the organic and aqueous volume fractions occurred. This effect was more pronounced at 83 °C, where the middle phase volume fraction also was slightly larger compared to 95 °C. A variation of the oil/water ratio α did not affect the microemulsion phase considerably.

Investigation on Drop Size Distribution. The occurrence of the third liquid phase was also visualized using the endoscope measurement technique. Figure 6 depicts the droplet appearance inside the stirred tank under 2-phase (left) and 3-phase conditions (right). Under two-phase conditions (e.g., $T = 60$ °C) an o/w emulsion occurs. An increase of the temperature led to the formation of the 3-phase system, where the third phase occurred. The third liquid phase changed the dispersion conditions of the system toward multiple emulsions, where the middle phase is dispersed inside the dispersed aqueous phase. Details about the identification of the phases are given in previous studies.^{19,20}

The drop size distribution under both conditions can be determined using image analysis. Figure 7 (left) depicts the drop size distributions in the 2-phase area (o/w emulsion) and the overall drop size distribution of the 3-phase area (multiple emulsion). An increase of the droplet size and widening of the drop size distribution can be observed as a function of temperature. The droplet sizes in the 3-phase area were also

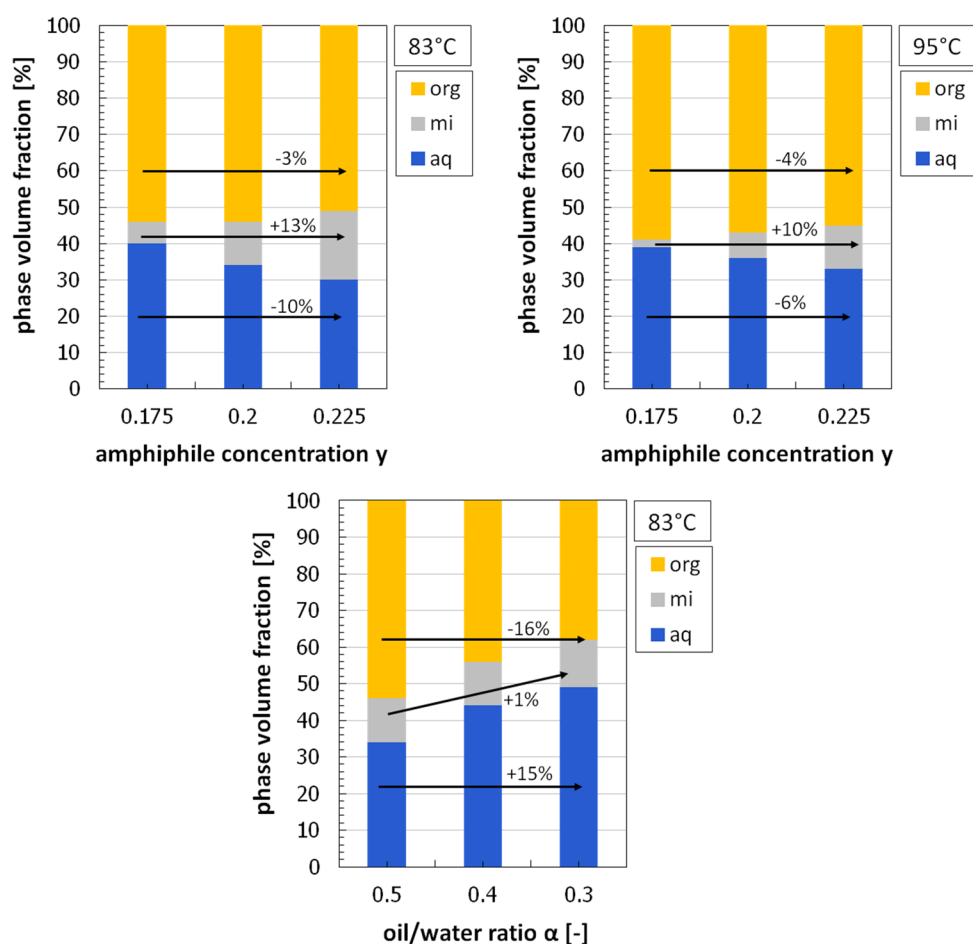


Figure 5. Phase volume fractions for different mixtures of 1-dodecene/water/C4E2. Top: At 83 and 95 °C with constant $\alpha = 0.5$. Bottom: At 83 °C with constant $\gamma = 0.2$. Phase volume fractions (phase heights) were determined by optical methods.

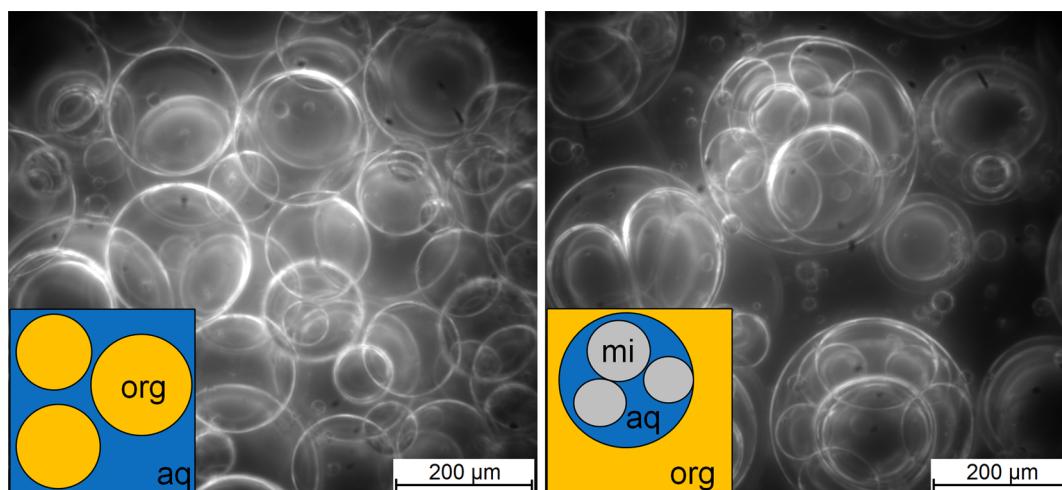


Figure 6. Drop images of the 1-dodecene/water/C4E2 multiphase system at 60 °C (2-phase area) and 83 °C (3-phase area).

determined separately: outer droplets = aqueous phase, inner droplets = emulsion phase (Figure 7, right).

Influence of Amphiphile Concentration on Hydroformylation. The reaction was tested with different C4E2 concentrations to identify the optimal amount of amphiphile. Due to the findings for the decomposition of catalyst at higher amphiphile concentrations (during investigation of phase behavior, see above), γ was not raised above 0.2 in these

experiments. In general, an increased amount of C4E2 in the mixture (and by that a larger emulsion phase, see Figure 5) benefits the reaction. For concentrations below $\gamma = 0.1$ the hydroformylation performed very poorly, resulting in almost no conversion after a 4 h reaction time (Figure 8). For $\gamma = 0.1$ a conversion of 3.5% was reached with a 1.4% yield in linear aldehyde ($\text{TOF} = 7.3 \text{ h}^{-1}$). The yield could be increased to 9.1% ($\text{TOF} = 53.8 \text{ h}^{-1}$) with a γ of 0.2, whereas formation of

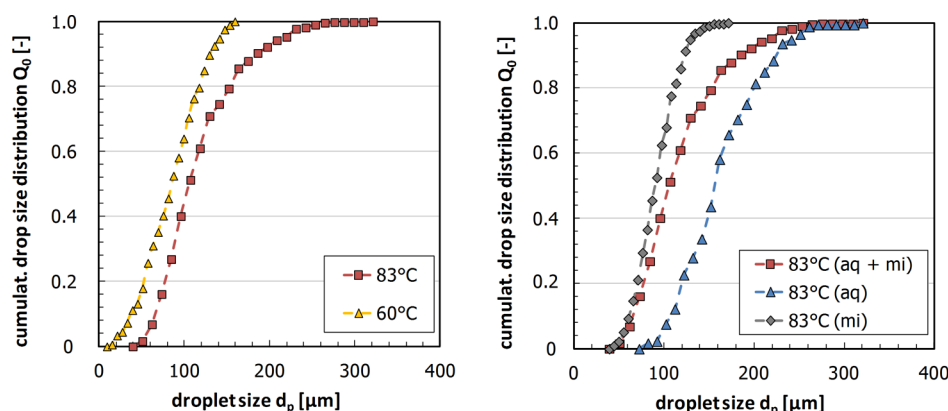


Figure 7. Overall drop size distribution in the 2-phase area at 60 °C and the 3-phase area at 83 °C (left). Overall and separated drop size distribution in the 3-phase area (right) at 500 rpm stirring speed in steady state.

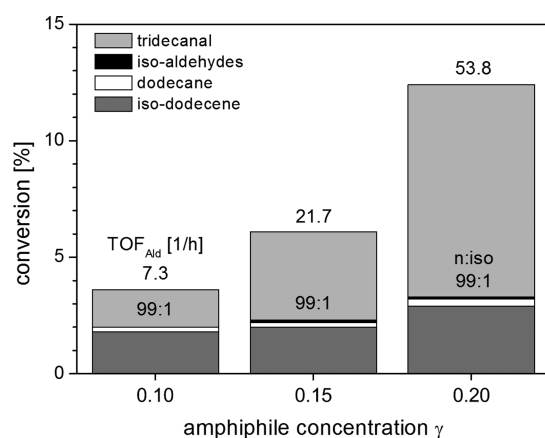


Figure 8. Effect of amphiphile concentration. Test conditions: $[\text{Rh}(\text{acac}) (\text{CO})_2] = 0.05 \text{ mmol}$, $\text{SulfoXantPhos} = 0.2 \text{ mmol}$, 1-dodecene = 120 mmol, water ($\alpha = 0.5$), $V_R = 50 \text{ mL}$, $T = 95 \text{ }^\circ\text{C}$, $p = 15 \text{ bar}$, stirring speed = 1200 rpm, $t_R = 4 \text{ h}$. Statistic deviation of conversion: $\pm 3\%$.

side products increased only slightly. The n:iso selectivity in the hydroformylation remained unchanged at 99:1 for each experiment, indicating that catalyst decomposition was not an issue for the applied C4E2 concentrations. In consequence we chose to apply a γ of 0.2 in all following experiments.

Influence of Catalyst Composition. Different metal-to-ligand ratios were tested to identify the optimal catalyst composition in terms of activity and long-term stability. The results are displayed in Figure 9. The selectivity of the catalyst was almost the same in each experiment. We found that an increase of metal-to-ligand ratio from 1:4 to 1:10 had a beneficial effect on the activity of catalyst. For a ratio of 1:10 approximately 15.3% of 1-dodecene was converted after 4 h reaction time with a yield of 12.6% in linear aldehyde, compared to 11.8% conversion (9.1% linear aldehyde) for a ratio of 1:4 (TOFs = 73.7 h^{-1} and 53.8 h^{-1} , respectively). These results were in contradiction to our assumption that a higher concentration of ligand should reduce the reaction rate due to the increased formation of inactive catalyst species bearing more than one SulfoXantPhos ligand. This partial deactivation of the applied rhodium-SulfoXantPhos catalyst was found by Hamerla et al.²¹ for the hydroformylation of 1-dodecene in microemulsion systems with nonionic surfactants. We assume that in the case of SFMEs this deactivation might be compensated by an enhancement in stability of the applied

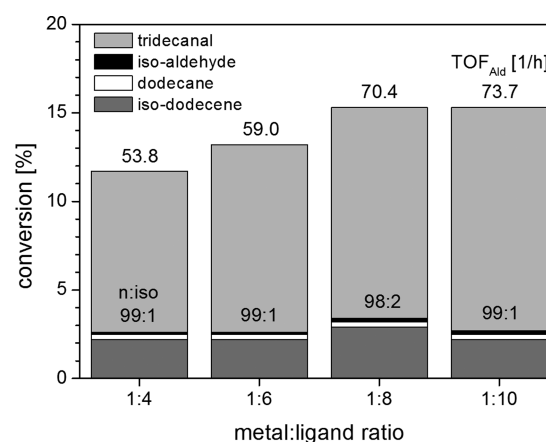


Figure 9. Effect of metal-to-ligand ratio. Test conditions: $[\text{Rh}(\text{acac}) (\text{CO})_2] = 0.05 \text{ mmol}$, 1 dodecene = 120 mmol, water ($\alpha = 0.5$), $\gamma = 0.2$, $V_R = 50 \text{ mL}$, $T = 95 \text{ }^\circ\text{C}$, $p = 15 \text{ bar}$, stirring speed = 1200 rpm, $t_R = 4 \text{ h}$. Statistic deviation of conversion: $\pm 3\%$.

emulsions due to higher amounts of ligand. Since SulfoXantPhos is surface active by itself²² it could have an additional stabilizing effect on the droplets in the SFME, which would be beneficial for mass transport and hence for the reaction rate. According to these results, a metal-to-ligand ratio of 1:10 was used for further investigation.

Influence of Oil Fraction. We investigated the influence of oil fraction on the hydroformylation in the applied SFME, to determine the optimal amount of oil with respect to reaction rate and yield. The oil fraction was varied between $\alpha = 0.3$ and $\alpha = 0.7$ (see Table 1). Interestingly the amount of oil seems to have only a slight but indistinct impact on the reaction rate. For

Table 1. Results for Different Weight Fractions of Oil

alpha (1-dodecene/ water)	TOF _{Ald} [h ⁻¹]	m(tridecanal) [g] ^a	selectivity (n:iso aldehyde)
0.3	68.6	2.33	99:1
0.4	77.5	2.66	99:1
0.5	73.7	2.52	99:1
0.6	51.9	1.78	99:1
0.7	71.2	2.41	99:1

^aAfter 4 h reaction time. $[\text{Rh}(\text{acac}) (\text{CO})_2] = 0.05 \text{ mmol}$, $\text{SulfoXantPhos} = 0.5 \text{ mmol}$, $\gamma = 0.2$, $V_R = 50 \text{ mL}$, $T = 95 \text{ }^\circ\text{C}$, $p = 15 \text{ bar}$, stirring speed = 1200 rpm.

the lowest α value of 0.3, reaction performed slightly slower (TOF = 68.6 h⁻¹) than for $\alpha = 0.5$ (TOF = 73.7 h⁻¹), whereas the TOF was found to be the highest at $\alpha = 0.4$ (TOF = 77.5 h⁻¹). With the exception of the experiment for $\alpha = 0.6$ (TOF = 51.9 h⁻¹) all TOFs lie in the range of $\pm 10\%$. Together with the results from the experiments with varying C4E2 concentration (see Figure 8), this ultimately leads us to the assumption that the reaction mainly takes place in the middle phase and at the interfacial area of the multiple emulsion droplets. Since the size of middle phase can only be adjusted by the amount of amphiphile in the system, as depicted in Figure 5, the concentration of substrate in this phase should not have changed between the experiments with different α (and therefore the reaction rate too). Due to slightly better results, we finally chose to apply $\alpha = 0.4$ instead of $\alpha = 0.5$ for further investigation.

Influence of Syngas Pressure. After optimization of the composition of the reaction medium the influence of syngas pressure on the hydroformylation was tested in the range of 2 to 25 bar. The results are displayed in Figure 10. The

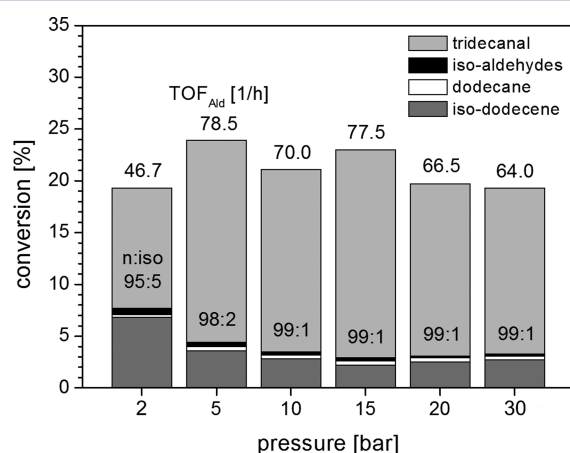


Figure 10. Effect of syngas pressure. Test conditions: [Rh(acac)(CO)₂] = 0.05 mmol, SulfoXantPhos = 0.5 mmol, 1-dodecene = 80 mmol, water ($\alpha = 0.4$), $\gamma = 0.2$, $V_R = 50$ mL, $T = 95$ °C, stirring speed = 1200 rpm, $t_R = 4$ h. Statistic deviation of conversion: $\pm 3\%$.

experiments showed that the hydroformylation performs best at 5 and 15 bar with conversions of roughly 24% after 4 h reaction time (TOFs = 78.5 h⁻¹ and 77.5 h⁻¹, respectively) and slightly slower at 10 bar (21% conversion, TOF = 70.0 h⁻¹). At a pressure of 2 bar the catalyst activity was comparably high but featured rather low reaction selectivity. The n:iso selectivity decreased to 95:5, and approximately 40% of converted 1-dodecene were isomerization products. An explanation for this finding could be the low partial pressure of CO. Markert et al.²³ showed for the hydroformylation of 1-dodecene with a rhodium-biphenos catalyst that a reduced partial pressure of carbon monoxide leads to an increase of the rate of the reversible isomerization reaction as well as the rate of hydrogenation. At syngas pressures higher than 15 bar the reaction rate seems to decrease slowly with an increase of pressure. At 25 bar the TOF value was only 64.0 h⁻¹, whereas selectivity remained unchanged. This result was expected and is a well-known effect in hydroformylation reactions.^{23,24} The inhibition of the reaction rate can be explained by increased formation of several inactive catalyst species with increasing CO concentration. As conclusion from these experiments we

decided to keep the pressure at 15 bar for further investigation. Although the reaction performed slightly faster at 5 bar and thus might be preferential from an economic point of view, we also considered selectivity and long-term stability of the catalyst for our decision.

Influence of Temperature. Different reaction temperatures were tested from 75 to 95 °C in 5 °C steps. The results show very clearly an increase of reaction rate with the temperature: After 4 h reaction time at 75 °C conversion of 1-dodecene was found to be 12.8% (TOF = 41.0 h⁻¹) which linearly increased to 23.4% at 95 °C (TOF = 77.5 h⁻¹) while selectivity of the catalyst remained on the same value in all experiments (Figure 11). The experimental data show that the

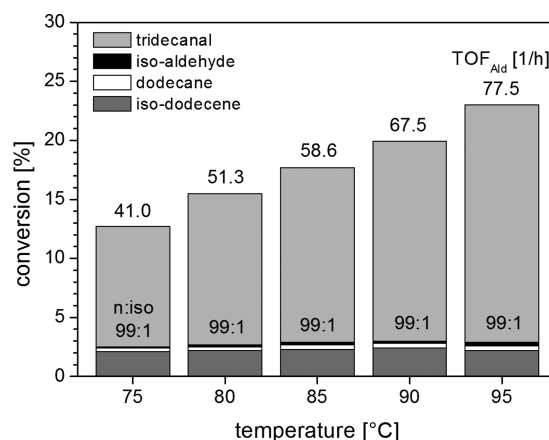


Figure 11. Effect of reaction temperature. Test conditions: [Rh(acac)(CO)₂] = 0.05 mmol, SulfoXantPhos = 0.5 mmol, 1-dodecene = 80 mmol, water ($\alpha = 0.4$), $\gamma = 0.2$, $V_R = 50$ mL, $p = 15$ bar, stirring speed = 1200 rpm, $t_R = 4$ h. Statistic deviation of conversion: $\pm 3\%$.

phase behavior of the applied SFME has no influence on reaction rate and a simple Arrhenius approach is sufficient to describe temperature dependency. The initial rates of the experiments were calculated and plotted in an Arrhenius diagram (Figure 12). Activation energy of the hydroformylation was calculated to be 53.9 kJ/mol which is in good accordance to the literature data collected with single phase systems.²⁵

Recycling Experiment. The gathered data from the previous experiments were used to optimize the reaction parameters for the rhodium-catalyzed hydroformylation in the

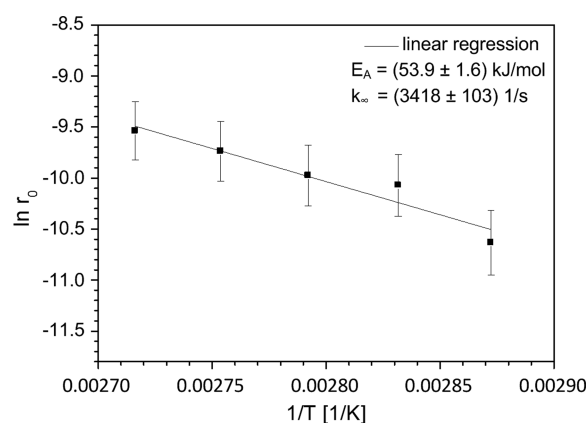


Figure 12. Arrhenius plot for the investigated reaction system. r_0 was calculated from syngas consumption at the start of the reaction.

applied SFME. To finally investigate and prove the applicability of SFMEs for chemical processing we performed a recycling experiment over 5 cycles including all optimal reaction settings. For this purpose the reactor was cooled down to room temperature and depressurized after each run. Next, the reactor was opened, the oil phase was decanted (after complete phase separation), and then the new substrate was added. In addition, we had to add some C4E2 after each run since GC measurements showed that small amounts of C4E2 leave the reactor together with the oil phase (roughly 1 g per recycle, which is 11 wt % of the applied amphiphile). After replenishing the reactor, it was closed and heated up again for the next run.

Following this procedure, the catalyst could be successfully recycled for four times and performed the hydroformylation reaction in a total of five runs with very high selectivity toward the desired product (Figure 13). Thus, the proof of concept for

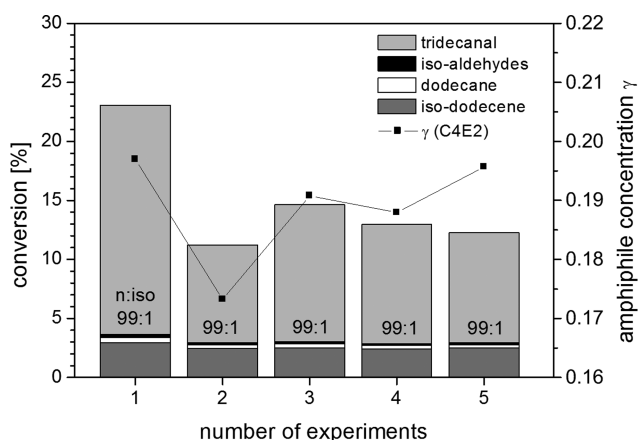


Figure 13. Recycling experiment. Test conditions: $[\text{Rh}(\text{acac})(\text{CO})_2] = 0.05 \text{ mmol}$, SulfoXantPhos = 0.5 mmol, 1-dodecene = 80 mmol, water ($\alpha = 0.4$), $\gamma = 0.2$, $V_R = 50 \text{ mL}$, $T = 95 \text{ }^\circ\text{C}$, $p = 15 \text{ bar}$, stirring speed = 1200 rpm, $t_R = 4 \text{ h}$. Statistic deviation of conversion: $\pm 3\%$.

the application of SFMEs as switchable reaction media in homogeneous catalysis is given. However, the results show a considerable decrease in activity of the catalyst after the first recycle. The TOF decreases by nearly 50% from 73.4 h^{-1} to 38.0 h^{-1} between the first and second run. The decrease is mainly due to the low C4E2 concentration in this run, since the loss of C4E2 in the extracted oil phase had been higher than expected. Thus, the value of γ decreased from 0.20 to roughly 0.175, which has a considerable impact on the rate of reaction

as already shown in Figure 8. The C4E2 concentration could be increased for the subsequent runs, leading to higher conversions. However, the activity of catalyst still decreased slightly with every new recycling step. We assume that this decrease could be due to catalyst deactivation by decomposition which had been already observed during the first phase separation experiments (see discussion of Figure 4). Oxidation of the catalyst by oxygen could also be part of the reason for catalyst deactivation, since the reactor had to be opened between the runs for the renewal of the oil phase. An indication for this assumption could be that the catalyst solution lost its characteristic yellow color during the recycling experiment and changed to light brown. Unfortunately, we have no evidence of the quantitative amount of remaining active catalyst after the fifth run, since this information would require the implementation of highly extensive in situ measurement techniques.

4. SUZUKI COUPLING

The Pd/SPhos catalyzed Suzuki coupling of 1-chloro-2-nitrobenzene and 4-chlorobenzeneboronic acid to 4'-chloro-2-nitrobiphenyl was carried out in heptane/water/C4E2 as reaction medium (Figure 14).

In contrast to the hydroformylation reaction, where 1-dodecene is used as a reactant and oily compound at the same time, heptane was used as a nonpolar component to dissolve the hydrophobic reactants. Suzuki coupling reactions have already been investigated in microemulsion systems of technical grade surfactants. It was demonstrated that 3ϕ microemulsion systems provide the best conditions for the reaction and the simultaneous separation of hydrophobic products, the catalyst complex, and salts produced during the reaction from the inorganic base.^{26,27}

At first, the phase behavior for the reaction mixture with C4E2 as the amphiphile was studied, and the obtained phase diagram after the coupling reaction is shown in Figure 15. Between an amphiphile concentration of 0 and 0.6 the 2ϕ and 3ϕ states are observed. In comparison to Figure 4, for the Suzuki coupling reaction the 3ϕ region is shifted to lower temperatures and covers a range of about 30–40 $^\circ\text{C}$.

If classical surfactants are applied to formulate a microemulsion system, the range for the 3ϕ region is often very small (about 5–10 $^\circ\text{C}$); therefore, a change in the composition of the reaction mixture can easily lead to a change in the phase behavior, e.g. from 3ϕ to 2ϕ state. This is a challenge, if a continuous process is aspired, but a successful example for a

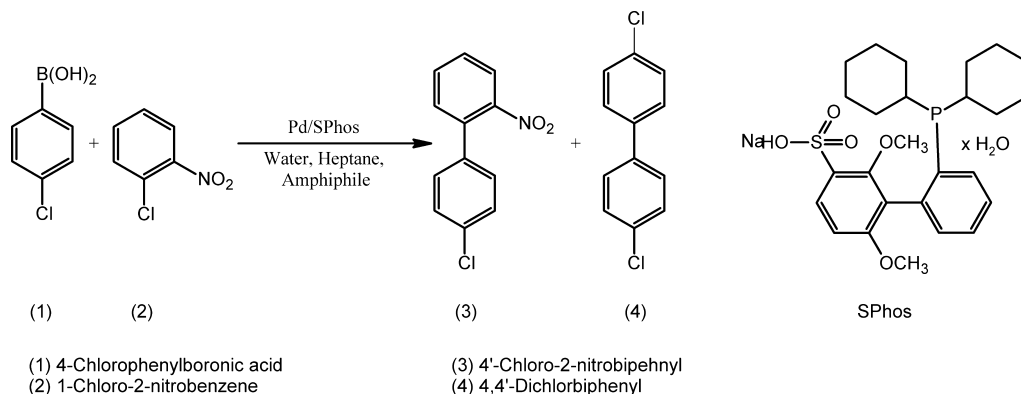


Figure 14. Suzuki coupling reaction with the applied water-soluble ligand.

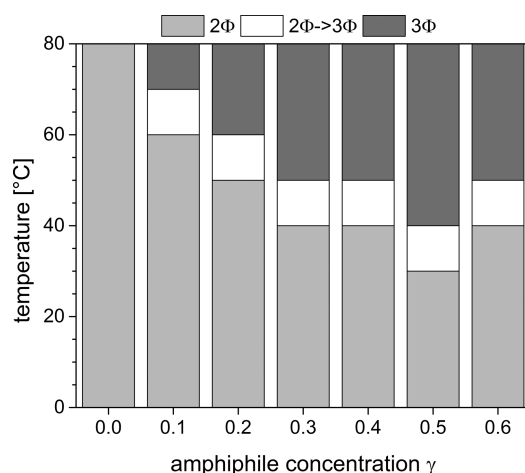


Figure 15. Phase behavior after reaction of 1-chloro-2-nitrobenzene (3 mmol) and 4-chlorobenzeneboronic acid (3 mmol) with K_2CO_3 (4 mmol) as base and Pd/SPhos as catalyst complex (Pd/SPhos = 1/3, 33.42 μ mol Pd) in heptane/water/C4E2 ($\alpha = 0.5$).

continuous operation of a hydroformylation reaction in a miniplant using 1-dodecene/water/Marlipal 24/70 as reaction medium is presented in refs 18 and 28. This example shows that it is possible to apply a microemulsion system in a combined reaction and separation process. However, the lower sensitivity of the phase behavior for the C4E2 based SFME toward smaller changes in the composition of the reaction mixture is of advantage. In addition, phase separation is much faster than in microemulsion systems, where the time for phase separation increases significantly when approaching the phase boundaries, but there are new challenges when C4E2 is used as an amphiphile instead of a conventional surfactant. The properties of the microemulsions system which are needed to have a favorable interaction with the catalyst complex, as we have already shown in ref 29 for microemulsion systems, are missed. For the 3 Φ microemulsion system, we would expect a higher catalyst concentration in the middle phase if water-soluble ligands are used. In contrary, we found for the C4E2 system that the Pd/SPhos catalyst complex used for the Suzuki coupling reaction accumulates in the middle phase, whereby a Pd/TPPTS complex accumulates mainly in the aqueous-excess phase. The short-chained amphiphilic structure of C4E2 is responsible for a more solvent-like behavior of the middle phase so that now the polarity of the catalyst complex is more important than its amphiphilic nature.

The Suzuki coupling reaction was performed at different C4E2 concentrations. As shown in Figure 16, the conversion and selectivity are slightly lower for the 2 Φ system but increase when the 3 Φ system is obtained, where yields up to 90% are achievable. When the amphiphile concentration is increased further, conversion and yield decrease again. As shown in Figure 5, the volume fractions within the 3 Φ system depend on the amphiphile concentration, whereby in the case of heptane, the volume of the middle phase increases and the volumes of the water and oil excess phase decrease. As the Pd/SPhos catalyst is located in the middle phase, its concentration will decrease with C4E2 concentration (dilution) and the reaction will slow down.

Although the 3 Φ system is the desired state for separation, the higher volume fraction of the middle phase is disadvantageous for the Suzuki coupling reaction. As already mentioned, for this reaction the oily phase is composed by heptane and the

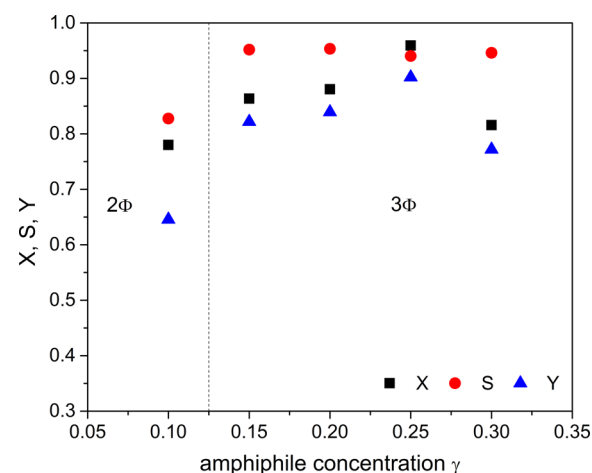


Figure 16. Conversion, selectivity, and yield as a function of the C4E2 concentration for the Suzuki coupling of 1-chloro-2-nitrobenzene (3 mmol) and 4-chlorobenzeneboronic acid (3 mmol) with K_2CO_3 (4 mmol) as base and Pd/SPhos as catalyst complex (Pd/SPhos = 1/3, 33.42 μ mol Pd) in heptane/water/C4E2 ($\alpha = 0.5$). Reaction temperature = 60 $^{\circ}C$ and reaction time = 120 min.

reactants/products within. Therefore, we have to consider the partitioning of the product between the individual phases. As shown by Volovych et.²⁷ for a C4E2 concentration of 15% only 56% of the product is located in the oil excess phase and the rest accumulates in the middle phase. Since heptane is not as hydrophobic as 1-dodecene, more heptane is dissolved in the middle phase with increasing C4E2 concentration so that the middle phase becomes more hydrophobic. If the oil excess phase should be used further, e.g. in tandem reactions, or high product removal is desired after one single reaction, the C4E2 concentration should be kept low. Again, we found an optimum in C4E2 concentration of 20%. The obtained yields for the Suzuki coupling reaction were already sufficient; therefore, we investigated the catalyst recycling and the increase in reactant concentration to achieve a higher space-time yield. For the recycling experiments, the oil and water excess phases after reaction containing the product and the salts were replaced by the same amount of heptane, water, and fresh reactants. As in the hydroformylation experiments, we found that C4E2 also leaches into the excess phases and has to be replaced in order to stabilize the phase behavior. Without any other modification, three runs could be carried out with the same catalyst, whereby the reaction time for each run was reduced to 20 min. The results are shown in Table 2.

Obviously, there is a strong decrease in the catalytic activity between the runs. To find the reason, we determined the catalyst leaching into the excess phases. We found a minor

Table 2. Conversion, Selectivity, and Yield for the Pd/SPhos Catalyzed Suzuki Coupling with Catalyst Recycling^a

run	conversion (X)	selectivity (S)	yield (Y)
1	0.87	0.91	0.79
2	0.41	0.86	0.35
3	0.22	0.81	0.18

^a1-Chloro-2-nitrobenzene (3 mmol) and 4 chlorobenzeneboronic acid (3 mmol) with K_2CO_3 (4 mmol) as base and Pd/SPhos as catalyst complex (Pd/SPhos = 1/3, 33.42 μ mol Pd) in heptane/water/C4E2 ($\alpha = 0.5$). Reaction temperature = 60 $^{\circ}C$ and reaction time = 20 min.

leaching of about 8% of Pd in three runs, but about 25% of SPhos already leached in a single run. A strong ligand leaching was also observed earlier by Nowothnick et al. for TPPTS.²⁶ Based on the Pd and SPhos losses, there are several possibilities to explain the lower activity, e.g. change in the Pd/SPhos ratio. However, the selectivity changes only slightly, and we can assume that the main reaction is still carried out by the Pd/SPhos complex but only at lower concentrations. It might be possible that some Pd is reduced but stabilized by the C4E2, which can explain that still 92% of Pd are present. As the C4E2 system is relatively new, further investigations are necessary. As this trend was also observed for the microemulsion systems²⁷ and could finally be solved by adding fresh ligand after a single run, we can expect the same behavior for the SFME.

Finally, we were interested in an increased productivity of the reaction system for which the reactant amounts were increased by a factor of 5 from 3 to 15 mmol. Within 15 min 98% conversion was achieved, but the selectivity decreased to 87% attributed to the high concentration of activated boronic acid able to perform the homocoupling reaction. It should be mentioned that the reaction at 60 °C was carried out in the upper 2Φ region due to a hydrophilic shift at higher reactant concentrations. To re-establish the 3Φ region, a reaction solution must be cooled down to 30 °C. We performed the reaction at 30 °C so that after the reaction separation can be done without a change in temperature; but activity was lower than expected, and 94% conversion and 85% selectivity were obtained after a reaction time of 120 min. We can summarize that the SFME can also be used for a combined reaction and separation process for the Suzuki coupling reaction, but further investigation is necessary to optimize the performance.

5. CONCLUSION AND OUTLOOK

In this contribution, we have shown that aqueous surfactant-free multiphase emulsions are feasible reaction media for homogeneously catalyzed reactions. A short-chain amphiphile, like diethylene glycol butyl ether (C4E2), is able to solubilize hydrophobic substrates in an aqueous environment and thus support the catalytic reaction and facilitate catalyst recycling in its active form. Preliminary investigations by the use of an endoscope measurement technique shown, that the applied reaction mixture for hydroformylation reaction consisting of 1-dodecene, water, and the amphiphile C4E2, formulates a multiphase system that has temperature dependent phase behavior similar to microemulsion systems (MES). Moreover, the switch from 2-phase to 3-phase conditions changed the dispersion conditions of the system from o/w emulsion toward multiple emulsions, where the emulsion phase was dispersed inside the continuous phase. Semibatch experiments for the rhodium-catalyzed hydroformylation of 1-dodecene in these systems showed under optimized reaction conditions a conversion of 23.4% (TOF = 77.5 h⁻¹) after 4 h reaction time. Interestingly, the results from the kinetic experiments let us assume that the reaction behavior of hydroformylation in SFMEs is more comparable to reactions in thermomorphic multicomponent systems (TML) than in MES. It seems like the reaction mainly takes place in the middle phase, and the reaction rate is strongly dependent on the amount of amphiphile in the system. This indicates the solvent properties of a medium polarity solvent mixture, rather than a highly dispersed MES. In recycling experiments the applied Rhodium-SulfoXantPhos catalyst could be successfully recycled for four times, maintaining its very high linear-to-branched selectivity of

99:1. The Suzuki coupling reaction of 1-chloro-2-nitrobenzene and 4-chlorobenzenboronic acid could also be successfully performed in aqueous SFMEs at yields up to 90%. Catalyst recycling was proven in general but needs further investigation in order to optimize the performance.

In summary, the results of the lab-scale experiments demonstrated the potential of surfactant-free multiphase emulsions as switchable reaction media for homogeneous catalysis and established the basis for more research using these systems, including the prospect of the design of a continuous process.

AUTHOR INFORMATION

Corresponding Author

*E-mail: tobias.pogrzeba@tu-berlin.de.

ORCID

Tobias Pogrzeba: 0000-0003-3727-9589

Notes

The authors declare no competing financial interest.

ACKNOWLEDGMENTS

This work is part of the Collaborative Research Center/Transregio 63 "Integrated Chemical Processes in Liquid Multiphase Systems" (subprojects A2 and B8). Financial support by the Deutsche Forschungsgemeinschaft (DFG, German Research Foundation) is gratefully acknowledged (TRR 63). Furthermore, the authors gratefully acknowledge the support of the company Umicore for sponsoring the rhodium catalyst "Acetylacetonato-dicarbonylrhodium(I) (CAS: 14874-82-9)".

ABBREVIATIONS

2φ = two phase

3φ = three phase

C4E2 = diethylene glycol butyl ether, C₄H₉(C₂H₄O)₂OH

MES = microemulsion system

SFME = surfactant-free multiphase emulsion

SPhos = 2'-dicyclohexylphosphino-2,6-dimethoxy-sodium salt

SX = SulfoXantphos, 4,5-bis(diphenylphosphino)-9,9-dimethylxanthene

TMS = thermomorphic multicomponent solvent

TOF = turnover frequency

REFERENCES

- (1) Leitner, W. Supercritical Carbon Dioxide as a Green Reaction Medium for Catalysis. *Acc. Chem. Res.* **2002**, *35*, 746.
- (2) Jessop, P. G.; Mercer, S. M.; Heldebrant, D. J. CO₂-Triggered Switchable Solvents, Surfactants, and Other Materials. *Energy Environ. Sci.* **2012**, *5*, 7240.
- (3) Schäfer, E.; Brunsch, Y.; Sadowski, G.; Behr, A. Hydroformylation of 1-Dodecene in the Thermomorphic Solvent System Dimethylformamide/Decane. Phase Behavior – Reaction Performance – Catalyst Recycling. *Ind. Eng. Chem. Res.* **2012**, *51*, 10296.
- (4) Schwarze, M.; Pogrzeba, T.; Volovych, I.; Schomäcker, R. Microemulsion Systems for Catalytic Reactions and Processes. *Catal. Sci. Technol.* **2015**, *5*, 24.
- (5) Winsor, P. A. Hydrotrophy, Solubilisation and Related Emulsification Processes. Part I. *Trans. Faraday Soc.* **1948**, *44*, 376.
- (6) Kahlweit, M.; Strey, R.; Busse, G. Microemulsions: A Qualitative Thermodynamic Approach. *J. Phys. Chem.* **1990**, *94*, 3881.
- (7) Sottmann, T.; Stubenrauch, C. *Microemulsions: Background, New Concepts, Applications, Perspectives*; John Wiley & Sons: Chichester, 2009.

- (8) Smith, G. D.; Donelan, C. E.; Barden, R. E. Oil-Continuous Microemulsions Composed of Hexane, Water, and 2-Propanol. *J. Colloid Interface Sci.* **1977**, *60*, 488.
- (9) Keiser, B. A.; Varie, D.; Barden, R. E.; Holt, S. L. Detergentless Water Oil Microemulsions Composed of Hexane, Water, and 2-Propanol. 2. Nuclear Magnetic Resonance Studies, Effect of Added NaCl. *J. Phys. Chem.* **1979**, *83*, 1276.
- (10) Borys, N. F.; Holt, S. L.; Barden, R. E. Detergentless Water/oil Microemulsions. III. Effect of KOH on Phase Diagram and Effect of Solvent Composition on Base Hydrolysis of Esters. *J. Colloid Interface Sci.* **1979**, *71*, 526.
- (11) Knickerbocker, B. M.; Pesheck, C. V.; Davis, H. T.; Scriven, L. E. Patterns of Three-Liquid-Phase Behavior Illustrated by Alcohol-Hydrocarbon-Water-Salt Mixtures. *J. Phys. Chem.* **1982**, *86*, 393.
- (12) Khmelnitsky, Y. L.; Van Hoek, A.; Veeger, C.; Visser, A. J. W. G. Detergentless Microemulsions as Media for Enzymatic Reactions: Spectroscopic and Ultracentrifugation Studies. *J. Phys. Chem.* **1989**, *93*, 872.
- (13) Klossek, M. L.; Touraud, D.; Zemb, T.; Kunz, W. Structure and Solubility in Surfactant-Free Microemulsions. *ChemPhysChem* **2012**, *13*, 4116.
- (14) Xu, J.; Yin, A.; Zhao, J.; Li, D.; Hou, W. Surfactant-Free Microemulsion Composed of Oleic Acid, N-Propanol, and H₂O. *J. Phys. Chem. B* **2013**, *117*, 450.
- (15) Fischer, V.; Marcus, J.; Touraud, D.; Diat, O.; Kunz, W. Toward Surfactant-Free and Water-Free Microemulsions. *J. Colloid Interface Sci.* **2015**, *453*, 186.
- (16) Marcus, J.; Touraud, D.; Prévost, S.; Diat, O.; Zemb, T.; Kunz, W. Influence of Additives on the Structure of Surfactant-Free Microemulsions. *Phys. Chem. Chem. Phys.* **2015**, *17*, 32528.
- (17) Goedheijt, M. S.; Kamer, P. C. J.; van Leeuwen, P. W. N. M. A Water-Soluble Diphosphine Ligand with a Large "Natural" Bite Angle for Two-Phase Hydroformylation of Alkenes. *J. Mol. Catal. A: Chem.* **1998**, *134*, 243.
- (18) Pogrzeba, T.; Müller, D.; Hamerla, T.; Esche, E.; Paul, N.; Wozny, G.; Schomäcker, R. Rhodium-Catalyzed Hydroformylation of Long-Chain Olefins in Aqueous Multiphase Systems in a Continuously Operated Miniplant. *Ind. Eng. Chem. Res.* **2015**, *54*, 11953.
- (19) Hohl, L.; Paul, N.; Kraume, M. Dispersion Conditions and Drop Size Distributions in Stirred Micellar Multiphase Systems. *Chem. Eng. Process.* **2016**, *99*, 149.
- (20) Hohl, L.; Schulz, J.; Paul, N.; Kraume, M. Analysis of Physical Properties, Dispersion Conditions and Drop Size Distributions in Complex Liquid/liquid Systems. *Chem. Eng. Res. Des.* **2016**, *108*, 210.
- (21) Hamerla, T.; Rost, A.; Kasaka, Y.; Schomäcker, R. Hydroformylation of 1-Dodecene with Water-Soluble Rhodium Catalysts with Bidentate Ligands in Multiphase Systems. *ChemCatChem* **2013**, *5*, 1854.
- (22) Schmidt, M.; Pogrzeba, T.; Stehl, D.; Sachse, R.; Schwarze, M.; von Klitzing, R.; Schomäcker, R. Verteilungsgleichgewichte von Liganden in Mizellaren Lösungsmittelsystemen. *Chem. Ing. Tech.* **2016**, *88*, 1.
- (23) Markert, J.; Brunsch, Y.; Munkelt, T.; Kiedorf, G.; Behr, A.; Hamel, C.; Seidel-Morgenstern, A. Analysis of the Reaction Network for the Rh-Catalyzed Hydroformylation of 1-Dodecene in a Thermomorphic Multicomponent Solvent System. *Appl. Catal., A* **2013**, *462–463*, 287.
- (24) Deshpande, R. M.; Kelkar, A. A.; Sharma, A.; Julcour-lebigue, C.; Delmas, H. Kinetics of Hydroformylation of 1-Octene in Ionic Liquid-Organic Biphasic Media Using Rhodium Sulfoxantphos Catalyst. *Chem. Eng. Sci.* **2011**, *66*, 1631.
- (25) Bhanage, B. M.; Divekar, S. S.; Deshpande, R. M.; Chaudhari, R. V. Kinetics of Hydroformylation of 1-Dodecene Using Homogeneous HRh(CO) (PPh₃)₃ Catalyst. *J. Mol. Catal. A: Chem.* **1997**, *115*, 247.
- (26) Nowothnick, H.; Blum, J.; Schomäcker, R. Suzuki Coupling Reactions in Three-Phase Microemulsions. *Angew. Chem., Int. Ed.* **2011**, *50*, 1918.
- (27) Volovych, I.; Neumann, M.; Schmidt, M.; Buchner, G.; Yang, J.-Y.; Wölk, J.; Sottmann, T.; Strey, R.; Schomäcker, R.; Schwarze, M. A Novel Process Concept for the Three Step Boscalid® Synthesis. *RSC Adv.* **2016**, *6*, 58279.
- (28) Illner, M.; Müller, D.; Esche, E.; Pogrzeba, T.; Schmidt, M.; Schomäcker, R.; Wozny, G.; Repke, J.-U. Hydroformylation in Microemulsions: Proof of Concept in a Miniplant. *Ind. Eng. Chem. Res.* **2016**, *55*, 8616.
- (29) Pogrzeba, T.; Müller, D.; Illner, M.; Schmidt, M.; Kasaka, Y.; Weber, A.; Wozny, G.; Schomäcker, R.; Schwarze, M. Superior Catalyst Recycling in Surfactant Based Multiphase Systems – Quo Vadis Catalyst Complex ? *Chem. Eng. Process.* **2016**, *99*, 155.

PAPER 6

Halloysites Stabilized Emulsions for Hydroformylation of Long Chain Olefins

Regine von Klitzing, Dimitrij Stehl, Tobias Pogrzeba, Reinhard Schomäcker, Renata Minullina, Abhishek Panchal, Svetlana Konnova, Rawil Fakhrullin, Joachim Koetz, Helmuth Möhwald, and Yuri Lvov

Advanced Materials Interfaces, 2016, 1600435

Online Article: <http://onlinelibrary.wiley.com/doi/10.1002/admi.201600435/full>

ActiveView PDF: <http://onlinelibrary.wiley.com/doi/10.1002/admi.201600435/epdf>

Reprinted (adapted) with permission from “Halloysites Stabilized Emulsions for Hydroformylation of Long Chain Olefins; Regine von Klitzing, Dimitrij Stehl, Tobias Pogrzeba, Reinhard Schomäcker, Renata Minullina, Abhishek Panchal, Svetlana Konnova, Rawil Fakhrullin, Joachim Koetz, Helmuth Möhwald, and Yuri Lvov. Advanced Materials Interfaces, 2016, 1600435.” Copyright (2016) John Wiley and Sons.

Halloysites Stabilized Emulsions for Hydroformylation of Long Chain Olefins

Regine von Klitzing, Dimitrij Stehl, Tobias Pogrzeba, Reinhard Schomäcker, Renata Minullina, Abhishek Panchal, Svetlana Konnova, Rawil Fakhrullin, Joachim Koetz, Helmuth Möhwald, and Yuri Lvov*

Halloysites as tubular aluminosilicates are introduced as inexpensive natural nanoparticles to form and stabilize oil–water emulsions. This stabilized emulsion is shown to enable efficient interfacial catalytic reactions. Yield, selectivity, and product separation can be tremendously enhanced, e.g., for the hydroformylation reaction of dodecene to tridecanal. In perspective, this type of formulation may be used for oil spill dispersions. The key elements of the described formulations are clay nanotubes (halloysites) which are highly anisometric, can be filled by helper molecules, and are abundantly available in thousands of tons, making this technology scalable for industrial applications.

of the halloysite surface increases the resulting emulsion stability.^[7–9] The arrangement parallel to the interface allows for larger contact area, and the mechanical stiffening may suppress fluctuations, that otherwise facilitates droplet coalescence. Halloysite clay nanotubes were first proposed as an efficient oil emulsifier in ref. [7] The formation of Pickering emulsions with surfactant loaded clay nanotubes (dioctyl sodium sulfosuccinate salt, Span 80, and lecithin) further improved oil dispersibility and connected this halloysite technology with

the traditional methods of preparing amphiphile stabilized emulsions.

Halloysite is a natural tubular aluminosilicate clay mineral that can be mined from deposits in thousands of tons at purity of 95%–99%.^[10] The nanotubes vary in length between 400 and 2000 nm, with a diameter of 40–60 nm and a lumen of 10–20 nm (Figure 1). The unique properties of halloysite such as low cost, environmental friendliness, biocompatibility, and hollow structure made it possible to use these nanotubes as a cargo for loading and slow release of active molecules such as drugs, anticorrosion agents, and surfactants.^[10–13] In the present paper, the application of pristine and hydrophobized halloysite nanotubes (HNTs) is described for model petroleum and dodecene emulsification in an attempt to generalize interfacial architectures for these clay nanotubes. The impact of dodecene/water emulsions for catalysis is demonstrated.

1. Introduction

Emulsions may be produced with addition of nano/microparticles accumulated at the droplets' interface, that stabilize them against coalescence in nonmiscible liquids. These emulsions named after one of the technique pioneers, S. Pickering,^[1] may be useful for liquid/liquid catalysis and for emulsification of spilled oil.^[2] Particles of silica, latex, or even bacterial cells are able to stabilize oil-in-water emulsions by assembly at the liquid–liquid interface^[3–6] using natural clay nanotubes is widening emulsification possibilities. Additional hydrophobization

Prof. R. von Klitzing, D. Stehl, T. Pogrzeba,
Prof. R. Schomäcker
Institute of Chemistry
Berlin Technische Universität
Berlin 10623, Germany

Dr. R. Minullina, A. Panchal, Prof. Y. Lvov
Institute for Micromanufacturing
Louisiana Tech University
Ruston, LA 71270, USA
E-mail: ylvov@latech.edu

S. Konnova, Prof. R. Fakhrullin
Institute of Fundamental Biology and Medicine
Kazan Federal University
Kazan, 420008 Tatarstan, Russia

Prof. J. Koetz
Institute of Chemistry
University of Potsdam
Potsdam 14476, Germany

Prof. H. Möhwald
Max Planck Institute for Colloids and Interfaces
Golm 14424, Germany



DOI: 10.1002/admi.201600435

2. Results and Discussion

2.1. Control of the Structure of Halloysite Pickering Emulsions

In order to get high yield and selectivity during catalysis and for oil spill remediation, the structure of the emulsions had to be controlled and tailored. As oil, either the model petroleum or dodecene was used. Halloysites were added at different concentrations. The degree of hydrophobization of the halloysite tubes was varied, and halloysites of different sizes were used.

The vortexing time does not essentially affect the average diameter of the oil droplets in case of a halloysite content of 0.25 wt%. In contrast, in presence of 0.5–1 wt% halloysites, the droplets get smaller with increasing vortexing time from

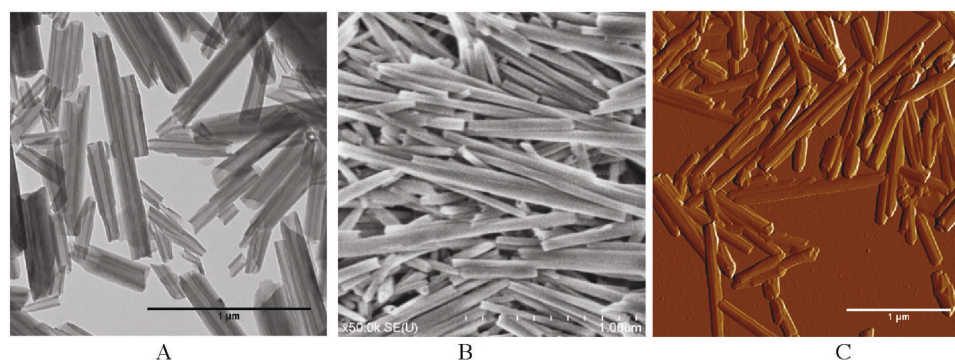


Figure 1. A) Transmission electron microscopy (TEM), B) scanning electron microscopy (SEM), and C) atomic force microscopy (AFM) images of halloysite (sample from Applied Minerals Inc.).

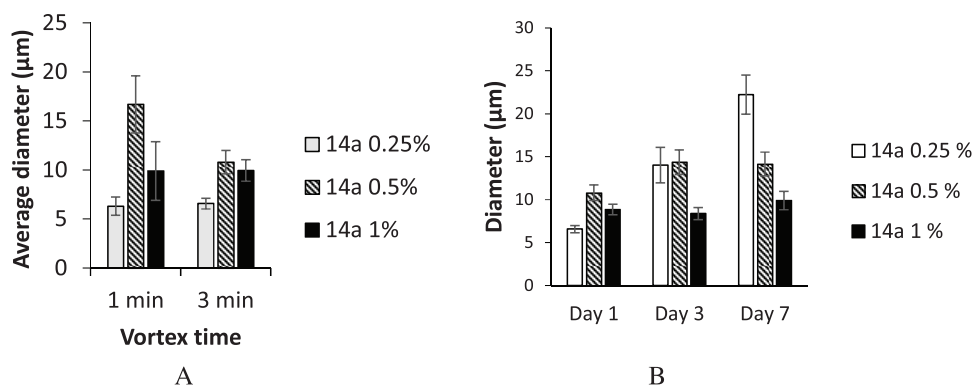


Figure 2. Average diameter of the Pickering emulsion droplets formed with model petroleum (oil phase) in water and 0.25, 0.5, and 1 wt% of pristine halloysite measured A) after different durations of vortexing and B) after several days (for 1 min vortexing time). The oil:water volume ratio was 1:3. The respective mean diameters are obtained from measurements of about 200 droplets each and the error is an average deviation.

1 to 3 min (Figure 2). For the following experiments, the vortexing time was kept fixed at 1 min.

In the next step, the storage stability of the emulsions was investigated in terms of changes in droplet size. The average diameter of the emulsions formed with 0.25 wt% of pristine halloysite significantly increases from 6 to 22 µm after 7 d (blue bars in Figure 2B), but less significant changes in diameter were observed in case of emulsions formed with 0.5–1 wt% of pristine halloysite (orange and grey bars). Obviously, an increase in halloysite concentration leads to denser packing at the oil/water interface, which stabilizes the droplets against coalescence. This highest studied halloysite concentration of 1 wt% was used for further formulation.

Size effects of halloysites on the droplet size distribution were studied with 1 wt% HMDS hydrophobized halloysite (Figure 3). Short halloysite nanotubes had average length of 400 nm, medium length halloysite had the average length of 750 nm, and long halloysite had an average length of 1500 nm.^[8]

The average droplet diameter is not affected by the length of the halloysites in the range 0.5–1.5 µm (Figure 3), though longer tubes provided a narrower size distribution of the droplets. An explanation might be the higher resistance of long halloysite tubes against droplet coalescence, which prevents the formation of the “distribution tail” toward larger droplets. For shorter halloysite tubes, it is difficult to visualize the tube location on the oil droplet, but longer tubes were well visible, and

they are oriented laterally on the droplet surface (Figure 4); cryo-SEM images for dodecene droplets shown further in Figure 7C as well indicate lateral positioning of the tubes on the droplet surface.

In order to imitate the salinity of sea water and to measure its impact, studies in fresh water, at 0.2 M and, finally, at 0.6 M of sodium chloride were carried out. The concentration of halloysite was fixed at 1 wt%, which was found as the best concentration in terms of stability. The halloysites were hydrophobized by HMDS or ODTMS.

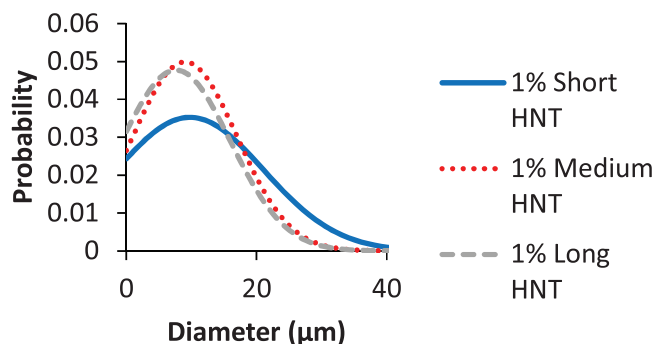


Figure 3. Diameter distribution of model petroleum droplets after one week in emulsions formed with 1 wt% of halloysite (HNT) of three different lengths.

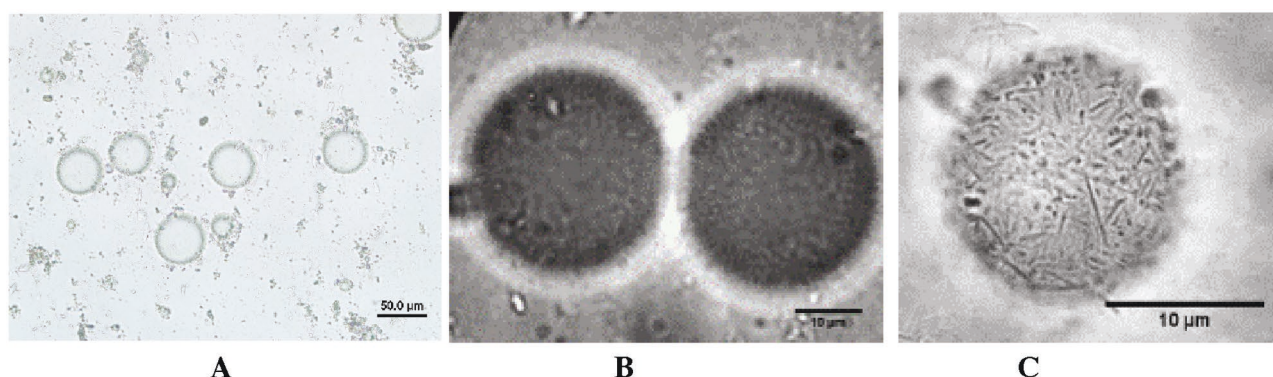


Figure 4. Optical images of 1 wt% halloysite emulsions with 30% oil (model petroleum): A,B) halloysite in model sea water at 0.6 M NaCl, and C) optical image at the same condition but with long 1.5 μm halloysite, allowing visualization of the tube location. Oil:water volume ratio was 1:3.

Using pristine halloysite in pure and salted water leads to a broad distribution of oil droplets with an average diameter of ca. 170 μm in case of pure water and ca. 100 μm in case of salty 0.2 and 0.6 M NaCl water (Figure 5A). The halloysites with medium hydrophobization with HMDS (contact angle of 30°) in pure water form emulsions with an average diameter of 18 μm which slightly increases in salty water (Figure 5B). The most stable emulsions with the smallest droplet diameters of $4.0 \pm 1.5 \mu\text{m}$ were obtained with ODTMS-hydrophobized halloysite (Figure 5C). Therefore, this formulation was considered the best among the studied ones for model petroleum emulsification. The halloysite emulsification of dodecene for catalysis as well yielded oil droplet diameters of ca. 4 μm . An explanation for the effect of salt might be the screening of the electrostatic repulsion between pristine halloysite nanotubes in presence of salts. The screening leads to denser packing of halloysites at the oil/water interface and to a decrease in droplet size. In case of hydrophobized halloysites, salt has no effect on the interaction. The dense packing of the surface active halloysites leads to smaller droplets.

2.2. Halloysite Based Oil Emulsions for Catalysis

Pickering emulsions stabilized with halloysite nanotubes are promising candidates for catalysis. It had already been shown, that emulsions stabilized by nano- or microparticles are potential systems for hydroformylation.^[4,14,15] A long chain olefin (dodecene) can be hydroformylated to tridecanal by using halloysite stabilized Pickering emulsions. Dodecene presented

the oil phase and the water-soluble amphiphilic rhodium (Rh)-based catalyst was solubilized in the water phase. Although silica particles and halloysites are both hydrophilic and have the same surface chemistry, their emulsions behave differently. In case of silica stabilized emulsions, the water:oil ratio determines the type of emulsion: oil-in-water emulsion (o/w) or water-in-oil emulsion. Up to 70% of the dispersed phase can be added until the emulsions show an inversion. In case of halloysite stabilization, the Pickering emulsions were always of o/w-type irrespective of the water/dodecene ratio. Figure 6C–F shows fluorescence microscope images of water:dodecene mass ratios of 1:3 (Figure 6C,E) and 3:1 (Figure 6D,F). The fluorescein dyed emulsions (Figure 6C,D) show dispersed oil droplets in the water phase. Also oil droplets can be observed in the nil red dyed emulsions (Figure 6E,F). Thus, the emulsion type of pristine halloysite stabilized emulsions remains always an o/w-emulsion. They follow the Bancroft rule, meaning that the continuous phase corresponds to the phase in which the particles are dispersible.

Due to the type of the Pickering emulsions (o/w-emulsion), the oil phase is not completely dispersible in the water phase at the water:dodecene mass ratio of 1:3 (Figure 6A) and the emulsion shows an excess of dodecene phase at the top. However, at the inversed mass ratio of water:dodecene 3:1 (Figure 6B), a completely dispersed oil phase appears and the excess of dodecene cannot be detected. The droplet size is not essentially affected by the oil:water ratio.

Figure 7A shows an optical microscopy image of dodecene droplets in the water phase. Furthermore, Figure 7B shows halloysites, which have adsorbed fluorescein and become visible in

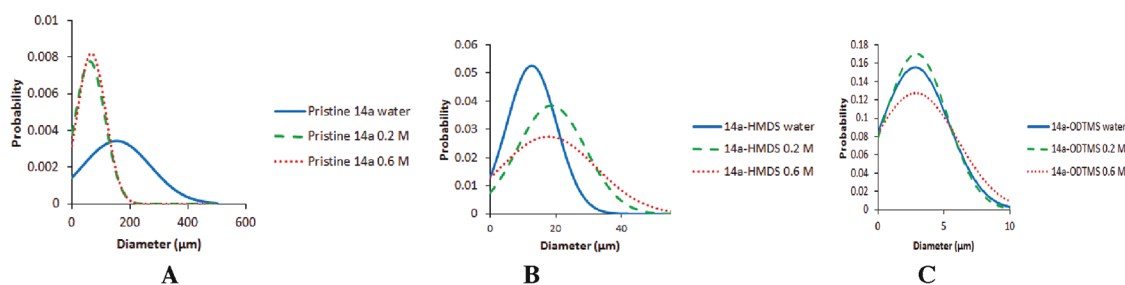


Figure 5. Size distribution of oil droplets after one week. Emulsions were formed with 1 wt% of A) pristine, B) HMDS, and C) ODTMS hydrophobized halloysite in pure water and in aqueous 0.2 and 0.6 M of NaCl.

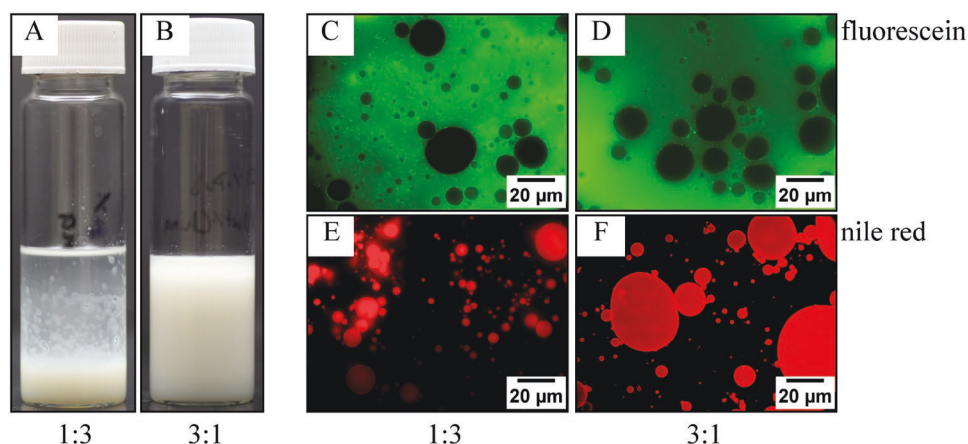


Figure 6. A,B) Images of halloysite stabilized emulsions at the mass ratios of 1:3 and 3:1. C–F) Fluorescence microscope images of the emulsions. C,D) The water phase was dyed with fluorescein (0.01 mg mL^{-1}), and E,F) the dodecene phase was dyed with nil red (0.01 mg mL^{-1}). C,E) Water to oil mass ratio of 1:3, D,F) water to oil mass ratio of 3:1.

the fluorescence microscope as green lines. It can be observed that the halloysites are attached at the oil/water interface, but the orientation of the halloysites does not really become clear from this fluorescence microscope image.

Another important difference between halloysite and silica stabilized emulsions is, that silica particles with extreme contact angles ($\theta < 20^\circ$ for hydrophilic and $\theta > 160^\circ$ for hydrophobic treatment) cannot stabilize emulsions^[4] while Pickering emulsions can be stabilized by hydrophilic tubule (pristine) halloysites. This supports the conclusion that the shape of the nanoparticles has an important effect on the stabilization as theoretically analyzed in.^[8] For example, the cylindrical (aspect ratio: 20:1) elongated particles have five times higher droplet surface detachment energy than the same mass spherical particles.^[8] Freeze fracture cryo scanning electron microscopy shows that the halloysite tubes are oriented laterally at the surface of the ca. 3–10 μm diameter dodecene droplets (Figure 7C). This explains the large resistance against coalescence.

If high energy ultrasonication is used for dodecene formulations, emulsions can be formulated without any particles added, but they are not filterable and much less stable against coalescence than Pickering emulsions. The rhodium-based catalyst used for hydroformylation of olefins contains an amphiphilic ligand, which acts as coemulsifier and may enhance the emulsification process. The addition of the catalyst leads to an

increase of the volume of the emulsion phase. Further experiments showed that stirring in the reactor at 1200 rpm of only water phase (with the catalyst) and dodecene phase shows no significant product yield.

The results of the hydroformylation of 1-dodecene to tridecanal (aldehyde) are shown in **Figure 8**. The halloysite (pristine, $750 \pm 200 \text{ nm}$) stabilized emulsions show a quite high product mass ratio in the reactor with more than 36 wt% after 24 h. The amount of byproduct (iso-aldehyde) remains very low during the whole reaction time. The product selectivity is excellent with an *n*:iso (tridecanal:iso-aldehydes) ratio of 99:1. Other compounds like iso-dodecene, which do not contribute to the reaction, are not shown in the plot.

After the reaction, the water phase with the catalyst can be easily separated from tridecanal by membrane filtration. The emulsion can be concentrated to more than 90% without breakthrough of the dodecene phase, meaning that the oil droplets remain stable against coalescence. This is a great advantage in comparison to many other strategies for catalysis of hydroformylation. The Pickering emulsions have very high overall process efficiency in terms of product yield, selectivity, and separation. This is a proof of concept for a novel strategy using halloysite stabilized emulsions for catalysis. Besides, in comparison to compact particles like silica, the lumen of the halloysites can be filled with drugs or additives for further perspectives.

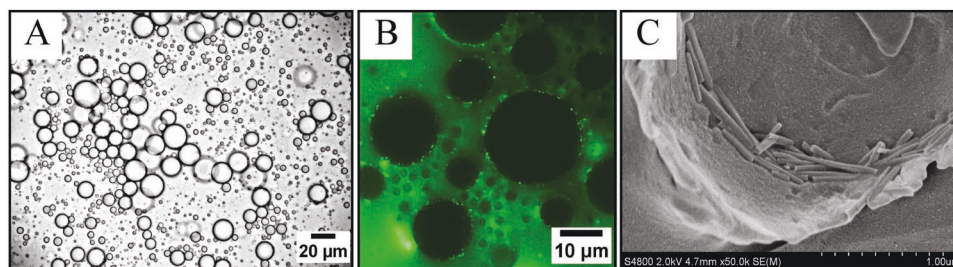


Figure 7. Dodecene-in-water emulsion stabilized by halloysites (water to dodecene ratio 3:1, 0.5 wt% halloysites). A) Optical microscopy image. B) Water phase doped with fluorescein. C) Freeze-fracture cryo SEM picture of a 3–10 μm sized dodecene droplet coated with halloysites in water.

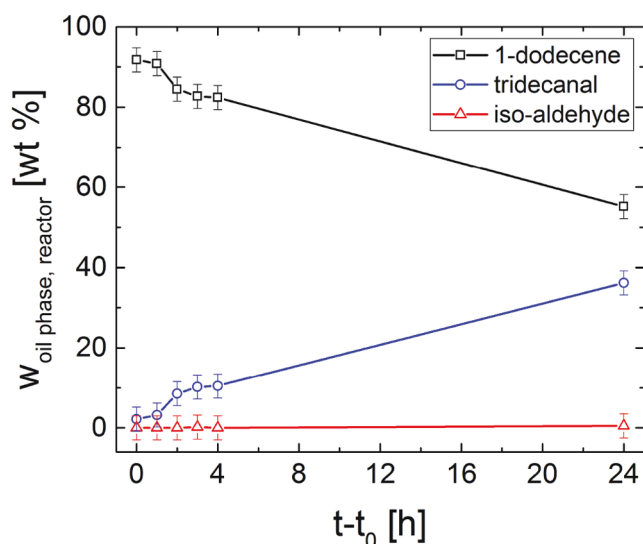


Figure 8. Hydroformylation of 1-dodecene to tridecanal (and undesired iso-aldehydes) during 24 h of reaction time and reaction conditions of 15 bar syngas (1:1 $H_2:CO$), 95 °C and stirring speed of 1200 rpm: The reactant contains also about 5% of iso-dodecene which reacts very slowly and does not change in concentration; $t = 0$: time, where the synthesis gas is added, t_0 : warming up of the reactor; $c_{Rh-cat} = 4.2 \text{ mmol L}^{-1}$ and the concentration of SulfoXantPhos was 17.8 mmol L^{-1} . $w_{oil \text{ phase, reactor}}$: mass ratio of the components in the oil phase (in reactor). For the Pickering emulsion, 24 g water with the catalyst, 8 g 1-dodecene, and 0.16 g (0.50 wt%) of pristine halloysites ($750 \pm 200 \text{ nm}$) were used.

2.3. Halloysite Nanotube Safety

Nanomaterial safety is a critical factor in industrial applications, making questionable the development of carbon nanotubes and graphene emulsions which may cause danger for ecology if used in large quantities.^[16–18] One may also question if elongated particles are more dangerous than more compact ones, considering the discussions about asbestos. However, halloysite clay nanotubes are the safest of the dispersed clays (montmorillonite, kaolin, and bentonite) and are much friendlier to the environment than carbon nanomaterials. This was proven for human cells, soil and fresh water microorganisms, and for small animal consumption.^[10,17,18]

Here it is shown that halloysite nanotubes do not significantly inhibit the viability and growth of bacterial cells. First, real-time monitoring of cell growth (Figure 9A) has confirmed, that the cells exhibit the typical growth patterns, although higher concentrations (2.5 mg mL^{-1}) somewhat reduce the growth rate. However, this might be explained by the more effective settlement of halloysite-treated cells and formation of biofilms rather than planktonic growth, as in case of intact cells and lower concentrations of halloysites. Although halloysite is generally known to be safe, no data were reported on the interactions of halloysite with bacteria. *A. borkumensis* cells are gram-negative marine species with relatively thin cell walls. Real-time growth monitoring was performed in thermostated plates where the cells had full access to nutrients and oxygen, therefore the increase of optical density corresponds to increasing cell numbers. This approach is more

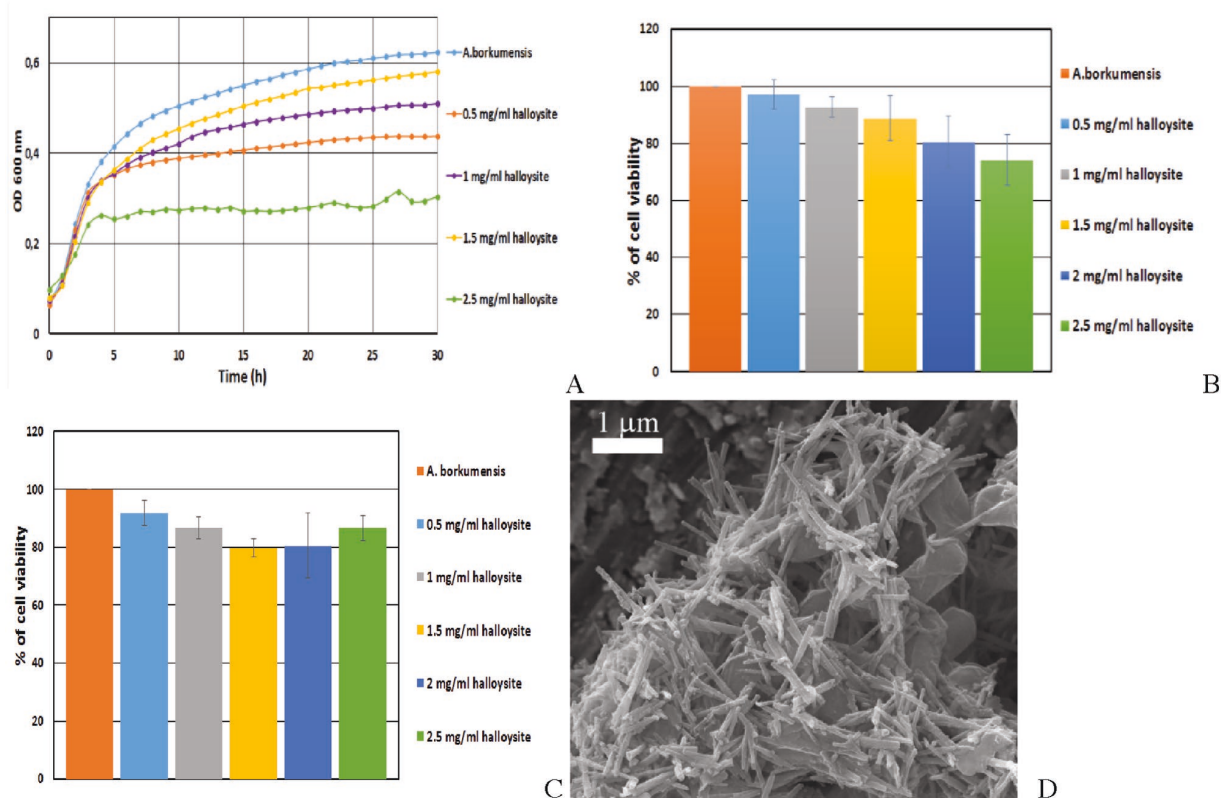


Figure 9. Viability of pristine halloysite-treated *A. borkumensis* cells: A) real-time growth monitoring curves, B) resazurin test results, C) MTT test results, D) scanning electron micrograph of the bacteria added in pristine halloysite dispersion.

reliable than colony forming unit count, since it demonstrates the population increase in situ.

To investigate the enzymatic activity of halloysite-treated *A. borkumensis* cells, we employed a set of colorimetric assays (MTT (3-(4,5-dimethylthiazol-2-yl)-2,5-diphenyltetrazolium bromide) assay and resazurin assay). These tests are used to evaluate the physiological activity of enzymatic cellular ensembles. Resazurin is reduced by bacterial enzymes within the cells producing the pink pigment resorufin, and we found, that the redox enzymatic activity was not severely inhibited in halloysite-treated cells (Figure 9). The MTT-test results also indicate that there is no severe reduction in enzymatic activity of NAD(P) H (nicotinamide adenine dinucleotide phosphate)-dependent oxidoreductases. A slight reduction in enzymatic activity was observed at higher concentrations of halloysite (2.5 mg mL^{-1}), which correlates well with the growth monitoring. One can see, that halloysite nanotubes are comparable in sizes with bacteria and do not penetrate into the cell interior (Figure 9C). Halloysite is safe in the concentration range up to few mg mL^{-1} for *A. borkumensis*, and even higher nanoclay concentrations are safe for whole organisms, such as microworms or animal digesting.^[17]

The results obtained on oil emulsification and halloysite safety promise further technology extension for petroleum spill remediation. Pickering emulsification can proceed with energies low enough to be afforded by ocean turbulence, and stability of droplets extends over more than a week. The oil/water interface is roughened, which is favorable for bacteria proliferation. In order to contain the petroleum spill in Deepwater Horizon, Gulf of Mexico, seven million liters of hydrocarbon amphiphilic dispersants were applied at the leaking spot for oil emulsification.^[19,20] This allowed to disperse petroleum spots and could result in faster bioremediation of the spill by naturally occurring degrading microorganisms such as *A. borkumensis*.^[21–23] One of the main goals of spilled oil halloysite emulsification is to optimize its consumption via degrading bacteria, and this may be reached: (1) by maximizing the oil surface area which is inversely proportional to the droplet radius (e.g., decreasing the oil droplet diameter from 1 mm to 10 μm increases the resulting multiplied droplets' surface 100 times), and (2) by increasing of the droplet surface roughness, improving bacterial cell attachment and proliferation. We proved halloysite safety for *A. borkumensis* as one of the established bacterial organisms for both aliphatic and conjugated oil component decomposition, and its use for oil emulsification looks very promising. A halloysites dispersion preparation does not need much energy and can be achieved with few minutes vortexing, which is comparable with sea-wave energy.

3. Conclusions

Using well-defined 50 nm diameter halloysite clay nanotubes for oil emulsification allows for architectural control over oil-in-water droplets. Optimization of the nanotubes' length between 0.4 and 1.5 μm and their surface hydrophobicity through silanization allowed designing oil droplets with diameters of 3–5 μm stable in pure water and

even in high molarity salt solutions, like sea water. Contrary to other clays, halloysite nanotubes do not need prior exfoliation and may be used for emulsification directly in pristine powder form.

The oil-in-water emulsions allowed for efficient hydroformylation reactions using an aqueous Rh-catalyst. This gave efficient dodecene conversion to tridecanal with simple aqueous catalyst separation from the product. This novel strategy of halloysite stabilized emulsions for catalysis is more efficient than using spherical nano/microparticles like silica. Besides, the nanotubes can be filled with reaction enhancing chemicals providing synergetic effects during their slow and controlled release.

The halloysite tubes are abundantly available and ecologically friendly nanoparticles, enabling formation and stabilization of oil emulsions. We are expecting additional development in making use of adsorption of aligned clay nanotubes at the oil droplet interfaces, which promises further attractive applications including oil spill remediation.

4. Experimental Section

Halloysites: Halloysite clay of 95%–99% purity from three sources was used: first from Applied Minerals Inc, NY. Two other halloysite samples from Henan Province, Z. Bing, China, and I-Minerals Inc. (Canada) would be referred correspondingly.

Halloysites—Hydrophobization of Halloysites: Hexamethyldisilazane (HMDS) and octadecyltrimethylsilazane (ODTMS) were purchased from Sigma-Aldrich. 500 mg halloysite and 10 mL hexamethyldisilazane were mixed in 60 mL isopropanol and sonicated for 30 min. The sonication was important to break down clumps and aggregates of the nanotubes and expose singular tubes to the silane compound. The mixture was put under a reflux condenser and the reaction was allowed to run for 20 h at 80 °C. Octadecyltrimethylsilazane had an aliphatic C18 chain attached to a single silane center, which promised higher hydrophobization. Different ratios of halloysite: ODTMS were added to 30 mL of toluene, and the mixture refluxed for ≈ 24 h at 80 °C. The optimal ratio to maximize the contact angle was identified as 1:4.5 (g mL^{-1}). After the reaction with the silanes, the halloysites were thoroughly washed and dried at 60 °C overnight.

A contact angle instrument OCA (Future Digital Scientific Corp.) was used to analyze the contact angle of pristine and hydrophobized halloysites. Therefore, a sessile water drop was deposited on the pressed halloysite pellet, and the contact angle was measured. In order to tune the contact angle of the halloysites, they were hydrophobized with HMDS and ODTMS achieving a water contact angle of $30^\circ \pm 2^\circ$ and $98^\circ \pm 3^\circ$, respectively, as compared with $16^\circ \pm 1^\circ$ for pristine halloysite (Figure 10).

Halloysites—Halloysite Length Distributions: To study the influence of the halloysites' length on the size distribution of the emulsion

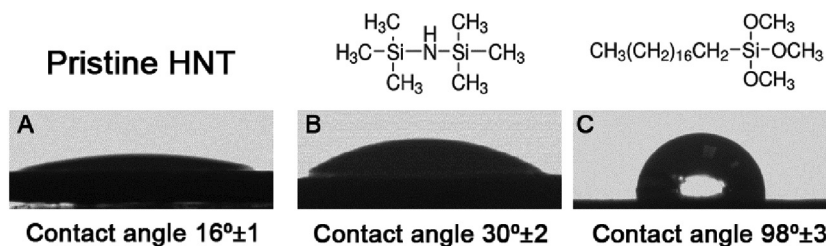


Figure 10. Contact angle of pure water on the surface of a pressed pellet of A) pristine halloysite-HNT, halloysite hydrophobized B) with HMDS and C) with ODTMS.

droplets, three different types of halloysite nanotubes were used for the formulation: short halloysite supplied by Applied Minerals (USA) with average length of 500 ± 200 nm which would be referred as halloysite. Medium length halloysite from Henan Province (China) with the average length of 750 ± 200 nm and long halloysite supplied by I-Minerals (Canada) with the length of 1500 ± 500 nm were used in few special cases and would be referred correspondingly. The halloysites were hydrophobized with HMDS and ODTMS to ensure the formation of more stable emulsions working also in sea water. The size of the oil droplets was measured 1 d after the formulation of emulsions.

Formulation of Pickering Emulsions: As oil phase, either pure dodecene or model Louisiana sweet petroleum (50 wt% of hexane, 40 wt% of decane, and 10 wt% of naphthalene) were used. Hexane, decane, and naphthalene were purchased from Sigma-Aldrich. Two formulation routes were tested: (a) in case of model petroleum, it was mixed with water with a volume ratio oil:water 1:3. Then 0.25–1 wt% of dry powder of the halloysite nanotubes were added on top and the dispersion was vortexed at 3200 rpm for 1–3 min. To disperse halloysite aggregates, the mixture was ultrasonicated for 5–10 min (40 kHz) and again vortexed for 1–3 min. The formation of emulsions was proved with optical microscopy. The oil droplet size distributions were measured 1, 3, and 7 d after the preparation. (b) In case of dodecene as oil phase, first the halloysites were dispersed in water and emulsified with dodecene afterward by ultrasonication. Both strategies gave homogeneous emulsions.

Formulation of Pickering Emulsions—Effect of Salinity: For studying salt effects on the stability of the halloysite, emulsions with pure water and with aqueous solutions containing sodium chloride (0.2 and 0.6 M) were fabricated. This range of molarity covered fresh to sea water. The size distribution of the oil droplets was measured after storing the emulsions for 7 d without any agitation.

Formulation of Pickering Emulsions—Catalytic Reaction: For the catalytic hydroformylation, 1-dodecene (8 g, purity >95%, Merck, Germany) was used; it was a reactant for the oil phase in the Pickering emulsions. The mass ratio of water:1-dodecene was 3:1. The catalyst precursor was $[\text{Rh}(\text{acac})(\text{CO}_2)]$ (25.8 mg) from Umicore, Germany. SulfoxantPhos (313.8 mg) from Molisa, Germany was used as a water soluble ligand. Rhodium catalyzed hydroformylation of long-chain olefins in aqueous multiphase systems in a continuously operated miniplant. The reaction conditions were as follows: 15 bar of syngas (1:1 H_2 :CO), with an internal reaction temperature of 95 °C and stirring speed of the aeration stirrer of 1200 rpm. Pristine halloysites (0.16 g, 0.50 wt%) with the length 750 ± 200 nm were used for the emulsion. The emulsion samples were taken hourly (1, 2, 3, 4, and 24 h) and diluted with acetone. Halloysites were removed from the liquid phase by centrifugation (relative centrifugal force = 14100 g, Eppendorf, MiniSpin plus). The supernatant liquid phase was analyzed by gas chromatography (Hewlett-Packard model 5890, series II). RTX-5MS capillary column, flame ionization detection, and nitrogen as carrier gas were used. For the temperature program and details of the used column, see the Supporting Information.

Formulation of Pickering Emulsions—Characterization of Halloysite Particles: Transmission electron microscopy (TEM) was carried out with Zeiss EM 912 at 120 kV. An Auriga (Carl Zeiss) scanning electron microscope (SEM) was used to analyze the structure of the halloysites. For SEM studies, all samples were placed on glass/aluminum stubs, sputter-coated with 60% Au–40% Pd alloy using a Q150R (Quorum Technologies) instrument. The images were obtained at 3×10^{-4} Pa working pressure, 10 kV accelerating voltage. Atomic force microscopy (AFM) images were obtained with a Dimension FastScan instrument (Bruker, USA) and Peak Force Tapping mode in air. ScanAsystAir cantilevers (nominal tip radius – 2 nm, spring constant – 0.4 N m^{-1}) (Bruker) were used. AFM images were processed using Nanoscope Analysis software v 1.7 (Bruker).

Formulation of Pickering Emulsions—Droplet Size Distributions in Emulsions: To analyze the droplet size distributions, an optical microscope (Nikon Eclipse E2300) was used. The size of the oil droplets was measured by analysis of digital images taken under the optical microscope. Images were collected as follows: 10 μL of emulsions were diluted to the final

volume of 100 μL to allow medium density of oil droplets in the field of view. To avoid the damage of oil droplets during microscopy, two vertical lines across the slide were drawn with a wax pencil forming a rectangular well. Then 20 μL of the diluted sample were placed in the well, and then covered with the coverslip. Images were captured under 10 \times or 20 \times objective magnifications. The collected images were used for analysis with Image J software (NIH) resulting in Gaussian distribution curves of the particle sizes. Emulsions were formed with *n*-hexadecane in artificial sea water as described above and 0.5 wt% of ODTMS hydrophobized halloysites.

Formulation of Pickering Emulsions—Type of the Emulsions and Halloysites Location: A fluorescence optical microscope (Axio Imager A1, Zeiss) was used to analyze the type of the emulsions. Images were collected as follows: 3 μL of emulsions were placed on a microscope slide and covered with a cover slip. Images were captured under 50 \times objective magnification. Furthermore, a cryo-SEM (Hitachi, S-4800) was used to analyze the dodecene Pickering emulsion and the orientation of the halloysites at the interface.

Formulation of Pickering Emulsions—*Alkanovorax borkumensis* (*A. borkumensis*): *A. borkumensis* bacteria was purchased from American Type Culture Collection (ATCC 700651). Bacteria growth media (marine agar, marine broth) were purchased from BD Difco (USA). Microbial culture *A. borkumensis* was obtained from ATCC (ATCC 700651) and cultivated on marine broth (37.4 g L^{-1}) with 10 g L^{-1} pyruvate.

Supporting Information

Supporting Information is available from the Wiley Online Library or from the author.

Acknowledgements

R.v.K., D.S., T.P., and R.S. acknowledge the Collaborative Research Center “Integrated Chemical Processes in Liquid Multiphase Systems” coordinated by the Technische Universität Berlin and supported by the Deutsche Forschungsgemeinschaft (DFG-TRR 63, TP A2 and B6). R.F. and S.K. thank the support from the Russian Science Foundation, grant No 14-14-00924. The authors thank Vijay John and Diane Blake, Tulane University, USA for results discussions. This research was made possible in part by a grant from The Gulf of Mexico Research Initiative. Data were publicly available through the Gulf of Mexico Research Initiative Information & Data Cooperative (GRIIDC) at <https://data.gulfresearchinitiative.org/data/R5.x288.000:0001/>.

Received: May 13, 2016

Revised: August 10, 2016

Published online:

- [1] S. Pickering, *J. Chem. Soc., Trans.* **1907**, 91, 2001.
- [2] S. Crossley, J. Faria, M. Shen, D. E. Resasco, *Science* **2010**, 327, 68.
- [3] E. Nyankson, O. Owoseni, V. John, R. Gupta, *Ind. Eng. Chem. Res.* **2015**, 54, 9328.
- [4] a) B. P. Binks, S. O. Lumsdon, *Langmuir* **2000**, 16, 2539; b) B. P. Binks, S. O. Lumsdon, *Langmuir* **2000**, 16, 8622; c) B. P. Binks, C. P. Whitby, *Langmuir* **2004**, 20, 1130.
- [5] D. J. Voorn, W. Ming, A. M. van Herk, *Macromolecules* **2006**, 39, 2137.
- [6] P. Wongkongkatep, K. Manopwisedjaroen, P. Tipsoth, S. Archakunakorn, T. Pongtharangkul, M. Suphantharika, K. Honda, I. Hamachi, J. Wongkongkatep, *Langmuir* **2012**, 28, 5729.
- [7] O. Owoseni, E. Nyankson, Y. Zhang, S. Adams, J. He, G. McPherson, A. Bose, R. Gupta, V. John, *Langmuir* **2014**, 30, 13533.

- [8] O. Owoseni, Y. Zhang, Y. Su, J. He, G. McPherson, A. Bose, V. John, *Langmuir* **2015**, *31*, 13700.
- [9] Y. Hou, J. Jiang, K. Li, Y. Zhang, J. Liu, *J. Phys. Chem. B* **2014**, *118*, 1962.
- [10] Y. Lvov, W. Wang, L. Zhang, R. Fakhrullin, *Adv. Mater.* **2016**, *28*, 1227.
- [11] W. Wei, E. Abdullayev, A. Hollister, D. Mills, Y. M. Lvov, *Macromol. Mater. Eng.* **2012**, *297*, 645.
- [12] E. Abdullayev, R. Price, D. Shchukin, Y. Lvov, *ACS Appl. Mater. Interfaces* **2009**, *1*, 1437.
- [13] G. Cavallaro, G. Lazzara, S. Milioto, F. Parisi, V. Sanzillo, *ACS Appl. Mater. Interfaces* **2014**, *6*, 606.
- [14] M. Bookstaver, M. P. Godfrin, A. Bose, A. Tripathi, *J. Pet. Sci. Eng.* **2015**, *129*, 153.
- [15] a) M. Pera-Titus, L. Leclercq, J.-M. Clacens, F. De Campo, V. Nardello-Rataj, *Angew. Chem.* **2015**, *127*, 2028; b) M. Pera-Titus, L. Leclercq, J.-M. Clacens, F. De Campo, V. Nardello-Rataj, *Angew. Chem., Int. Ed. Engl.* **2015**, *54*, 2006.
- [16] G. Fakhrullina, F. Akhatova, Y. Lvov, R. Fakhrullin, *Environ. Sci.: Nano* **2015**, *2*, 54.
- [17] M. Kruchkova, Y. Lvov, R. Fakhrullin, *Environ. Sci.: Nano* **2016**, *3*, 442.
- [18] Y. Kasai, H. Kishira, T. Sasaki, K. Syutsubo, K. Watanabe, S. Harayama, *Environ. Microbiol.* **2002**, *4*, 141.
- [19] R. M. Atlas, T. C. Hazen, *Environ. Sci. Technol.* **2011**, *45*, 6709.
- [20] S. Kleindienst, M. Seidel, K. Ziervogel, S. Grim, K. Loftis, S. Harrison, S. Y. Malkin, M. J. Perkins, J. Field, M. L. Sogin, *Proc. Natl. Acad. Sci. USA* **2015**, *112*, 14900.
- [21] S. Kleindienst, J. H. Paul, S. B. Joye, *Nat. Rev. Microbiol.* **2015**, *13*, 388.
- [22] J. E. Kostka, O. Prakash, W. A. Overholt, S. J. Green, G. Freyer, A. Canion, J. Delgadio, N. Norton, T. C. Hazen, M. Huettel, *Appl. Environ. Microbiol.* **2011**, *77*, 7962.
- [23] S. A. Konnova, Y. M. Lvov, R. F. Fakhrullin, *Langmuir* **2016**, *32*, DOI:10.1021/acs.langmuir.6b01743.

PAPER 7

Hydroformylation in Microemulsions: Proof of Concept in a Miniplant

Markus Illner, David Müller, Erik Esche, Tobias Pogrzeba, Marcel Schmidt, Reinhard Schomäcker, and Jens-Uwe Repke

Industrial & Engineering Chemistry Research, 2016, 55, 8616-8626

Online Article: <http://pubs.acs.org/doi/10.1021/acs.iecr.6b00547>

ActiveView PDF: <http://pubs.acs.org/doi/ipdf/10.1021/acs.iecr.6b00547>

Reproduced (or 'Reproduced in part') with permission from "Hydroformylation in Microemulsions: Proof of Concept in a Miniplant; Markus Illner, David Müller, Erik Esche, Tobias Pogrzeba, Marcel Schmidt, Reinhard Schomäcker, and Jens-Uwe Repke. Industrial & Engineering Chemistry Research, 2016, 55, 8616-8626." Copyright (2016) American Chemical Society.

Hydroformylation in Microemulsions: Proof of Concept in a Miniplant

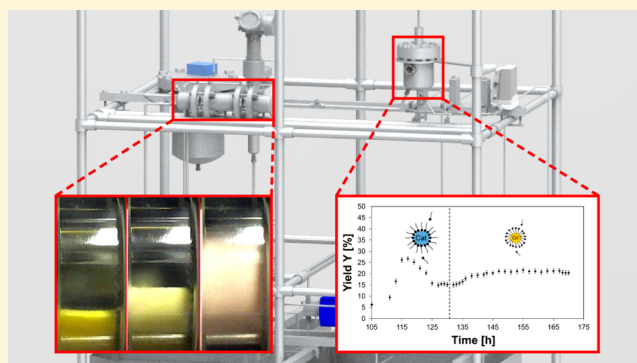
Markus Illner,^{*,†,||} David Müller,^{*,‡,||} Erik Esche,[†] Tobias Pogrzeba,[§] Marcel Schmidt,[§] Reinhard Schomäcker,[§] Günter Wozny,[†] and Jens-Uwe Repke[†]

[†]Process Dynamics and Operations Group, Technische Universität Berlin, Strasse des 17. Juni 135, Sekr. KWT-9, D-10623 Berlin, Germany

[§]Department of Chemistry, Technische Universität Berlin, Strasse des 17. Juni 135, Sekr. TC8, D-10623 Berlin, Germany

[‡]Evonik Technology & Infrastructure GmbH, Process Technology & Engineering, Paul-Baumann-Strasse 1, 45772 Marl, Germany

ABSTRACT: The implementation of the hydroformylation reaction for the conversion of long-chain alkenes into aldehydes still remains challenging on an industrial scale. One possible approach to overcoming this challenge is to apply tunable systems employing surfactants. Therefore, a novel process concept for the hydroformylation of long-chain alkenes to aldehydes in microemulsions is being investigated and developed at Technische Universität Berlin, Germany. To test the applicability of this concept for the hydroformylation in microemulsions on a larger scale, a miniplant has been constructed and operated. This contribution presents the proof of concept for hydroformylation in microemulsions carried out during a 200 h miniplant operation. Throughout the operation a stable aldehyde yield of 21% and a catalyst loss in the product phase below 0.1 ppm were achieved, which confirms previous lab scale findings. Additionally, solution strategies for a stable continuous operation to overcome challenges such as foaming, phase separation issues, and coalescence dynamics are discussed herein.



1. INTRODUCTION

One of the world's most important applications of homogeneous catalysis on an industrial scale is the reaction known as hydroformylation.^{1,2} Today, production plants for hydroformylation products have reached a capacity of 11 million tons per year.^{3–5} The reaction, also known as oxo synthesis, was originally discovered in 1938 by Otto Roelen.⁶ In the presence of an adequate transition metal, such as cobalt (Co) or rhodium (Rh), unsaturated hydrocarbons (alkenes) react with carbon monoxide and hydrogen to form linear or branched aldehydes (Figure 1). In general, *n*-aldehydes are desired as intermediates for subsequent reactions toward alcohols, detergents, softening agents, flavorings, and other chemicals and are of great value by themselves.

A steady move from cobalt to rhodium-based catalysts has taken place during the past few decades. The main reasons were

higher achievable activities and selectivities at overall milder reaction conditions.⁵ Additionally, improvements regarding the normal:iso selectivity of the reaction have been obtained by selecting and modifying the employed catalysts with stereoactive ligands.^{5,9} Obviously, these advancements have come at the cost of more expensive catalyst complexes.

Therefore, increasing effort has been made on developing process concepts with a special focus on catalyst recovery. The Ruhrchemie/Rhône Poulenc (RCH/RP) process presents a milestone in the process development of the hydroformylation reaction.³ A major advantage of this biphasic process is the solubilization of the highly reactive ligand-modified rhodium-based catalyst complex in an aqueous phase. In principle, separation of the product can easily be achieved by simple means of phase decantation. Catalyst leaching via the product stream of the process, which is the standard disadvantage of homogeneous catalysis, becomes negligible. Additionally, as discussed by Haumann et al.,¹⁰ the operating conditions of the RCH/RP process are mild with pressures below 60 bar and temperatures around 120 °C. Given that negligible amounts of

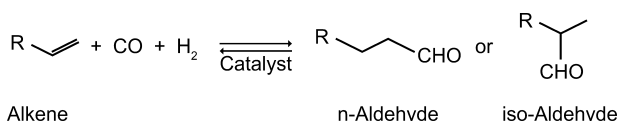


Figure 1. Reaction equation of the hydroformylation reaction. R is an alkyl group.^{7,8}

Received: February 8, 2016

Revised: July 18, 2016

Accepted: July 21, 2016

Published: July 21, 2016

catalyst are lost via the product phase, no side reactions are observed in subsequent distillation steps. However, a major drawback of the process lies in its limitation to short-chain alkenes. Since alkenes longer than hexene have a limited solubility in the aqueous phase, which results in a severe decrease of reactivity, they are inadequate for the RCH/RP process.¹¹ For longer-chain alkenes Börner et al.⁵ report that the conversion is carried out in single phase reactions at severe process conditions (up to 300 bar and 200 °C), using mainly cobalt catalysts. Modifying the catalysts with phosphines, these process conditions can be lowered significantly. Nevertheless, these processes suffer from lower selectivities toward the desired aldehydes and thus a rather costly product separation. Consequently, switching the feedstock toward long-chain alkenes remains challenging for the chemical industry to date.

To overcome this hurdle, a novel process concept is currently under investigation within the Collaborative Research Center InPROMPT/TRR 63 and presented in this contribution. Therein, a surfactant is added to the system, to enhance the miscibility between the long-chain alkene and an aqueous catalyst solution leading to the formation of a microemulsion. A highly hydrophilic ligand-modified rhodium catalyst is used to achieve high selectivities at mild process conditions.²

To carry out the hydroformylation reaction, the catalyst needs to be activated. This is done by introducing synthesis gas into the system. Carbon monoxide transforms the catalyst into its active species.¹² With carbon monoxide and hydrogen as reactants present, the formation of aldehydes starts immediately. After the reaction step, the mixture is led into a phase separation unit, within which the thermomorphic behavior of the micellar system can be exploited to separate and recycle the catalyst from the oily product. The process concept can thus be summarized as a mixer–settler concept shown in Figure 2.

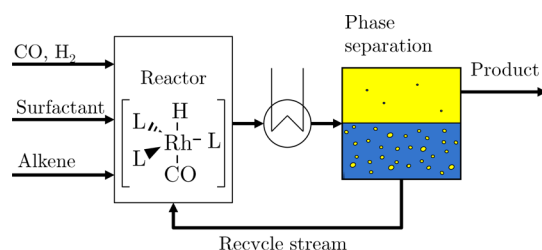


Figure 2. Process concept for the hydroformylation of long-chain alkenes in microemulsions.¹³

In order to investigate this novel concept at a larger scale, a miniplant has been designed, constructed, and operated at Technische Universität Berlin (TU Berlin). Therein, the hydroformylation of 1-dodecene as a model, biobased olefin using a nonionic surfactant is carried out.

The aim of this contribution is to present the results from long-term miniplant operation and to discuss the applicability of such a process concept. Keeping an eye on economic viability and sustainability, the presented results are analyzed regarding specific targets:

- long-term stable application of ligand-modified rhodium-based catalysts for high reaction activity and normal:iso selectivity
- realization of a homogeneous catalysis at mild reaction conditions (low pressures and low temperatures)

- adequate separation of the catalyst complex from the product phase after the reaction

Additionally, special attention is given to challenges which have arisen during the implementation of this concept as well as strategies to overcome these challenges.

2. BACKGROUND INFORMATION

The following sections discuss the state of the art of microemulsions as reaction media and their capabilities for catalyst recovery. Consequently, characteristics of oil–water–surfactant systems and phenomena exploited to achieve the desired process steps are highlighted.

2.1. State of the Art and Preliminary Investigations.

To date, various applications of surfactant containing reaction systems have been reported. Among them, several organic applications such as reduction, oxidation, and coupling reactions at C=C bonds can be found.^{14,15} For long-chain alkenes of chain lengths up to C₁₆, a feasible application of homogeneously catalyzed hydroformylation using micellar reaction media was presented by Van Vyve and Renken in 1999¹⁶ for alkenes. Also, Li et al.¹⁷ reported increased selectivities and higher reaction yields for the conversion of 1-dodecene in biphasic mixed micelle systems, depending on the surfactant composition and micellar state. The direct influence of surfactants on the reaction performance was the main focus of the studies of Haumann et al. in 2002.¹⁰ They reported the hydroformylation of 1-dodecene in microemulsions using water-soluble ligands. Compared to those, biphasic water–oil systems showed no significant conversion of long-chain alkenes to aldehydes. The addition of a surfactant, however, enables the reaction. The main challenge lies in determining an appropriate surfactant. The surfactant selection is crucial for both the reaction performance and the subsequent product separation.¹⁸ The thermomorphic behavior of micellar systems (see section 2.2) and therefore also the distribution of the catalyst between all formed phases strongly depend on the surfactant's properties.¹⁹ Furthermore, high reaction rates, clear phase separation, and catalyst recovery also have to be realized as continuous operations in a technical system to estimate economic viability. Regarding the process concept in Figure 2, no continuous operation on a miniplant or any comparable scale was reported until now.

2.2. General Phase Separation Characteristics of Oil–Water–Surfactant Systems. The addition of sufficient amounts of surfactant to an oil and water mixture leads to the formation of a microemulsion. From a macroscopic point of view a microemulsion can be regarded as homogeneous. On a microscopic scale it is heterogeneous with coexisting, nanometer-thin hydrophobic and hydrophilic layers.^{20,21} For the application here, a microemulsion can be used in two ways. It acts as a tunable solvent, which on the one hand increases the interfacial area during the reaction, and on the other hand changes its phase separation behavior dependent on temperature.²² Thus, the reaction can be carried out in a homogeneous mixture followed by a fast and pure phase separation in a settler.²³ However, for this purpose the phase separation characteristics of oil–water–surfactant systems must be well understood.²⁴

The phase separation characteristics of a microemulsion system formed with nonionic surfactants can be described by Kahlweit's fish diagram. The diagram is created by slicing Gibbs' phase prism of an oil–water–surfactant system at an oil

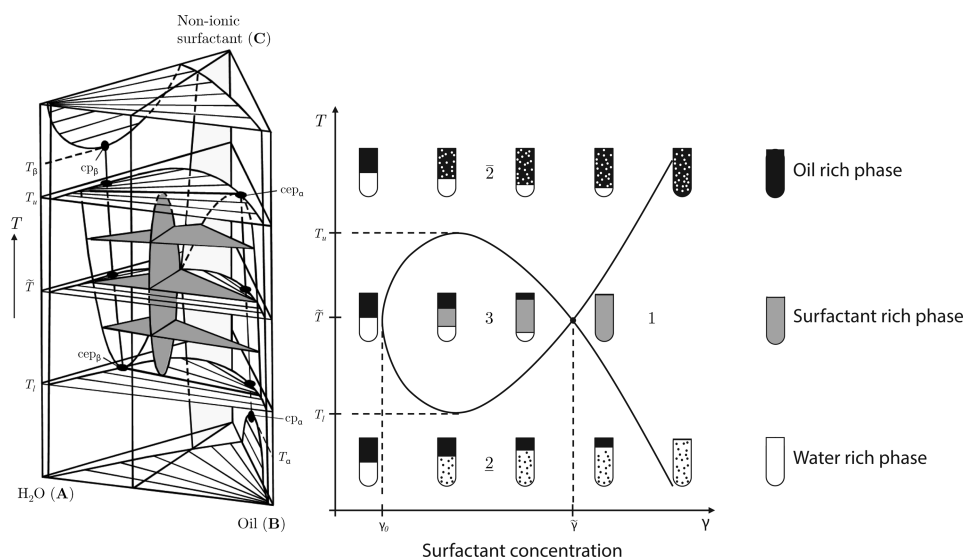


Figure 3. Gibbs' phase prism of oil–water–surfactant mixtures at different temperatures (left) and Kahlweit's fish (right). The figures are based on and partially redrawn in accordance with the original images presented in ref 25.

to water ratio of 1:1. Thus, the various phase states at different temperatures and surfactant concentrations become visible. Figure 3 shows a qualitative sketch of Gibbs' phase prism for an arbitrary oil–water–surfactant system and Kahlweit's fish therein.

A closer look at Kahlweit's fish reveals several distinct phase states. The fish's body (micellar system) is established in case a sufficient amount of surfactant is present (greater than the critical micellar concentration, γ_0). A two-phase regime (2) is created at low surfactant concentrations and low temperatures. This is governed by a water and surfactant rich emulsions phase at the bottom and an oily excess phase on top. As mentioned by Müller et al., "the surfactant is mainly dissolved in the water-rich phase due to its higher solubility there at lower temperatures. Hence, an oil-in-water (o/w) microemulsion is formed. This regime can be desired for the product separation step of a mixer–settler process as a pure product phase can be removed while recycling the surfactant and water (aqueous catalyst solution)."²⁶ By increasing the temperature, a three-phase region (3) is established in which the bulk of the surfactant is located in a middle phase. In coexistence with this middle phase an oil-rich top phase and a water-rich bottom phase appear. Here, the catalyst is also mainly located in the middle phase, whereas the oily excess phase still remains free of catalyst.¹⁹ Given its pure oil phase, this region is desirable for the separation step. Two more regions are shown in Figure 3. The first is the single-phase region on the right-hand side (fish's fin). Obviously this region may be suitable for the reaction, but inadequate for separation purposes. The second undesired region is the upper two-phase (2̄) region. There, the surfactant lies dissolved in the top phase. This may be problematic, because phase separation would lead to drastic surfactant and water loss with the product phase. The surfactant as well as the water (catalyst solution) trapped therein would have to be replenished and separated in additional separation steps from the product.¹⁹

Regarding the phase separation dynamics, microemulsion systems show a distinct reduction of the separation time in the three-phase region (3) compared to the two-phase regions (2, 2̄). Depending on the applied surfactant, the required time for achieving an equilibrium state increases by several orders of

magnitude on leaving this area.¹⁹ Hence, for the construction of a decanter with reasonable residence time, solely the three-phase region is of interest. However, this causes two major challenges toward process design and control. First, the concentration dependent location of Kahlweit's fish needs to be intensively investigated for the considered component system in the miniplant. Second, the temperature only offers a small operational window regarding the temperature in the decanter. Using this information on the general phase separation characteristics, the miniplant, and the settler in particular, was constructed and operated. Here, an approach described by Müller et al.²⁶ was applied, to systematically tackle the unit design for such a multiphase system.

3. MATERIALS AND METHODS

At this point, the applied substances as well as the constructed miniplant are introduced. A miniplant operation schedule is presented to highlight applied operation strategies and discuss their influence on the system. Additionally, operational challenges and solution approaches are discussed.

3.1. Materials. The applied substances can be categorized into several groups: reactants, catalyst compounds, solubilizing substances, and products.

The first reactant is 1-dodecene (CAS Registry Number 112-41-4, purchased from VWR), a C₁₂ alkene, which is used as an exemplary unsaturated, long-chain hydrocarbon. The second reactant is synthesis gas with a composition of 1:1 mol % CO:H₂ with a purity of 5.0 purchased from Linde.

The applied catalyst consists of a rhodium-based precursor [Rh(acac)(CO)₂] (CAS Registry Number 14874-82-9), sponsored by Umicore, and the water-soluble ligand SulfoXantPhos (sulfonated form of XantPhos, CAS Registry Number 161265-03-8), purchased from MOLISA GmbH. Both precursor and ligand are dissolved in water.

The miscibility of 1-dodecene and the catalyst solution is enabled by the nonionic surfactant Marlipal 24/70 (CAS Registry Number 68439-50-9), sponsored by Sasol Germany GmbH. Additionally, Na₂SO₄, purchased from Th. Geyer, is added in small amounts as a separation enhancing additive.

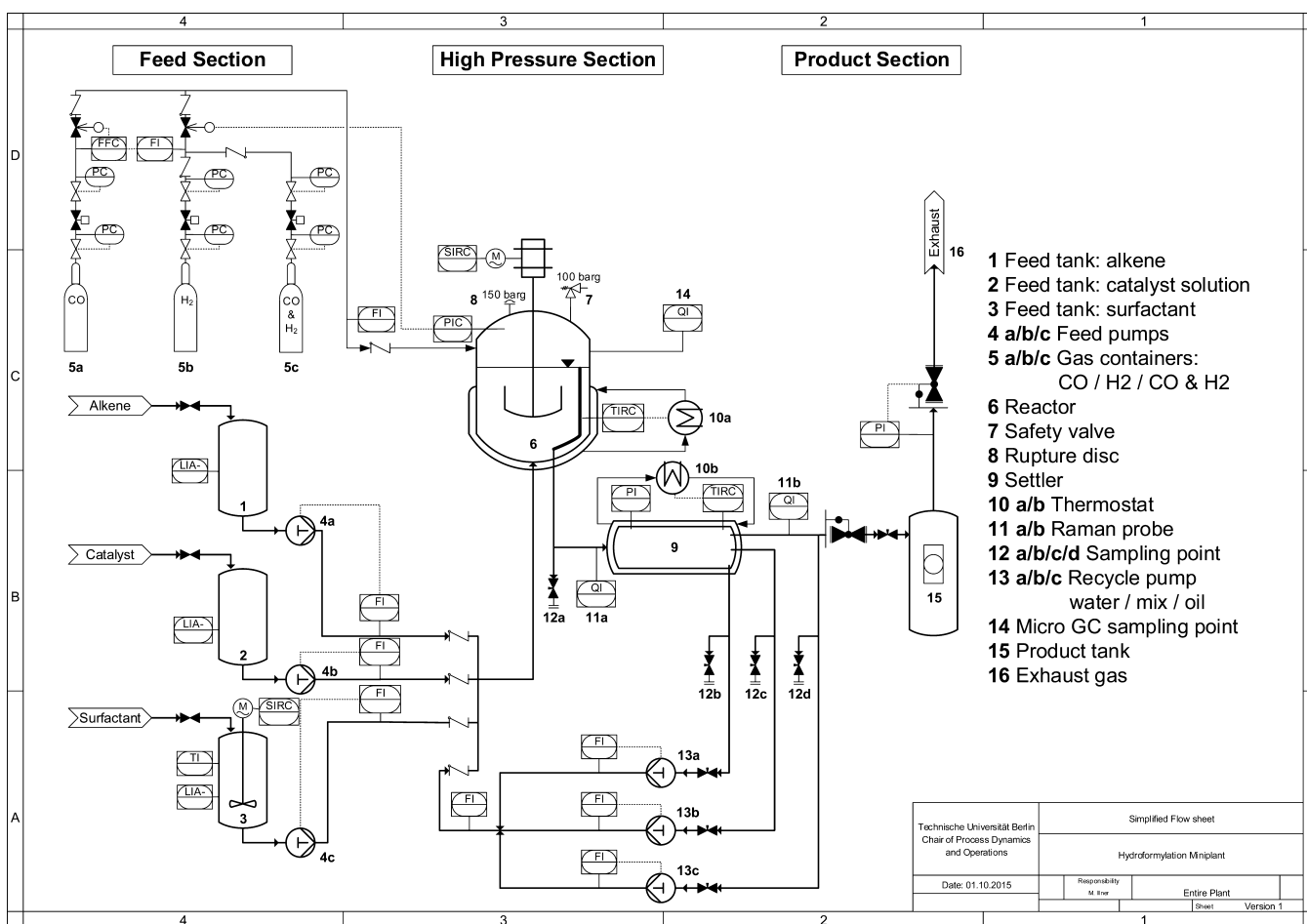


Figure 4. P&ID of the miniplant at TU Berlin.

For the initial mixture of the miniplant operation campaign mass fractions of roughly 44.52×10^{-2} g/g water, 46.00×10^{-2} g/g alkene, and 8.00×10^{-2} g/g surfactant were used. Additionally, 1.00×10^{-2} g/g Na_2SO_4 , 0.03×10^{-2} g/g precursor, and 0.45×10^{-2} g/g were applied.

3.2. Technical Realization: Miniplant at TU Berlin.

3.2.1. Process Design. A simplified piping and instrumentation diagram (P&ID) of the miniplant at TU Berlin is shown in Figure 4. As described by Müller,²⁷ the miniplant consists of three sections. The feed section contains the feed tanks and feed pumps for the liquid components 1-dodecene, catalyst solution, and surfactant.²⁷ Additionally, the feed section holds the gas bottles for synthesis gas, pure hydrogen, and pure carbon monoxide. The feeds of 1-dodecene (4a), catalyst solution (4b), and nonionic surfactant (4c) can be regulated to a maximum values of 840, 400, and 200 g/h, respectively.

The lower part of Figure 5 shows a three-dimensional (3-D) image created with Solid Edge and a photo of the feed section with the tanks and pumps for the liquids.

The mixer-settler section consists of a reactor and a decanter. The reactor has a maximum volume of 1500 mL. The liquid mixture is stirred with a gassing stirrer featuring a Rushton turbine with a maximum speed of 2880 rpm. Within the reactor, baffles are installed to avoid vortex formation and a drain is positioned at roughly 70% height to guarantee a constant liquid level. The second unit, the decanter or settler, consists of several modules with three separate drains. These drains are located at the bottom (water phase), in the middle

(surfactant-rich middle phase), and at the top (oil phase). Each drain is connected to a separate pump (13a–c) so that each of the phases can be recycled differently back into the reactor with maximum flow rates of up to 1000 g/h. The bottom part of Figure 5 shows a 3-D image and a photo of the mixer-settler section. Figure 6 shows the custom-made settler. Two cylindrical gauge glasses enable the observation of the phase separation before and after passing through a knitted wire section in the middle of the settler. A detailed description of the settler and the knitted wire for enhancement of the phase separation can be found in the contribution by Müller et al.²⁶

The third section, the product storage section, consists of a product container for the liquid components and a depressurization unit for the removal of synthesis gas from the system. To remove oxygen from the system before the reaction, a vacuum pump is installed above the depressurization unit.

3.2.2. Automation and Analytics. The miniplant is fully automated with SIEMENS PCS 7 allowing for the online monitoring of more than 50 sensors from the control room. From there, operators are also able to control the process with several actuators (pumps, control valves, magnetic valves).

Regarding the analytics, two offline gas chromatographs (Agilent HP-5 column with an FID analyzer) are employed for an accurate hourly composition analysis. Second, an offline inductively coupled plasma optical emission spectrometer (ICP-OES; Varian ICP-OES 715 ES) is used to estimate the rhodium amount in the product phase. The sample positions of the liquids are located at the top, middle, and bottom drains of

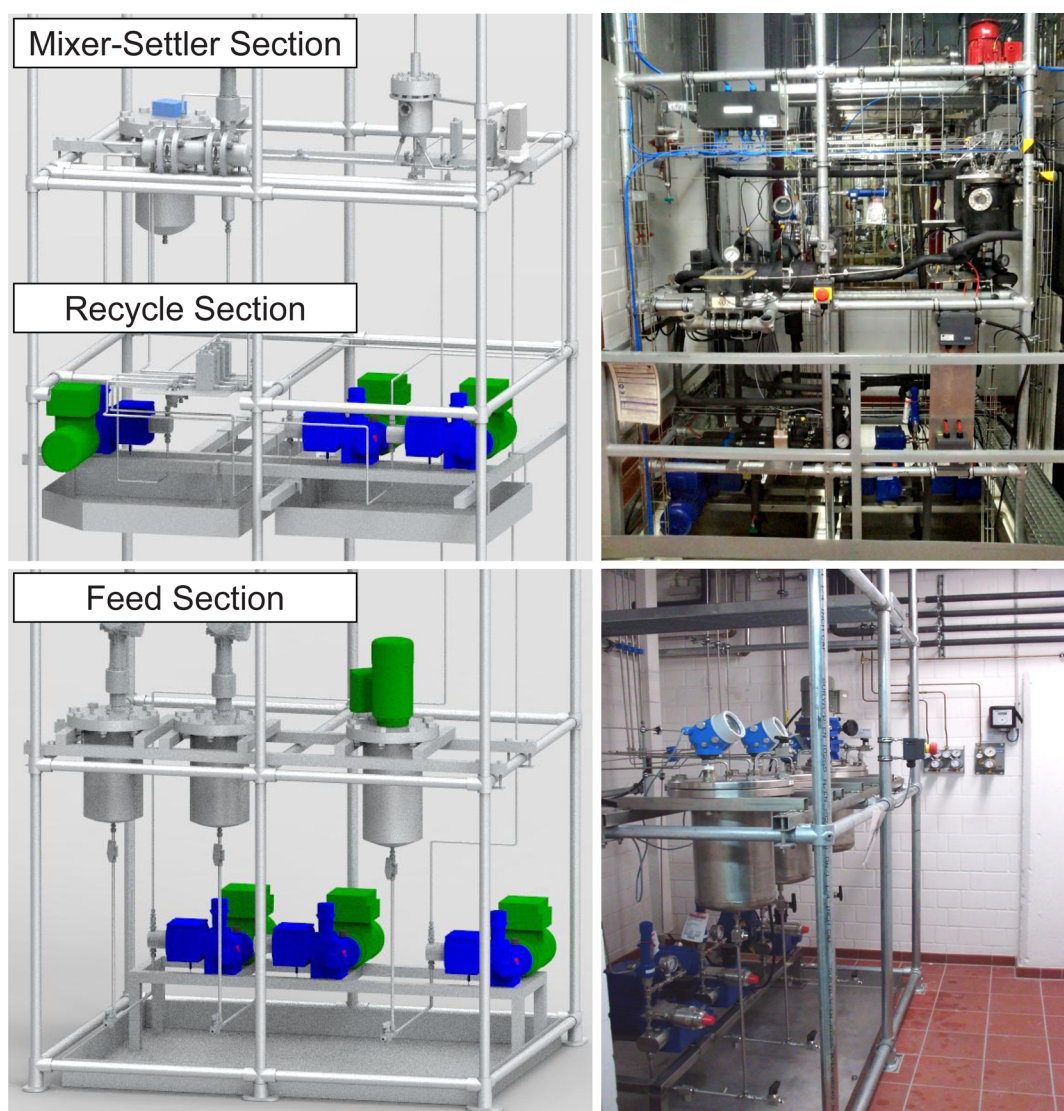


Figure 5. (top) Three-dimensional image (left) and photo (right) of the mixer–settler and recycle section. (bottom) Three-dimensional image (left) and photo (right) of the feed section of the miniplant at TU Berlin.²⁷

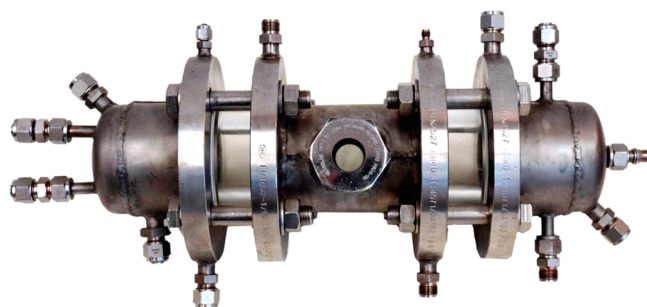


Figure 6. Self-constructed decanter/settler installed in the miniplant. The depicted setup contains a gauge glass, a knitted fabric from Rhodius GmbH (inside, not visible), and two cylindrical sight glasses.²⁶ The center piece with the small gauge glass is one of several modules. The settler length and volume can thus be increased by attaching additional modules in the middle.

the settler and of the reactor (see 12a–d in Figure 4). The gas composition is measured online with a micro gas chromatograph (micro-GC; molecular sieve 5 Å column). Additionally, an online Raman spectrometer (Kaiser Optical Systems RXN1,

NIR probe) has been installed for a fast analysis of the liquids entering the settler.

3.2.3. Safety Concept. Finally, it must be mentioned that considerable efforts have been made to guarantee a safe operation of the miniplant. The surrounding area of the plant is classified as an “explosion zone II” seeing that hazardous and explosive components are used during the reaction which may leak into the surroundings. Therefore, an extensive HAZOP analysis has been carried out during which technical and operative countermeasures to potential hazards were defined.

Following the concept of multiple layers of protection described by Seborg et al.²⁸ and based on the proceedings of the American Institute of Chemical Engineers from 1993,²⁹ these countermeasures are systematically applied. At the process design layer, all units are constructed or bought according to the regulations for an explosion zone II and according to the regulations for the temperature classes for 1-dodecene and synthesis gas. The necessary auxiliary equipment, such as thermostats, the offline gas chromatographs, online Raman spectrometers, gas feeds, and control cabinet of the process control system, not designated for an “explosion zone

Table 1. Simplified Miniplant Operation Schedule with Applied Process Parameters for Several Operation Modes (Cases 1–4)

	case 1	case 2	case 3	case 4
operation hours [h]	0–80	80–92	92–108	108–150
operation mode	continuous	full recycle	continuous	continuous
residence time reactor [h]	0.50	3.18	2.80	2.80
residence time settler [h]	0.58	3.53	3.15	3.15
recycle rate [g/h]	1500	250	250	250
recycle ratio (oil:mix:water)	0.19:0.57:0.24	0.40:0.20:0.40	0.40:0.28:0.32	0.24:0.52:0.24
feed rate dodecene [g/h]	100	0	30	30
gas supply	synthesis gas	synthesis gas	synthesis gas	synthesis gas

II", are located outside of the miniplant's housing. Basic process control features allow for indication of alarms in case of sensor malfunction or violated process value limits. As a safety interlock, H₂ and CO concentrations are monitored with gas detectors on each floor. Additionally, critical process values, such as reactor pressure and temperature, are tracked with the process control system. In case of emergency, nitrogen is automatically flooded into the plant and simultaneously all liquid and other gas feeds are shut down. The physical protection layer is equipped with pressure relief valves, venting synthesis gas to the flare. To prevent the spread of a fire, the miniplant has been set up in a separate three-story high room. In case of an explosion, magnetic flaps open to the outside to prevent structural damage to the miniplant's housing. On top of that, a ventilation system is installed to prevent an accumulation of synthesis gas in the room, which guarantees a 10-fold air exchange per hour. For liquid leakage multiple collection basins are in place to contain hazardous components.

3.3. Miniplant Operation Challenges. Prior to the miniplant operation, a number of preliminary experiments and shorter miniplant operations were carried out,^{26,30} which led to the identification of several challenges and methods to overcome them.

The first challenge was foaming in several sections of the miniplant, especially during the depressurization. The applied oil–water–surfactant system tends to foam whenever stronger degassing occurs. This undesirable effect has been described by several authors.^{8,31} Foaming in general can cause problems, since mass and heat transfer is limited by foam itself. This issue can be avoided though by degassing more slowly or expansion into tanks with a large surface to volume ratio and an appropriate gas holdup. Additionally, it has been observed that certain oil–water–surfactant mixtures with a high water content tend to establish a foam that remains stable for a longer period of time. Therefore, a water concentration below a critical level of 35 wt % was ensured for all conducted plant operations and the original depressurization unit was replaced by a suitably larger one.

The second issue was an inseparable liquid mixture in the decanter after catalyst activation with synthesis gas.^{32,33} The phase separation of the oil–water–surfactant system with catalyst present was investigated in multiple steps in the lab. Without synthesis gas, the separation takes place as desired. Once synthesis gas is added to the system, a separation can take multiple hours or even last indefinitely. A reason for this is the strong surface activity of the catalyst complex and changing electric charges of the molecule once CO is attached to it. We assume that the appearing surface activity of the catalyst complex is due to a change in geometry between the nonactivated and activated complex, which was recently discussed by Pogrzeba et al.³⁴ This stops micelles from

coalescing and thus hinders the phase separation. To counter this issue, the addition of small amounts of Na₂SO₄ (same quantity as catalyst, 300 ppm) has proven to be successful. It was decided to introduce a larger mass fraction of Na₂SO₄ of 1 wt % to ensure the countereffect at all times.

The third challenge was that, despite the presence of Na₂SO₄ in the plant, the kinetics of the phase separation was too slow. Consequently, coalescence accelerators (knitted fabrics) were implemented in the settler. A more detailed discussion can be found in ref 26.

3.4. Process Conditions and Operation Schedule. The following section introduces a description of reaction conditions and modes of operation for the subsequent discussion of long-term miniplant results. The overall duration of the miniplant operation including start-up and shutdown was more than 200 h long. The plant was operated in a three-shift system with a team of overall 17 operators and lab assistants.

3.4.1. Reaction. According to lab-scale experiments, the reaction pressure was set to 15 bar gauge pressure, along with a constant reactor temperature of 95 °C.^{34,35} The stirrer speed has been varied between 600 and 1500 rpm depending on the emulsion state. Within this range, it was guaranteed that the stirrer operates in gassing mode, thus ensuring sufficient dissolution of synthesis gas in the reaction mixture. The reaction conditions were not changed throughout the operation campaign. Thus, influences on the reaction rates were not related to temperature or pressure.

Several products were created during the reaction. The desired product was the linear aldehyde 1-tridecanal. Possible byproducts of the reaction mechanism are the isomers of tridecanal, the hydrogenated form of 1-dodecene (*n*-dodecane), and *cis/trans* isomers of 1-dodecene. A detailed description of the reaction network is given by Markert et al.³⁶

To evaluate the reaction performance, the yield of the main product 1-tridecanal is defined as the ratio of the *n*-aldehyde mass fraction to the mass fraction of all reaction educts and products, i.e. the 1-tridecanal mass fraction divided by the mass fraction of all oily components. Given that 1-dodecene is the main reactant and all reaction products are formed from this component, the total mass fraction of all oily components corresponds to the theoretical mass of product.

$$Y_{1\text{-tridecanal}} = \frac{w_{1\text{-tridecanal}}}{w_{\text{oil}}}$$

3.4.2. Modes of Operation. The miniplant operation was divided into several operation modes, in order to influence the reaction by manipulating feed rate, product purge, and residence time. After inertization of the system with N₂, alkene, catalyst solution, and surfactant were fed into the plant with feed streams set to meet the concentrations described in section 3.1. Subsequently, the plant was operated in full recycle mode

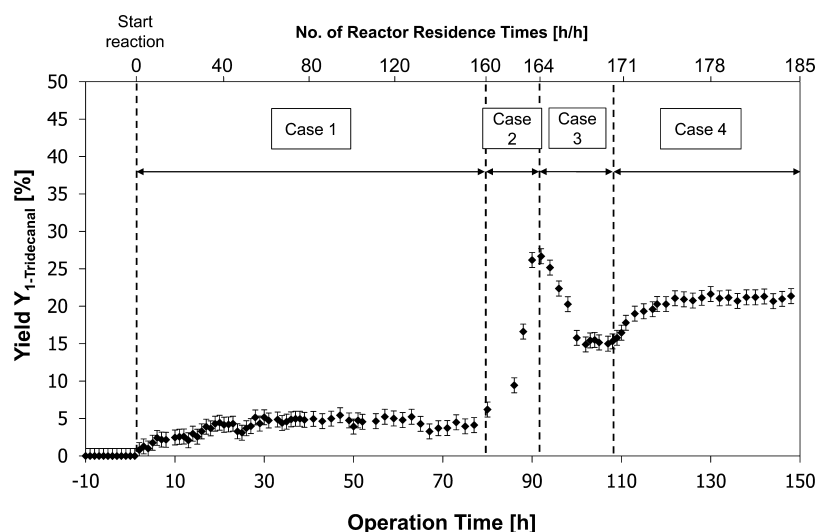


Figure 7. Miniplant operation results. Yield of 1-tridecanal in the reactor over time. Reactor residence times as ratio of operation time to the current residence time in the reactor are indicated to assess process stability.

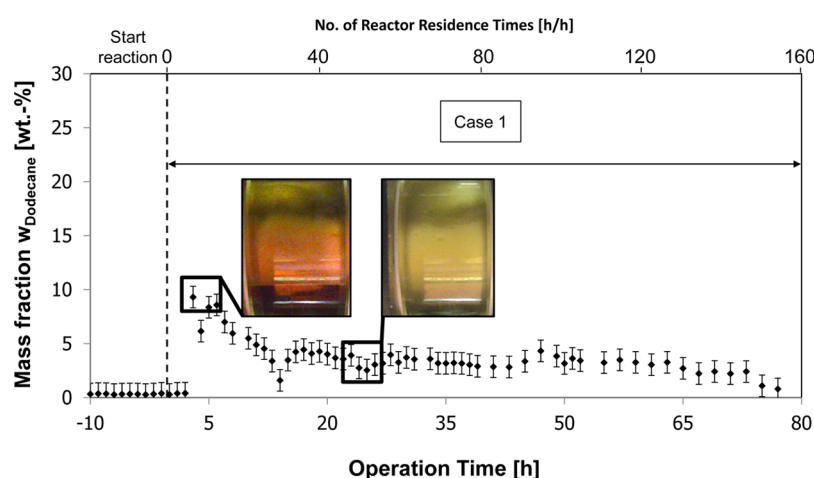


Figure 8. Miniplant operation results of case 1. Mass fraction of the hydrogenation byproduct *n*-dodecane. Settler's sight glass pictures given above indicate the activity of the catalyst (red, inactive; yellow, active).

without activation of the catalyst with synthesis gas. Therefore, no reaction took place. During this start-up phase, different settler residence times were implemented by manipulating the recycle stream rates with the aim of determining optimal phase separation conditions and to stabilize the process before initiating the reaction.

After this phase, the system was pressurized with synthesis gas. This defines the start of the actual operation (operation time = 0 h) for all further discussions. With stable phase separation and *n*-aldehyde yield being the main targets for the miniplant operation, different scenarios were performed within the operation schedule. Table 1 shows relevant process parameter sets for those scenarios (cases) allowing to relate changes in, e.g., residence times or recycle ratios to given results in the next section.

Case 1 represents a continuous operation mode with reaction, during which a low reactor residence time was chosen to demonstrate a stable aldehyde yield over a reasonable number of residence times. Based on the reactor's residence time of 0.5 h, a 1-tridecanal yield of 7% was expected from lab scale investigations.^{34,35}

A full recycle operation in case 2 was used to increase the aldehyde yield in the reactor. In this mode, settler outlet streams were fed back into the reactor, with the alkene feed turned off. Synthesis gas though was fed into the system and partially purged to maintain the ideal ratio of CO to H₂. The operation mode was changed from continuous to full recycle operation to shorten the time needed to achieve higher yields and thus also shorten the required length of the plant operation. Apart from the deactivated alkene feed, the yield increase was achieved with an increased reactor residence time.

Subsequently, a stable continuous operation with the aim of a higher yield compared to case 1 was established in case 3. Given the data in Table 1, a total recycle flow rate of 250 g/h was established, causing a reactor residence time of approximately 2.8 h in the reactor. This corresponds to a yield of 25%, which was expected according to lab experiments.

Case 4 investigated the influence of the ratio between the settler outlet streams—and thus the residence times of the corresponding phases inside the settler—on yield and process viability.

Note that reaction temperature and pressure were kept constant at 95 °C and 15 bar throughout all described cases.

3.4.3. Disturbances. In order to evaluate the recorded experimental data, unavoidable systematic or random disturbances and their impact on the process have to be considered.

Concentration measurements of reactants, products, and byproducts were carried out via offline gas chromatography implying manual sampling. Hence, the total liquid amount inside the plant was reduced each time and needed to be replenished systematically according to the extracted components. With three samples (reactor, oil phase, water phase) a total of 30 g was extracted every hour. This equals roughly 1.2% of the total liquid amount in the plant's high pressure section. Given the analysis result, the specific amounts of pure components were calculated. Hence, these component masses were re-fed to diminish the influence on the overall component concentrations inside the plant, especially the loss of catalyst.

4. RESULTS OF THE MINIPLANT OPERATION

In this section, long-term miniplant operation results are presented. Here, the two major aspects of the reaction and phase separation performance are evaluated and linked to the operation schedule.

4.1. Reaction Performance and Product Yield. The product yield is one of the main performance indicators of the reaction. Based on the GC results of the reactor samples (position 12a in the P&ID diagram in Figure 4), the 1-tridecanal yield for all operational modes is depicted in Figure 7.

Referring to operation time 0 h in Figure 8, an increase of the yield is visible, as this marks the start of the reaction. During a period of 20 h the yield increased to an average maximum value of 6.8% for the reaction mode of case 1. This value is consistent with preliminary lab experiments.³⁵ Temporary decreases in reaction yield were observable at operation hours 25 and 68. This was mainly caused by extended sampling for additional tests, whereas 1-dodecene was re-fed to maintain a constant amount of reaction mass. Overall, a stable yield over an uninterrupted period of more than 100 residence times was achieved for operation case 1. This generally highlights the catalyst stability as no decomposition and according reaction slowdown were observed. Therefore, unknown effects in the technical system (contaminants, side reactions), which are prone to trigger catalyst decomposition, were not observable.

As a next step, an operation mode with higher yield was desired to increase profitability. Here, a yield increase of 20 percentage points was achieved within 12 h (case 2). The reaction rate during that time frame is again in accordance with lab experiments.

Subsequently, the continuous operation was reestablished (case 3). Here, the 1-tridecanal yield declined drastically and evened out to a new steady-state point at a yield of 15%. However, for case 4 an immediate increase of 6 percentage points and stabilization of the 1-tridecanal yield was observed. Figure 7 depicts a continuous operation for operation hours 120–150. The extent of the yield increase is not solely explicable with perturbations given that the residence time was kept constant. In this case the increase was caused by a changed ratio between the recycle streams for oil, water, and surfactant. Referring to Table 1, the middle phase recycle stream, in which the majority of surfactant is located, was proportionally increased. The streams of oil and water phase recycle were at comparable levels for this part of the operation.

A higher recycle rate for the surfactant compared to the catalyst solution and oil phase could have caused surfactant concentration shifts or reduced surfactant accumulations in the settler. Thus, the surfactant concentration in the reactor could have increased. Linking yield and higher surfactant concentrations in the reactor, a positive effect of the surfactant concentration on the reaction yield is assumed.

4.2. Byproduct Formation. The reaction in Figure 1 represents a complex reaction network, which contains the formation of several byproducts.^{12,36} One major side reaction is the hydrogenation of *n*-dodecene toward *n*-dodecane. Therefore, the formation of this component is shown exemplarily in Figure 8, to discuss the selectivity of the reaction.

On initiating the reaction, a significant formation of *n*-dodecane was observed with mass fractions of up to 10 wt %. For this initial period the dodecane yield actually exceeded the 1-tridecanal yield. Later, the amount of *n*-dodecane declined to values below 1 wt % as it was slowly purged from the process and was led into the product container (position 15 in Figure 4). It is assumed that the hydrogenation took place during the first hours of the operation and was then successfully suppressed by full catalyst activation. Supporting this hypothesis, photos showing the separated reaction medium in the settler are given in Figure 8. Preliminary lab scale investigations showed that the inactive catalyst (no synthesis gas in the system) shows a deep red color, while the activated form is bright yellow. Given that, it is assumed that the catalyst was not completely activated with synthesis gas during the first hours after the reaction initiation, since a red colored reaction medium was observed. A possible intermediate species of the catalytic cycle might be prone to support hydrogenation reactions.¹² With the applied low residence times for case 1, a sufficient activation was achieved in a short time frame.

The other byproducts of interest are all isomers of 1-tridecanal. In this contribution they are summarized as isotridecanal. Negligible to no amounts of isotridecanal were measured during the entire operation.

4.3. Phase Separation. The investigation of the phase separation behavior for the miniplant operation is the second main result of interest. As stated before, efficient recovery and recycle of the catalyst as well as product isolation are crucial for the shown process concept. Referring to Kahlweit's fish in Figure 3 and the subsequent discussion, this can be reached by maintaining a three-phase separation state. Figure 9 depicts this, marking the three relevant phases.

To evaluate the separation performance, Figure 10 depicts the total amount of oily components in the oil phase outlet of the settler. Here, the sum of mass fractions of all reaction educts and products is considered. The data was gathered from GC analysis of oil phase samples (position 12d in PI diagram Figure 4). Here, total oil mass fractions close to 1 mark an ideal phase separation with almost no catalyst solution or surfactant contained in the oily phase.

As an overall result, it can be stated that the phase separation was stable throughout all discussed operation modes (cases 1–4), in total, for an operation time of more than 150 h.

The optimal separation temperature for maintaining a three-phase system as depicted in Figure 9 is influenced by component concentrations in the system and changed flow rates, which can induce concentration shifts or accumulations. Therefore, control actions on the settler temperature had to be carried out accordingly to maintain a stable phase separation. For this, a prediction model for the optimal separation

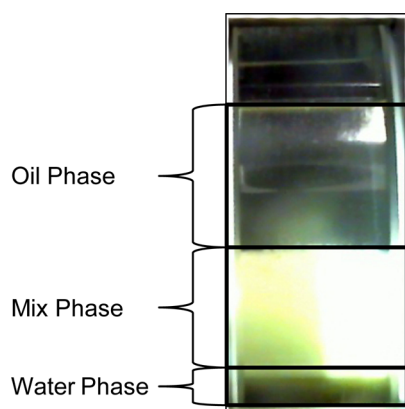


Figure 9. Photo of settler's sight glass with an ideal phase separation state. A surfactant rich phase is surrounded by a clear oily product phase and a catalyst containing water phase.

temperature, as described by Müller et al.,²⁶ was used. With this, a minimum oil content of 95 wt % could be achieved for all operational modes. Deviations from an ideal pure oil phase were caused by partial solubilization of surfactant in the oil phase and drastic changes in process operation conditions.

To this end, especially the change between batch and continuous operation caused highly dynamic disturbances, leading to a reduced separation quality (see start of case 1 in Figure 10, switching from case 1 to case 2 and switching from case 2 to case 3). Additionally, the necessary refeeding of surfactant and catalyst solution due to sample losses caused temporary perturbations at some operational points (see middle of case 1 and end of case 4). These dynamic concentration shifts impede tracking the optimal temperature for the phase separation and several control actions needed to be performed to regain an optimal separation state.

The separation behavior in dependence of the settler temperature showed the expected correlations. Referring to results obtained by Müller et al.,²⁶ increasing product concentrations lead to lower separation temperatures required to maintain a three-phase separation. The observation was verified throughout the campaign. Thus, the applicability of the prediction model was given.

Interestingly, the coalescence support with knitted wire fabrics led to overall excellent phase separation dynamics. This was observed with gauge glasses before and after the settler internals. The improved coalescence achieved with the knitted wire fabrics resulted in a successful separation, regardless of the emulsion's state at the settler inlet.

Concerning the rhodium loss, ICP-OES measurements confirmed results from previous miniplant operations. In case an almost pure oil phase was established, rhodium concentrations of around 0.1 ppm and below were observed. The rhodium concentrations in most of our samples lay below the detectability limit of the ICP-OES. This result is similar to lab-scale test tube results.

5. CONCLUSIONS AND OUTLOOK

With this contribution a long-term miniplant operation is presented for the hydroformylation of long-chain alkenes (C_{12} alkene) in micellar systems. Here, the applicability of a proposed process concept using a microemulsion system is demonstrated with a stable phase separation and an efficient catalyst recovery. Moreover, a stable product yield of 21% was achieved. The surfactant-supported reaction system enabled the hydroformylation of long-chain alkenes at mild reaction conditions (95 °C and 15 bar). Hence, this contribution presents the proof of concept for realizing a homogeneously catalyzed hydroformylation in microemulsions during a 200 h long miniplant operation.

However, some challenges still remain. Based on the results, it can be seen that there are critical process parameters which have a drastic influence on the performance of the plant and the dynamics of the system. Among these are the recycle ratio of the three streams in the settler and the accumulation of certain components, such as catalyst and surfactant, in the settler. Throughout the miniplant operation the latter led to reduced reaction rates as phase mediation and catalytic mass were reduced.

In terms of profitability, higher yields should be strived for. This is to be achieved by increasing the reactor residence time and simultaneously manipulating the recycle flows of the three phases. This effect outlines one field for future research. Additionally, the introduction of larger amounts of catalyst into the system, increasing the reactor pressure from 15 to 20 bar, or

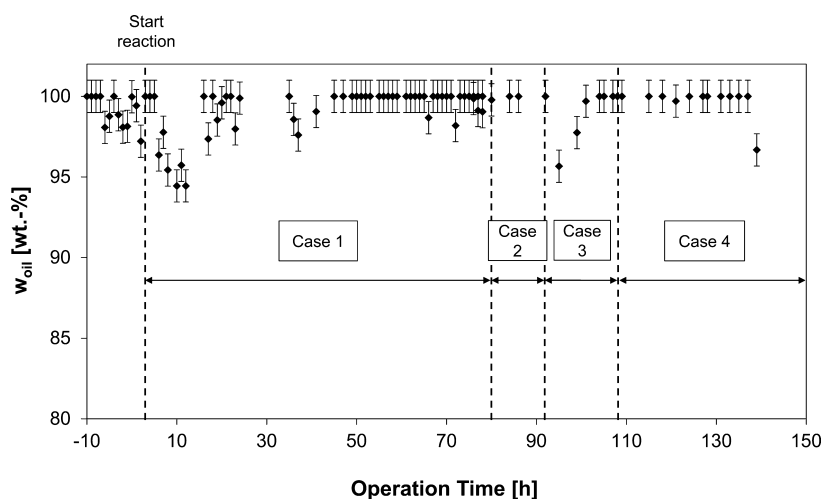


Figure 10. Miniplant operation. Phase separation quality depicted as the total amount of oily components in the oil phase of the settler. Results are given for the total time of operation.

raising the temperature are possible and planned options for future investigations. Moreover, the catalyst stability is to be proven in a long-term operation without sampling and hence, no replenishing.

Concluding, in this contribution it was successfully shown how surfactants can under realistic conditions be employed to enable homogeneous catalysis and simultaneously enable pure phase separation in a multiphase system. The authors hope to have inspired ideas and presented possible solutions for similar process concepts, in which comparable challenges of reactions followed by catalyst separation and product isolation are being tackled.

AUTHOR INFORMATION

Corresponding Authors

*E-mail: markus.illner@tu-berlin.de.

*E-mail: david-nicolas.mueller@evonik.de.

Author Contributions

Markus Illner and David Müller have contributed equally to this article and are both considered primary authors.

Notes

The authors declare no competing financial interest.

ACKNOWLEDGMENTS

This work is part of the Collaborative Research Center "Integrated Chemical Processes in Liquid Multiphase Systems" (Subproject B4) coordinated by the Technische Universität Berlin. Financial support by the German Research Foundation (Deutsche Forschungsgemeinschaft, DFG) is gratefully acknowledged (TRR 63). Furthermore, the authors gratefully acknowledge the support of Umicore N.V. for sponsoring the rhodium catalyst precursor "acetylacetonatodicarbonylrhodium(I) (CAS Registry Number 14874-82-9)", Sasol Ltd. for the surfactant used in the described experiments, the support of SIEMENS AG for sponsoring the entire process control system SIMATIC PCS7 for the automation of the miniplant, and Rhodius GmbH for sponsoring the knitted fabrics. Finally, the support of the Federal Institute for Materials Research and Testing (BAM) is gratefully acknowledged. A special thanks is given to Dr. Michael Maiwald and his team of the Federal Institute for Materials Research and Testing (BAM) for lending the Raman spectrometer for the miniplant campaign.

REFERENCES

- (1) Kummer, R. *New Synthesis with Carbon Monoxide*. Herausgegeben von J. Falbe, Springer-Verlag, Berlin 1980. XIV, 465 S., Geb. DM 244.00. *Angew. Chem.* **1982**, *94*, 156.
- (2) Hamerla, T.; Rost, A.; Kasaka, Y.; Schomäcker, R. Hydroformylation of 1-Dodecene with Water-Soluble Rhodium Catalysts with Bidentate Ligands in Multiphase Systems. *ChemCatChem* **2013**, *5* (7), 1854.
- (3) Kohlpaintner, C. W.; Fischer, R. W.; Cornils, B. Aqueous Biphasic Catalysis: Ruhrchemie/Rhône-Poulenc Oxo Process. *Appl. Catal., A* **2001**, *221* (1–2), 219.
- (4) Wiese, K.-D.; Obst, D. Catalytic Carbonylation Reactions: Hydroformylation. In *Topics in Organometallic Chemistry*; Springer: Berlin, 2006; pp 1–33.
- (5) Franke, R.; Selent, D.; Börner, A. Applied Hydroformylation. *Chem. Rev.* **2012**, *112* (11), 5675.
- (6) Cornils, B.; Herrmann, W. a.; Rasch, M. Otto Roelen, Pioneer in Industrial Homogeneous Catalysis. *Angew. Chem., Int. Ed. Engl.* **1994**, *33*, 2144.
- (7) Kupka, J. *Hydroformylierung von 1-Octen in Mikroemulsion*. Ph.D. Dissertation, Technische Universität Braunschweig, 2006.
- (8) Miyagawa, C. C.; Kupka, J.; Schumpe, A. Rhodium-Catalyzed Hydroformylation of 1-Octene in Micro-Emulsions and Micellar Media. *J. Mol. Catal. A: Chem.* **2005**, *234* (1–2), 9.
- (9) Fell, B.; Papadogianakis, G. Rhodiumkatalysierte Mizellare Zweiphasenhydroformylierung von N-Tetradecen-1 Mit Grenzflächenaktiven Sulfobetainderivaten Des Tris(2-Pyridyl)phosphans Als Wasserlösliche Komplexliganden. *J. Mol. Catal.* **1991**, *66* (2), 143.
- (10) Haumann, M.; Koch, H.; Hugo, P.; Schomäcker, R. Hydroformylation of 1-Dodecene Using Rh-TPPTS in a Microemulsion. *Appl. Catal., A* **2002**, *225* (1–2), 239.
- (11) Wachsen, O.; Himmler, K.; Cornils, B. Aqueous Biphasic Catalysis: Where the Reaction Takes Place. *Catal. Today* **1998**, *42* (4), 373.
- (12) Kiedorf, G.; Hoang, D. M.; Müller, A.; Jörke, A.; Markert, J.; Arellano-Garcia, H.; Seidel-Morgenstern, A.; Hamel, C. Kinetics of 1-Dodecene Hydroformylation in a Thermomorphic Solvent System Using a Rhodium-Biphenyl Catalyst. *Chem. Eng. Sci.* **2014**, *115*, 31.
- (13) Müller, M.; Kasaka, Y.; Müller, D.; Schomäcker, R.; Wozny, G. Process Design for the Separation of Three Liquid Phases for a Continuous Hydroformylation Process in a Miniplant Scale. *Ind. Eng. Chem. Res.* **2013**, *52* (22), 7259.
- (14) Dwars, T.; Paetzold, E.; Oehme, G. Reactions in Micellar Systems. *Angew. Chem., Int. Ed.* **2005**, *44* (44), 7174.
- (15) Yonehara, K.; Ohe, K.; Uemura, S. Highly Enantioselective Hydrogenation of Enamides and Itaconic Acid in Water in the Presence of Water-Soluble Rhodium(I) Catalyst and Sodium Dodecyl Sulfate. *J. Org. Chem.* **1999**, *64* (26), 9381.
- (16) Van Vyve, F.; Renken, A. Hydroformylation in Reverse Micellar Systems. *Catal. Today* **1999**, *48* (1–4), 237.
- (17) Li, M.; Li, Y.; Chen, H.; He, Y.; Li, X. Studies on 1-Dodecene Hydroformylation in Biphasic Catalytic System Containing Mixed Micelle. *J. Mol. Catal. A: Chem.* **2003**, *194* (1–2), 13.
- (18) Schwarze, M.; Pogrzeba, T.; Seifert, K.; Hamerla, T.; Schomäcker, R. Recent Developments in Hydrogenation and Hydroformylation in Surfactant Systems. *Catal. Today* **2015**, *247*, 55.
- (19) Pogrzeba, T.; Müller, D.; Illner, M.; Schmidt, M.; Kasaka, Y.; Weber, a.; Wozny, G.; Schomäcker, R.; Schwarze, M. Superior Catalyst Recycling in Surfactant Based Multiphase Systems – Quo Vadis Catalyst Complex? *Chem. Eng. Process.* **2016**, *99*, 155.
- (20) Holmberg, K. Organic Reactions in Microemulsions. *Eur. J. Org. Chem.* **2007**, *2007*, 731.
- (21) Schomäcker, R.; Holmberg, K. Reactions in Organised Surfactant Systems. In *Microemulsions: Background, New Concepts, Applications, Perspectives*; Subenrauch, C., Ed.; John Wiley & Sons Ltd.: Chichester, U.K., 2009; pp 148–177.
- (22) Schwarze, M.; Pogrzeba, T.; Volovych, I.; Schomäcker, R. Microemulsion Systems for Catalytic Reactions and Processes. *Catal. Sci. Technol.* **2015**, *5* (1), 24.
- (23) Müller, D.; Minh, D. H.; Merchan, V. A.; Arellano-Garcia, H.; Kasaka, Y.; Müller, M.; Schomäcker, R.; Wozny, G. Towards a Novel Process Concept for the Hydroformylation of Higher Alkenes: Mini-Plant Operation Strategies via Model Development and Optimal Experimental Design. *Chem. Eng. Sci.* **2014**, *115*, 127.
- (24) Kahlweit, M.; Strey, R.; Haase, D.; Kunieda, H.; Schmeling, T.; Faulhaber, B.; Borkovec, M.; Eicke, H.-F.; Busse, G.; Eggers, F.; et al. How to Study Microemulsions. *J. Colloid Interface Sci.* **1987**, *118* (2), 436.
- (25) Stubenrauch, C. *Microemulsions: Background, New Concepts, Applications, Perspectives*; Stubenrauch, C., Ed.; John Wiley & Sons, Ltd.: Chichester, U.K., 2009.
- (26) Müller, D.; Esche, E.; Pogrzeba, T.; Illner, M.; Schomäcker, R.; Wozny, G.; Leube, F. Systematic Phase Separation Analysis of Surfactant Containing Systems for Multiphase Settler Design. *Ind. Eng. Chem. Res.* **2015**, *54* (12), 3205.
- (27) Müller, D. *Development of Operation Trajectories Under Uncertainty for a Hydroformylation Mini-Plant*. Ph.D. Dissertation, Technische Universität Berlin, 2015.

- (28) Seborg, D. E.; Mellichamp, D. A.; Edgar, T. F.; Doyle, F. J., III. *Process Dynamics and Control*; John Wiley & Sons: Chichester, U.K., 2011.
- (29) AIChE Center for Chemical Process Safety. *Guidelines for Safe Automation of Chemical Processes*; AIChE: New York, 1993.
- (30) Müller, D.; Esche, E.; Hamerla, T.; Rost, A.; Kasaka, Y. Enabling Hydroformylation in Micro-Emulsion Systems: Long-Term Performance of a Continuously Operated Mini-Plant. Presented at the AIChE Annual Meeting, San Francisco, CA, 2013.
- (31) Torres, R.; Podzimek, M.; Friberg, S. E. E. Foaming of Microemulsions I. Microemulsions with Ionic Surfactants. *Colloid Polym. Sci.* **1980**, 258, 855.
- (32) Ding, H.; Bartik, B.; Hanson, B. E. Surface Active Phosphines for Catalysis under Two-Phase Reaction Conditions. P(menthyl) $[(CH_2)_8C_6H_4-p-SO_3Na]_2$ and the Hydroformylation of Styrene. *J. Mol. Catal. A: Chem.* **1995**, 98 (95), 117.
- (33) Karakhanov, E. a; Kardasheva, Y. S.; Runova, E. a; Semernina, V. a. Surface Active Rhodium Catalysts for Hydroformylation of Higher Alkenes in Two-Phase Systems. *J. Mol. Catal. A: Chem.* **1999**, 142 (3), 339.
- (34) Pogrzeba, T.; Müller, D.; Hamerla, T.; Esche, E.; Paul, N.; Wozny, G.; Schomaecker, R. Rhodium Catalysed Hydroformylation of Long-Chain Olefins in Aqueous Multiphase Systems in a Continuously Operated Miniplant. *Ind. Eng. Chem. Res.* **2015**, 54, 11953.
- (35) Hamerla, T. *Hydroformylierung Langkettiger Olefine Mit Zweizähnigen Rhodium-Komplexen in Mizellaren Lösungen Und Mikroemulsionen*. Ph.D. Dissertation, Technische Universität Berlin, 2014; p 132.
- (36) Markert, J.; Brunsch, Y.; Munkelt, T.; Kiedorf, G.; Behr, A.; Hamel, C.; Seidel-Morgenstern, A. Analysis of the Reaction Network for the Rh-Catalyzed Hydroformylation of 1-Dodecene in a Thermomorphic Multicomponent Solvent System. *Appl. Catal., A* **2013**, 462–463, 287.

PAPER 8

Microemulsion Systems as Switchable Reaction Media for the Catalytic Upgrading of Long-Chain Alkenes

Tobias Pogrzeba, Markus Illner, Marcel Schmidt, Jens-Uwe Repke, and Reinhard Schomäcker

Chemie Ingenieur Technik, 2017, 89, 459-463

Online Article: <http://onlinelibrary.wiley.com/doi/10.1002/cite.201600140/full>

ActiveView PDF: <http://onlinelibrary.wiley.com/doi/10.1002/cite.201600140/epdf>

Reprinted (adapted) with permission from “Microemulsion Systems as Switchable Reaction Media for the Catalytic Upgrading of Long-Chain Alkenes; Tobias Pogrzeba, Markus Illner, Marcel Schmidt, Jens-Uwe Repke, and Reinhard Schomäcker. Chemie Ingenieur Technik, 2017, 89, 459-463.” Copyright (2017) John Wiley and Sons.

Microemulsion Systems as Switchable Reaction Media for the Catalytic Upgrading of Long-Chain Alkenes

Tobias Pogrzeba^{1,*}, Markus Illner², Marcel Schmidt¹, Jens-Uwe Repke², and Reinhard Schomäcker¹

DOI: 10.1002/cite.201600140

The application of microemulsion systems as switchable reaction media for the rhodium-catalyzed hydroformylation of 1-dodecene is herein reported. The influence of temperature and the selected surfactant on the reaction kinetics was investigated. In addition, the feasibility of a process concept for these reaction systems was tested within 100 hours continuous mini-plant operation, showing similar product yield and reaction selectivity as on the lab-scale. Alongside, a stable steady state operation was achieved, showing an efficient phase separation and recycling of surfactant and catalyst.

Keywords: Hydroformylation, Microemulsions, Mini-plant, Process design, Switchable solvents

Received: September 29, 2016; *revised:* January 27, 2017; *accepted:* February 03, 2017

1 Introduction

The selection of an appropriate solvent is certainly one of the biggest obstacles for the development of chemical processes. Since an optimal yield is not a solely satisfying objective in terms of green chemical processing, the selection criteria for solvents imply an integrated consideration of the process, including aspects of resource and energy efficiency as well as sustainability. Unfortunately, most industrial applications involve more than one step, especially in downstream processing, where typically each step requires a different solvent that has to be removed again once its task is done. In terms of process sustainability, that strategy is highly wasteful and contributes to wastage of energy and materials. To overcome this, one would need a solvent that can transform itself, changing its properties to enable several applications. Fortunately, these systems do already exist: Switchable solvents, meaning liquids that can be reversibly switched from one state to another, could unfold a great potential for process intensification, if applied in a subtle way. Several different approaches of switchable solvent systems have already been reported in literature, like supercritical media based on CO₂ [1], switchable-polarity solvents [2], thermomorphic multicomponent solvents [3] or microemulsion systems (further denoted as MES) [4].

In terms of green processing the application of water as solvent is highly desirable but carries the issue of poor reactant solubility in case of hydrophobic reactants. A way to bring organic substrates and water together is to add a surfactant to the reaction mixture, which enables many interesting applications for water-soluble catalysts in homogeneous catalysis. For example performing catalytic reactions in microemulsion systems, which are ternary mixtures consist-

ing of oil, water, and a surfactant (often non-ionic surfactants are chosen in this context). Microemulsions provide a high interfacial area between the polar and non-polar domains during the reaction. Additionally, their phase separation behaviour can be manipulated through temperature changes and thus makes them switchable solvent systems. According to Winsor, microemulsions are thermodynamically stable and can be either a one-phase system (Winsor IV) or part of a multiphase system (Winsor I, II, or III) in which the microemulsion can be of three different types: water-in-oil (w/o), oil-in-water (o/w) or bicontinuous; the phase behaviour is described in detail in literature [4–6].

The switchability of MES enables chemical processes in aqueous media with high reaction rates and efficient catalyst recycling. To proof the applicability of MES as switchable reaction media, an integrated process concept for the rhodium-catalyzed hydroformylation of 1-dodecene on a mini-plant scale is currently under investigation. In this contribution the results of a long-term operation, in which a highly selective reaction as well as a stable phase separation with feasible catalyst recycling could be achieved continuously for 100 hours in total, are presented. Also a number of results from kinetic lab-scale experiments that show an interesting reaction behavior dependent on temperature

¹Tobias Pogrzeba, Marcel Schmidt, Prof. Reinhard Schomäcker
tobias.pogrzeba@tu-berlin.de

Technische Universität Berlin, Department of Chemistry, Straße des 17. Juni 124, 10623 Berlin, Germany.

²Markus Illner, Prof. Jens-Uwe Repke

Technische Universität Berlin, Department of Process Dynamics and Operation, Straße des 17. Juni 135, 10623 Berlin, Germany.

and surfactant chain-length are highlighted. The obtained results are of great importance for understanding these complex reaction systems and contribute to further development and enhancement of chemical processes in MES.

2 Experimental

In lab-scale the hydroformylation reactions were performed in a 100 mL stainless steel high-pressure vessel (Premex Reactor AG) equipped with a gas dispersion stirrer and mounted in an oil thermostat (Huber, K12-NR). The typical reaction conditions for the hydroformylation were 15 bar of synthesis gas (1:1 mixture, purity 2.1), an internal reactor temperature of 65–110 °C, and a stirring speed of 1200 rpm. The reaction mixture usually consisted of 1-dodecene (VWR, 95 %), water (HPLC grade), a non-ionic surfactant from the Marlipal® 24 series (Sasol), the rhodium precursor [Rh(acac)(CO)₂] (Umicore), and the ligand SulfoXantphos (Molisa). A more detailed description of experimental set-up and reaction procedure can be found in [7]. The important parameters (oil content α , surfactant concentration γ , selectivity S , and TOF) for the evaluation of experimental data were calculated as shown in Eqs. (1)–(4), where m is the mass, n is the amount of substance, 1-dodecene is the substrate and tridecanal is the product.

$$\alpha = \frac{m_{\text{Oil}}}{m_{\text{Oil}} + m_{\text{Water}}} \quad (1)$$

$$\gamma = \frac{m_{\text{Surfactant}}}{m_{\text{Oil}} + m_{\text{Water}} + m_{\text{Surfactant}}} \quad (2)$$

$$S(n : \text{iso}) = \frac{n_{\text{Product}}}{n_{\text{iso-Aldehydes}}} \quad (3)$$

$$\text{TOF} = \frac{n_{t=0, \text{Substrate}} Y(t)}{n_{\text{cat}} t} \quad (4)$$

The mini-plant system, which is schematically depicted in Fig. 1, consists of a feed section holding containers for the applied substances, a main reaction section holding the

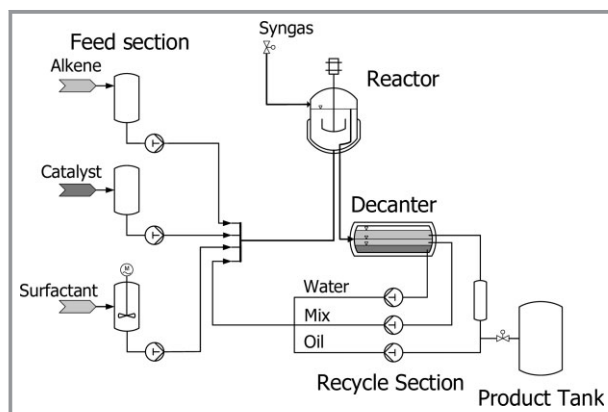


Figure 1. Schematic setup of the mini-plant system for the continuous hydroformylation of 1-dodecene in MES.

reactor (1.5 L), and a separation unit (decanter, 0.5 L). Here, a decanter with three drains was installed to adjust the phase separation for the MES and enable a reliable separation of the product containing oil phase from the surfactant and catalyst rich mix phase and the lower aqueous solution [8]. The mini-plant is fully automatized with SIEMENS PCS7 and meets ATEX zone 2 specifications [9]. Offline gas chromatography (Agilent HP-5 column, FID) and online raman spectroscopy (RXN1 NIR, Kaiser Optical Systems) were used for liquid sampling and thus, evaluating separation success and reaction performance. Rhodium leaching into the product phase is determined by an ICP-OES (Varian ICP-OES 715 ES).

3 Results and Discussion

The rhodium-catalysed hydroformylation of 1-dodecene in microemulsion systems (Fig. 2) is investigated by our research group for several years [7, 10, 11]. In previous experiments it was found that the aliphatic surfactants from the Marlipal® series provide good results as emulsifier for the applied reaction mixture. By the application of the surfactant Marlipal® 24/70, 31.3 % yield of aldehyde (98 % linear product) were obtained after 4 h reaction time under optimized reaction conditions: $\alpha = 0.5$, $\gamma = 0.08$, 95 °C reaction temperature, 15 bar syngas pressure, 1200 rpm stirring speed, and 1:4 metal-to-ligand ratio.

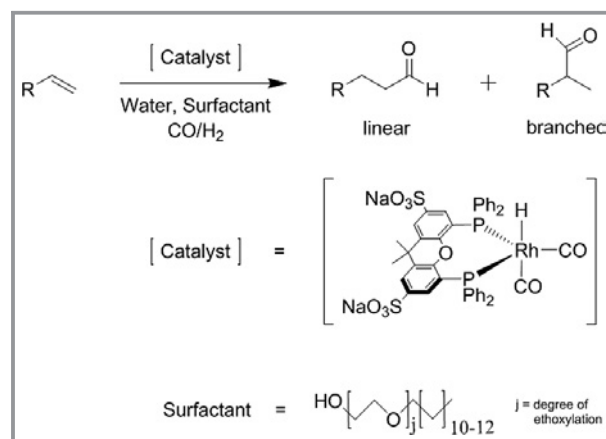


Figure 2. Hydroformylation reaction in microemulsion systems, structures of the applied rhodium catalyst and of the non-ionic surfactants (Marlipal® 24 series).

To gain deeper understanding of the mechanisms behind homogeneous catalysis in MES, it is highly necessary to thoroughly investigate the influence of surfactants and temperature on catalytic reactions in these systems, since both have simultaneous impact on reaction rate and phase behaviour. In order to do this, the influence of temperature on the hydroformylation of 1-dodecene with respect to reaction rate and selectivity for a fixed composition of the reaction mixture was investigated. The results are depicted

in Fig. 3. Interestingly, the reaction rate increased exponentially within the investigated temperature range and indicated a simple Arrhenius behaviour. At 68 °C a TOF of 50 h⁻¹ was achieved which could be raised to 380 h⁻¹ at 110 °C, while the selectivity towards the linear product remained at very high value of 98 %. These results were slightly unexpected, since the MES underwent two phase transitions between 68 and 82 °C that completely changed the type of microemulsion (oil-in-water → bicontinuous → water-in-oil). As it was already shown, the switch in phase behaviour leads to a noticeable change of mass transfer in the MES [12]. In addition, the type of microemulsion dictates the continuous phase for the reaction mixture since the catalyst follows the surfactant into the corresponding microemulsion phase due to its amphiphilic character. However, that all seems to have no immediate influence on the reaction rate in the presented experiment. Hence it was assumed that MES feature kinetically controlled two-phase reactions, which is also indicated by the Arrhenius behaviour of the hydroformylation (Fig. 3). In addition, an activation energy of 59 kJ mol⁻¹ could be calculated for the reaction which is in good accordance to literature data collected for the applied catalyst in single phase systems. Considering a two-phase reaction, the surfactant should play an even greater role for the reaction conditions in MES than expected since catalysis mainly takes place at the oil-water interface, where all the reactants are located and bound by the surfactant. Thus the ability of the surfactant to work as emulsifier for the applied reaction system determines the size of the interfacial area for the reaction and, in addition, also the local concentrations of reactants at the interface that are relevant for catalysis. Simply said, the better the surfactant performs, the higher is the possible outcome of the reaction.

To further investigate this matter, an experiment was performed in which the hydroformylation was carried out with

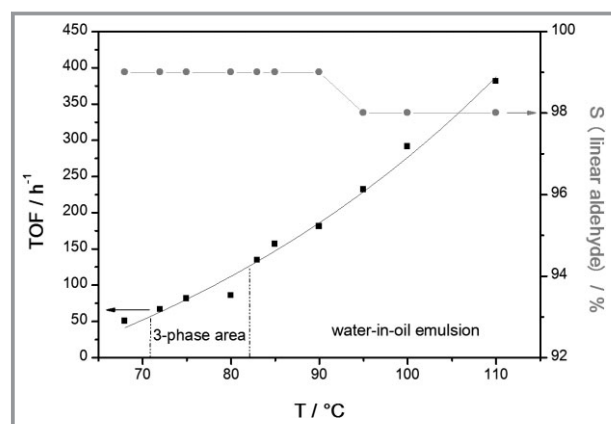


Figure 3. Turnover frequency and selectivity as function of temperature. Test conditions: 15 bar, 1200 rpm, 120 mmol 1-dodecen, $\alpha = 0.5$, $\gamma = 0.08$ (Marlipal 24/70), 1 wt % Na₂SO₄, 0.05 mmol (0.04 mol %) Rh(acac)(CO)₂, 0.2 mmol SulfoXantphos, V_R = 50 mL. TOFs were calculated after 1 h reaction time. Arrows indicate the corresponding axis.

several related surfactants from the Marlipal® series (the results are shown in Fig. 4). All reaction parameters were kept constant for every run to ensure that the degree of ethoxylation of the surfactant was the only essential variable for the reaction. The degree of ethoxylation, meaning the amount of ethoxylate groups in the surfactant-chain, was varied between 5 and 9 (Marlipal® 24/70 has an average of 7). The experimental results indicate that the applied surfactant indeed plays a greater role for the reaction than just emulsifying the two-phase systems. In case of the investigated hydroformylation an enhanced hydrophilicity of surfactant (meaning a higher ethoxylation degree) seems to be beneficial. The reaction rate was found to be the highest at an ethoxylation degree of 9 (Marlipal® 24/90). A TOF of 309 h⁻¹ was calculated for this surfactant which is an increase of 51 % in comparison to 205 h⁻¹ for an ethoxylation degree of 5 (Marlipal® 24/50). This finding could be explained by a higher density of the surfactant film that enhances the adsorption of reactants at the oil-water interface and, by that, increases the reaction rate. In the same time, a change in the degree of ethoxylation has an impact on the resulting phase behaviour of the applied MES. However, the change in phase behaviour had again no noticeable influence on the reaction since the results show only a slight linear increase of the reaction rate without an abrupt rising in between that would indicate a major change of mass transfer conditions. All things considered, these results alone are not sufficient for an accurate explanation of the impact of surfactants on homogeneous catalysis and thus this topic requires more investigation. But they do point out the high optimization potential of chemical processes in microemulsion systems with respect to higher space-time yields.

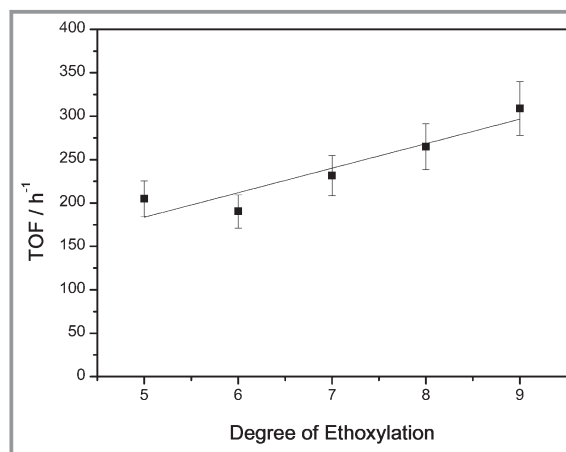


Figure 4. Turnover frequency vs degree of ethoxylation. Test conditions: 95 °C, 15 bar, 1200 rpm, 120 mmol 1-dodecen, $\alpha = 0.5$, $\gamma = 0.08$ (Marlipal 24/XX), 1 wt % Na₂SO₄, 0.05 mmol (0.04 mol %) Rh(acac)(CO)₂, 0.2 mmol SulfoXantphos, V_R = 50 mL. TOFs were calculated after 1 h reaction time.

3.1 Mini-Plant Operation

The proof of concept for the hydroformylation in MES is performed within the technical mini-plant system. The conducted mini-plant campaign was carried out as 100 hours continuous operation, covering different operational modes from start-up, full recycle mode to increase product yield and long-term steady state continuous operation. Referring to the lab-scale results an initial mixture of 50 % α and 8 % γ was applied, including 0.04 mol % rhodium precursor, 0.2 mol % SulfoXantphos and 1.00 wt % Na_2SO_4 . The reaction conditions, determined on the lab-scale as well, were set to 15 bar(g) pressure and 95 °C.

A trajectory for the total conversion of 1-dodecene and yield of tridecanal was obtained from the mini-plant campaign, depicted in Fig. 5. After feeding and starting up the plant, the reaction was successfully initiated. From here on a full recycle operation was performed to quickly increase yield. At operation hour 35, the continuous operation was started with the introduction of fresh 1-dodecene and extraction of the product-containing organic phase. Consequently, the conversion slightly decreased and stabilized at a new level of 41 %, which could be sustained during the steady-state operation for more than 50 hours. With a reaction residence time of 6.5 hours for the continuous operation, these results are in good accordance to lab-scale find-

ings. The product yield stabilized at around 39 %, showing an excellent overall reaction selectivity of 95 % towards the desired aldehyde. In addition, the product was obtained with a linear to branched selectivity of 99 %. Again, this is in very good accordance to previous findings in lab. Moreover, a continuous phase separation could be accomplished, leading to a remarkably pure organic phase (educt and product content of 99.8 %) and very low rhodium leaching into the product phase (lower than 0.1 ppm). Thus, an efficient separation and recycling of surfactant and catalyst could be shown by the mini-plant operation, which demonstrates the applicability of MES as reaction media in continuous chemical processes.

4 Conclusions and Outlook

In this contribution, it is shown that microemulsion systems are feasible reaction media for homogeneously catalysed reactions and continuous chemical processes in aqueous media. The mini-plant experiments proved the applicability of MES and demonstrated that their switchability can be exploited in an integrated process with reaction and subsequent recycling of surfactant and catalyst. However, these multiphase systems require a profound knowledge of the influence of parameters regarding reaction

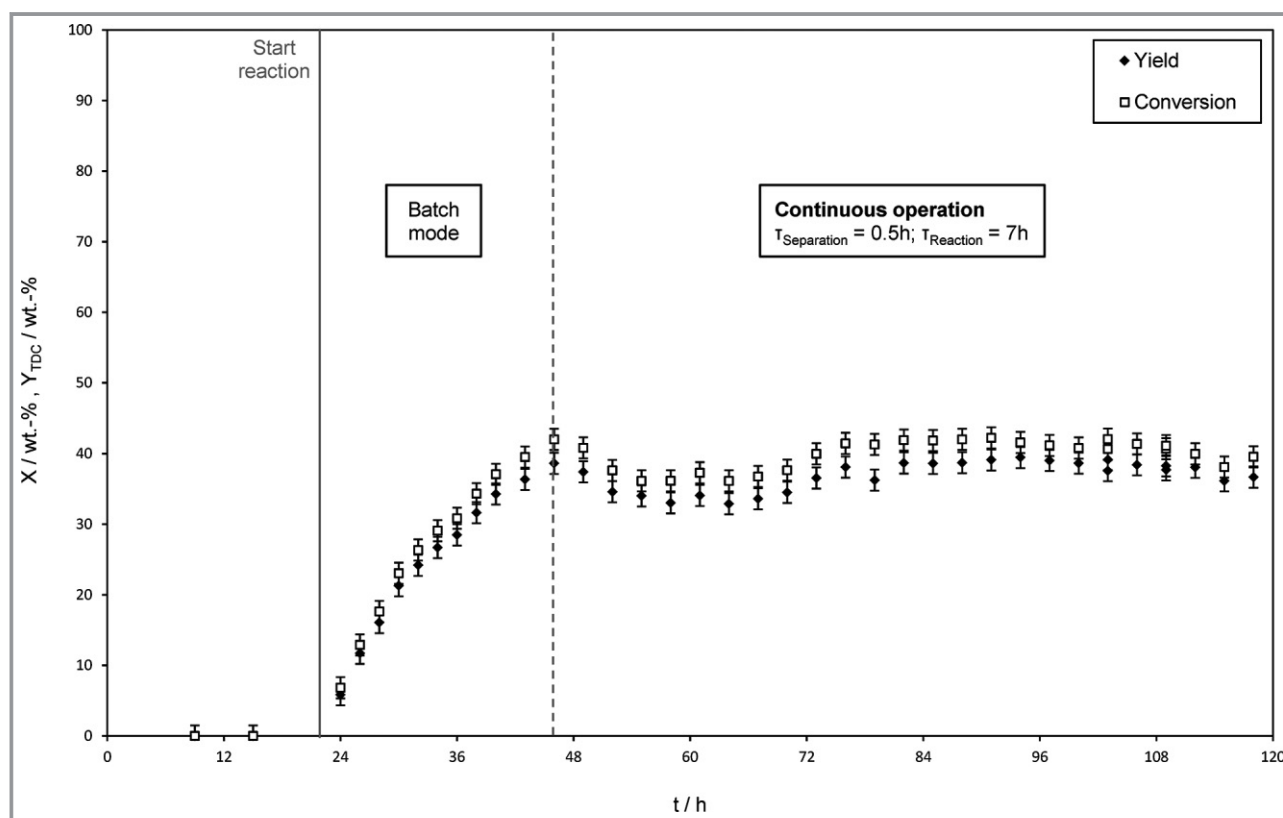


Figure 5. Mini-plant operation results, total conversion of 1-dodecene and yield of tridecanal over time. Reaction residence time indicates equivalent reaction time of a batch experiment.

and separation. In particular, the applied surfactant has a strong impact on the outcome of a reaction. Further investigations on this matter are mandatory to fully understand the role of the surfactant and, by that, enhance the operability of MES in technical systems.

This work is part of the Collaborative Research Center/Transregio 63 "Integrated Chemical Processes in Liquid Multiphase Systems" (subprojects A2 and B4). Financial support by the Deutsche Forschungsgemeinschaft (DFG, German Research Foundation) is gratefully acknowledged (TRR 63). Furthermore, the authors gratefully acknowledge the support of the company Umicore for sponsoring the rhodium catalyst "Acetylacetonatodicarbonylrhodium(I)" (CAS: 14874-82-9).

Symbols used

m	[kg]	mass
n	[mol]	amount of substance
S	[-]	selectivity
t	[h]	time
T	[°C]	temperature
TOF	[h ⁻¹]	turnover frequency
X	[-]	conversion
Y	[-]	yield
α	[-]	oil-to-water ratio
γ	[-]	surfactant concentration

Abbreviations

MES	Microemulsion system
SulfoXantphos	4,5-Bis(diphenylphosphino)-9,9-dimethylxanthene

References

- [1] W. Leitner, *Acc. Chem. Res.* **2002**, 35 (9), 746 – 56.
- [2] P. G. Jessop, S. M. Mercer, D. J. Heldebrant, *Energy Environ. Sci.* **2012**, 5 (6), 7240 – 7253.
- [3] E. Schäfer, Y. Brunsch, G. Sadowski, A. Behr, *Ind. Eng. Chem. Res.* **2012**, 51 (31), 10296 – 10306.
- [4] M. Schwarze, T. Pogrzeba, I. Volovych, R. Schomäcker, *Catal. Sci. Technol.* **2015**, 5 (1), 24 – 33.
- [5] M. Kahlweit, R. Strey, G. Busse, *J. Phys. Chem.* **1990**, 94 (10), 3881 – 3894.
- [6] P. A. Winsor, *Trans. Faraday Soc.* **1948**, 44, 376 – 398.
- [7] T. Pogrzeba, D. Müller, T. Hamerla, E. Esche, N. Paul, G. Wozny, R. Schomäcker, *Ind. Eng. Chem. Res.* **2015**, 54 (48), 11953 – 11960.
- [8] D. Müller, E. Esche, T. Pogrzeba, M. Illner, F. Leube, R. Schomäcker, G. Wozny, *Ind. Eng. Chem. Res.* **2015**, 54 (12), 3205 – 3217.
- [9] M. Müller, Y. Kasaka, D. Müller, R. Schomäcker, G. Wozny, *Ind. Eng. Chem. Res.* **2013**, 52 (22), 7259 – 7264.
- [10] T. Hamerla, A. Rost, Y. Kasaka, R. Schomäcker, *ChemCatChem* **2013**, 5 (7), 1854 – 1862.
- [11] A. Rost, M. Müller, T. Hamerla, Y. Kasaka, G. Wozny, R. Schomäcker, *Chem. Eng. Process.* **2013**, 67, 130 – 135.
- [12] T. Hamerla, N. Paul, M. Kraume, R. Schomäcker, *Chem. Ing. Tech.* **2013**, 85 (10), 1530 – 1539.

PAPER 9

Understanding the Role of Nonionic Surfactants during Catalysis in Microemulsion Systems on the Example of Rhodium-Catalyzed Hydroformylation

Tobias Pogrzeba, Marcel Schmidt, Natasa Milojevic, Carolina Urban, Markus Illner, Jens-Uwe Repke, and Reinhard Schomäcker

Industrial & Engineering Chemistry Research, 2017, 56, 9934-9941

Online Article: <http://pubs.acs.org/doi/abs/10.1021/acs.iecr.7b02242>

ActiveView PDF: <http://pubs.acs.org/doi/ipdf/10.1021/acs.iecr.7b02242>

Reproduced (or 'Reproduced in part') with permission from "Understanding the Role of Nonionic Surfactants during Catalysis in Microemulsion Systems on the Example of Rhodium-Catalyzed Hydroformylation; Tobias Pogrzeba, Marcel Schmidt, Natasa Milojevic, Carolina Urban, Markus Illner, Jens-Uwe Repke, and Reinhard Schomäcker. Industrial & Engineering Chemistry Research, 2017, 56, 9934-9941." Copyright (2017) American Chemical Society.

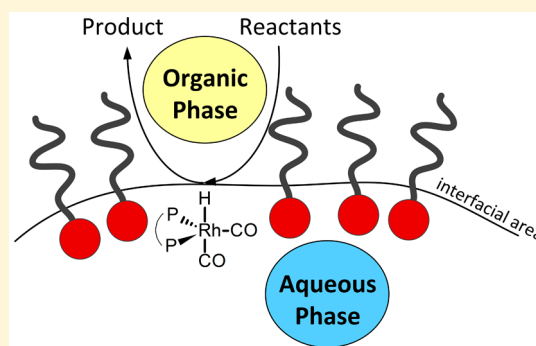
Understanding the Role of Nonionic Surfactants during Catalysis in Microemulsion Systems on the Example of Rhodium-Catalyzed Hydroformylation

Tobias Pogrzeba,^{*,†} Marcel Schmidt,[†] Natasa Milojevic,[†] Carolina Urban,[†] Markus Illner,[‡] Jens-Uwe Repke,[‡] and Reinhard Schomäcker[†]

[†]Department of Chemistry, Technische Universität Berlin, Straße des 17. Juni 124, Sekr. TC-8, Berlin D-10623, Germany

[‡]Chair of Process Dynamics and Operation, Technische Universität Berlin, Straße des 17. Juni 135, Sekr. KWT-9, Berlin D-10623, Germany

ABSTRACT: The application of microemulsion systems as switchable reaction media for the rhodium-catalyzed hydroformylation of 1-dodecene is being reported. The influence of temperature, phase behavior, and the selected nonionic surfactant on the reaction has been investigated. The results revealed that the structure and the hydrophilicity (degree of ethoxylation) of the applied surfactant can have a strong impact on the performance of the catalytic reaction in microemulsion systems, in particular on the reaction rate. The surfactant determines the boundary conditions for catalysis (interfacial area, local concentrations) and can also interact with the catalyst at the oil–water interface and hinder the reaction. In addition to the discussion of the experimental results, we present a proposal for the impact of surfactant-based reaction media on the reaction mechanism of the catalyst reaction.



1. INTRODUCTION

The use of water as solvent in transition metal-catalyzed chemistry is today still rather unusual and rarely the first choice of a chemist. To be fair, this is not very surprising because the poor solubility of most organic educts in water makes it difficult to perform reactions in aqueous media and to predict their results. However, if we want to make a switch to a greener chemistry and reduce the environmental implications of our work, we should start to intensify the efforts in research of catalysis in aqueous media. As Lipshutz et al. pointed out recently,¹ the path toward greener chemistry offers exciting opportunities and surprises associated with this new environment for catalysis, which should attract the interest of many scientists worldwide. To enable the transfer of the already established organic transition metal-catalyzed chemistry into the medium water, micellar catalysis can provide the crucial “solution” for substrate and catalyst solubilization and subsequent reaction under mild conditions.^{2–6} Often it is sufficient to employ a suitable surfactant or a micelle producing agent to solubilize the reactants and to enable the reaction. However, in case of the application of expensive transition metal catalysts in such media, an old problem occurs again that is already known from homogeneous organic solutions: the recovery of the catalyst. One possible way to tackle this problem in micellar media is the application of filtration techniques, for example, ultrafiltration. A catalyst that is embedded in the micelles can be retained during the ultrafiltration process if a micelle rejecting membrane is

applied. With this so-called micellar enhanced ultrafiltration (MEUF) technique, the active catalyst can be recycled within the retentate and reused for reaction.^{7,8} Another approach to combine reaction and catalyst recycling in micellar systems is the utilization of microemulsion systems (MES) as switchable solvents. Microemulsions are ternary mixtures consisting of a nonpolar component, water, and a surfactant (often nonionic surfactants are chosen in this context). Because of the strong surface activity of the surfactant, microemulsions provide a high interfacial area between the polar and nonpolar domains during the reaction. Additionally, their phase separation behavior can be manipulated through temperature changes and thus makes them switchable solvent systems. According to Winsor, microemulsions are thermodynamically stable and can be either a one-phase system (Winsor IV) or part of a multiphase system (Winsor I, II, or III) in which the microemulsion can be of three different types: water-in-oil (w/o), oil-in-water (o/w), or bicontinuous; the phase behavior is described in detail in the literature.^{9–11} The switchability of microemulsion systems offers many interesting options for chemical processes with industrial relevance in aqueous media, like Suzuki and Heck coupling reactions^{12,13} as substeps in the total synthesis of complex organic molecules (e.g., total synthesis of Boscalid¹⁴).

Received: May 31, 2017

Revised: August 2, 2017

Accepted: August 18, 2017

Published: August 18, 2017

Another application is the rhodium-catalyzed hydroformylation of long-chained alkenes that has already been performed successfully in a continuously operated mini-plant over a 200 h campaign.^{15,16}

Regarding the already numerous examples for transition metal catalysis in surfactant-based reaction media, it seems to be only a question of time until the first industrial application in these systems becomes reality. However, these complex multiphase systems require a profound knowledge of the influence of a variety of system parameters regarding reaction and separation. In particular, the applied surfactant seems to have a strong impact on the result of a reaction, which is today still not completely understood and raises the question of how catalysis works in these systems. To gain more knowledge about the role of the surfactant during catalysis, we decided to investigate the rhodium-catalyzed hydroformylation of 1-dodecene in microemulsion systems in a detailed study with regards to phase behavior of the MES, concentration and hydrophilicity of surfactant, and temperature dependency of the reaction. The obtained results are of great importance for understanding these complex reaction systems and contribute to further development and enhancement of chemical processes in surfactant-based reaction media.

2. MATERIALS AND METHODS

2.1. Chemicals. The reactant 1-dodecene (95%) and water (HPLC grade) were purchased from VWR. The precursor (acetylacetonato)dicarbonylrhodium(I) [Rh(acac)(CO)₂] was contributed by Umicore, Germany. The water-soluble ligand 2,7-bissulfonate-4,5-bis(diphenylphosphino)-9,9-dimethylxanthene (SulfoXantphos, SX) was purchased from Molisa, where it was synthesized according to a procedure described by Goedheijt et al.¹⁷ The syngas (1:1 mixture of CO and H₂, purity 2.1 for CO and 2.1 for H₂) was purchased from Air Liquide. The technical grade nonionic surfactants from the Marlipal 24 series were contributed by Sasol Germany. To adjust the ionic strength, we used sodium sulfate (Na₂SO₄, 99%) purchased from Merck. All of the chemicals were used without further purification.

2.2. Preparation of Catalyst Solution. For the preparation of the catalyst complex, 12.9 mg (0.05 mmol, 1 equiv) of [Rh(acac)(CO)₂] and 156.7 mg (0.20 mmol, 4 equiv) of SulfoXantphos were evacuated three times in a Schlenk tube and flushed with argon. The solvent (5 g of degassed water, HPLC grade) was added through a septum. The catalyst solution then was stirred overnight at room temperature to ensure the formation of the catalyst complex.

2.3. Investigation on Phase Behavior. Investigations on the phase behavior of the microemulsion systems were performed by using small glass reactors (50 mL volume) with a heating jacket. The lid of such a reactor offers connections for sampling, for vacuum establishment, and argon inertization. We investigated the phase behavior of several microemulsion systems consisting of 1-dodecene/water/nonionic surfactant. The applied nonionic surfactant from the Marlipal 24 series was varied with respect to the degree of ethoxylation (EO), from Marlipal 24/50 (average EO = 5) to Marlipal 24/90 (average EO = 9). In addition, every mixture consisted of 1.0 wt % sodium sulfate, 0.04 mol % [Rh(acac)(CO)₂], and 0.16 mol % SulfoXantphos. The oil-to-water ratio was kept constant for all experiments at $\alpha = 0.5$ with an amount of 95 mmol (16 g) of 1-dodecene (rhodium/ligand/alkene ratio = 1/4/2500). The amount of surfactant was varied from 1 to 16 wt % ($\gamma = 0.01$ to

0.16). For each sample, the different amounts of oil, water, sodium sulfate, and the particular surfactant were weighted into the reactor and evacuated and flushed with argon at least three times. The catalyst solution then was injected with a syringe. We studied the phase behavior from 50 to 90 °C in 2 °C steps. The microemulsions were stirred during the heating periods by a magnetic stirrer. After the desired temperature was reached, the stirrer was stopped and the phase separation was observed.

The important composition parameters to characterize the MES are the weight fractions of oil (α) and surfactant (γ) (eq 1), which are calculated from the mass m of the corresponding component:

$$\alpha = \frac{m_{\text{oil}}}{m_{\text{oil}} + m_{\text{H}_2\text{O}}} \quad \gamma = \frac{m_{\text{Surf}}}{m_{\text{oil}} + m_{\text{H}_2\text{O}} + m_{\text{Surf}}} \quad (1)$$

2.4. Hydroformylation Experiments. The hydroformylation reactions were performed in a 100 mL stainless steel high-pressure vessel from Premex Reactor AG, equipped with a gas dispersion stirrer and mounted in an oil thermostat from Huber (K12-NR). The reactor setup has already been illustrated in previous contributions.¹⁵ The typical reaction conditions for the hydroformylation were 15 bar pressure of syngas, an internal reactor temperature of 65–120 °C, and a stirring speed of 1200 rpm, using a gas dispersion stirrer. The reaction mixture usually consisted of 120 mmol (20 g) of 1-dodecene, water (HPLC grade, $\alpha = 0.5$), 1.0 wt % sodium sulfate, surfactant (Marlipal 24 series), and catalyst solution. The ratio of rhodium/ligand/alkene was 1/4/2500 in every experiment.

The reaction was performed as described in the following. At first the reactor was filled with the desired amounts of alkene, water, sodium sulfate, and surfactant. The catalyst solution then was transferred by a syringe to the reactor. The reactor was closed and evacuated and purged with nitrogen at least three times. The stirrer was started at a rate of 500 rpm, and the reactor was heated to the desired temperature. After reaching the temperature, the stirring was slowed (200–300 rpm), and the reactor was pressurized with syngas. The reaction was started by increasing the stirring speed again to 1200 rpm. For the evaluation of reaction progress, samples were withdrawn at several time intervals via a sampling valve and analyzed by gas chromatography (GC). To ensure homogeneous liquid sampling, the stirring speed was not changed, while the samples were taken from the reactor. No further purification steps were performed to isolate the product from the reaction mixture before the samples were measured via GC. In addition, consumption of syngas during the experiments has been recorded via the mass flow controller.

The important parameters (conversion X , yield Y , selectivity S , and TOF) for the evaluation of experimental data were calculated as shown in eqs 2–5, where n is the amount of substance, 1-dodecene is the substrate, and 1-tridecanal is the product.

$$X(t) = \frac{n_{t=0, \text{Substrate}} - n_{t, \text{Substrate}}}{n_{t=0, \text{Substrate}}} \quad (2)$$

$$Y(t) = \frac{n_{t, \text{Product}}}{n_{t=0, \text{Substrate}}} \quad (3)$$

$$S(n:\text{iso}) = \frac{n_{\text{Product}}}{n_{\text{iso-Aldehydes}}} \quad (4)$$

$$\text{TOF}_{\text{Ald}} = \frac{n_{t=0, \text{Substrate}} \cdot Y_{\text{Ald}}(t)}{n_{\text{cat}} \cdot t} \quad (5)$$

2.5. Analysis. Reaction progress and selectivity of hydroformylation reactions were analyzed by gas chromatography on a Shimadzu model GC-2010, equipped with a Supelcowax 10 capillary column, a flame ionization detection analyzer, and nitrogen as carrier gas.

3. RESULTS AND DISCUSSION

3.1. Phase Behavior of the Microemulsion Systems.

The phase behavior of the investigated microemulsion systems consisting of 1-dodecene, water, and varying technical grade surfactants from the Marlipal 24 series (Figure 1) was recorded

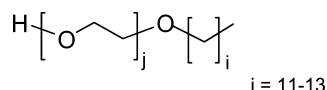


Figure 1. Structure of the applied surfactants from the Marlipal 24 series (j = degree of ethoxylation (EO)). EO increases from Marlipal 24/50 (average j = 5) to Marlipal 24/90 (average j = 9).

in the form of phase diagrams as illustrated exemplarily in Figure 2a for 1-dodecene/water/Marlipal(24/70). The presence of sodium sulfate and the rhodium catalyst in the mixture led to a shift of the phase boundaries to lower temperatures in comparison to the pure microemulsion system.¹⁸ The applied nonionic surfactants are characterized by their degree of ethoxylation, which is responsible for the hydrophilic character of each surfactant. The hydrophilicity increases with the number of ethoxylate groups in the surfactant chain and affects the phase behavior of the resulting MES. While the shape of the “fish” in the phase diagram (as in Figure 2a) follows a general pattern for each of the investigated surfactants due to their related chemical structure, the phase boundaries are shifted to lower or higher temperatures with changing EO (see Figure 2b). It is also apparent that the three-phase area becomes slightly larger with an increasing EO number. The information about the position of the “fish” in the phase diagram is of great importance for the application of a MES in a chemical process, because it marks the switchable area that is essential for reaction and catalyst recycling in these systems. At the same time, it is also a good indicator for the temperature range at which the application of a particular MES for a reaction is feasible or not. The reason for this is that every surfactant has its own specific working area (temperature range), which is determined by its chemical structure. In this particular area, the surfactant shows the strongest surface activity and therefore the highest ability to function as emulsifier and thus provides the most stable emulsions. In case of the investigated surfactants (Figure 2b), the results indicate that the optimal operation temperature of the corresponding MES increases with increasing EO number (or rather hydrophilicity).

3.2. Hydroformylation of 1-Dodecene. The rhodium-catalyzed hydroformylation of 1-dodecene in microemulsion systems (Figure 3) has been investigated by our working group for several years by now.^{15,19,20} In previous experiments, we found the aliphatic surfactants from the Marlipal series to provide good results as emulsifier for this reaction. By the application of the surfactant Marlipal 24/70, 31.3% yield of aldehyde (98% linear product) has been obtained after 4 h reaction time under optimized reaction conditions: α = 0.5, γ =

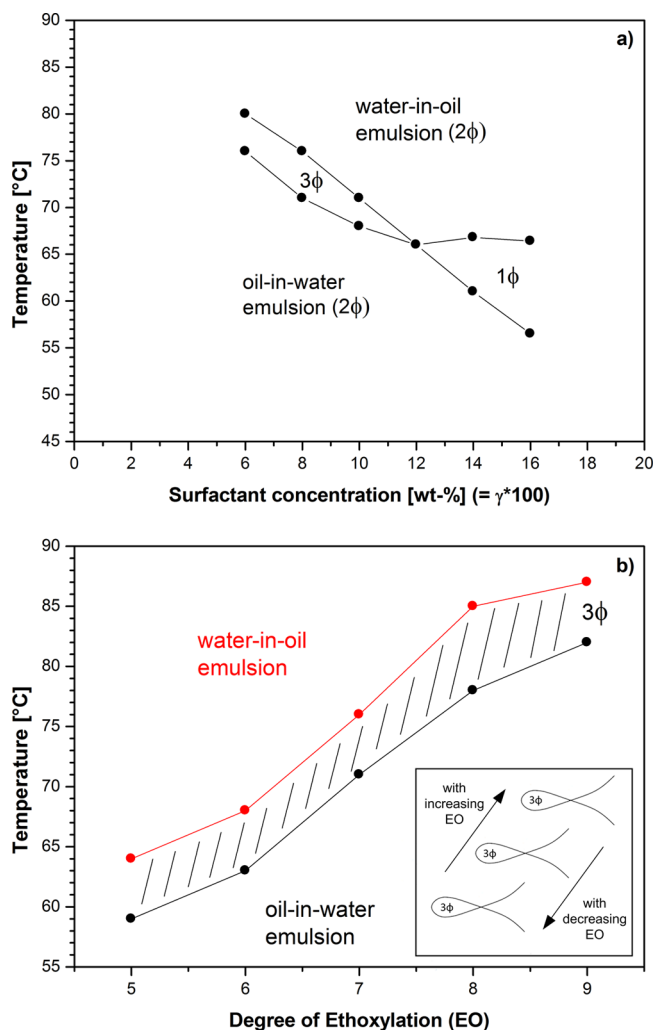


Figure 2. (a) Phase diagram of 1-dodecene/water/Marlipal(24/70) for α = 0.5 with 1.0 wt % Na_2SO_4 , 0.04 mol % $[\text{Rh}(\text{acac})(\text{CO})_2]$, and 0.16 mol % SulfoXantphos. (b) Temperature shift of the three-phase area as a function of degree of ethoxylation with 1-dodecene/water/Marlipal(24/50–90) for α = 0.5 and γ = 0.08 with 1.0 wt % Na_2SO_4 , 0.04 mol % $[\text{Rh}(\text{acac})(\text{CO})_2]$, and 0.16 mol % SulfoXantphos.

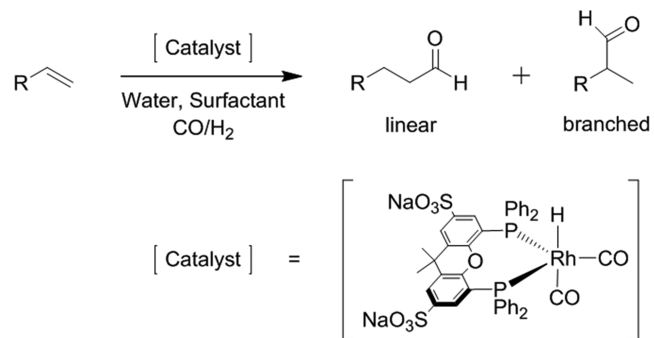


Figure 3. Hydroformylation reaction in microemulsion systems and the applied rhodium catalyst.

0.08, 95 °C reaction temperature, 15 bar syngas pressure, 1200 rpm stirring speed, and 1:4 metal-to-ligand ratio. The applied catalyst remains stable during the entire reaction time, and no sign of catalyst degradation can be observed. Recycling of the catalyst within the aqueous phase is easily possible by temperature-induced phase separation with a very low leaching

of Rh (<1 ppm) into the organic phase.^{21,22} The successful transition of the reaction system into an integrated process on a mini-plant scale has been reported recently.¹⁶

3.3. Effect of Salt Addition. Preceding the discussion of general effects of surfactants in hydroformylation, we would like to explain the use of Na_2SO_4 in the reaction mixture. The decision to add a salt to the reaction system originates from observations during the first continuous operation of the process (integrated reaction and separation) on miniplant scale, in which almost no phase separation of the reaction mixture could be achieved. This finding was in strong disagreement to the lab scale results where the separation of the system has always been achievable. In consequence, a systematic analysis of the separation dynamics of the reaction mixture was performed in a temperature and pressure controlled glass reactor with a gas dispersion stirrer to ensure realistic process conditions during the experiments. The experimental setup and procedure has already been reported in ref 23. In Figure 4 is illustrated the

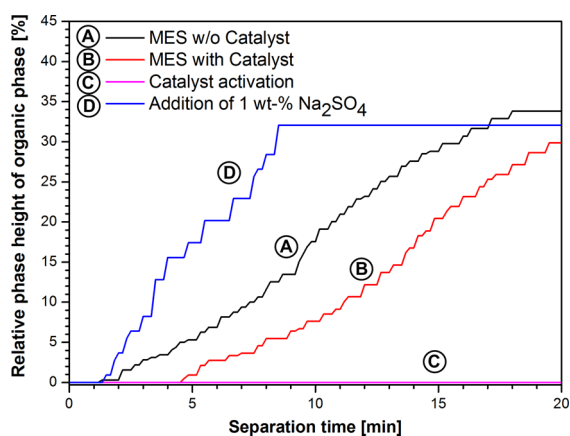


Figure 4. Relative height of organic (product) phase over separation time under process conditions. All experiments were performed at 85 °C and 10 bar pressure of argon (for A+B) or 10 bar pressure of syngas (C+D). MES was formulated from 1-dodecene, water, and Marlupal 24/70 ($\alpha = 0.5$, $\gamma = 0.08$). Additionally, 0.04 mol % $[\text{Rh}(\text{acac})(\text{CO})_2]$ and 0.16 mol % SulfoXantphos were added for B, C, and D.

evolution of the organic phase during the phase separation for the four crucial experiments of the screening. It becomes apparent that the activation of the rhodium catalyst with syngas inhibits the separation of the reaction system drastically. The separation time of the system increased from 18 min for the pure MES (Figure 4A) to around 25 min after the addition of catalyst (Figure 4B) and in the end to over several hours after the addition of syngas (Figure 4C). Moreover, it has to be noted that a complete separation of the reaction mixture under these conditions could not be observed. The surface activity of the applied catalyst complex has been observed only recently during parameter studies in lab scale.¹⁵ However, such a strong impact of the catalyst on the phase separation was not to be expected and has not been reported before in the literature for other MES. To overcome this undesirable effect for the continuous operation, the reaction mixture has been modified by the addition of 1.0 wt % Na_2SO_4 . With this adjustment of the ionic strength in the aqueous part of the reaction mixture, the effect of the catalyst complex as an ionic, surface active substance could be mostly suppressed by electrostatic screening. As a result, the separation dynamic of the system was

significantly improved, and thus the separation time decreased to roughly 8 min (Figure 4D).

Subsequent to these findings, we investigated the effect of the addition of Na_2SO_4 on the reactivity and stability of the catalyst during hydroformylation reaction. For this purpose, the reaction was performed with varying concentrations of Na_2SO_4 . The experimental results are shown in Figure 5. In

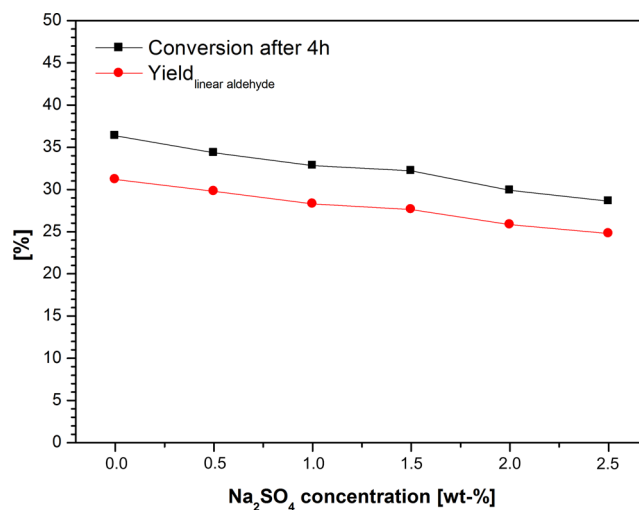


Figure 5. Effect of Na_2SO_4 concentration on hydroformylation reaction. Test conditions: 0.04 mol % $\text{Rh}(\text{acac})(\text{CO})_2$, 0.16 mol % SulfoXantphos, 120 mmol of 1-dodecene, water ($\alpha = 0.5$), $\gamma = 0.08$ (Marlipal 24/70), $V_R = 50$ mL, $T = 95$ °C, $p = 15$ bar, stirring speed = 1200 rpm, $t_R = 4$ h. Statistic deviation of results: $\pm 3\%$.

general, the reaction rate decreased with increasing amount of salt. The yield of linear aldehyde was reduced by roughly 1.2% per 0.5 wt % Na_2SO_4 as compared to the reaction without salt after 4 h reaction time (31.3% yield). For 1.0 wt % Na_2SO_4 in the system, a yield of 28.9% could be obtained. The most likely explanation for these results is an increasing destabilization of the MES with higher amounts of salt, which leads to larger emulsion droplets and consequently to a smaller interface for the reaction. Apart from the reactivity, the selectivity of the reaction remained unchanged at a high 98:2 ratio of linear to branched aldehydes, which proves the stability of the catalyst in the modified reaction mixture. The catalyst stability has also been tested in long-term experiments over 48 h with no sign of catalyst degradation. Concluding the results for separation and reaction, the application of Na_2SO_4 is a feasible method to enable the phase separation of the reaction mixture under process conditions with only minor implications on catalysis. Thus, we decided to apply the salt in the reaction mixture for all following experiments, including the experiments presented in Figure 2.

3.4. Effect of Temperature and Phase Behavior. The hydroformylation of 1-dodecene was carried out at different temperatures between 68 and 120 °C. In general, the formation of the linear aldehyde could be increased by using higher temperatures (see Figure 6). Until 110 °C the reaction rate increased exponentially with the temperature and indicated a simple Arrhenius behavior. After 1 h reaction time, a TOF of 50 h^{-1} was achieved at 68 °C, which could be raised to 380 h^{-1} at 110 °C, while the selectivity toward the linear product remained at a very high value of 98%. As was recently reported in ref 24, an activation energy of 59 kJ/mol could be calculated

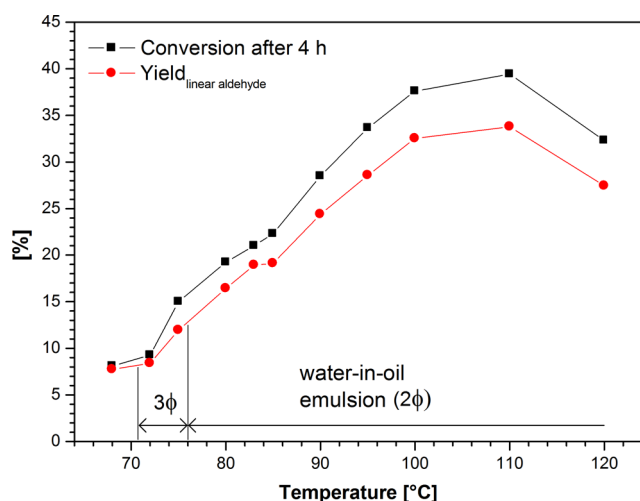


Figure 6. Effect of temperature on hydroformylation reaction. Test conditions: 0.04 mol % $\text{Rh}(\text{acac})(\text{CO})_2$, 0.16 mol % SulfoXantphos, 120 mmol of 1-dodecene, water ($\alpha = 0.5$), $\gamma = 0.08$ (Marlipal 24/70), 1 wt % Na_2SO_4 , $V_R = 50$ mL, $p = 15$ bar, stirring speed = 1200 rpm, $t_R = 4$ h. Statistic deviation of results: $\pm 3\%$.

for the hydroformylation, which is in good accordance with literature data collected for the applied catalyst in single phase systems.²⁵ However, a decrease of reaction rate could be observed at temperatures higher than 110 °C, which is related to the applied surfactant. Regarding the phase behavior of the reaction mixture (shown in Figure 2a and also indicated in Figure 6), the optimal working area of Marlipal 24/70 as emulsifier is in the range of 70–80 °C. The application at far higher temperatures leads to a destabilization of the microemulsion system because the ability of the surfactant to work as an emulsifier is constantly decreasing with increasing temperature. In consequence, the droplet size of the emulsion increases, which leads to a smaller interfacial area and thus rising mass transfer limitations of the reaction.

Interestingly, the phase behavior of the microemulsion system has no noticeable influence on the reaction. The MES underwent two phase transitions between 68 and 82 °C that completely changed the type of microemulsion (oil-in-water (2ϕ) \rightarrow bicontinuous (3ϕ) \rightarrow water-in-oil (2ϕ)). However, these changes of the emulsion type did not lead to an abrupt alteration of the reaction rate that would indicate a major change of mass transfer conditions. To further investigate this matter, an experiment was performed in which the reaction was carried out in each of the three microemulsion types at a constant temperature of 85 °C and constant values of α and γ . Therefore, the phase behavior of the MES was adjusted by different amounts of Na_2SO_4 in the mixtures. The results of this experiment are depicted in Figure 7. The reaction was performed with nearly similar rates for the oil-in-water (o/w) and the bicontinuous emulsion resulting in a conversion of roughly 24% and 25% after 4 h reaction time, respectively. As expected, the hydroformylation in the water-in-oil (w/o) emulsion was slightly slower due to the higher amount of salt in the mixture (compare with Figure 5). The results of this experiment confirm that the phase behavior of MES has no significant influence on the reaction rate of the hydroformylation due to the kinetic control of the reaction. This finding however is in clear contradiction to the conclusions from earlier works of Rost et al.²⁰ and Hamerla et al.¹⁹ in which the hydroformylation of 1-dodecene in MES was found to

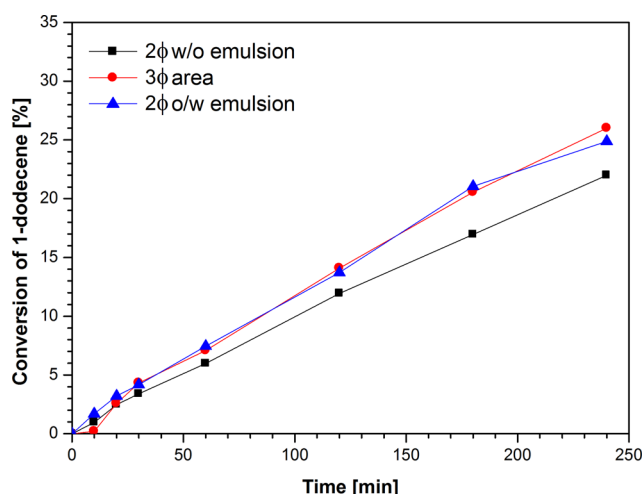


Figure 7. Effect of phase behavior on hydroformylation reaction. Test conditions: 0.04 mol % $\text{Rh}(\text{acac})(\text{CO})_2$, 0.16 mol % SulfoXantphos, 120 mmol of 1-dodecene, water ($\alpha = 0.5$), $\gamma = 0.08$ (Marlipal 24/90), $V_R = 50$ mL, $T = 85$ °C, $p = 15$ bar, stirring speed = 1200 rpm, $t_R = 4$ h. Amount of Na_2SO_4 : 0.1 wt % for 2ϕ o/w emulsion, 1.0 wt % for 3ϕ area, 3.0 wt % for 2ϕ w/o emulsion. Statistic deviation of results: $\pm 3\%$.

perform the fastest inside the 3ϕ area. The experiments that led the authors to their conclusion at that time were very similar to that from Figure 7 in this contribution. However, the main and very important difference between the earlier experiments and the one presented here is that they did adjust the phase behavior of their MES by changing the applied type of surfactant. Unfortunately, that was not the appropriate approach to perform this particular experiment. Although all of the received experimental data were correct, the interpretation was mistaken because they did mainly observe the influence of the chemical structure and chain length of the applied surfactants on the reaction rate of the hydroformylation and not the influence of the phase behavior. As we recently reported in ref 26, the constitution of the surfactant can have a relatively strong impact on reactions in MES. For instance, different functional groups of the surfactant can interact with the catalyst during catalysis and inhibit the reaction rate. In addition, the hydrophilicity (chain length, degree of ethoxylation) of the surfactant influences the reaction rate as well. This matter will be further discussed in the following section.

3.5. Degree of Ethoxylation. To investigate the influence of the surfactant chain length on the hydroformylation reaction, we varied the degree of ethoxylation (EO) from 5 to 9 (Marlipal 24/50 to 24/90). It was found that the reaction rate and EO number are in linear dependency at a constant reaction temperature; see Figure 8. However, it depends on the applied temperature whether it is a linear decrease or increase of the rate with increasing EO number. As explained in section 3.1, this is mainly due to the specific ability of the applied surfactants to work as emulsifiers for the reaction system, which changes with temperature. During the investigation on phase behavior in Figure 2b, it became evident that a higher EO number equals a higher temperature required for the surfactants to work efficiently. This characteristic is reflected in Figure 8 and gives an explanation why the reaction performs best at 80 °C with the short chained Marlipal 24/50, while at 95 °C the longest chained surfactant Marlipal 24/90 is clearly superior. Also, the higher density of the surfactant film with an increasing EO might enhance the adsorption of reactants at the

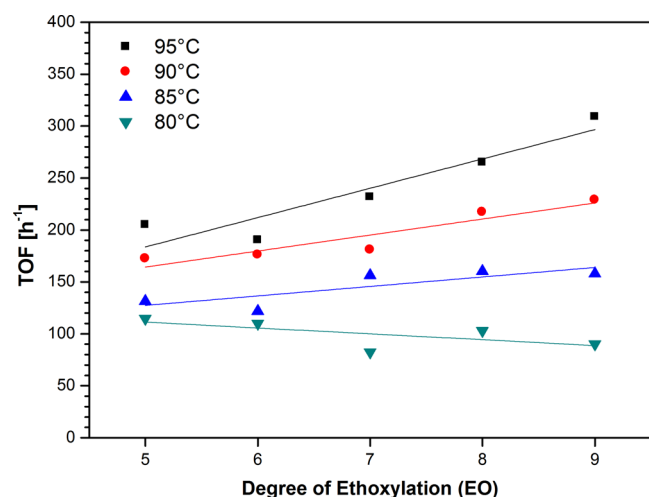


Figure 8. Degree of ethoxylation versus TOF for different reaction temperatures. Test conditions: 0.04 mol % Rh(acac)(CO)₂, 0.16 mol % SulfoXantphos, 120 mmol of 1-dodecene, water ($\alpha = 0.5$), $\gamma = 0.08$ (Marlipal 24 series), 1 wt % Na₂SO₄, $V_R = 50$ mL, $p = 15$ bar, stirring speed = 1200 rpm, $t_R = 1$ h. Statistic deviation of results: $\pm 3\%$.

oil–water interface and by that increase the reaction rate. Furthermore, it should be mentioned that the temperature dependency of the reaction for each applied surfactant confirms the findings in Figure 6. For better comparability, we listed the experimental results for a reaction temperature of 95 °C in Table 1. For Marlipal 24/50, an aldehyde yield of 25% was achieved after 4 h reaction time with a very high selectivity of 99% toward the linear product. By changing the EO number of the surfactant to 9 (Marlipal 24/90), the yield could be increased to 38%. To show that this is a general characteristic of these systems, we added the experimental results of a different

Table 1. Results for the Hydroformylation of 1-Dodecene with Different Surfactants at Constant Temperature^a

no.	surfactant	conversion 1-dodecene [%]	yield (linear aldehyde) [%]	n:iso selectivity
1	Marlipal 24/50	28	25	99:1
2	Marlipal 24/60	25	24	98:2
3	Marlipal 24/70	34	29	98:2
4	Marlipal 24/80	38	33	98:2
5	Marlipal 24/90	43	38	98:2
6	Marlophen NPS ^b	4	4	99:1
7	Marlophen NP6 ^b	8	6	99:1
8	Marlophen NP7 ^b	10	9	98:2
9	Marlophen NP9 ^b	15	13	98:2

^aReaction conditions [1–5]: 0.04 mol % Rh(acac)(CO)₂, 0.16 mol % SulfoXantphos, 120 mmol of 1-dodecene, water ($\alpha = 0.5$), $\gamma = 0.08$, 1 wt % Na₂SO₄, $V_R = 50$ mL, $T = 95$ °C, $p = 15$ bar, stirring speed = 1200 rpm, $t_R = 4$ h. Statistic deviation of results: $\pm 3\%$. Reaction conditions [6–9]: 0.05 mol % Rh(acac)(CO)₂, 0.25 mol % SulfoXantphos, 180 mmol of 1-dodecene, water ($\alpha = 0.88$), $\gamma = 0.10$, $V_R = 50$ mL, $T = 110$ °C, $p = 40$ bar, stirring speed = 1000 rpm, $t_R = 4$ h. ^bData extracted from ref 26.

type of nonionic surfactant to Table 1. The surfactants from the Marlophen NP series contain an aromatic ring in their hydrophobic part instead of a solely aliphatic chain like in the Marlipal series. It is evident that the dependency of reaction rate and EO is similar for both types of surfactants. However, it is an interesting observation that the different structure of the Marlophen surfactants turned out to be not beneficial for the rate of the hydroformylation. We assume that the aromatic ring of the surfactant hinders the catalytic reaction, most probably through electronic interactions with the catalyst at the oil–water interface.⁵ This leads to much lower aldehyde yields after 4 h reaction time as compared to Marlipal under mostly comparable reaction conditions.

3.6. Effect of Surfactant Concentration. The hydroformylation of 1-dodecene was carried out at different surfactant concentrations at a constant reaction temperature of 95 °C. In general, it was found that a higher concentration of surfactant leads to an increase in aldehyde yield after the same reaction time (see Figure 9). The yield increased from roughly

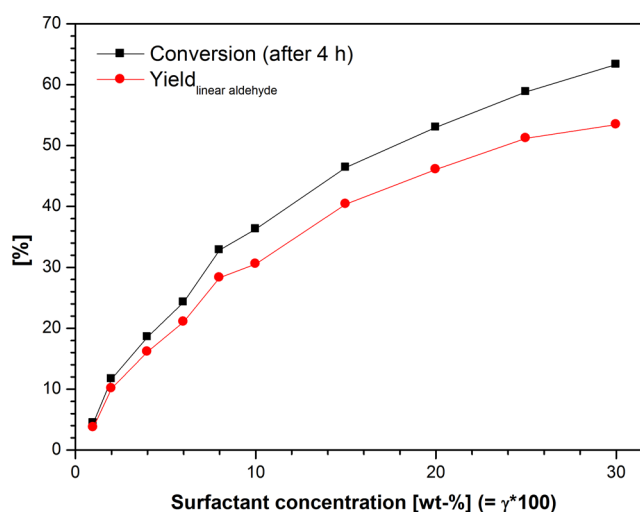


Figure 9. Effect of surfactant concentration on hydroformylation reaction. Test conditions: 0.04 mol % Rh(acac)(CO)₂, 0.16 mol % SulfoXantphos, 120 mmol of 1-dodecene, water ($\alpha = 0.5$), Marlipal 24/70, 1 wt % Na₂SO₄, $V_R = 50$ mL, $T = 95$ °C, $p = 15$ bar, stirring speed = 1200 rpm, $t_R = 4$ h. Statistic deviation of results: $\pm 3\%$.

4% with 1 wt % surfactant in the mixture to 53% with 30 wt % surfactant. The selectivity toward the linear product remained unchanged at a value of 98% in all experiments. In the case where no surfactant was applied in the mixture, no reaction progress could be observed during 4 h reaction time, confirming that the surfactant is needed to enable the hydroformylation. It stands out that the rate of the reaction continues to increase with the surfactant concentration (illustrated in Figure 10) even after the MES already became a macroscopic one-phase microemulsion (for $\gamma > 0.12$). Considering the biphasic character of the system at $\gamma < 0.12$, more surfactant in the mixture generally means a larger interfacial area for the reaction and thus a higher potential reaction rate. In addition, the reaction rate is not affected by mass transfer limitation, which has been experimentally verified (see Figure 11). However, the significant further increase of the reaction rate at higher surfactant concentration cannot be solely addressed to the larger interfacial area, because all of the reactants are already located in one emulsion phase. Thus, this

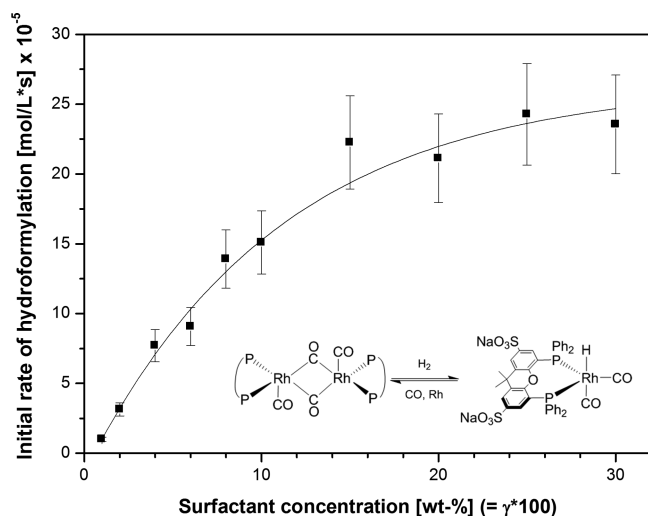


Figure 10. Effect of surfactant concentration on the rate of hydroformylation. Test conditions: 0.04 mol % Rh(acac)(CO)₂, 0.16 mol % SulfoXantphos, 120 mmol of 1-dodecene, water ($\alpha = 0.5$), Marlupal 24/70, 1 wt % Na₂SO₄, $V_R = 50$ mL, $T = 95$ °C, $p = 15$ bar, stirring speed = 1200 rpm, $t_R = 4$ h. Initial rates were calculated from syngas consumption. Statistic deviation of results: $\pm 15\%$.

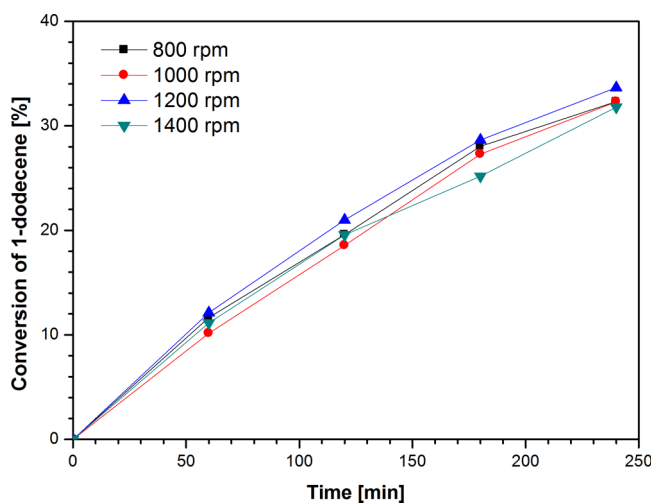


Figure 11. Effect of stirring speed on hydroformylation reaction. Test conditions: 0.04 mol % Rh(acac)(CO)₂, 0.16 mol % SulfoXantphos, 120 mmol of 1-dodecene, water ($\alpha = 0.5$), $\gamma = 0.08$ Marlupal 24/70, 1 wt % Na₂SO₄, $V_R = 50$ mL, $T = 95$ °C, $p = 15$ bar, $t_R = 4$ h. Statistic deviation of results: $\pm 3\%$.

finding could be explained by a change in the local catalyst concentration at the oil–water interface. It has to be clarified first, that while the interfacial area of the reaction system (corresponding to the volume of the emulsion phase) is increasing with the surfactant concentration, the total amount of catalyst in the system remains constant. This means that the catalyst, which is located at the interface within the emulsion phase due to its surface activity, should be more diluted when the volume of this particular phase is increased. In consequence, the local catalyst concentration in the emulsion phase should decrease with increasing surfactant concentration. It is already known that rhodium catalysts with bidentate phosphine ligands, in particular the here applied rhodium sulfoxantphos catalyst, are able to form inactive dimeric catalyst species.^{19,27} Because the equilibrium between monomer and

dimer is influenced by the concentration of catalyst (see drawing in Figure 10), a decrease of the local catalyst concentration in the emulsion phase should lead to a higher amount of the monomeric species and thus to a higher reaction rate. This would also give an explanation for the diminishing increase of the reaction rate at higher surfactant concentrations, because the equilibrium should be already strongly shifted to the monomer.

At last, it has to be mentioned that a too high concentration of surfactant in the MES bears a major drawback considering catalyst recycling. To maintain a good and fast switchability of the MES and, by that, enable an easy catalyst recycling, it is necessary to work with surfactant concentrations that do not exceed the 3 ϕ area (fish body) in the phase diagram. The 3 ϕ area is the most feasible state of the MES for catalyst recycling, because the phase separation performs here the fastest and most of the catalyst is located in the middle phase of the system together with the surfactant.²¹ Higher surfactant concentrations would make it necessary to separate the system in one of the 2 ϕ systems, which would lead to longer separation times and higher potential losses of surfactant and catalyst into the product phase. Considering these points, the surfactant concentration of the investigated MES in Figure 9 should not exceed 12 wt % ($\gamma = 0.12$, compare with Figure 2a) to be applicable in an integrated chemical process.

4. CONCLUSION

The performed experiments demonstrated that catalysis in microemulsion systems can be affected by several parameters, with the applied surfactant in a major role. To summarize this newly gained knowledge, Figure 12 schematically illustrates the

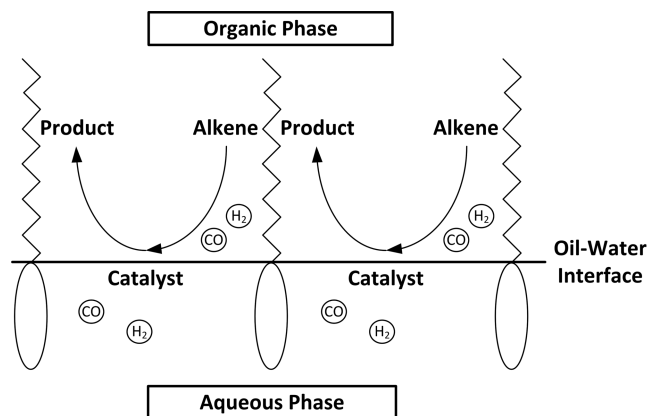


Figure 12. Schematic illustration of two-phase catalysis in micro-emulsions systems on the example of the hydroformylation reaction.

impact of the MES on the catalytic reaction. We assume that the catalyst complex is mainly located at the oil–water interface due to its surface activity. Consequently, the reaction should mainly take place at the interface as well. Regarding the temperature dependency of the investigated reaction (Figure 6), it seems likely to assume that the hydroformylation of long-chain alkenes in MES is a kinetically controlled two-phase reaction. With that, the role of the surfactant in these multiphase systems is of utmost importance. In its function as emulsifier, the surfactant determines the stability of the MES and the local concentrations at the oil–water interface, which are both important requirements for catalysis in MES (Figure 8). In addition, the surfactant provides the interfacial area for

the reaction and in consequence can also interact with the catalyst because both are in immediate vicinity to each other at the interface. Thus, it is possible that the catalytic reaction might be hindered by the surfactant due to electronic interactions with the catalyst (Table 1). All aspects considered, these findings point out the good applicability of MES as switchable reaction media in homogeneous catalysis and their high optimization potential for any given application by the choice of a proper surfactant.

AUTHOR INFORMATION

Corresponding Author

*E-mail: tobias.pogrzeba@tu-berlin.de.

ORCID

Tobias Pogrzeba: 0000-0003-3727-9589

Notes

The authors declare no competing financial interest.

ACKNOWLEDGMENTS

This work is part of the Collaborative Research Center/Transregio 63 "Integrated Chemical Processes in Liquid Multiphase Systems" (subprojects A2 and B4). Financial support by the Deutsche Forschungsgemeinschaft (DFG, German Research Foundation) is gratefully acknowledged (TRR 63). Furthermore, we gratefully acknowledge the support of the company Umicore for sponsoring the rhodium catalyst acetylacetonato-dicarbonylrhodium(I) (CAS: 14874-82-9).

ABBREVIATIONS

2 ϕ = two phase

3 ϕ = three phase

EO = degree of ethoxylation

MES = microemulsion system

SX = SulfoXantphos, 4,5-bis(diphenylphosphino)-9,9-dimethylxanthene

TOF = turnover frequency

REFERENCES

- (1) Lipshutz, B. H.; Gallou, F.; Handa, S. Evolution of Solvents in Organic Chemistry. *ACS Sustainable Chem. Eng.* **2016**, *4*, 5838.
- (2) Dwars, T.; Paetzold, E.; Oehme, G. Reactions in Micellar Systems. *Angew. Chem., Int. Ed.* **2005**, *44*, 7174.
- (3) Lipshutz, B. H.; Taft, B. R. Heck Couplings at Room Temperature in Nanometer Aqueous Micelles. *Org. Lett.* **2008**, *10* (7), 1329.
- (4) Lipshutz, B. H.; Ghorai, S.; Abela, A. R.; Moser, R.; Nishikata, T.; Duplais, C.; Krasovskiy, A.; Gaston, R. D.; Gadwood, R. C. TPGS-750-M: A Second-Generation Amphiphile for Metal-Catalyzed Cross-Couplings in Water at Room Temperature. *J. Org. Chem.* **2011**, *76* (11), 4379.
- (5) Schwarze, M.; Milano-Brusco, J. S.; Stempel, V.; Hamerla, T.; Wille, S.; Fischer, C.; Baumann, W.; Arlt, W.; Schomäcker, R. Rhodium Catalyzed Hydrogenation Reactions in Aqueous Micellar Systems as Green Solvents. *RSC Adv.* **2011**, *1* (3), 474.
- (6) La Sorella, G.; Strukul, G.; Scarso, A. Recent Advances in Catalysis in Micellar Media. *Green Chem.* **2015**, *17*, 644.
- (7) Dwars, T.; Haberland, J.; Grassert, I.; Oehme, G.; Kragl, U. Asymmetric Hydrogenation in a Membrane Reactor: Recycling of the Chiral Catalyst by Using a Retainable Micellar System. *J. Mol. Catal. A: Chem.* **2001**, *168* (1–2), 81.
- (8) Schwarze, M.; Schmidt, M.; Nguyen, L. A. T.; Drews, A.; Kraume, M.; Schomäcker, R. Micellar Enhanced Ultrafiltration of a Rhodium Catalyst. *J. Membr. Sci.* **2012**, *421–422*, 165.
- (9) Winsor, P. A. Hydrotrophy, Solubilisation and Related Emulsification Processes. Part I. *Trans. Faraday Soc.* **1948**, *44*, 376.
- (10) Kahlweit, M.; Strey, R.; Busse, G. Microemulsions: A Qualitative Thermodynamic Approach. *J. Phys. Chem.* **1990**, *94*, 3881.
- (11) Schwarze, M.; Pogrzeba, T.; Volovych, I.; Schomäcker, R. Microemulsion Systems for Catalytic Reactions and Processes. *Catal. Sci. Technol.* **2015**, *5*, 24.
- (12) Nowothnick, H.; Blum, J.; Schomäcker, R. Suzuki Coupling Reactions in Three-Phase Microemulsions. *Angew. Chem., Int. Ed.* **2011**, *50*, 1918.
- (13) Volovych, I.; Kasaka, Y.; Schwarze, M.; Nairoukh, Z.; Blum, J.; Fanun, M.; Avnir, D.; Schomäcker, R. Investigation of Sol–gel Supported Palladium Catalysts for Heck Coupling Reactions in O/w-Microemulsions. *J. Mol. Catal. A: Chem.* **2014**, *393*, 210.
- (14) Volovych, I.; Neumann, M.; Schmidt, M.; Buchner, G.; Yang, J.-Y.; Wölk, J.; Sottmann, T.; Strey, R.; Schomäcker, R.; Schwarze, M. A Novel Process Concept for the Three Step Boscalid® Synthesis. *RSC Adv.* **2016**, *6*, 58279.
- (15) Pogrzeba, T.; Müller, D.; Hamerla, T.; Esche, E.; Paul, N.; Wozny, G.; Schomäcker, R. Rhodium-Catalyzed Hydroformylation of Long-Chain Olefins in Aqueous Multiphase Systems in a Continuously Operated Miniplant. *Ind. Eng. Chem. Res.* **2015**, *54*, 11953.
- (16) Illner, M.; Müller, D.; Esche, E.; Pogrzeba, T.; Schmidt, M.; Schomäcker, R.; Wozny, G.; Repke, J.-U. Hydroformylation in Microemulsions: Proof of Concept in a Miniplant. *Ind. Eng. Chem. Res.* **2016**, *55*, 8616.
- (17) Goedheijt, M. S.; Kamer, P. C. J.; Leeuwen, P. W. N. M.; Van, A. Water-Soluble Diphosphine Ligand with a Large "Natural" Bite Angle for Two-Phase Hydroformylation of Alkenes. *J. Mol. Catal. A: Chem.* **1998**, *134*, 243.
- (18) Kasaka, Y.; Bibouche, B.; Volovych, I.; Schwarze, M.; Schomäcker, R. Investigation of Phase Behaviour of Selected Chemical Reaction Mixtures in Microemulsions for Technical Applications. *Colloids Surf., A* **2016**, *494*, 49.
- (19) Hamerla, T.; Rost, A.; Kasaka, Y.; Schomäcker, R. Hydroformylation of 1-Dodecene with Water-Soluble Rhodium Catalysts with Bidentate Ligands in Multiphase Systems. *ChemCatChem* **2013**, *5*, 1854.
- (20) Rost, A.; Müller, M.; Hamerla, T.; Kasaka, Y.; Wozny, G.; Schomäcker, R. Development of a Continuous Process for the Hydroformylation of Long-Chain Olefins in Aqueous Multiphase Systems. *Chem. Eng. Process.* **2013**, *67*, 130.
- (21) Pogrzeba, T.; Müller, D.; Illner, M.; Schmidt, M.; Kasaka, Y.; Weber, A.; Wozny, G.; Schomäcker, R.; Schwarze, M. Superior Catalyst Recycling in Surfactant Based Multiphase Systems – Quo Vadis Catalyst Complex? *Chem. Eng. Process.* **2016**, *99*, 155.
- (22) Nowothnick, H.; Rost, A.; Hamerla, T.; Schomäcker, R.; Müller, C.; Vogt, D. Comparison of Phase Transfer Agents in the Aqueous Biphasic Hydroformylation of Higher Alkenes. *Catal. Sci. Technol.* **2013**, *3* (3), 600.
- (23) Müller, D.; Esche, E.; Pogrzeba, T.; Illner, M.; Leube, F.; Schomäcker, R.; Wozny, G. Systematic Phase Separation Analysis of Surfactant Containing Systems for Multiphase Settler Design. *Ind. Eng. Chem. Res.* **2015**, *54*, 3205.
- (24) Pogrzeba, T.; Illner, M.; Schmidt, M.; Repke, J.-U.; Schomäcker, R. Microemulsion Systems as Switchable Reaction Media for the Catalytic Upgrading of Long-Chain Alkenes. *Chem. Ing. Tech.* **2017**, *89* (4), 459.
- (25) Bhanage, B. M.; Divekar, S. S.; Deshpande, R. M.; Chaudhari, R. V. Kinetics of Hydroformylation of 1-Dodecene Using Homogeneous HRh(CO)(PPh₃)₃ Catalyst. *J. Mol. Catal. A: Chem.* **1997**, *115*, 247.
- (26) Schwarze, M.; Pogrzeba, T.; Seifert, K.; Hamerla, T.; Schomäcker, R. Recent Developments in Hydrogenation and Hydroformylation in Surfactant Systems. *Catal. Today* **2015**, *247*, 55.
- (27) Deshpande, R. M.; Kelkar, A. A.; Sharma, A.; Julcour-lebigue, C.; Delmas, H. Kinetics of Hydroformylation of 1-Octene in Ionic Liquid-Organic Biphasic Media Using Rhodium Sulfoxantphos Catalyst. *Chem. Eng. Sci.* **2011**, *66*, 1631.

PAPER 10

(manuscript only)

Kinetics of Hydroformylation of 1-Dodecene in Microemulsion Systems using Rhodium Sulfoxantphos Catalyst

Tobias Pogrzeba, Markus Illner, Marcel Schmidt, Natasa Milojevic, Jens-Uwe Repke, and Reinhard Schomäcker

Industrial & Engineering Chemistry Research, submitted Dec 2017

Kinetics of hydroformylation of 1-dodecene in microemulsion systems using rhodium sulfoxantphos catalyst

Tobias Pogrzeba^{,1}, Markus Illner², Marcel Schmidt¹, Natasa Milojevic¹, Jens-Uwe Repke², Reinhard Schomäcker¹*

¹ Department of Chemistry, Technische Universität Berlin, Straße des 17. Juni 124, Sekr. TC-8, D-10623 Berlin, Germany.

² Chair of Process Dynamics and Operation, Technische Universität Berlin, Straße des 17. Juni 135, Sekr. KWT-9, D-10623 Berlin, Germany.

**Email: tobias.pogrzeba@tu-berlin.de*

Abstract

The hydroformylation of 1-dodecene has been performed in microemulsions systems using rhodium sulfoxantphos as catalyst. Preliminary experiments proved these aqueous multiphase systems to enable the reaction with good yield and very high selectivity towards the linear aldehyde (about 60 % yield with n:iso ratio of 98:2 after 24 h reaction time). Catalyst recycling is easily possible by simple phase separation after the reaction, maintaining the activity and very high selectivity. The investigation of process parameters showed a first order dependence of the initial rate with respect to the 1-dodecene concentration, and a more complex behavior with respect to catalyst concentration and syngas pressure. Based on an earlier proposed mechanism and the gained experimental data an adapted kinetic model has been derived, including the unique influences of the regarded multiphase system on the reaction (in particular the surfactant concentration and ligand to metal ratio). The identified model formulation and parameter set for the reaction system enabled the calculation of reaction trajectories which are in good accordance to the observed trends from experimental data.

1. Introduction

After the industrial success of propylene hydroformylation catalyzed by the water-soluble $\text{HRh}(\text{CO})(\text{TPPTS})_3$ complex in the Ruhrchemie/Rhône-Poulenc process, aqueous biphasic reaction systems have opened a new perspective for homogeneous catalysis with transition metal complexes. However, the low water solubility of long chained substrates limited the scope of applications for water-soluble catalysts in biphasic catalysis. Often enough it is sufficient to employ a suitable surfactant or a micelle producing agent to solubilize the reactants in water and to enable the reaction. The so-called micellar enhanced catalysis offers the possibility to transfer the already established organic transition metal-catalyzed chemistry into the reaction medium water under very mild reaction conditions ¹⁻⁵. A very efficient approach to combine reaction and catalyst recycling in micellar systems is the utilization of microemulsion systems (MES) as switchable solvents ^{6,7}. The switchability of MES offers many interesting options for integrated chemical processes with industrial relevance in aqueous media, like Suzuki and Heck coupling reactions ^{8,9} or rhodium-catalyzed hydroformylation of long-chained alkenes ¹⁰⁻¹². The rhodium-catalyzed hydroformylation of 1-dodecene in microemulsion systems (Fig. 1) is being investigated by our working group for several years by now ^{10,13,14}. In these preliminary experiments we found the aliphatic surfactants from the Marlupal series provide good results as emulsifier for the applied reaction system. The results from a typical continuous hydroformylation experiment are illustrated in Fig. 2. The reaction performs highly selective due to the applied Rh-sulfoxantphos catalyst with an aldehyde yield of about 60 % (n:iso ratio of 98:2) after 24 h reaction time. The isomerization of 1-dodecene occurs very slowly, the amount of isododecenes in the mixture increases from 4 to 6 wt-% during reaction. The formation of side products is also insignificant with only 2 wt-% of hydrogenation product after 24 h. The catalyst remains stable during the entire reaction time and no sign of catalyst degradation can be observed. Recycling of the catalyst is easily possible by temperature induced phase separation with a very low leaching of Rh (< 1ppm) into the organic phase ^{7,15}. The successful transition of the reaction system into an integrated process on a mini-plant scale has been reported recently ^{11,12}.

Although alkene hydroformylation has been investigated in microemulsion systems for several years by now, no detailed study on the reaction kinetics has been reported yet.

However, it would be of great interest to investigate the influence of different process parameters on the activity and selectivity of the applied rhodium catalyst, in order to achieve a more precise model to describe the hydroformylation in a continuous process. An important question that has to be answered is in which points the kinetics of the reaction in aqueous micellar media differs from the reaction in homogeneous media. As we reported recently ¹⁶, the applied surfactant can have a strong impact on the results of a catalytic reaction. In case of the investigated hydroformylation it was found that an increase of surfactant concentration generally leads to an increase of the reaction rate. Interestingly, this increase in reaction rate cannot be solely addressed to a larger interfacial area of the microemulsion system due to a higher surfactant concentration. Since the applied Rh-sulfoxantphos catalyst is surface active itself, it should be mainly located at the oil-water interface of the microemulsion regardless of the size of the interfacial area. Thus, this finding could be explained by a change in the local catalyst concentration at the oil-water interface, which directly influences the activity of the catalyst. A “dilution” of catalyst at the interface should have an impact on several catalyst preequilibria leading to the formation of more active rhodium species under reaction conditions. As a consequence, the corresponding rate equation of the hydroformylation has to be modified according to these differences to enable the description of the catalytic reaction in microemulsion systems.

We herein report the detailed kinetics of the hydroformylation of 1-dodecene using a water-soluble Rh-sulfoxantphos catalyst in a microemulsion system, consisting of water, non-ionic surfactant Marlipal 24/70, and 1-dodecene as organic phase. In addition, the experimental kinetic information is used together with rate equations based on the mechanistic description for the homogeneous system by Kiedorf et al. ¹⁷ to conduct a parameter estimation for the microemulsion system. To account for influences of the emulsion system, additional concentration dependencies are implemented, to describe the reaction trajectory for the supposed system accordingly.

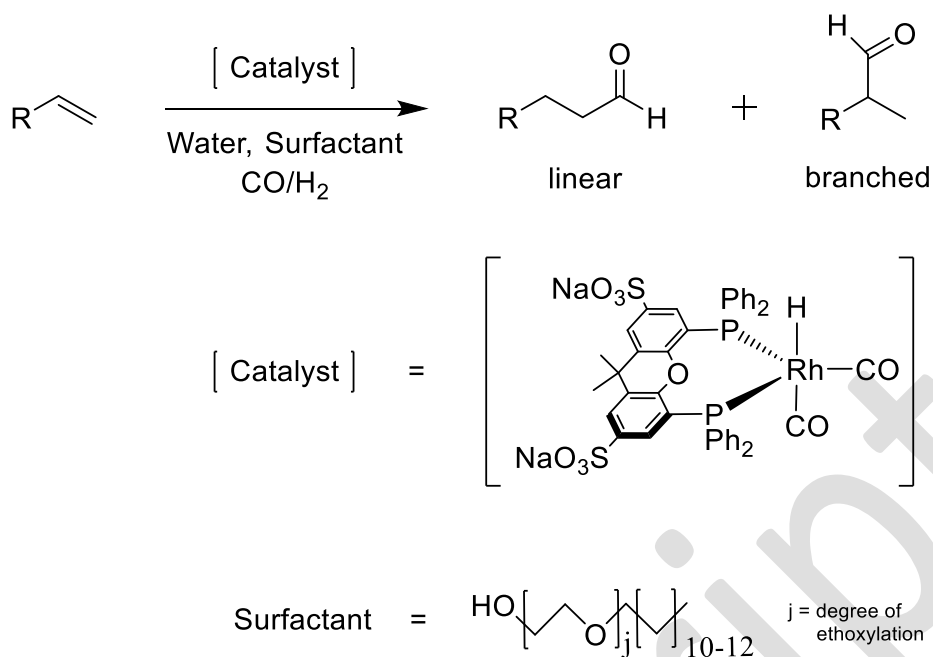


Fig. 1. Hydroformylation reaction in microemulsion systems, structure of the applied Rh-sulfoxantphos catalyst and structure of the non-ionic surfactant Marlipal 24/70 (with $j = 7$).

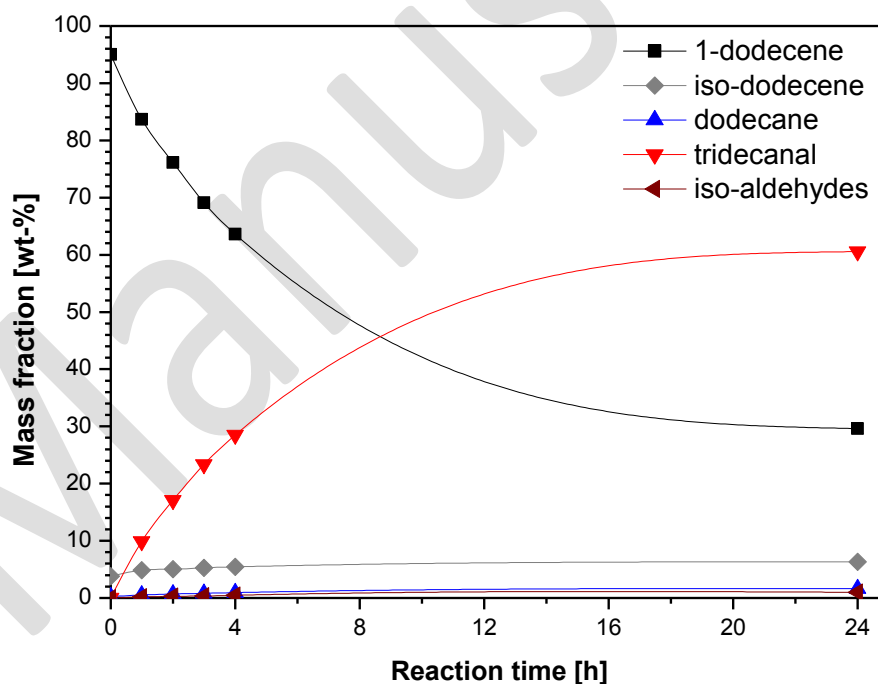


Fig. 2. Hydroformylation of 1-dodecene in a microemulsion system. Test conditions: $\text{Rh(acac)(CO)}_2 = 1.0 \times 10^{-3}$ mol/L, sulfoxantphos:Rh ratio=4:1 (P:Rh ratio=8:1), 1-dodecene= 2.4 mol/L, water=20 g ($\alpha = 0.5$), surfactant=3.5 g ($\gamma = 0.08$), 1 wt-% Na_2SO_4 , total liquid volume: 50 mL; $T = 95^\circ\text{C}$, $p = 15$ bar, stirring speed=1200 rpm, and reaction time: 24 h. Statistic deviation of results: $\pm 3\%$.

2. Materials and methods

2.1. Chemicals

The reactant 1-dodecene (95%) and the water (HPLC grade) were purchased from VWR. The precursor (acetylacetonato)dicarbonylrhodium(I) $\text{Rh}(\text{acac})(\text{CO})_2$ was contributed by Umicore, Germany. The water soluble ligand 2,7-Bissulfonate-4,5-bis(diphenylphosphino)-9,9-dimethylxanthene (sulfoxantphos, SX) was purchased from Molisa, where it was synthesized according to a procedure described by Goedheijt et al.¹⁸. The syngas (1:1 mixture of CO and H_2 , purity 2.1 for CO and 2.1 for H_2) was purchased from Air Liquide. The technical grade non-ionic surfactant Marlipal® 24/70 was contributed by Sasol. To adjust the ionic strength we used sodium sulfate (Na_2SO_4 , 99%) purchased from Merck. All the chemicals were used without further purification.

2.2. Preparation of catalyst solution

For the preparation of a typical experiment, $\text{Rh}(\text{acac})(\text{CO})_2$ and sulfoxantphos were mixed in the desired ratio (usually 1:4) in a Schlenk tube and inertized using Schlenk technique. The solvent (5 g degassed water, HPLC grade) was added through a septum. Then the catalyst solution was stirred over night at room temperature to ensure the formation of the catalyst complex.

2.3. Experimental set-up and procedure

The hydroformylation reactions are performed in a 100 mL stainless steel high-pressure vessel from Premex Reactor AG, equipped with a gas dispersion stirrer and mounted in an oil thermostat from Huber (K12-NR). The reactor setup has already been illustrated in previous contributions¹³. The typical reaction conditions for the hydroformylation were 15 bar pressure of syngas, an internal reactor temperature of 95°C, and a stirring speed of 1200 rpm. The important composition parameters to characterize the applied MES are the weight fractions of oil (α) and surfactant (γ) (Equation 1), which are calculated with the mass m of the corresponding component:

$$\alpha = \frac{m_{oil}}{m_{oil} + m_{H_2O}} \quad \gamma = \frac{m_{Surf}}{m_{oil} + m_{H_2O} + m_{Surf}} \quad (1)$$

The reaction mixture usually consisted of 2.4 mol/L (20 g) 1-dodecene, 20 g water ($\alpha=0.5$), 3.5 g Marlupal® 24/70 ($\gamma=0.08$), 61.4×10^{-3} mol/L (1 wt-%) Na_2SO_4 , 1.0×10^{-3} mol/L catalyst and sulfoxantphos:Rh ratio=4:1 (P:Rh ratio=8:1).

The reactions were performed as described in the following. At first the reactor was filled with the desired amounts of alkene, water, sodium sulfate, and surfactant. Then the catalyst solution was transferred with a syringe to the reactor. The reactor was closed and evacuated and purged with nitrogen for at least three times. The stirrer was started at a rate of 500 rpm and the reactor was heated up to the desired temperature. After reaching the temperature the stirring was slowed down (200-300 rpm) and the reactor was pressurized with syngas. Then the reaction was started by increasing the stirring speed again to 1200 rpm. For the evaluation of reaction progress, samples were withdrawn at several time intervals via a sampling valve and analyzed by gas chromatography (GC). To ensure homogeneous liquid sampling, the stirring speed was not changed, while the samples were taken from the reactor. No further purification steps were performed to isolate the product from the reaction mixture before the samples were measured via GC. In addition, consumption of syngas during the experiments has been recorded via the mass flow controller.

The important parameters (yield Y and TOF) for the evaluation of experimental data were calculated as shown in Equation 2 and 3, where n is the amount of substance, 1-dodecene is the substrate and 1-tridecanal is the product. The initial rates of hydroformylation were calculated from the consumption of syngas.

$$Y(t) = \frac{n_{t,Product}}{n_{t=0,Substrate}} \quad (2)$$

$$TOF_{Ald} = \frac{n_{t=0,Substrate} \cdot Y_{Ald}(t)}{n_{cat} \cdot t} \quad (3)$$

2.4. Analysis

Reaction progress and selectivity of hydroformylation reactions were analyzed by gas chromatography on a Shimadzu model GC-2010, equipped with a Supelcowax 10 capillary column, a flame ionization detection analyzer, and nitrogen as carrier gas.

Manuscript

3. Results and Discussion

3.1. Kinetic study of hydroformylation of 1-dodecene

There are only a few reports on the kinetics of alkene hydroformylation in microemulsion systems available although it has been investigated for several years by now. The main reason for this is that it requires a profound knowledge about the role of the surfactants during catalysis in these complex multiphase systems ¹⁶ to clearly isolate the effect of the reaction conditions on kinetics. In order to study the kinetics of a reaction, it is also important to ensure that the experiments are carried out under kinetic control. For that matter, a number of experiments at different stirring speed has been performed and showed that the rate of reaction was independent of the stirring speed beyond 800 rpm. This investigation was conducted under the following standard conditions: 2.4 mol/L (20 g) 1-dodecene, 20 g water ($\alpha = 0.5$), 3.5 g surfactant ($\gamma = 0.08$), 61.4×10^{-3} mol/L (1 wt-%) Na_2SO_4 , 1.0×10^{-3} mol/L catalyst and sulfoxantphos:Rh ratio=4:1 (P:Rh ratio=8:1), temperature of 95 °C, and p=15 bar. With the confirmation of kinetic regime, all further experiments were carried out at 1200 rpm in order to completely exclude mass transfer limitation. For a better understanding of the following kinetic studies, we would like to point out that all stated concentrations of 1-dodecene, catalyst, and sodium sulfate were calculated for the entire reaction volume. In addition, the surfactant concentration was kept constant at 8 wt-% ($\gamma = 0.08$) for all experiments in order to exclude the special influence of the surfactant on the reaction kinetics from the results of this study. As a final remark, the stated initial rates of hydroformylation were calculated from syngas consumption under the assumption that the high selectivity of the catalyst leads to a nearly exclusive formation of n-tridecanal and iso-aldehydes at the beginning of the reaction.

The effect of 1-dodecene concentration, catalyst concentration, ligand:Rh ratio, and syngas pressure on the initial rate of hydroformylation is shown in Fig. 4,6,8 and 9, respectively. The proposed mechanism for Rh-catalyzed hydroformylation using sulfoxantphos as a ligand in aqueous media is presented in Fig. 3 and based on the widely accepted work of Evans and Wilkinson ¹⁹. In addition, it is assumed in our case that $\text{Rh}(\text{CO})_2(\text{acac})$ reacts with sulfoxantphos in the presence of CO and H_2 to give principally species (1a) ²⁰, which is in equilibrium to the non-selective unmodified Rh-tetracarbonyl complex (1b) ²¹ and the catalytically inactive Rh-dimer (1c) ^{22,23} under reaction conditions. CO dissociation from

species (1a) gives the 16 valence electron Rh-complex (2). The interaction of alkene with (2) leads to an alkene coordinated species (3), which is converted to an alkyl species (4). Further steps in the catalytic cycle involve a dicarbonyl species (5), an acyl species (6a), the formation of the dihydrogen complex (7), and finally the reductive elimination of the aldehyde.

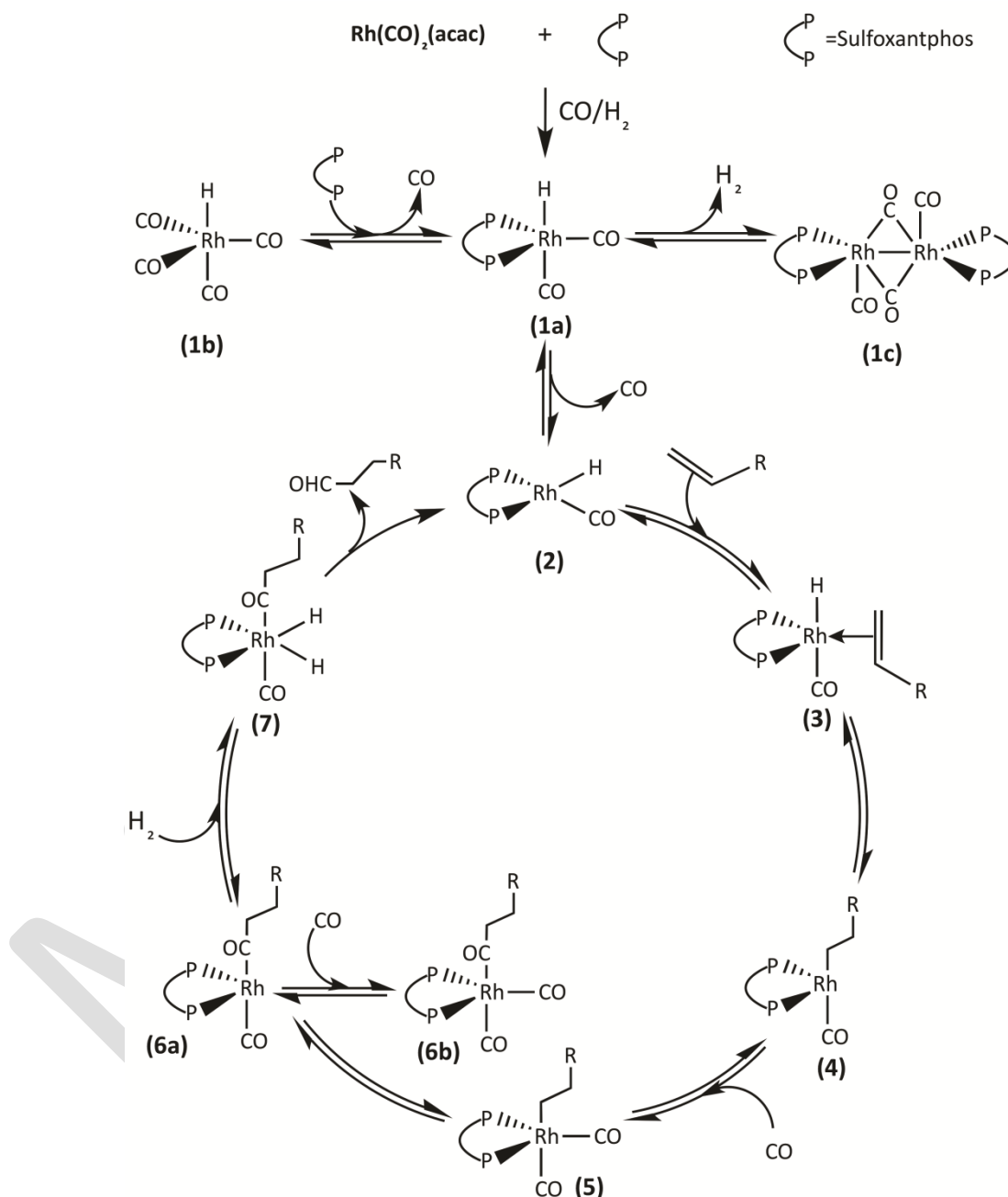


Fig. 3. Mechanism of rhodium-catalyzed hydroformylation of alkenes using a bidentate diphosphine ligand. For a clearer view only the path of n-selective hydroformylation is illustrated.

3.1.1. Effect of 1-dodecene concentration

The initial concentration of 1-dodecene in the reaction mixture was varied from 0.24 to 2.4 mol/L. In order to keep the mass of organic phase at a constant value of 20 g in every experiment, n-decane was additionally added to the mixture to compensate the missing amount of 1-dodecene in the microemulsion system. The other reaction conditions were kept constant. The results are presented in Fig. 4. The reaction rate was found to increase linearly with the 1-dodecene concentration, indicating a first order dependence. Due to the surface activity of the applied Rh-sulfoxantphos catalyst, the hydroformylation takes mainly place at the oil-water interface in the microemulsion system (see Fig. 5). Since 1-dodecene is not a strongly coordinating olefin, higher concentrations at the interface will be necessary to generate more of the olefin coordinated Rh complex (Fig. 3, species 3) and thus will lead to an enhancement in reaction rate.

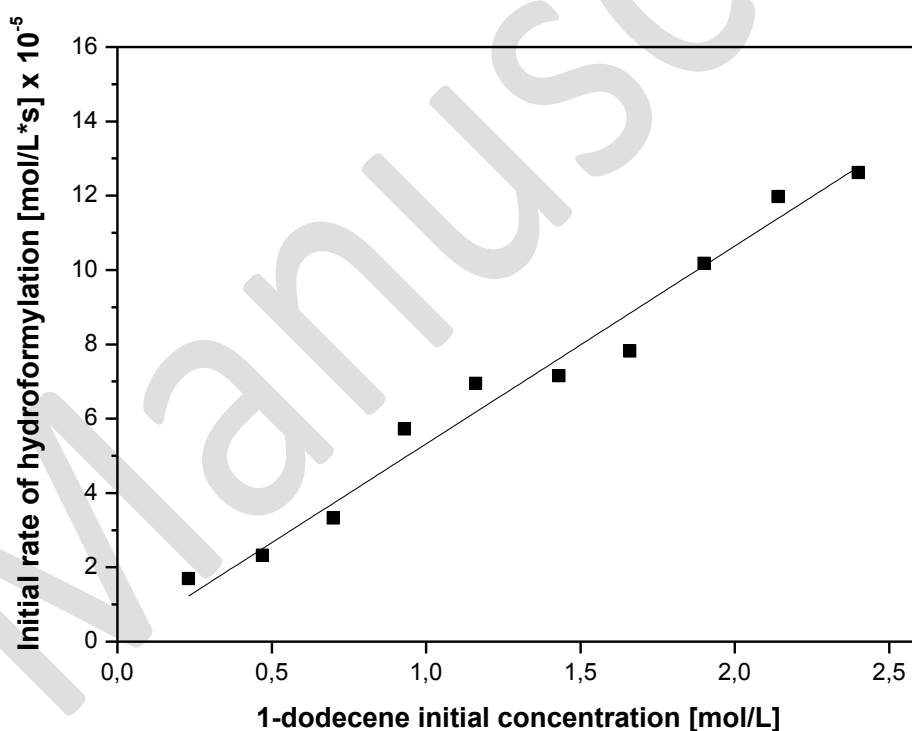


Fig. 4. Effect of 1-dodecene initial concentration on the initial rate of hydroformylation. Test conditions: $\text{Rh}(\text{acac})(\text{CO})_2 = 1.0 \times 10^{-3}$ mol/L, sulfoxantphos:Rh ratio=4:1 (P:Rh ratio=8:1), 1-dodecene + n-decane (20 g organic phase in total), water=20 g ($\alpha = 0.5$), surfactant=3.5 g ($\gamma=0.08$), 1 wt-% Na_2SO_4 , total liquid volume: 50 mL; $T=95$ °C, $p=15$ bar, stirring speed=1200 rpm. Statistic deviation of results: $\pm 15\%$.

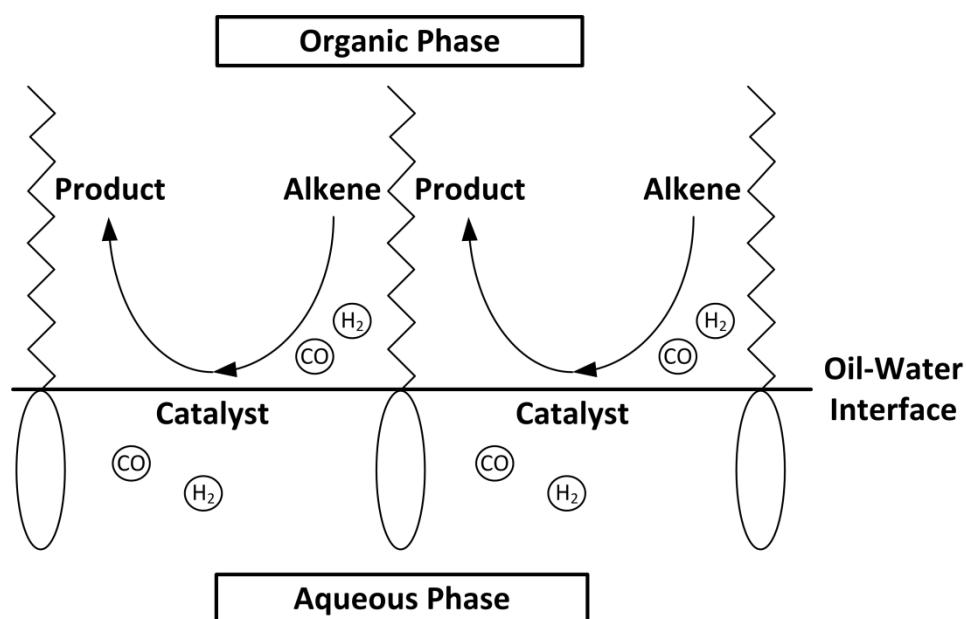


Fig. 5. Schematic illustration of two-phase catalysis in microemulsion systems on the example of the hydroformylation reaction. Picture taken from ¹⁶.

3.1.2. Effect of catalyst concentration

The effect of the concentration of the catalyst (with constant sulfoxantphos:Rh ratio of 4:1) was investigated at two different temperatures while keeping the pressure and 1-dodecene concentration constant. The results are shown in Fig. 6. It was observed that the reaction rate generally increases with increasing catalyst concentration. This was expected since an increasing catalyst concentration should enhance the concentration of active catalyst species in the mixture and thus the rate of reaction. Interestingly, the dependency of the reaction rate from the catalyst concentration can be divided in two different regions with linear dependence. At low catalyst concentrations the increase of the rate is significantly higher than at high concentrations, which indicates that not all Rh atoms are working as catalysts at the same TOF dependent on the catalyst loading in the reaction mixture. This behaviour is illustrated in Fig. 7 for the experiments at 95 °C. With increasing catalyst concentration the TOF at first increases to roughly 680 1/h and constantly decreases for higher concentrations. In addition, the n:iso selectivity of the hydroformylation is significantly lower at catalyst concentrations below 0.25 mmol/L, which indicates that the Rh-sulfoxantphos complex is not the only active catalyst under these conditions. Most probably this reaction behaviour is due to the two preequilibria of the active Rh-sulfoxantphos complex (Fig. 3, species 1a) with the corresponding dimeric Rh species (1c) and the unmodified Rh species (1b). At low catalyst concentrations the formation of the unmodified species could be enhanced due to the relatively low concentration of sulfoxantphos compared to the concentration of CO in solution. This would explain the rather high activity (TOF) of the catalyst in combination with the low n:iso selectivity. For initial catalyst concentrations higher than 0.25 mmol/L the formation of dimer could be enhanced and thus the TOF should constantly decrease with increasing catalyst concentration.

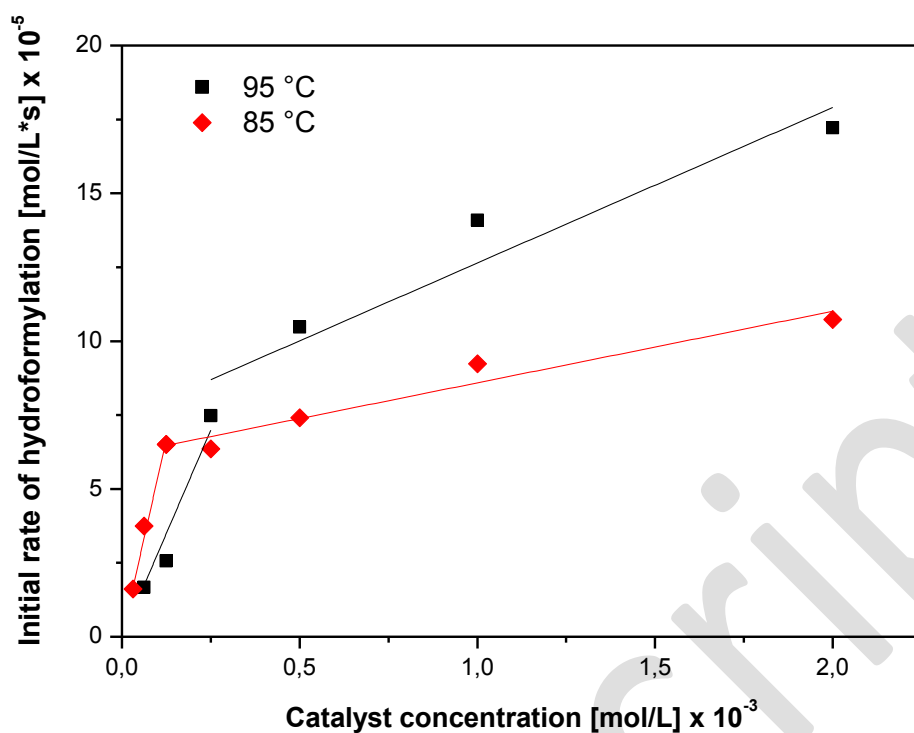


Fig. 6. Effect of catalyst concentration on the initial rate of hydroformylation. Test conditions: sulfoxantphos:Rh ratio=4:1 (P:Rh ratio=8:1), 1-dodecene=2.4 mol/L, water=20 g ($\alpha = 0.5$), surfactant=3.5 g ($\gamma=0.08$), 1 wt-% Na₂SO₄, total liquid volume: 50 mL; p=15 bar, stirring speed=1200 rpm. Statistic deviation of results: $\pm 15\%$.

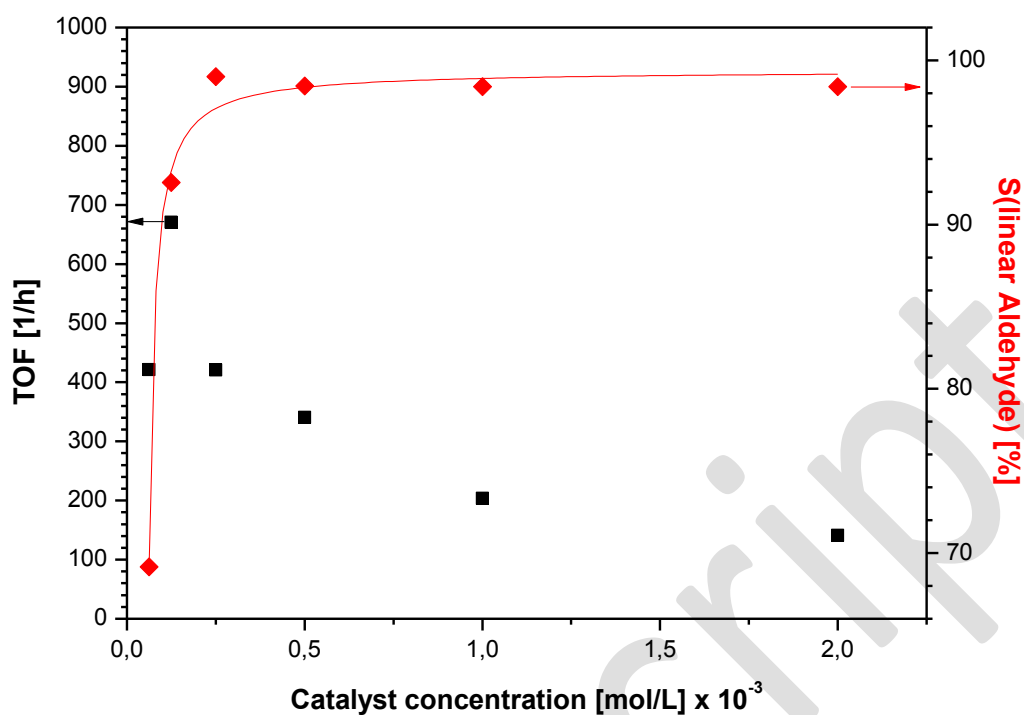


Fig. 7. Effect of catalyst concentration on turnover frequency and selectivity of hydroformylation. Test conditions: sulfoxantphos:Rh ratio=4:1 (P:Rh ratio=8:1), 1-dodecene= 2.4 mol/L, water=20 g ($\alpha = 0.5$), surfactant=3.5 g ($\gamma=0.08$), 1 wt-% Na₂SO₄, total liquid volume = 50 mL, T = 95 °C, p = 15 bar, stirring speed = 1200 rpm, TOFs were calculated after 1 h reaction time. Statistic deviation of results: $\pm 3\%$.

3.1.3. Effect of ligand:Rh ratio

The sulfoxantphos:Rh ratio was varied from 1:1 to 8:1 while the other reaction parameters were kept constant. The results are presented in Fig. 8. It was observed that the reaction rate is decreased with increasing amount of ligand in the mixture. This was expected, since a higher ligand-to-metal ratio usually leads to the inhibition of the reaction rate due to a higher concentration of ligand at the metal centers, which hinders the substrates to coordinate. For the ratios of 1:1 and 2:1 it has to be noted that the chemoselectivity and the n:iso selectivity of the hydroformylation have been significantly lower than expected (with an n:iso selectivity of 62:38 and 81:19 respectively). This indicates, that a sulfoxantphos:Rh ratio of at least 3:1 is needed for the exclusive formation of the desired catalyst species under the chosen reaction conditions. Higher ratios offer no additional benefit for the catalytic reaction.

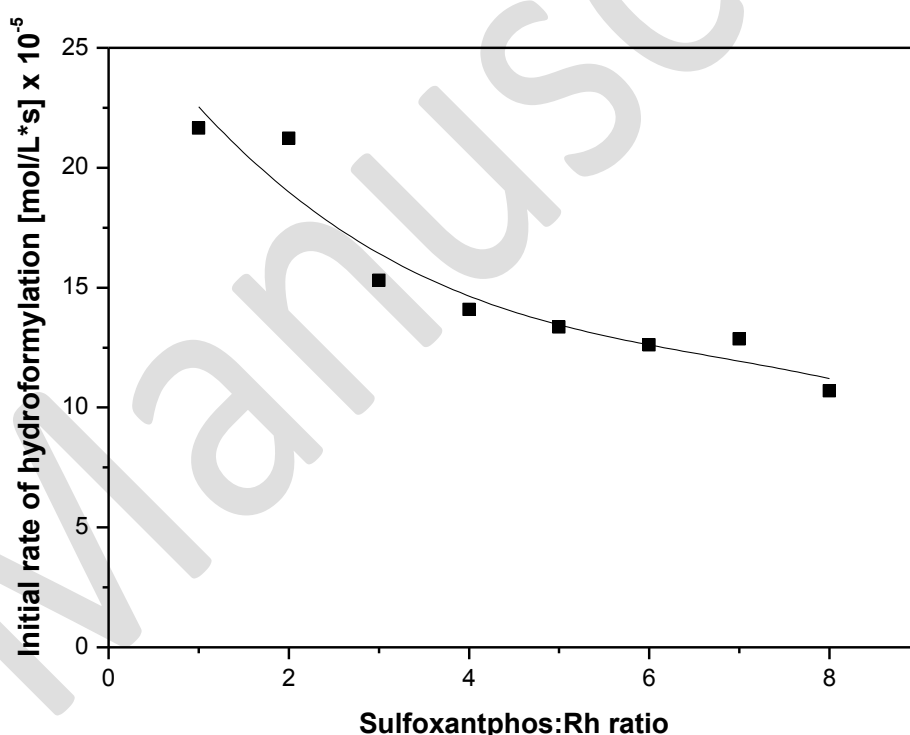


Fig. 8. Effect of sulfoxantphos:Rh ratio on the initial rate of hydroformylation. Test conditions: Rh(acac)(CO)₂=1.0 x 10⁻³ mol/L, 1-dodecene=2.4 mol/L, water=20 g (α = 0.5), surfactant=3.5 g (γ =0.08), 1 wt-% Na₂SO₄, total liquid volume: 50 mL; T=95 °C, p=15 bar, stirring speed=1200 rpm. Statistic deviation of results: \pm 15%.

3.1.4. Effect of syngas pressure

The effect of syngas pressure has been investigated in range of 1 to 40 bar while the other reaction conditions were kept constant. The reaction rate showed a complex dependency on the pressure, as seen in Fig. 9. It first increased strongly and then decreased with further increase in pressure, exhibiting a maximum at about 10 bar. This characteristics is very typical for hydroformylation reactions and mainly due to the increase of the partial pressure of CO. It has already been observed for several homogeneous and biphasic reaction systems using different catalysts ^{24–29}. Generally, the hydroformylation reaction is driven by the concentrations of CO and H₂ in the reaction mixture since both are substrates. However, it is also inhibited by side reactions leading to the formation of inactive dicarbonyl rhodium species (Fig. 3, species 6b) which is increased with an increasing CO pressure. As a result the concentration of active catalyst species is reduced and hence the reaction rate is decreased. This means that the apparent reaction order of CO shifts with the partial pressure: It starts at a positive value at low CO concentrations in solution, passes zero, and then has a negative value for higher CO concentrations. The effect of the H₂ partial pressure on the hydroformylation reaction is usually of positive order and can be of zero order at higher pressures. The increase of reaction rate with H₂ pressure can be explained by the formation of the dihydrogen complex (Fig. 3, species 7) which is a mandatory step in the catalytic cycle. However, the oxidative addition of hydrogen to the acyl complex is not generally rate determining for the hydroformylation and in competition with the coordination/insertion of the olefin double-bond to be the rate determining step. Dependent on (I) the ligand type and (II) on the steric interaction between ligand and substrate the RDS can differ for the same catalyst and thus makes a general prediction very difficult ^{26,30}.

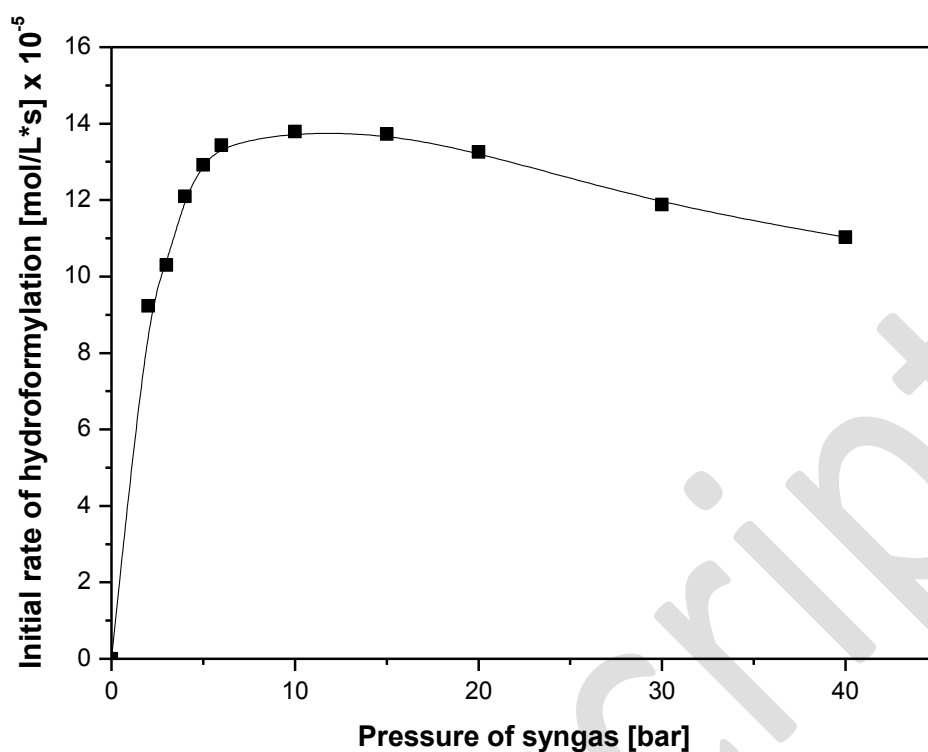


Fig. 9. Effect of syngas pressure on the initial rate of hydroformylation. Test conditions: $\text{Rh}(\text{acac})(\text{CO})_2 = 1.0 \times 10^{-3} \text{ mol/L}$, sulfoxantphos:Rh ratio=4:1 (P:Rh ratio=8:1), 1-dodecene= 2.4 mol/L, water=20 g ($\alpha = 0.5$), surfactant=3.5 g ($\gamma=0.08$), total liquid volume: 50 mL; $T=95^\circ\text{C}$, stirring speed=1200 rpm. Statistic deviation of results: $\pm 15\%$.

3.2. Formulation approach for an adapted kinetic model

The application and stable operation of complex process concepts, using innovative tunable solvent systems, such as the proposed microemulsion system is often aided by process systems engineering methods³¹. Herein, adequate process models are crucial for performing tasks like data reconciliation, state estimation or (dynamic) optimization. With regard to the formulation of kinetic models, a rigorous description is often not available or complicated by coupled kinetic and mass transfer phenomena. One approach to cope with this is to use kinetic models, in which available microkinetic or mechanistic models can be coupled with information about additional influences on the kinetics in the regarded system. To illustrate a possible procedure, a short systematic workflow is presented in Fig. 10 and subsequently performed for the microemulsion system at hand.

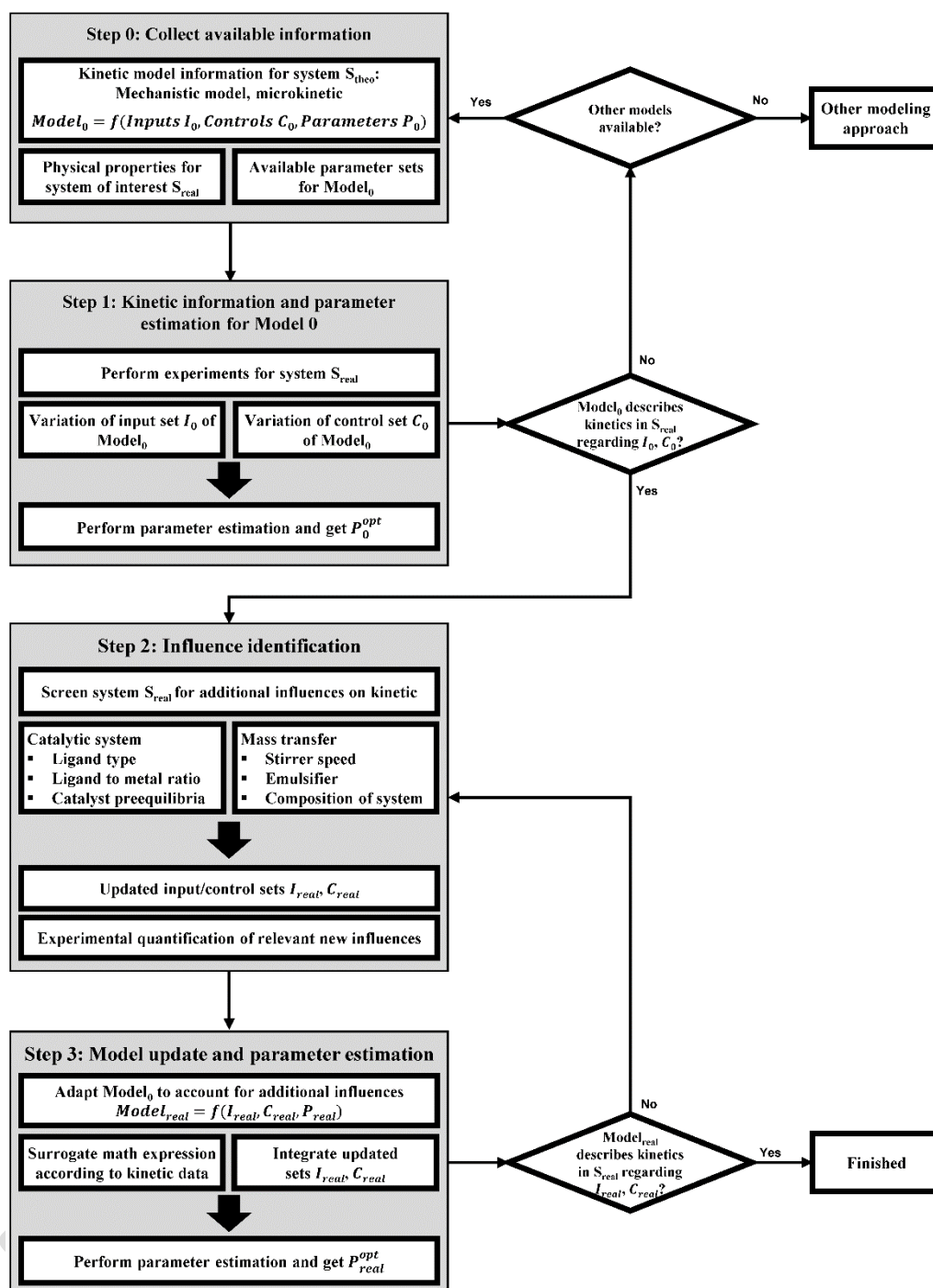


Fig. 10. Workflow for the adaption of microkinetic or mechanistic models to describe reaction trajectories for system with inherent additional influences.

3.2.1. Reaction network and available kinetic models

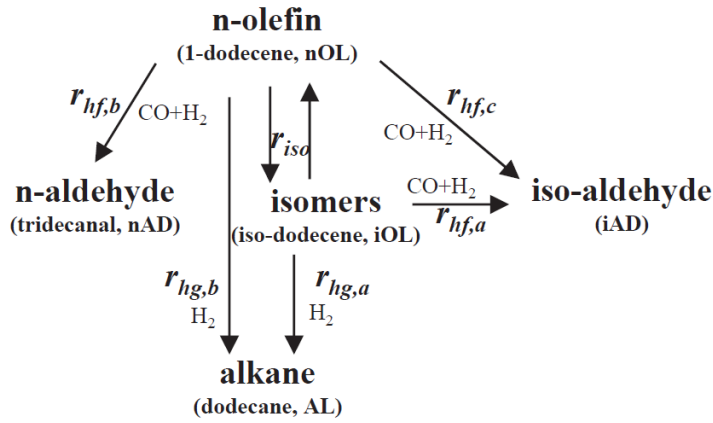


Fig. 11. Reaction network for the hydroformylation. Taken from ¹⁷.

Using the procedure in Fig. 10, **Step 0** marks the initialization step in which a review of available descriptions of the considered reaction system is performed, including model parameters if possible. For the reaction system at hand, a mechanistic rate equation system was developed by Kiedorf et al. ¹⁷ identifying 6 main reactions of isomerization, hydrogenation and hydroformylation depicted in Fig. 11. The structure of the rate equations is exemplarily shown in Eq. 4, in which k_{Hyfo}^{ref} represents the rate constant, $K_{x,Hyfo}$ inhibition factors, $E_{A,Hyfo}$ the activation energy and $[X]$ concentrations of components in the system. This formulation (*Model₀*) allows for calculating the effects of the amount of active catalyst in the system, concentrations of dissolved gases (CO , H_2), temperature, and pressure. However, the performed experiments and subsequent parameter estimation were carried out for a homogeneous catalytic system, using a rhodium-biphephos catalyst. Thus, the reported kinetic parameters are not valid for the discussed microemulsion system, but represent a suitable initial guess (Parameters P_0) for subsequent parameter estimations.

$$Rate_{Hyfo} = \frac{[Rh(CO)_2H]}{1 + K_{eq,cat,a} \cdot [CO] + K_{eq,cat,b} \cdot \frac{[CO]}{[H_2]}} \cdot \quad (4)$$

$$k_{Hyfo}^{ref} \exp\left(\frac{-E_{A,Hyfo}}{R} \cdot \left(\frac{1}{T} - \frac{1}{T_{ref}}\right)\right) [CO][H_2][alkene]$$

$$\cdot \frac{1}{1 + K_{a,Hyfo} \cdot [alkene] + K_{b,Hyfo} \cdot [CO][alkene] + K_{a,Hyfo} \cdot [CO][H_2][alkene]}$$

3.2.2. Model adaption

To retain a model description for the hydroformylation in microemulsion systems, a re-estimation parameter is necessary (**Step 1** in Fig. 10), using dynamic experimental data with variation of the model inputs I_0 (concentrations) and controls C_0 (e.g. pressure and temperature). This was exemplarily done using the framework described by Müller et al.³² to derive parameter set P_0^{opt} . Note, that a detailed description of the parameter estimation framework, the quality of the estimation (parameter variance, co-variances and identifiability) is waived at this point to keep the discussion short and focused.

The estimation result is depicted in Fig. 12. Additional information of the relative deviation between model and experiment is given in Tab. 1. For a constant ligand to metal ratio, as well as equal oil-to-water ratio and surfactant concentration, an adequate determination of the kinetic parameters was achieved. The experimental results for 1-dodecene and tridecanal are predicted with minimal deviations, which mainly arise from fluctuations of the measurements. Thus, Model₀ is suitable to describe the reaction kinetics under defined conditions, which are limited to the model inherent inputs and controls. If the structure of Model₀ is not suitable to describe the system, other initial kinetic models or modeling approaches, like a fully empiric model generation might be tested.

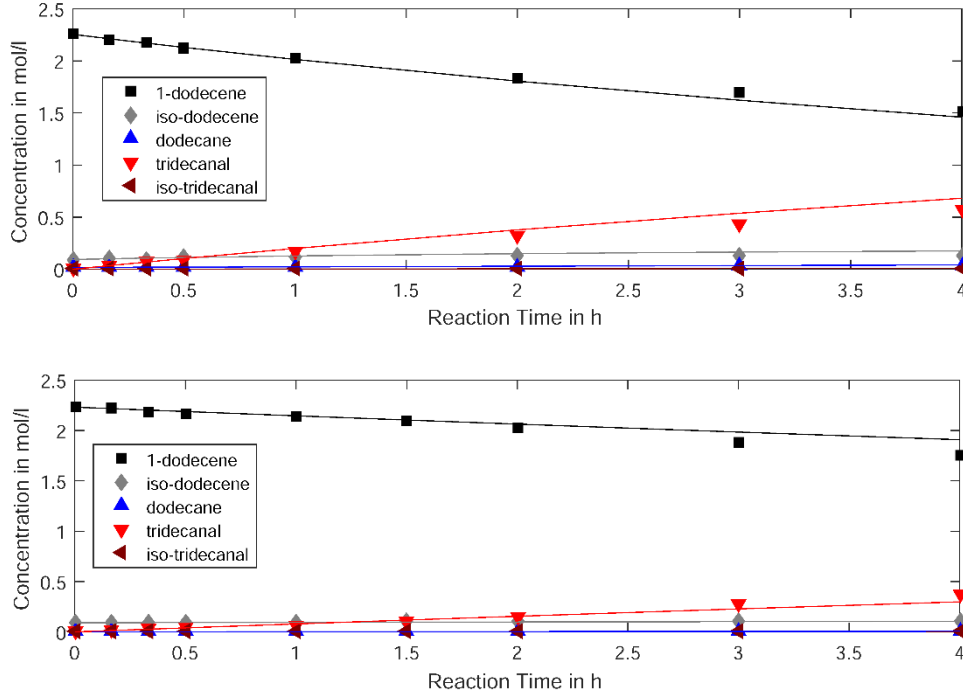


Fig. 12. Parameter estimation results using the mechanistic model of Kiedorf et al. ¹⁷ for experimental test conditions: $\text{Rh}(\text{acac})(\text{CO})_2 = 1.0 \times 10^{-3} \text{ mol/L}$, sulfoxantphos:Rh ratio=4:1 (P:Rh ratio=8:1), 1-dodecene=2.4 mol/L, water=20 g ($\alpha = 0.5$), surfactant=3.5 g ($\gamma=0.08$). Top: $T=95 \text{ }^\circ\text{C}$, $p=15 \text{ bar}$, Bottom: $T=85 \text{ }^\circ\text{C}$, $p=30 \text{ bar}$. Markers represent experimental data, full lines corresponding model responses.

Continuing with **Step 2** of Fig. 10, additional influences of the microemulsion system and the catalyst are to be identified by the use of screening experiments. Exemplarily, the gained model (Model_0 , using parameters P_0^{opt}) is applied for the representation of experiments with varied controls regarding the catalytic system and the composition of the microemulsion system. Here, large deviations occur throughout all components (see Fig. 13 and Tab. 1). This result is rather expected, because the presented kinetic studies in section 3.2 and the findings of Pogrzeba et al. ¹⁶ mark key influences on the kinetics for the microemulsion system, which need to be considered in a subsequent experimental quantification and adaption of the model equations (**Step 3** of Fig. 10).

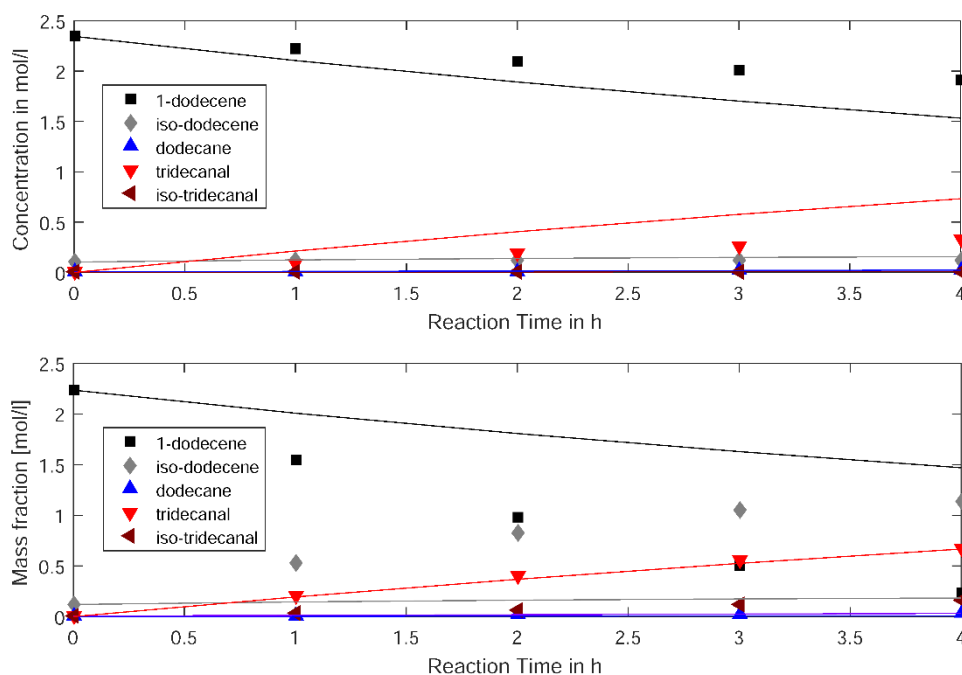


Fig. 13. Model representation for the hydroformylation of 1-dodecene using a rhodium-sulfoxantphos catalyst in a microemulsion system. Test conditions: $T=95\text{ }^{\circ}\text{C}$, $p=15\text{ bar}$ $\text{Rh}(\text{acac})(\text{CO})_2=1.0 \times 10^{-3}\text{ mol/L}$, 1-dodecene=2.4 mol/L, water=20 g ($\alpha = 0.5$), surfactant=3.5 g ($\gamma=0.08$). Top: sulfoxantphos:Rh ratio=4:1, surfactant=1.7 g ($\gamma=0.04$); Bottom: sulfoxantphos:Rh ratio=2:1, surfactant=3.5 g ($\gamma=0.08$). Markers represent experimental data, full lines corresponding model responses.

Adaption for ligand to metal ratio

Using ligand modified rhodium catalysts, the ligand species is prone to alter catalyst activity and selectivity¹⁰. In principle, this could be handled within the reaction rate expression of Eq. 4. But following the catalytic cycle in Fig. 3 and considering the present kinetic information for the microemulsion system, it is obvious that one must also account for the depicted catalyst preequilibria, which highly influence the specific reaction rates and thus overall main product yield and the regioselectivity (see Fig. 6-8). Incorporating this information into the kinetic model is desired to predict and avoid undesired reaction conditions in which side reactions such as hydrogenation or isomerization are promoted. However, since the quantification of the different catalytic species in the catalytic cycle during the reaction is not possible, a profound derivation of a rate expression for the preequilibria is not accessible. As a surrogate, the parameterized ligand to metal ratio is used to adapt the reaction rate of each reaction within the reaction network (see exemplarily

Eq. 5). The mathematical formulation was chosen to match the observed trajectories of the reactants from experimental data.

$$Rate^*_{Hyfo} = \frac{K_{eq,Lig}}{1 + [SX]^{n_{eq,Lig}_{Hyfo}}} \cdot Rate_{Hyfo} \quad (5)$$

Adaption for surfactant concentration

Recently, Pogrzeba et al. ¹⁶ showed the influence of the surfactant concentration on the hydroformylation reaction. It could be demonstrated that the surfactant concentration has a significant and complex influence on the reaction rates of the hydroformylation network. It was assumed that this complex reaction behaviour is due to the local concentrations of the rhodium catalyst at the oil-water interface of the microemulsion, leading to a shift of the catalyst preequilibria. Again, these local concentration (detection level of measurement devices), as well as the structure of the microemulsion (nanometer scale of droplets) itself are inaccessible. Thus, the collected kinetic information regarding the variation of surfactant concentration was analyzed and transferred to a surrogate model structure according to Eq. 6. Note that for the reduction of parameters $K_{eq,Lig}$, $K_{eq,Surfactant}$ and the corresponding efficiency factor for each reaction in the reaction network are combined to one parameter $k^{ref,**}_{Hyfo}$.

$$Rate^{**}_{Hyfo} = \frac{K_{eq,Lig} \cdot [Surfactant] \cdot K_{eq,Surfactant}}{1 + [SX]^{n_{eq,Lig}_{Hyfo}}} \cdot Rate_{Hyfo} \quad (6)$$

$$k^{ref,**}_{Hyfo} = K_{eq,Lig} \cdot K_{eq,Surfactant} \cdot k^{ref}_{Hyfo} \quad (7)$$

Having the adapted model equations (Model_{real}) and the kinetic information from the conducted screening experiments, a parameter estimation was carried out to estimate the updated parameter set P^{opt}_{real} . Using this approach, a model formulation and parameter set has been identified for the system at hand and in the investigated ranges of inputs and controls. Here, reaction trajectories are described in good accordance to observed

experimental data (see Fig. 14 and Tab. 1). This holds not only for varied temperatures and pressures, as for Model₀, but also for varied catalyst specific controls (ligand to metal ratio) and microemulsion specific controls (surfactant concentration).

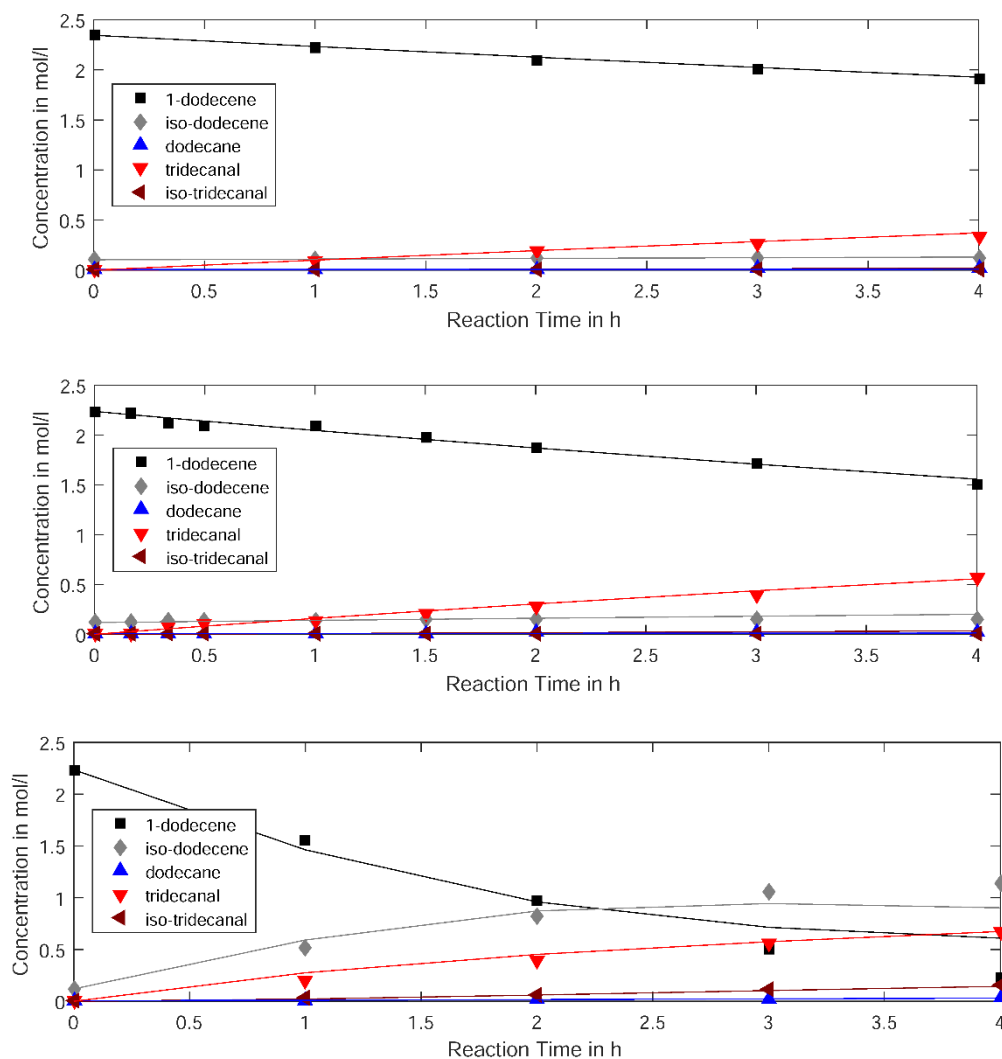


Fig. 14. Model representation using the adapted reaction kinetic equations. Test conditions: $T=95\text{ }^{\circ}\text{C}$, $p=15\text{ bar}$ $\text{Rh}(\text{acac})(\text{CO})_2=1.0 \times 10^{-3}\text{ mol/L}$, $1\text{-dodecene}=2.4\text{ mol/L}$, $\text{water}=20\text{ g}$ ($\alpha = 0.5$), $\text{surfactant}=3.5\text{ g}$ ($\gamma=0.08$). Top: $\text{sulfoxantphos}:\text{Rh}$ ratio=4:1, $\text{surfactant}=1.7\text{ g}$ ($\gamma=0.04$); Middle: $\text{sulfoxantphos}:\text{Rh}$ ratio=2:1, $\text{surfactant}=3.5\text{ g}$ ($\gamma=0.08$); Bottom: $\text{sulfoxantphos}:\text{Rh}$ ratio=4:1, $\text{surfactant}=3.5\text{ g}$ ($\gamma=0.08$). Markers represent experimental data, full lines corresponding model responses.

Table 1. Comparison of the estimation results for Model₀ and Model_{real} for differing variation of inputs: Temperature (T), pressure (p), sulfoxantphos:Rh ratio [SX], and surfactant concentration [Surfactant]. The relative deviation between model and experiment for each component in the regarded set of experiments is depicted. Additionally, estimated parameter are listed for the adapted model (rate equations according to Kiedorf et al. ¹⁷).

Component	Model ₀ Variation of T, p	Model ₀ Variation of T, p, [SX], [Surfactant]	Model _{real} Variation of T, p, [SX], [Surfactant]
1-dodecene	1.63%	35.07%	4.52%
iso-dodecene	0.48%	23.67%	2.73%
iso-tridecanal	< 0.01%	3.5 %	0.54%
dodecane	0.18%	< 0.01%	0.21%
tridecanal	1.43%	6.42%	1.42%
Hydroformylation			
$k_{Hyfo,a}^{ref,**} = 7.895 \cdot 10^3 \frac{L^3}{g_{cat} \cdot min \cdot mol^2}$			
$E_{A,Hyfo,a} = 120844 \frac{J}{mol}$			
$n_{Hyfo,a}^{eq,Lig} = 0.002$			
$k_{Hyfo,b}^{ref,**} = 4.885 \cdot 10^7 \frac{L^3}{g_{cat} \cdot min \cdot mol^2}$			
$E_{A,Hyfo,b} = 59000 \frac{J}{mol}$			
$n_{Hyfo,b}^{eq,Lig} = 0.854$			
$k_{Hyfo,b}^{ref,**} = 6.650 \cdot 10^{-5} \frac{L^3}{g_{cat} \cdot min \cdot mol^2}$			
$E_{A,Hyfo,b} = 59000 \frac{J}{mol}$			
$n_{Hyfo,c}^{eq,Lig} = 0.999$			
$K_{a,Hyfo} = 4.816 \cdot 10^{-3} \frac{L}{mol}$			
$K_{b,Hyfo} = 1.826 \cdot 10^{-2} \frac{L}{mol}$			
$K_{c,Hyfo} = 5.908 \cdot 10^4 \frac{L}{mol}$			
Hydrogenation			
$k_{Hyd,a}^{ref,**} = 46.486 \frac{L^2}{g_{cat} \cdot min \cdot mol}$			
$E_{A,Hyd,a} = 102260 \frac{J}{mol}$			
$n_{Hyfo,b}^{eq,Lig} = 0.002$			
$k_{Hyd,b}^{ref,**} = 3.568 \cdot 10^4 \frac{L^2}{g_{cat} \cdot min \cdot mol}$			
$E_{A,Hyd,b} = 76105 \frac{J}{mol}$			
$n_{Hyfo,b}^{eq,Lig} = 0.999$			
$K_{a,Hyd} = 3.311 \frac{L}{mol}$			
$K_{b,Hyd} = 0.368 \frac{L}{mol}$			
$K_{c,Hyd} = 2.916 \cdot 10^4 \frac{L}{mol}$			
Catalyst Equilibrium			
$K_{eq,cat,a} = 8505.973 \frac{L}{mol}$			
$K_{eq,cat,b} = 1$			
Isomerization			
$k_{Iso}^{ref,**} = 4.878 \cdot 10^4 \frac{L}{g_{cat} min}$			
$E_{A,iso} = 136891 \frac{J}{mol}$			
$n_{Hyfo,b}^{eq,Lig} = 3.668$			
$\Delta G_{R,Iso} = 1099.999 \frac{J}{mol}$			
$K_{a,Iso} = 132.859 \frac{L}{mol}$			
$K_{b,Iso} = 8.134 \cdot 10^{-3} \frac{L}{mol}$			

4. Conclusion

In this contribution, the kinetics of hydroformylation of 1-dodecene in microemulsion systems using the $\text{Rh}(\text{CO})_2(\text{acac})/\text{Sulfoxantphos}$ catalyst system has been investigated. The reaction rate was found to be in first order with respect to alkene concentration and fractional order with respect to catalyst and ligand concentration. The dependency of the rate on syngas pressure was found to be rather complex, exhibiting a maximum at about 10 bar. This observation indicates an inhibition of the reaction at higher pressures, most probably due to the high partial pressure of CO. Based on the derived data an adaption of an existing microkinetic model was performed applying a systematic approach. Using this, a kinetic model, which incorporates the identified additional influences on the hydroformylation reaction in microemulsions was formulated, whereas first kinetic parameters were estimated. Thus, the mismatch between model and experiments was significantly reduced.

Acknowledgements

This work is part of the Collaborative Research Center/ Transregio 63 "Integrated Chemical Processes in Liquid Multiphase Systems" (subprojects A2, B4, C4). Financial support by the Deutsche Forschungsgemeinschaft (DFG, German Research Foundation) is gratefully acknowledged (TRR 63). Furthermore, the authors gratefully acknowledge the support of the company Umicore for sponsoring the rhodium catalyst "Acetylacetonato-dicarbonylrhodium(I) (CAS: 14874-82-9)".

Abbreviations

2 ϕ = two phase

3 ϕ = three phase

EO = degree of ethoxylation

MES = microemulsion system

SX = SulfoXantphos, 4,5-bis(diphenylphosphino)-9,9-dimethylxanthene

TOF = turnover frequency

References

- (1) Lipshutz, B. H.; Gallou, F.; Handa, S. Evolution of Solvents in Organic Chemistry. *Sustain. Chem. Eng.* **2016**, *4*, 5838.
- (2) Dwars, T.; Paetzold, E.; Oehme, G. Reactions in Micellar Systems. *Angew. Chem. Int. Ed. Engl.* **2005**, *44*, 7174.
- (3) Lipshutz, B. H.; Abela, A. R. Micellar Catalysis of Suzuki-Miyaura Cross-Couplings with Heteroaromatics in Water. *Org. Lett.* **2008**, *10*, 5329.
- (4) Schwarze, M.; Milano-Brusco, J. S.; Strempele, V.; Hamerla, T.; Wille, S.; Fischer, C.; Baumann, W.; Arlt, W.; Schomäcker, R. Rhodium Catalyzed Hydrogenation Reactions in Aqueous Micellar Systems as Green Solvents. *RSC Adv.* **2011**, *1*, 474.
- (5) La Sorella, G.; Strukul, G.; Scarso, A. Recent Advances in Catalysis in Micellar Media. *Green Chem.* **2015**, *17*, 644.
- (6) Schwarze, M.; Pogrzeba, T.; Volovych, I.; Schomäcker, R. Microemulsion Systems for Catalytic Reactions and Processes. *Catal. Sci. Technol.* **2015**, *5*, 24.
- (7) Pogrzeba, T.; Müller, D.; Illner, M.; Schmidt, M.; Kasaka, Y.; Weber, A.; Wozny, G.; Schomäcker, R.; Schwarze, M. Superior Catalyst Recycling in Surfactant Based Multiphase Systems – Quo Vadis Catalyst Complex? *Chem. Eng. Process.* **2016**, *99*, 155.
- (8) Nowothnick, H.; Blum, J.; Schomäcker, R. Suzuki Coupling Reactions in Three-Phase Microemulsions. *Angew. Chem. Int. Ed. Engl.* **2011**, *50*, 1918.
- (9) Volovych, I.; Kasaka, Y.; Schwarze, M.; Nairoukh, Z.; Blum, J.; Fanun, M.; Avnir, D.; Schomäcker, R. Investigation of Sol-gel Supported Palladium Catalysts for Heck Coupling Reactions in O/w-Microemulsions. *J. Mol. Catal. A Chem.* **2014**, *393*, 210.
- (10) Hamerla, T.; Rost, A.; Kasaka, Y.; Schomäcker, R. Hydroformylation of 1-Dodecene with Water-Soluble Rhodium Catalysts with Bidentate Ligands in Multiphase Systems. *ChemCatChem* **2013**, *5*, 1854.

- (11) Pogrzeba, T.; Illner, M.; Schmidt, M.; Repke, J.-U.; Schomäcker, R. Microemulsion Systems as Switchable Reaction Media for the Catalytic Upgrading of Long-Chain Alkenes. *Chemie Ing. Tech.* **2017**, *89*, 459.
- (12) Illner, M.; Müller, D.; Esche, E.; Pogrzeba, T.; Schmidt, M.; Schomäcker, R.; Wozny, G.; Repke, J.-U. Hydroformylation in Microemulsions : Proof of Concept in a Miniplant. *Ind. Eng. Chem. Res.* **2016**, *55*, 8616.
- (13) Pogrzeba, T.; Müller, D.; Hamerla, T.; Esche, E.; Paul, N.; Wozny, G.; Schomäcker, R. Rhodium-Catalyzed Hydroformylation of Long-Chain Olefins in Aqueous Multiphase Systems in a Continuously Operated Miniplant. *Ind. Eng. Chem. Res.* **2015**, *54*, 11953.
- (14) Rost, A.; Müller, M.; Hamerla, T.; Kasaka, Y.; Wozny, G.; Schomäcker, R. Development of a Continuous Process for the Hydroformylation of Long-Chain Olefins in Aqueous Multiphase Systems. *Chem. Eng. Process. Process Intensif.* **2013**, *67*, 130.
- (15) Nowothnick, H.; Rost, A.; Hamerla, T.; Schomäcker, R.; Müller, C.; Vogt, D. Comparison of Phase Transfer Agents in the Aqueous Biphasic Hydroformylation of Higher Alkenes. *Catal. Sci. Technol.* **2013**, *3*, 600.
- (16) Pogrzeba, T.; Schmidt, M.; Milojevic, N.; Urban, C.; Illner, M.; Repke, J.-U.; Schomäcker, R. Understanding the Role of Nonionic Surfactants during Catalysis in Microemulsion Systems on the Example of Rhodium-Catalyzed Hydroformylation. *Ind. Eng. Chem. Res.* **2017**, *56*, 9934.
- (17) Kiedorf, G.; Hoang, D. M.; Müller, A.; Jörke, A.; Markert, J.; Arellano-Garcia, H.; Seidel-Morgenstern, A.; Hamel, C. Kinetics of 1-Dodecene Hydroformylation in a Thermomorphic Solvent System Using a Rhodium-Biphephos Catalyst. *Chem. Eng. Sci.* **2014**, *115*, 31.
- (18) Goedheijt, M. S.; Kamer, P. C. J.; Leeuwen, P. W. N. M. Van. A Water-Soluble Diphosphine Ligand with a Large “ Natural ” Bite Angle for Two-Phase Hydroformylation of Alkenes. *J. Mol. Catal. A Chem.* **1998**, *134*, 243.
- (19) Evans, D.; Osborn, J. A.; Wilkinson, G. Hydroformylation of Alkenes By Use of Rhodium Complex Catalysts. *J. Chem. Soc.* **1968**, 3133.

- (20) Silva, S. M.; Bronger, R. P. J.; Freixa, Z.; Dupont, J.; van Leeuwen, P. W. N. . High Pressure Infrared and Nuclear Magnetic Resonance Studies of the Rhodium-Sulfoxantphos Catalysed Hydroformylation of 1-Octene in Ionic Liquids. *New J. Chem.* **2003**, 27, 1294.
- (21) Li, C.; Widjaja, E.; Chew, W.; Garland, M. Rhodium Tetracarbonyl Hydride: The Elusive Metal Carbonyl Hydride. *Angew. Chemie Int. Ed.* **2002**, 41, 3785.
- (22) Sandee, A. J.; Slagt, V. F.; Reek, J. N. H.; Kamer, P. C. J.; van Leeuwen, P. W. N. M. A Stable and Recyclable Supported Aqueous Phase Catalyst for Highly Selective Hydroformylation of Higher Olefins. *Chem. Commun.* **1999**, 1633.
- (23) Bronger, R. P. J.; Bermon, J. P.; Herwig, J.; Kamer, P. C. J.; van Leeuwen, P. W. N. . Phenoxaphosphino-Modified Xantphos-Type Ligands in the Rhodium-Catalysed Hydroformylation of Internal and Terminal Alkenes. *Adv. Synth. Catal.* **2004**, 346, 789.
- (24) Deshpande, R. M.; Chaudhari, R. V. Kinetics of Hydroformylation of 1-Hexene Using Homogeneous $\text{HRh}(\text{CO})(\text{PPh}_3)_3$ Complex Catalyst. *Ind. Eng. Chem. Res.* **1988**, 27, 1996.
- (25) Deshpande, R. M.; Purwanto, P.; Delmas, H. Kinetics of Hydroformylation of 1-Octene Using $[\text{Rh}(\text{COD})\text{Cl}]_2$ - TPPTS Complex Catalyst in a Two-Phase System in the Presence of a Cosolvent. *Ind. Eng. Chem. Res.* **1996**, 35, 3927.
- (26) Rooy, A. Van; Kamer, P. C. J.; Leeuwen, P. W. N. M. Van; Goubitz, K.; Fraanje, J.; Veldman, N.; Spek, A. L. Bulky Diphosphite-Modified Rhodium Catalysts: Hydroformylation and Characterization. *Organometallics* **1996**, 15, 835.
- (27) Rosales, M.; González, A.; Guerrero, Y.; Pacheco, I.; Sánchez-Delgado, R. A. Kinetics and Mechanisms of Homogeneous Catalytic Reactions Part 6 . Hydroformylation of 1-Hexene by Use of $\text{Rh}(\text{acac})(\text{CO})_2/\text{Dppe}$ [$\text{Dppe} = 1, 2\text{-Bis}(\text{Diphenylphosphino})\text{Ethane}$] as the Precatalyst. *J. Mol. Catal. A Chem.* **2007**, 270, 241.
- (28) Deshpande, R. M.; Kelkar, A. A.; Sharma, A.; Julcour-lebigue, C.; Delmas, H. Kinetics of Hydroformylation of 1-Octene in Ionic Liquid-Organic Biphasic Media Using Rhodium Sulfoxantphos Catalyst. *Chem. Eng. Sci.* **2011**, 66, 1631.

- (29) Jörke, A.; Gaide, T.; Behr, A.; Vorholt, A.; Seidel-Morgenstern, A.; Hamel, C. Hydroformylation and Tandem Isomerization – Hydroformylation of N-Decenes Using a Rhodium-BiPhePhos Catalyst : Kinetic Modeling , Reaction Network Analysis and Optimal Reaction Control. *Chem. Eng. J.* **2017**, *313*, 382.
- (30) Rooy, A. Van; Orij, E. N.; Kamer, P. C. J.; Leeuwen, P. W. N. M. Van. Hydroformylation with a Rhodium/Bulky Phosphite Modified Catalyst. Catalyst Comparison for Oct-1-Ene, Cyclohexene, and Styrene. *Organometallics* **1995**, *14*, 34.
- (31) Müller, D.; Illner, M.; Esche, E.; Pogrzeba, T.; Schmidt, M.; Schomäcker, R.; Biegler, L. T.; Wozny, G.; Repke, J.-U. Dynamic Real-Time Optimization under Uncertainty of a Hydroformylation Mini-Plant. *Comput. Chem. Eng.* **2017**, *106*, 836.
- (32) Müller, D.; Esche, E.; López C., D. C.; Wozny, G. An Algorithm for the Identification and Estimation of Relevant Parameters for Optimization under Uncertainty. *Comput. Chem. Eng.* **2014**, *71*, 94.